Allosteric Information Transfer through Inter-subunit Contacts in ATP-sensitive Potassium Channels

Thesis submitted for the degree of

Doctor of Philosophy

at the University of Leicester

by

Hussein Nori Rubaiy

Bpharm MPharmSc RPh

University Hospitals of Leicester, Leicester Royal Infirmary
School of Medicine
Department of Cardiovascular Sciences

March 2012

Abstract

Allosteric Information Transfer through Inter-subunit Contacts in ATP-sensitive Potassium (K_{ATP}) Channels

Hussein N. Rubaiy

K_{ATP} channels are ubiquitously expressed and link metabolic state to electrical excitability. In heart, in response to ischaemic stress, they play a protective role and in vascular smooth muscle regulation of vascular tone (vasorelaxation). Functional K_{ATP} channels are hetero-octamers composed of two subunits, a pore forming Kir6, which is a member of the inwardly rectifying potassium channels family and a regulatory sulphonylurea receptor (SUR). In response to nucleotides and pharmacological agents, SUR allosterically regulate K_{ATP} channel gating. Multidisciplinary techniques (molecular biology, biochemistry, electrophysiology, pharmacology) were used to study the allosteric regulation between these two heterologous subunits in K_{ATP} channels.

This project was divided into three major sub-projects: 1) Application of site directed mutagenesis and biochemical techniques to identify the cognate interaction domain on Kir6.2 for SUR2A-NBD2 (nucleotide binding domain 2). 2) Electrophysiological techniques to investigate the allosteric information transfer between heterologous subunits Kir6 and SUR2A. 3) Recombinant fusion protein to express and purify the cytoplasmic domains of Kir6.2 for structural analysis of the interaction between the two subunits.

This study reports on the identification of three cytoplasmic electrostatic interfaces between Kir6 and SUR2A involved in determining the sensitivity of K_{ATP} channel agonist, pinacidil, and antagonist, glibenclamide, from SUR2A to the Kir6 channel pore.

For structural study of cytoplasmic domains of Kir6.2, bacterial TM1070 was used as fusion partner with Kir6.2. A TM1070-Kir6.2 NC (CT-His6 tag) fusion construct expressed in Arctic Express competent cells permitted successful expression of folded cytoplasmic domains of Kir6.2 in near native form. Immobilized metal ion affinity chromatography, IMAC (Ni^{2+}), and gel filtration chromatography (GFC) column as second purification step were performed to purify this recombinant protein. The purification was confirmed by CBS and Western blot analysis.

Possibly, this new information on channel structure-function relationships may contribute to the design of novel and more effective drugs.

Acknowledgements

This PhD thesis represents a major milestone in my long journey within academics. I left my pharmacist profession when I received this great opportunity to pursue PhD studies at the Department of Cardiovascular Sciences. This period of time has been rewarding although very challenging and with many working hours.

With this, I want to take the opportunity to thank the people who made this journey bearable. A special thanks to my supervisor Bob Norman for all the advice and friendship. Also thanks to my co-supervisors Dave Lodwick, Nick Standen, and Mark Pfuhl and to research fellow Richard Rainbow.

I sincerely acknowledge the TH Wathes for providing financially in the form of a studentship.

A special thanks to the department staff; Carole Patrick, Barbara Horley, Hash Patel and Sonja Khemiri.

I would also like to thank Noel Davies and Nina Storey at the Department of Cell Physiology and Pharmacology. Thanks to my thesis committee, who guided me through all these years, John Mitcheson and Karl Herbert.

None of this journey would have been possible without the support of parents and family. I especially would like to thank my Mom and Dad, who have always given me all the love, support and motivation to succeed both academically and in life.

Without the love and support from my devoted wife, I would not be where I am now. She is always my right hand in everything and everywhere.

Finally, not only has this been an experience of a lifetime which will always be unforgettable during this time from the start having a daughter, Fatima, now age 7, I also received two additional angels two boys, Ali 2½ and Mehdi newborn. All three have given me such an enormous support and gave me many laughing moments, which facilitated my research.

Publications and Awards

Full Length

Lodwick D., Rainbow R.D., **Rubaiy H.N.**, Al-Johi M., Norman R.I.
Cytoplasmic Electrostatic Interactions Contribute to Functional Coupling in between Sulphonylurea Receptor (SUR) and Inward Rectifier Potassium Channel (Kir6) Subunits of K_{ATP} Channels. (*in preparation*)

Conference Publications

Rubaiy H.N., Lodwick D., Rainbow R.D., Norman R.I. **Dissecting Mechanisms of Information Transfer within a Cardiac Potassium Channel.** Seventh Festival of Postgraduate Research, Leicester 2011, **successful selected** among competing applicants, communicating and presenting your research to a wide audience and the general public, (June 2011).

Rubaiy H.N., Rainbow R.D., Al-Johi M., Lodwick D. and Norman R.I. **Sulphonylurea Receptors Regulate Kir6.2 Subunits Allosterically via a Salt Bridge in Cardiac K_{ATP} Channels.** Biophysical Journal, Volume 100, Issue 3, Supplement 1, 2 February 2011, Page 432a

Rubaiy H.N., Rainbow R.D., Al-Johi M., Lodwick D. and Norman R.I. **Inter-subunit Salt Bridges Communicate Glibenclamide Sensitivity to the ATP-sensitive Potassium Channel Pore**. Biochemical Society Annual Symposium Recent advance in membrane biochemistry, Cambridge, UK, Biochemical Society Transactions, 2011 in press

Press Release

Rubaiy H.N., New treatment hope for diabetes and cardiovascular diseases, Issued by University of Leicester Press Office on 03 June 2011

Award

A winner of **Highly Commended Award** at the 7th PG Research Festival 2011

Table of Contents

List of Figures

List of Tables

Abbreviations

ABC	ATP-binding cassette
ADP	Adenosine diphosphate
AGE	Agarose gel electrophoresis
Amp	Ampicillin
AMP-PCP	Adenylyl methylenediphosphate
AMP-PNP	Adenylyl imidodiphosphate
AP	Action potential
APS	Ammonium persulphate
ATP	Adenosine-5'-triphosphate
BLAST	Basic local alignment search tool
BK	Maxi-calcium activated potassium
BSA	Bovine serum albumin
^{o}C	Degrees centigrade
CBB	Coomassie brilliant blue
CBS	Coomassie blue staining
CFTR	Cystic fibrosis transmembrane conductance regulator
dH_2O	Distilled water
dNTPs	Deoxynucleotide triphosphate solution mix
DTT	Dithiothreitol
EDTA	Ethyldiamine tetra-acetate

g	Gram
GIRK1	G protein activated inwardly rectifying potassium channel
GFC	Gel filtration chromatography
hERG	Human ether-a-go-go
HEK	Human embryonic kidney
HHI	Hyperinsulinemic hypoglycemia of infancy
HRP	Horseradish peroxidase
IPTG	Isopropyl-beta-D-thiogalactopyranoside
IMAC	Immobilized metal ion affinity chromatography
k	Kilo
Kana	Kanamycin
K_{ATP} Channel	ATP-sensitive potassium channel
KCO	Potassium channel opener
Kir	Inwardly rectifying potassium channel
LSB	Laemmli sample buffer
MRP1	Multidrug resistance protein 1
min	Minutes
mitoK_{ATP}	Mitochondrial K_{ATP}
NBD	Nucleotide binding domain
NDM	Neonatal diabetes mellitus
NMR	Nuclear magnetic resonance
PAGE	Polyacrylamide gel electrophoresis
P_o	Channel open probability

PCR	Polymerase chain reaction
PIP_2	Phosphatidylinositol 4, 5-bisphosphate
RMP	Resting membrane potential
ROMK1	Renal outer medullary potassium channel
rpm	Revolutions per minute
s	Second
SAP	Shrimp alkaline phosphatase
sarcK_{ATP}	Sacrolemmal K_{ATP}
SDS	Sodium dodecyl sulfate
SEC	Size exclusion chromatography
SUR	Sulphonylurea receptor
TAE	Tris-acetate ETDA
TBS	Tris-buffered saline
TdP	Torsades des Pointes
TEMED	N,N,N',N'-Tetramethyl-1-,2-diaminomethane
TEV	Tobacco etch virus
TM	*Thermotoga Maritima*
TMD	Transmembrane domain
TWIK	Inwardly rectifying currents
TASK	Outwardly rectifying currents
UV	Ultraviolet

Amino Acid Abbreviations

Amino acid abbreviation	One-letter abbreviation	Three-letter
Alanine	A	Ala
Cysteine	C	Cys
Aspartic acid	D	Asp
Glutamic acid	E	Glu
Phenylalanine	F	Phe
Glycine	G	Gly
Histidine	H	His
Isoleucine	I	Ile
Lysine	K	Lys
Leucine	L	Leu
Methionine	M	Met
Asparagine	N	Asn
Proline	P	Pro
Glutamine	Q	Gln
Arginine	R	Arg
Serine	S	Ser
Threonine	T	Thr
Valine	V	Val
Tryptophan	W	Trp
Tyrosine	Y	Tyr

Chapter 1

Introduction

Ion Channels

Ion channels are located in the plasma membrane of all living cells. They form aqueous pores across the lipid bilayer and selectively allow particular inorganic ions, primarily Na^+, K^+, Ca^{2+} or Cl^- to pass through them. Only ions of appropriate size and charge can pass in a single file through the narrow channel. Each second up to ten million ions can pass through one open channel (Hille 2001).

The existence of ion channels was suggested by the British biophysicists Alan Hodgkin and Andrew Huxley in 1952 (Hodgkin and Huxley 1952) on publication of a theory of the nerve impulse. About a decade earlier, the two biophysicists with another pair, Curtis and Cole (K S Cole and Curtis 1938) had been able to measure, by using an intracellular micropipette, the full action potential of a squid giant axon (Hille 2001). An action potential is a transient, regenerating change in membrane potential that permits a wave of electrical excitation to pass along the plasma membrane of electrically excitable cells. It consists of two major phases; depolarization (a rapid change of the membrane potential from a negative to a positive value) and repolarisation (return of the membrane potential from a positive to a negative, -40 to -95 mV depending on the cell type) (Hille 2001). The existence of ion channels was confirmed in the late 1970s with an electrical recording technique known as the "patch clamp", invented by Erwin Neher and Bert Sakmann (Neher et al. 1978).

Ion	Intracellular (mM)	Extracellular (mM)
Na^+	5-20	130-160
K^+	130-160	4-8
Ca^{2+}	50-1000 nM	1.2-4
Cl^-	1-60	100-140

Table 1- 1 Intracellular and extracellular range of Na^+, K^+, Ca^{2+} and Cl^- ions found in mammalian cell.

Table 1-1 represents the intracellular and extracellular ranges of concentrations of ions, where of the largest concentration differences are of the calcium ion. Ion channels play an essential role in controlling many various physiological and pathological processes, therefore they are important drug targets (Hille 2001).

1.1 Potassium Channels

Potassium channels play significant roles in shaping the excitability and firing patterns of cells (Hille, 2001). Potassium channels are divided into four major classes based on their structure; two, four, six and seven transmembrane domain channels (figure 1-1). There is a large diversity within potassium channels including calcium activated, voltage-gated, twin pore domain, and inwardly rectifying channel subtypes. Even though there is this large diversity, the members of the channel family have similarities such as all of them have pore-lining P-loops with a consensus amino acid sequence (Shieh et al. 2000).

1.1.1 Voltage-gated Potassium Channels

The voltage-gated potassium channel family plays a crucial role during action potentials in returning the depolarized cell to a resting polarised state. Voltage-gated channels consist of six transmembrane domains, termed S1 - S6, with cytoplasmic N- and C- terminal regions (Isacoff et al. 1990). The structure of the channel is similar to the calcium activated potassium channel subtypes, though the maxi-calcium activated potassium (BK) channels have an extra transmembrane domain on the N-terminal of the channel (Hille 2001).

In terms of pharmacological safety, human ether-a-go-go, hERG, is a very important subfamily of human voltage-dependent potassium channels. Like the channels above, it consists of six transmembrane domains. The hERG channel mediates the repolarising I_{Kr} current in the cardiac action potential. A diverse array of drugs can block this

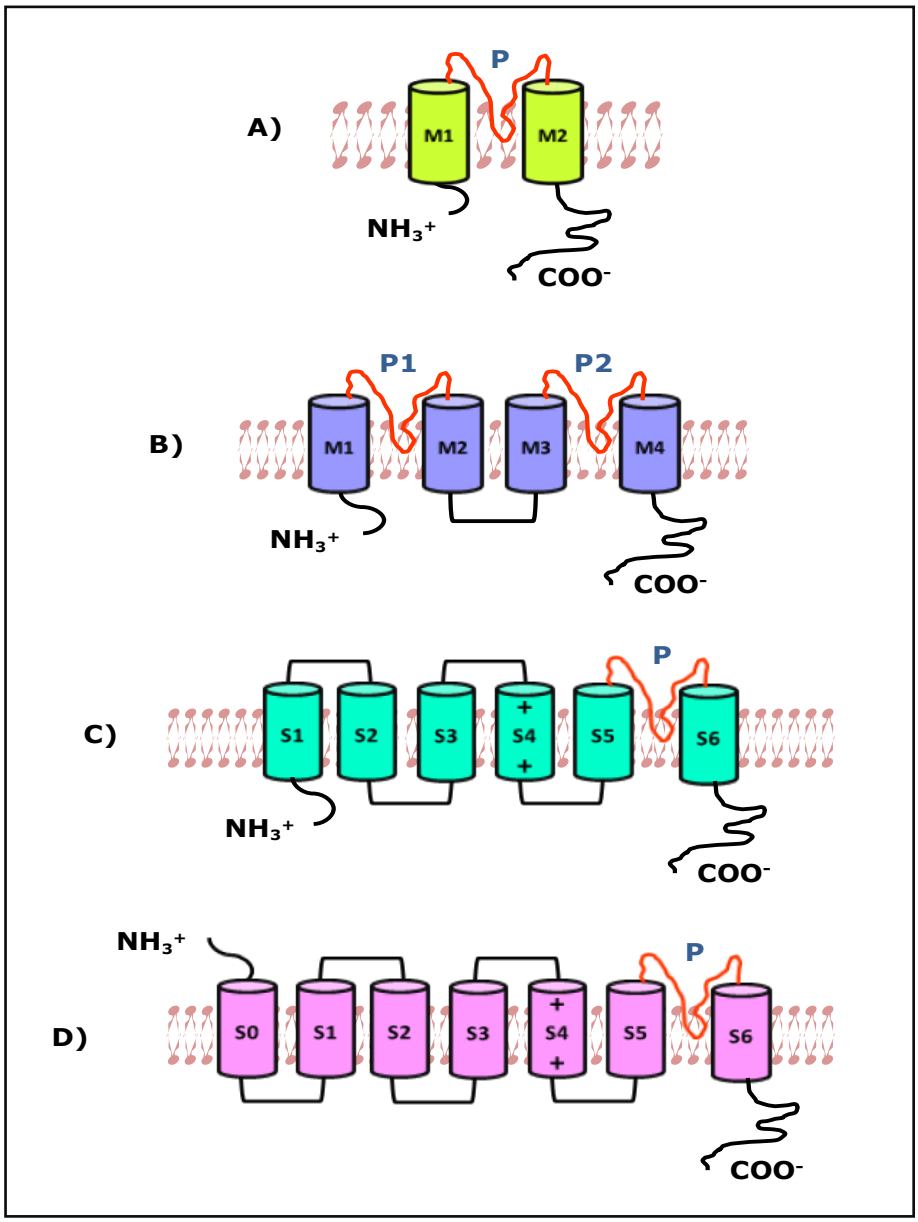

Figure 1-1 Proposed membrane topology of the four major classes of potassium channels.

The structure of potassium channels can be divided as follows. A) Represents two transmembrane domain channels (2-TM), M1 and M2 with a single pore loop (P) e.g. inward rectifier potassium channels. B) Four transmembrane domain channels with two pore loops e.g. leak channels (TWIK). C) Six transmembrane helix (S1-S6) channels that contain a single poor loop between S5 and S6 with a voltage sensor (positively charged amino acid residues) the S4 segment e.g. Kv1 and hERG channels. D) Seven transmembrane domain channels such as BK (Big Potassium or Maxi-K) channel.

channel, which leads to lengthening of the QT interval and the potentially fatal tachyarrhythmia Torsades des Pointes (TdP) (Gupta et al. 2007; Haverkamp et al. 2000).

1.1.2 Calcium Activated Potassium Channels

The calcium activated potassium (Kca) channel family includes three subfamilies; (1) small calcium sensitive potassium channels i.e. small conductance, (SK), (2) intermediate calcium sensitive potassium channels i.e. intermediate conductance, (IK) and (3) maxi-calcium sensitive potassium channels, i.e. big conductance, (BK) (Toro et al. 1998). Opening of calcium activated potassium channels is stimulated by an increase in the intracellular Ca^{2+} concentration. The channel is also activated by depolarization (Aidley 1996). The calcium activated potassium channels consist of six transmembrane domains.

1.1.3 Twin Pore Potassium Channels

Twin pore channels have small rectification[1] but no voltage dependent gating, since they lack a voltage-sensing domain. These channels can either exhibit inwardly (TWIK) or outwardly (TASK) rectifying currents (Hille 2001). The channel consists of four transmembrane domains and two pore regions which can assemble as functional dimers (Lesage and Lazdunski 2000). Another term for this group of channels is leak

[1] A nonlinear current-voltage relation occurs when the channel gating or conductance is affected by voltage.

channels. These channels are insensitive to most potassium channel blockers (Lesage and Lazdunski 2000).

1.1.4 Inwardly Rectifying Potassium Channels

The biophysical properties of inwardly rectifying potassium (Kir) channels is that they conduct inward current more readily than outward current (Doupnik et al. 1995; Nichols and Lopatin 1997). Kir channels are crucial for stabilizing the resting membrane potential and regulating excitability in many tissues (Hille, 2001; Doupnik et al. 1995). This group consists of seven sub-families; Kirl to Kir7. Kir channels comprise of two transmembrane domains (M1 and M2) with intracellular N- and C-terminal domains linked by a conserved pore domain (Bichet et al. 2003).

Ho et al (1993) and Kubo et al (1993) described the expression cloning of cDNAs encoding distinct inwardly rectifying K^+ channels. The Kir channels are dissimilar from voltage-gated K^+ channels since activation is not brought about by membrane depolarization and since a larger K^+ influx is allowed than efflux (Enkvetchakul et al. 2001).

To date, the Kir channel proteins that have been identified comprise between 360 to 500 amino acids in length. There are, in the Kir channel family, at least seven subfamilies now identified, Kir1.0 to Kir7.0 (Logothetis et al. 2007; Xie et al. 2007). All Kir members are regulated by the membrane phospholipid, phosphatidylinositol 4,5-bisphosphate (PIP_2), and some are also modulated by other regulatory factors or ligands, such as ATP and G-proteins, giving their common names, ATP-sensitive (K_{ATP}) and the G-protein-gated potassium channel (GRK) (Xie et al. 2007). Also, all members of the Kir channel family have the same basic structure, which consists of intracellular amino (N) and carboxyl (C) termini and two putative membrane spanning segments (M1 and M2) flanking a pore-forming P-loop and signature sequence (figure 1-2) (Xie et al. 2007).

1.2 K_{ATP} Channels

ATP-sensitive potassium (K_{ATP}) channels, which are unique among potassium channels, were first described by Akinori Noma in 1983 (Noma 1983). Noma stated that K_{ATP} channels in cardiac myocytes are reversibly inhibited by the nonhydrolytic binding of intracellular ATP. More recently, K_{ATP} channels have been identified in other tissues including pancreatic β-cells (Cook and Hales 1984), skeletal muscle cells (Spruce et al. 1985), neuronal cells (S. J. Ashcroft and Ashcroft 1990) and smooth muscle cells (Standen et al. 1989). The K_{ATP} channel has also been identified in the inner membrane of rat liver mitochondria, although the molecular identity of this K_{ATP} channel has not yet been determined (Inoue et al. 1991). The mitochondrial channel has been characterized pharmacologically in cells and in isolated bilayers. Many research groups have questioned its existence even, which makes this a very controversial area.

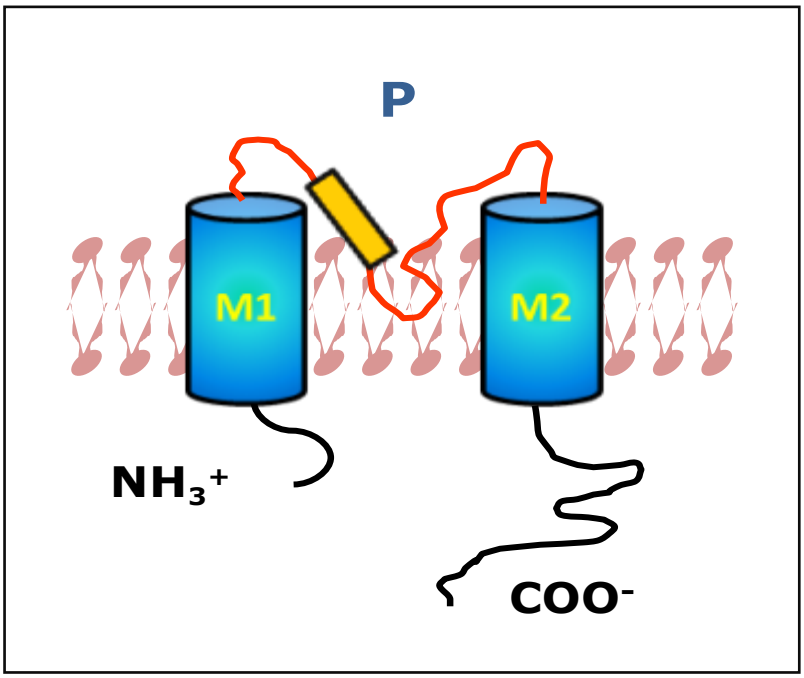

Figure 1-2 Suggested membrane topology of a Kir channel subunit.

Each subunit consists of two transmembrane helices M1 and M2 and a pore-forming region containing the pore-helix (P), and intracellular N- and C-termini.

This classification is provisional and there is a great necessity to confirm this classification by tissue and cellular localization work and to look for overlapping expression or co-assembly of subunit types (Aguilar-Bryan and Bryan 1999).

The classification of the K_{ATP} channels is mainly on pharmacological criteria by using the potassium channel openers (KCOs, agonists) or sulphonylureas (antagonists). K_{ATP} channels are identified by subunit combinations of sulphonylurea receptor (SUR), SUR1, SUR2A and SUR2B, and inward rectifier (Kir), Kir6.1, Kir6.2, in different tissue types (Aguilar-Bryan and Bryan 1999; Billman 2008).

1.2.1 Kir6

The Kir6 subfamily is a member of the Kir channel family (Isomoto et al. 1997) and comprises the pore forming component of the K_{ATP} channel (Bryan et al. 2004). There are two Kir6 isoforms, Kir6.1 and Kir6.2 (Farzaneh and Tinker 2008; Inagaki et al. 1995).

Sulphonylurea Receptor	Gene	Inward Rectifier	Gene	Tissue/Channel Subtype
SUR1	*ABCC8*	**Kir6.1** **Kir6.2**	*KCNJ8* *KCNJ11*	Mitochondria? Pancreatic β-cell/neuronal
SUR2A	*ABCC9*	**Kir6.1** **Kir6.2**		Cardiac muscle Cardiac/skeletal muscle
SUR2B	*ABCC9*	**Kir6.1** **Kir6.2**		Vascular smooth muscle Vascular smooth muscle

Table 1-2 Overview of K_{ATP} channel isoforms and theirs subtypes with corresponding gene and tissue localized subtypes.

This table illustrates that the K_{ATP} channels are widely expressed and play very important role in many cells/tissues. Based on cloning electrophysiological and pharmacological study, the K_{ATP} channels isoforms and subtypes were identified and classified as represented in the table. It is worth noting that the non-selectivity of some agents by binding to the sulphonylurea receptor can inhibit the β-cell, cardiac and smooth muscle types of K_{ATP} channel.

1.2.2 Sulphonylurea Receptor

Sulphonylurea receptor polypeptides are members of the ATP-binding cassette protein of the ABCC/MRP family. Human ABC protein genes are classified into seven subfamilies: ABCA to ABCG according to their gene structure, sequence homology and phylogenetic relations (Dean et al. 2001). There are two genes encoding three isoforms of SUR; SUR1, which is encoded by the ABCC8 gene and SUR2 which is encoded by the ABCC9 gene. The latter can be transcribed into two different isoforms, SUR2A and SUR2B (Aguilar-Bryan et al. 1998). These two SUR2 variants differ solely in the carboxyl-terminal due to alternative 3´-exon usage (Gabrielsson et al. 2004). In general, all ABC proteins contain a minimum of four structural domains: two transmembrane domains (TMDs) containing 6 to 8 transmembrane helices each and two cytosolic nucleotide binding domains (NBDs) which are involved in nucleotide binding and hydrolysis (Higgins 2001). SUR2 subunits consist of 17 transmembrane polypeptide segments clustered into three transmembrane domains (TMD), named TMD0, TMD1 and TMD2 (figure 1-3). TMD0 consists of the first five transmembrane segments and TMD1 and TMD2 consist of six segments each. There are two cytoplasmic nucleotide binding domains in each subunit. The first nucleotide binding domain, NBD1 is located between transmembrane segment 11 and 12 and the second, NBD2 is located beyond the last transmembrane segment number 17 and forms part of the C-terminal domain (Aguilar-Bryan et al. 1998; Walker et al. 1982).

SUR is a member of the ATP-binding cassette family of proteins and functions as transporters, ion channels and channel regulators in both prokaryotes and eukaryotes (Higgins 2001). Both the sequence and the structure of NBDs are highly conserved across all prokaryotic and eukaryotic ABC proteins. Each contains a conserved

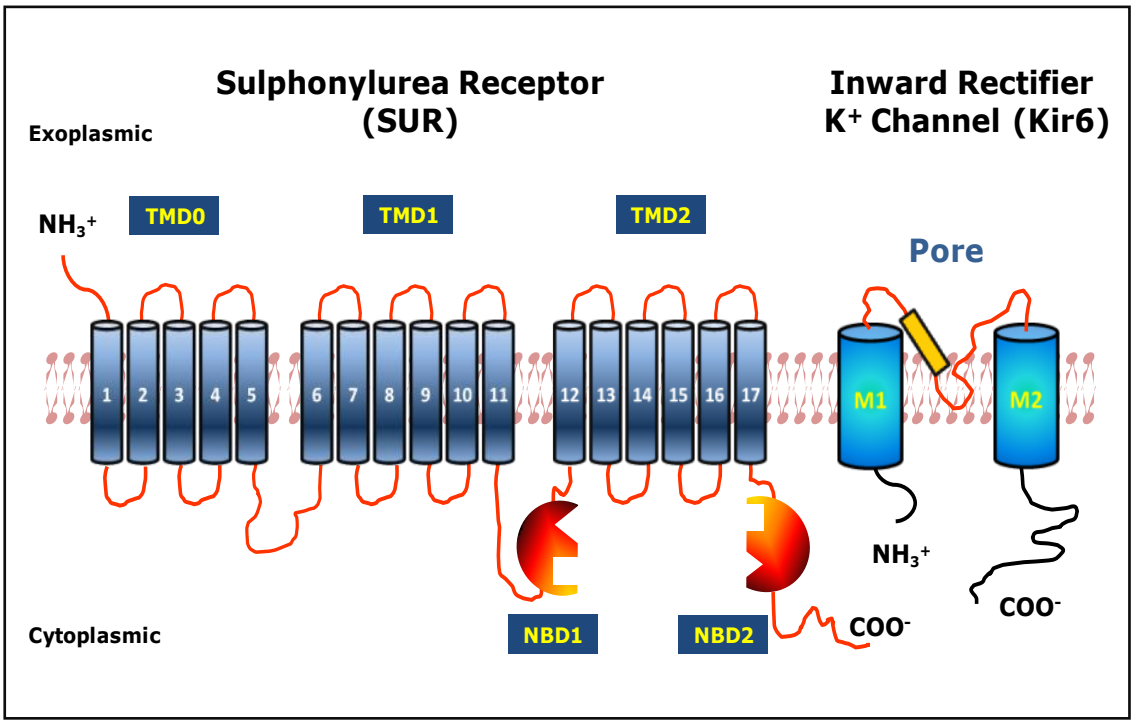

Figure 1-3 Subunit structure of K_{ATP} channels.

Schematic drawing showing the topology of the SUR and Kir6 subunits in K_{ATP} channels. The SUR subunit comprises the three transmembrane domains; TMD0, TMD1 and TMD2, the two nucleotide binding domains; NBD1 and NBD2, the extracellular N- and the intracellular C-termini and the pore-forming Kir subunit. Having in mind that K_{ATP} channels link metabolic state to electrical excitability by sensing ATP/ADP ratio and the cytoplasmic localization of NBD1 and 2 of SUR and N- and C-termini of Kir6, which raises the question of whether the cytoplasmic interactions between these two heterologous subunits of K_{ATP} channel may mediate allosteric information transfer.

Walker A (W_A) motif and a Walker B (W_B). These motifs catalyse ATP hydrolysis and it is believed that these motifs are important for nucleotide regulation of the ABC proteins' functional activity (Mannhold 2004).

1.3 K_{ATP} Channel Function

K_{ATP} channels couple cell metabolism to electrical activity in nerve, muscle and endocrine cells and play an important role in various cellular functions as sensors of intracellular ATP and ADP coupled to electrical function (Inagaki and Seino 1998). Under both physiological and pathological conditions the K_{ATP} channel may have important roles in many tissues (F. M. Ashcroft and Gribble 1998).

The K_{ATP} channel has a key role in the physiology of many cells and defects in the channel itself or in its regulation such as in hyper/hypo-glycemia, ischaemia, hormone secretion and excitability of muscles/neurons which causes human diseases (Seino 2003). Studies on mice have shown that K_{ATP} channels are involved in the protection against neuronal seizures and ischaemic stress in the heart and brain and in the regulation of vascular smooth muscle tone (Seino 2003). Furthermore studies on mice done, amongst others by Miki et al. (Miki et al. 2001a) and Chutkow et al. (Chutkow et al. 2001), have shown that the K_{ATP} channel clearly participates in glucose uptake of the skeletal muscles but the mechanism is still unclear. Other functions have been implicated such as vasodilatation (Quayle et al. 1997), secretion of pituitary hormone (Bernardi et al. 1993), K^+ recycling in renal epithelia (Tsuchiya et al. 1992), and oocyte maturation (Wibrand et al. 1992).

1.3.1 Pancreatic β-Cells

K_{ATP} channels are crucial in the regulation of glucose-induced insulin secretion (Inagaki and Seino 1998). In pancreatic β-cells, an increase in ATP/ADP ratio, which is generated by glucose uptake and metabolism, closes the K_{ATP} channels to elicit membrane depolarisation, calcium influx and a secretion of insulin, the primary hormone of glucose homeostasis.

In the pancreatic β-cell (figure 1-4), K_{ATP} channels are composed of the Kir6.2 pore with the SUR1 regulatory subunit and regulate insulin release. Insulin release is generated by the opening of voltage-gated Ca^{2+} channels and Ca^{2+} influx. In hyperglycaemia, an increased transport of glucose occurs into the β-cells which results in an elevated intracellular ATP, promoting closure of the K_{ATP} channels and membrane depolarization (Sattiraju et al. 2008). This K_{ATP} channel mechanism can be mimicked by sulphonylurea drugs, for example, glibenclamide, which inhibit the K_{ATP} channel directly in the pancreatic β-cells (figure 1-4). The inhibition causes cell membrane depolarization, opening of voltage-dependent calcium channels, thus triggering an increase in intracellular calcium into the β-cell which stimulates insulin release (Hussain and Cosgrove 2005).

K_{ATP} channel activating gene mutations are responsible for neonatal diabetes (F. M. Ashcroft 2010; Sattiraju et al. 2008). Gene defects due to loss of function have been associated with hyperinsulinemic hypoglycemia of infancy (HHI) (Sattiraju et al. 2008). This condition, which for the most part is sporadic, is characterized by hypoglycemia and associated with severe outcomes, such as seizures and mental retardation (Hussain and Cosgrove 2005). Autosomal recessive or dominant forms of HHI can be manifested by polymorphisms or mutations in either ABCC8 or KCNJ11(Dekelbab and Sperling 2006).

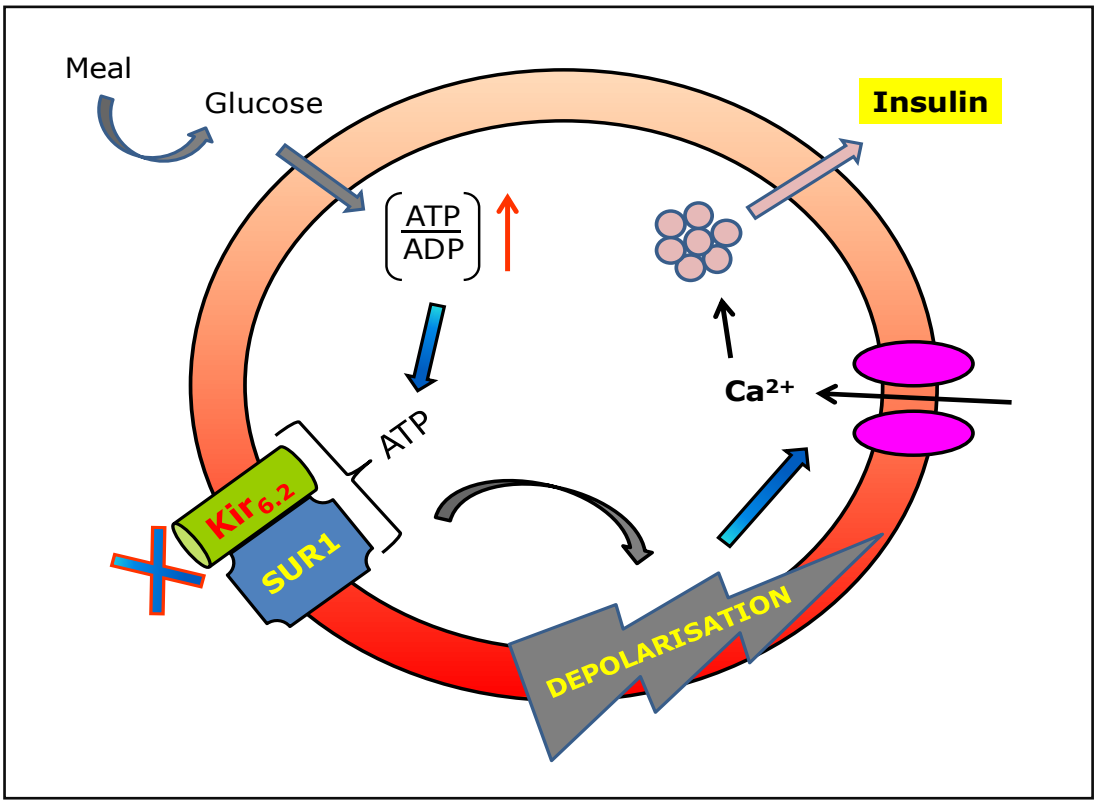

Figure 1-4 The K_{ATP} channel regulation of insulin release in pancreatic ß-cells.

When the glucose level increases it causes a rise in the ATP/ADP ratio and in its turn ATP binds to the K_{ATP} channel, which closes the channel. Depolarization of the membrane then opens the calcium channel which causes the insulin to release. This drawing illustrates the mimicked pathway which sulphonylurea drugs by acting to inhibit the K_{ATP} channels can increase insulin secretion, which is used in the treatment of type 2 diabetes.

1.3.2 Cardiac Cells

Potassium channels are critical to cardiac excitability because they play fundamental roles in setting the resting membrane potential, RMP, and in repolarisation of the action potential (AP). Under normal conditions, the cardiac sarcolemmal K_{ATP} channel is predominately closed (Deutsch et al. 1991). The channel activates during various forms of metabolic stress, including ischaemia, hypoxia, hyperglycemia, hypoglycaemia and inhibition of glycolysis and/or oxidative phosphorylation (Kwak et al. 1996; Yokoshiki et al. 1998). A shortening of the cardiac action potential results when intracellular ATP levels decrease (Nichols and Lederer 1991). In conditions such as hypoxia and ischaemia, the calcium entry to the myocyte is also reduced resulting in a reduction of mechanical contraction, amelioration of Ca^{2+} overload and energy sparing (Findlay 1994).

1.3.3 Vascular Smooth Muscle

Potassium channels regulate the membrane potential of smooth muscle, controlling the calcium entry through voltage-dependent calcium channels, and in so doing, the contractility through changes in intracellular calcium (Quayle et al. 1997).
In the vascular smooth muscle cells, K_{ATP} channels are thought to play important roles such as mediating the response of vascular smooth muscle to a variety of pharmacological and endogenous vasodilators and also to changes in metabolic activity that can directly influence blood flow in various tissues (Brayden 2002). Most of the K_{ATP} channels in the vascular muscle cells are rather insensitive to ATP and they are

activated by nucleoside diphosphates and inhibited by glibenclamide (M. Yamada et al. 1997).

1.3.4 Other Tissues

In addition to above, K_{ATP} channels have been identified in various other tissues including neurons, brain and skeletal muscle (Seino 2003). K_{ATP} channels have been shown to be expressed in several regions of the brain including the substantia nigra (Roper and Ashcroft 1995; Stanford and Lacey 1996) and in the hypothalamus (Ashford et al. 1990). Evidence has shown that the K_{ATP} channels are also expressed in the substantia nigra area of the brain, which consists of a layer of large pigmented nerve cells in the midbrain (Chien et al. 2004). It has been proposed that K_{ATP} channels may play a role in the suppression of seizures in ATP-depleted conditions (K. Yamada and Inagaki 2002).

In the hypothalamus, it is suggested that the K_{ATP} channel plays an interactive role with the pancreatic β-cell (Miki et al. 2001b). It is believed that the insulin secretion system and the glucagon secretion system are integrated in the maintenance of glucose homeostasis through a common K_{ATP} channel. Miki et al. (2001b) propose that when the blood glucose levels rise, K_{ATP} channels in pancreatic β-cells are inhibited resulting in insulin release and lowering of blood glucose. As the blood glucose level falls, the K_{ATP} channels in the hypothalamus stimulates glucagon release by the pancreatic α-cells resulting in a rise of blood glucose levels producing a counter balancing mechanism. With this the blood glucose levels can be held at a stable level.

In the skeletal muscles, K_{ATP} channels have been identified by electrophysiological methods (Davies 1990). The channels are mainly located in the plasma membrane, appear in all fibre types and are active in the resting human muscle. K_{ATP} channels located in the sarcolemma contribute significantly to the membrane permeability in resting human muscle and are important for the interstitial K^+ balance (Nielsen et al. 2003).

1.4 Ischaemic Preconditioning

Ischaemic preconditioning (IPC) is able to provide a powerful protection to ischaemic myocardium. The heart has natural abilities to adapt, which generates significant protection against lethal ischaemia. When exposed to a subsequent prolonged and potentially lethal ischaemia and reperfusion stress, the preconditioned heart has been shown to have reduced infarct size, less ultrastructural damage, higher ATP reserves, better recovery of mechanical function and fewer episodes of reperfusion arrhythmia (Carroll and Yellon 1999).

IPC consists of a series of brief intermittent periods of ischaemia, which protect the myocardium against a more prolonged ischaemic insult resulting in a distinct reduction of infarct size (Murry et al. 1986). IPC is divided into two phases; an early preconditioning and a second window of protection (SWOP) (Marber et al. 1993). The early phase protection, which occurs in the presence of a protein synthesis inhibitor (Thornton et al. 1990), lasts up to 3 hrs (Li et al. 1992; Zhuo et al. 2005). After 12 to 24 hrs a return of myocardial protection is observed (Kuzuya et al. 1993; Marber et al. 1993); a second phase, which lasts about 72 hrs though not as powerful as the previous

(Marber et al. 1993). It is thought that these two phases have different underlying mechanisms, however, the two appear to share the same triggers, that are mediated via G-protein receptors coupled to PKC (Downey and Cohen 1995).

It is thought that K_{ATP} channels are involved in both phases of IPC since it is proposed that the opening of the sarcolemma (sarcK_{ATP}) (Noma 1983) and mitochondrial K_{ATP} channel (mitoK_{ATP}) (Garlid et al. 1997) are involved in early preconditioning and the opening of myocardial K_{ATP} channel in the SWOP (Bernardo et al. 1999).

Noma presented a hypothesis that the opening of sarcK_{ATP} channels, which has been induced by hypoxia, ischaemia or pharmacological K_{ATP} openers, could enhance shortening of the cardiac action potential duration by accelerating repolarization (Noma 1983). By shortening the action potential, Ca^{2+} would be inhibited from entering into the cell and by so doing would prevent Ca^{2+} overload, resulting in an increase in viability of the cell. Studies suggest that blockade of K_{ATP} channels using blockers such as glibenclamide, abolishes ischaemic preconditioning in rats, rabbits, dogs, pigs and man (Speechly-Dick et al. 1995). The protection which is induced by the PKC activator dioctanoylglycerol is abolished by glibenclamide in human muscle (Speechly-Dick et al. 1995). Various findings have shown sarcK_{ATP} channel have a major involvement in IPC (W. C. Cole et al. 1991; Yao and Gross 1994a) and recent results show that sarcK_{ATP} channels may trigger IPC (Patel et al. 2002).

Data from various studies suggest that the sarcK_{ATP} channel may not be the sole mediator to be able to protect effects provided by K_{ATP} channels and IPC (Grover et al. 1995; Yao and Gross 1994b). The first evidence that the mitoK_{ATP} channel has a role in cardioprotection was made by Garlid et al. (Garlid et al. 1997). They found that diazoxide opened the mitoK_{ATP} channel with a concentration of 0.8 µmol/l of diazoxide

in comparison to 800 µmol/l needed to open the sarcK_{ATP} channel. However, it is still unclear, which role the mitoK_{ATP} channel has. Is it a trigger or a distal effector or maybe both, which some studies have shown (Gross and Fryer 1999; Schulz et al. 2001).

Studies have been done to show the involvement of both sarcK_{ATP} and mitoK_{ATP}. It has been indicated that during ischaemia the mitoK_{ATP} mediates the infarct size-reducing effect of adenosine-enhanced preconditioning, while sarcK_{ATP} channels modulate functional recovery (Toyoda et al. 2000).

Due to these findings it is believed that the K_{ATP} channel is an attractive candidate as the target or end-effector for both forms of preconditioning (Carroll and Yellon 1999).

1.5 K_{ATP} Channel Structure

K_{ATP} channels are members of the family of membrane spanning inward rectifier channel proteins. K_{ATP} channel complexes comprise a hetero-octamer (figure 1-5) formed by an inward-rectifying K^+ channel subunit (Kir6.x) and a sulphonylurea receptor (SURx) in a 4:4 stoichiometry (Enkvetchakul et al. 2001).

Subunit stoichiometry studies on K_{ATP} channels performed by Clement et al. measured that the molecular mass of the native K_{ATP} channel is 950 kDa. Since an octamer has a calculated protein mass of 4 x (177,000 + 43,000) = 880,000 Daltons plus mass due to glycosylation (Clement et al. 1997) a hetero-octameric $Kir6_4/SUR_4$ was proposed. In the next step, Clement et al. engineered fusion constructs of SUR1 with Kir6.2 to investigate the functional stoichiometry of Kir6.2 and SUR subunits whether a 1:1

SUR1:Kir6.2 stoichiometry was functional. Results showed that a 1:1 SUR1:Kir6.2 stoichiometry was sufficient to assemble functional K_{ATP} channels with the estimated molecular mass, which was also confirmed by others (Inagaki et al. 1997; S. Shyng and Nichols 1997). They continued by engineering a triple fusion, SUR1~$(Kir6.2)_2$. Although this construct did not generate functional K_{ATP} channels alone, the triple fusion was able to be "rescued" by co-expression with monomeric SUR1 resulting in functional K_{ATP} channels. This finding was supportive of octameric architecture of K_{ATP} channels. To confirm this finding, Clement et al. engineered another triple fusion construct with the Kir6.2 N160D subunit which showed strong rectification (Clement et al. 1997). A mixture of the two triple fusions; the weak inward rectifier, SUR1~ $(Kir6.2)_2$ with the strong inward rectifier Kir6.2 N160D, were rescued by SUR1. This channel had intermediate rectification properties indicating that both triple fusions, wild-type and N160D, must be present in the formation of the pore. As evidenced largely by Clement et al., a functional K_{ATP} channel is an octameric complex composed of four SUR subunits and four Kir6 subunit, i.e. a 4:4 stoichiometry (Clement et al. 1997).

It has been shown that there are various combinations of the Kir6 and SUR subunits isoforms, which reconstitute the functionally diverse K_{ATP} channel currents in different tissues (Aguilar-Bryan and Bryan 1999; Billman 2008). Binding of SUR to Kir subunits serves two purposes; first, to allow the translocation of the channel to the plasma membrane and, second to contribute to the regulation of the channel by interaction between two subunits (Burke et al. 2008).

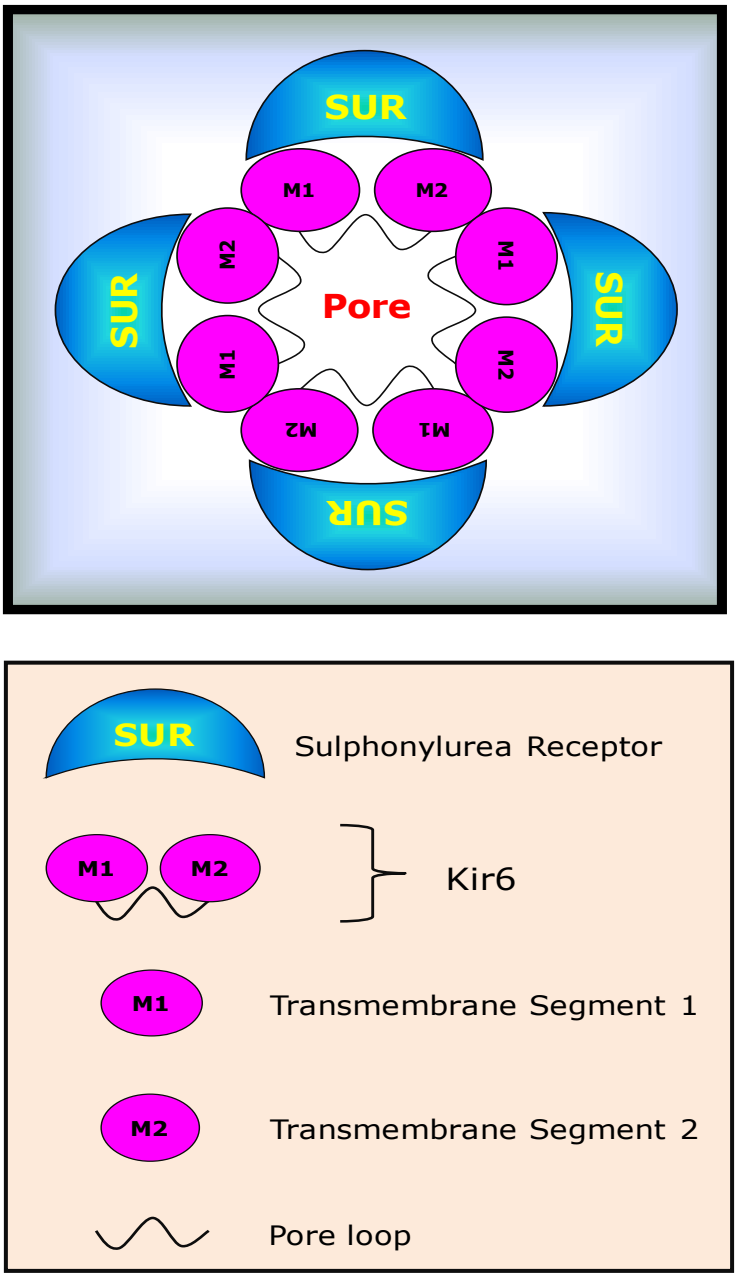

Figure 1-5 Diagrammatic illustration of a functional hetero-octameric complex ($Kir6_4/SUR_4$) structure of K_{ATP} channel.

Representation of the assembly of the two heterologous subunits to form functional K_{ATP} channels. These channels are hetero-octameric in structure comprising, in cardiac ventricular tissue, $Kir6.2_4$ / $SUR2A_4$. Viewed from the extracellular side of the plasma membrane.

1.6 Regulation of ATP-sensitive Potassium Channels by Intracellular ATP

A variety of intracellular factors, such as adenosine-5'-triphosphate (ATP), protein kinases e.g. protein kinase A (PKA) and protein kinase C (PKC) and nucleotide diphosphates, regulate K_{ATP} channel gating. This section will focus on intracellular ATP (ATP_i) regulation of K_{ATP} channels. K_{ATP} channels are potassium channels, which are sensitive to ATP_i or, more specifically, sensitive to intracellular ATP/ADP ratio (Ashcroft and Gribble 1998). This unique property of K_{ATP} channels links metabolic state to electrical excitability. Still today, the detailed mechanisms of these activation and inhibition pathways remain uncertain (Dupuis et al. 2008). When it was realized that K_{ATP} channels are encoded by an ABC protein (Misler et al. 1989), SUR1 or SUR2, and inward rectifier channel subunits (Kir6.1 or Kir6.2), a natural presumption was made that the inhibitory ATP binding should occur at the nucleotide binding domains (NBDs) of the SUR subunit (Koster et al. 1999).

Prior to discussing any details about ATP regulation of K_{ATP} channels, there is a need to understand the role of these channels. The role of K_{ATP} channels is to regulate cellular electrical excitability in response to the metabolic energy status of the cell. A prime function, therefore, is to sense the energy level of cells and this is best represented by the ratio ATP/ADP (F. M. Ashcroft 2005). In simple terms, Kir6 senses ATP concentration and SUR senses ADP concentrations. Neither alone would measure the energy status sufficiently, but both together provide more sensitive synergistic sensitivity, i.e., Kir6 is blocked by direct ATP binding and activated allosterically by ADP binding to SUR (Nichols et al. 1996), Tucker et al. 1997, Drain et al. 1998 and

Gribble et al. 1997). This means that SUR needs to be attached physically to Kir6 and to be coupled allosterically to communicate appropriately.

1.6.1 ATP-binding Site of the Pore-forming Kir6.2 Subunit

Understanding of nucleotide regulation of K_{ATP} channels is very important due to K_{ATP} channels coupling of the cell metabolism to electrical activity, which is of physiological and pathophysiological relevance (S. J. Ashcroft and Ashcroft 1990). By co-expressing the cloned, Kir6.2/SUR1 channels in *Xenopus Oocytes* and using inside-out patch (explained in the next Chapter), Drain et al. identified the sequence 333 FGNTIK 338 in the C-terminal of Kir6.2 to be part of the ATP binding site (Drain et al. 1998). Mutagenesis study and inside-out patches from *Xenopus oocytes* expressing wild type or Kir6.2 ΔC26 revealed the positive charged lysine at position 185 (K185) is required for high affinity ATP binding to Kir6.2 (Reimann et al. 1999). Based on X-ray crystal structures of KirBac1.1 (Kuo et al. 2003) and the intracellular domains of Kir3.1 (Nishida and MacKinnon 2002) a homological model of Kir6.2 was constructed and the ATP-binding site was identified (Antcliff et al. 2005). After that, with help of ligand docking, the position of the ATP-binding site was predicted. From functional studies, four ATP binding pockets have been identified (Markworth et al. 2000). These four are located about 17 °A below the plane of the membrane in the upper part of the cytosolic domain. The N- and C- domains of Kir6.2 are both intracellular and there is evidence from protein-protein interaction studies, which shows that there are physical interactions between the two domains (Jones et al. 2001; Tucker and Ashcroft 1999). It is believed that each N domain contributes to two

ATP-binding sites, one in the same subunit and the other in the adjacent subunit (Antcliff et al. 2005). Experiments done with fluorescence resonance energy transfer (FRET) showed that ATP binding influences the physical relationship of the N and C domains of adjacent subunits (Tsuboi et al. 2004). More specifically, in the N domain, residues 30-46 interact with residues in three separated regions of the C domain or an adjacent subunit. Within the same subunit, the main binding pocket is located at the interface between the N and C domains.

Residues 54-66 of Kir6.2, the slide helix, which links the transmembrane (TM) domains and cytosolic domains, might be involved in channel gating (Kuo et al. 2003). Investigations have only been carried out on R54 at the end of the N-terminal of the slide helix (Cukras et al. 2002; (Schulze et al. 2003) and by mutagenesis of the same region in Kir6.2 ΔC (Antcliff et al. 2005). In the latter, V59 was chosen to be mutated to glycine (V59G). The reason for this choice was that this mutation in Kir6.2 leads to reduced ATP sensitivity of the K_{ATP} channels producing neonatal diabetes with development delay, muscle weakness and epilepsy (Gloyn et al. 2004). Kir6.2 ΔC V59G mutations revealed a distinct increase in the intrinsic P_o, accompanied by a 10-fold reduction in ATP-sensitivity.

In humans, existing mutations of phenylalanine at position 35 (F35) to Valine (V) or Alanine (A) in the N-terminal of Kir6.2 and of the negatively charged glutamic acid at position 322 (E322) to positively charged lysine (K) in the C-terminal can cause permanent neonatal diabetes mellitus (PNDM). These most likely disrupt the adjacent E321-R32 ion pair (Sagen et al. 2004; Vaxillaire et al. 2004) and this can explain that the N and C domains of adjacent subunits contribute to the ATP binding site (Antcliff et al. 2005).

This finding is consistent with other studies; mutations in these regions impair channel inhibition by ATP (Cukras et al. 2002a; Drain et al. 1998; John et al. 2003; Proks et al. 1999; Reimann et al. 1999; Ribalet et al. 2003; Tucker et al. 1998) and, furthermore, if mutations in the N and C domains affecting ATP sensitivity are combined then the ATP sensitivity is further reduced (Proks et al. 1999). When positive charged arginine at position 201 (R201) was mutated, ATP sensitivity of Kir6.2 ΔC26 was distinctly reduced (Antcliff et al. 2005) and the results were similar for Kir6.2/SUR1 channels (S. L. Shyng et al. 2000); John et al. 2003; Ribalet et al. 2003). Also, when R201 was mutated to a negatively charged or uncharged residue, ATP inhibition was weakened and in Kir6.2 R201E/SUR1 inhibition of the channel did not occur even at millimolar concentration of ATP (Antcliff et al. 2005).

There is evidence suggesting that there is an electrostatic interaction between the positive charged lysine at position 185 (K185) and the β-phosphate ATP (Antcliff et al. 2005). When K185 is mutated to a negative charge (K185E), ATP inhibition was strongly impaired, however when K185 was mutated to arginine it only had a small effect in both Kir6.2 ΔC26 and Kir6.2/SUR1 (Tucker et al. 1997, 1998; Reimann et al. 1999; John et al. 2003). ATP sensitivity of Kir6.2 ΔC26 is also reduced when residues S184 and H186, which flank K185, were mutated. ATP sensitivity of the Kir6.2/SUR1 channel was also impaired when S184 is mutated (Tucker et al. 1998).

Located on the opposite side of the binding pocket to K185 is R50 of an adjacent Kir6.2 subunit; the N domain of the adjacent subunit loops across the C-terminal part of the binding pocket, meaning here that the side chain of R50 is located to one side of the entrance to the pocket, while K185 is located at the opposite side (Antcliff et al. 2005). In Kir6.2/SUR1 channels, ATP sensitivity was reduced when a cysteine was substituted at R50 (Trapp et al. 2003). It is believed that R50 is located close to the

γ-phosphate of ATP and it is also believed that R50 only disturbs the protein structure, allowing ATP to access its binding site (Antcliff et al. 2005).

Another residue G334, is located far from K185 in the primary sequence, however, in the three-dimensional model structure G334, is located close to both the β-phosphate of ATP and to K185 (Antcliff et sl. 2005). This result clarified the previous confusing finding that mutation of G334 to aspartate decreased ATP sensitivity distinctly (Drain et al. 1998).

Other studies have shown that a distinctive functional domain of the distal C-terminal domains of Kir 6.2 subunit is crucial for ATP inhibition (Drain et al. 1998). In this study K_{ATP} channels were expressed in *Xenopus* oocytes and by making chimaeras of Kir6.2 and Kir1.1, point mutagenesis and electrophysiological (patch-clamp) recording, the 334 GNTI 337 region of Kir6.2 was identified as part of the inhibitory ATP binding site (Drain et al. 1998).

The most important question, which needs to be answered, is how binding of ATP closes the pore. In ligand-gated channels, binding of ATP occurs at the interface between two subunits (Brejc et al. 2001). In addition, the structural models suggest that each monomer is connected to two other subunits and not just one (Antcliff et al. 2005). It is believed that ATP binding to one subunit influences the relative conformations of the two adjacent subunits and it may give us an understanding why the binding of a single ATP molecule is sufficient to close the pore (Antcliff et al. 2005). It is also believed that since the binding is located at the interface between subunits, it may be possible that the conformation of each monomer will not change dramatically upon ATP binding and, instead, nucleotide binding might mainly influence the relationship between the monomers (Antcliff et al. 2005).

The putative location of the ATP-binding site was identified with the help of a molecular model of the Kir6.2 tetramer. It is probable that Kir channels share a common structural basis for subunit assembly and the mechanism by which ligand binding is linked to opening and closing of the pore might also be similar. It is also suggested by embracing the outer part of Kir6.2, SUR1 may enhance ATP sensitivity. From the results of Antcliff's study, it is believed that gating of Kir6.2 by ATP may possibly involve changes in inter-subunit interactions and a hypothesis that flexible loops in the C-domain (204-209 and 289-299) help in translating conformational changes induced by ATP binding into movement of the slide helix which results in channel closure has been proposed (Antcliff et al. 2005).

As discussed above (section 1.5), functional K_{ATP} channels comprise hetero-octamers of four Kir6 and four accessory SUR subunits (Clement et al. 1997). This means there are four ATP-binding sites on Kir6.2 subunits and four binding events are possible (Craig et al. 2008). A recent study by Craig et al. in 2008 showed that a decrease in the burst and open time duration of the K_{ATP} channel occurred in the presence of ATP when it saturates at high ATP concentration (Craig et al. 2008) indicating that ATP must bind to the open as well as the closed state. An additional result from their study was that ATP binds to a single ATP binding site when the channel is open, which means that in an open state the channel has ATP bound to Kir6.2 most of the time (Craig et al. 2008). This study proposes that the four cytosolic domains of the Kir6.2 do not function independently but rather function together as a single gating unit. In other terms, ATP binds to each subunit independently and together contributes additively to the free energy of the open or closed states (Craig et al. 2008).

The ATP sensitivity of Kir6.2 can be enhanced by SUR to about 10-fold (Tucker et al. 1997). It is believed that the exposed position of the ATP-binding site in Kir6.2 may be achieved by SUR embracing the outer part of the binding site, perhaps by contributing additional residues that stabilize ATP binding, or by allosterically altering the structure of the binding site (Antcliff et al. 2005). ATP binding to the pore forming Kir 6.2 subunit, in the presence or absence of Mg^{2+} closes the channel and binding of MgATP or MgADP to NBDs of the regulatory SUR subunit increases the channel activity (Tammaro and Ashcroft 2007). The effects of ATP binding to the nucleotide binding domains, NBD1 and NBD2 of SUR subunits will be discussed in the next section.

1.6.2 The Effects of ATP Binding to the Nucleotide Binding Domains (NBDs) of SUR Subunits

As discussed (section 1.3, table 1-2), K_{ATP} channels in different tissues consist of different subtypes of SUR subunits and they differ in their responses to cellular metabolic state. The first biochemical study to analyse and compare the nucleotide-binding properties of NBDs of three SUR subtypes; SUR1, SUR2A and SUR2B was performed and the results showed that their different properties might explain partially the differential regulation of K_{ATP} channel subtypes (table 1-3) (Matsuo et al. 2000). In their study, a condition of radioligand binding and assembly was used to estimate the binding effect for the ATP and ADP to SUR subunit in native membranes.

The properties of nucleotide binding varied among SUR subtypes, the Mg^{2+} dependence of nucleotide binding of NBD2 of SUR1 was high, while that of SUR2A and SUR2B were low. The affinities of NBD1 of SUR1 for ADP, and especially for

ATP, were considerably higher than those of SUR2A and SUR2B. Notably, the affinities of NBD2 of SUR2B for ATP and ADP were considerably higher than those of SUR2A (Matsuo et al. 2000).

The differences between the SUR subtypes are that SUR2A shares 68% amino acid identity with SUR1. SUR2A and SUR2B share the majority of primary sequence, with the exception of the splicing variant of SUR2A in its C-terminal 42 amino acids (Inagaki et al. 1996); Isomoto et al. 1997). Between SUR2B and SUR1, the 42 amino acids in C-terminal of SUR2B are similar to those of SUR1. It has been reported (Babenko et al. 2000) that the last 42 amino acids of SUR are a major determent of ATP sensitivity in the Kir6 subunit. The sensitivity of Kir6 pores to inhibition by ATP may also be affected indirectly by the interaction of nucleotides with NBDs in the SUR subunits.

The properties of the two NBDs of SUR1 have been investigated (Matsuo et al. 1999). According to biochemical results, it is believed that NBD1 and NBD2 both work together in nucleotide binding. SUR1 binds 8-azido-ATP strongly at NBD1 and MgADP at NBD2. Mutations of either Walker A or B motifs of NBD1, K719M and D854N inhibit the high-affinity 8-azido-ATP binding of SUR1. However, the equivalent mutations in NBD2 do not affect ATP binding (Ueda et al. 1997). MgADP and MgATP stabilize binding of pre bound 8-azido-ATP to SUR1 and in NBD2, mutations of the Walker A and B motifs inhibit the stabilizing effect of MgADP and MgATP (Ueda et al. 1999). It has not been possible to detect nucleotide binding of NBD2 directly. The reason for this is probably due to the high-affinity ATP binding of NBD1 (Matsuo et al. 1999).

It is worth mentioning that the K_{ATP} channels subtypes have different sensitivities to ATP e.g. vascular smooth muscle K_{ATP} channels (Kir6.1/SUR2B) are stimulated by ADP and ATP and are not inhibited by ATP (M. Yamada et al. 1997).

Among all the SUR subtypes, there are similarities between their nucleotide binding properties. NBD1 is a Mg^{2+}-independent ATP- and ADP-binding site while nucleotide binding at NBD2 is Mg^{2+}-dependent. The 8-azido-ATP binds to NBD1 very firmly and does not dissociate at 0 °C. MgATP or MgADP binding to NBD2 stabilizes 8-azido-ATP binding at NBD1. NBD2 may possibly have ATPase activity, whereas NBD1 has shown no or little ATPase activity (Matsuo et al. 2000). There are also differences between the SUR subtypes such as nucleotide binding to NBD2 of SUR1 is highly Mg^{2+}-dependent, whereas Mg^{2+} dependence of nucleotide binding to NBD2 of SUR2A and SUR2B is much lower (Matsuo et al. 2000). The affinities of NBD1 of SUR1 for ADP, and particularly for ATP, are significantly higher than those of SUR2A and SUR2B (table 1-3). The affinity of NBD1 of SUR2B for ATP is relatively higher than that of SUR2A. Finally, the affinities of NBD2 of SUR2B for ATP and ADP are significantly higher than those of SUR2A. It is suggested that SUR1 has a higher ability to open Kir6.2 subunit channels than SUR2A and that the higher nucleotide binding affinities of SUR1 might explain this (table 1-3) (Matsuo et al. 1999; Matsuo et al. 2000).

A)

Subunit Combination	ATP Binding Affinity	Function
SUR1 + Kir6.2	High	Regulating insulin release
SUR2A + Kir6.2	Low	Regulating action potential duration
SUR2B + Kir6.1/Kir6.2	Intermediate to high	Regulating action potential duration and vasodilation

B)

SUR subtype	Nucleotide binding domain	ATP binding affinity (K_i , µM)	ADP binding affinity (K_i , µM)
SUR1	NBD1	4.4 ± 3.7	26 ± 8.6
	NBD2	60 ± 26	100 ± 26
SUR2A	NBD1	110 ± 41	86 ± 23
	NBD2	120 ± 39	170 ± 70
SUR2B	NBD1	51 ± 13	66 ± 7.5
	NBD2	38 ± 26	67 ± 40

Table 1-3 ATP- and ADP-dependence of K_{ATP} channel activity.

A) The table demonstrates the affinity of ATP binding to the different K_{ATP} channel subtypes. B) The table represents the ATP and ADP binding affinities determined for NBD domains from different SUR isoforms. Substantial evidence suggests that the nucleotide binding properties of the two NBDs of SUR revealed differences among SUR isoforms and K_{ATP} channel subtypes (Burke et al. 2008; Matsuo et al. 2000).

Both pancreatic and cardiac K_{ATP} channels contain Kir6.2 as the potassium channel pore components, however; they differ in their responses to cellular metabolic state. The reason for this is likely due to their different SUR subtypes (Matsuo et al. 2000). It has been shown that co-expression of Kir6.2/SUR1and Kir6.2/SUR2A reconstitutes pancreatic β-cell and cardiac muscle K_{ATP} channels type properties, respectively (Inagaki et al. 1995). These channel subtypes have differences in physiological functions, with different sensitivity to ATP (table 1-3), and have different responses to sulphonylurea drugs or potassium channel openers. Pancreatic β-cell K_{ATP} channels stay open under normal conditions to maintain membrane potential. Insulin secretion is triggered when the intracellular concentration of ATP is increased resulting from an increase of blood sugar concentration and the closure of the channel (Ashcroft and Gribble 1998; (Nichols et al. 1996). Under normal conditions, cardiac muscle K_{ATP} channels remain closed. When the intracellular concentration of ATP decreases under ischaemic stress, the channel opens to shorten action potential duration and protect the myocardium from lethal injury (Yokoshiki et al. 1998; Seino 1999).

A model of nucleotide stimulation of K_{ATP} channels through the SUR1 subunit was purposed, in which channel opening was induced by SUR1 binding ATP in NBD1 and ADP in NBD2 (Ueda et al. 1999). A working model of the function of the K_{ATP} channel in pancreatic β-cells was made as follows. When intracellular ADP concentration is high enough, SUR1 binds ATP in NBD1 and ADP in NBD2, cooperatively stimulating Kir6.2 to open the potassium channel. After a food intake, the plasma glucose concentration increases. This increase raises the cellular ATP concentration and along with a concomitant decrease in the cellular ADP concentration. This decrease in ADP concentration causes dissociation of ADP from NBD2 of SUR1. It is believed that ATP may bind to NBD2 after ADP dissociation, as

a result of the high cellular ATP concentration. However, SUR1 binding ATP at NBD2 cannot stimulate the channel. ATP, which has bound to NBD2, would then be hydrolyzed to ADP, and ADP would readily dissociate from NBD2. As a result, SUR1 would not stay long in the active state, when the cellular ADP concentration is low. ATP binds directly to Kir6.2 (Tanabe et al. 1999; Tanabe et al. 2000) and this binding is involved in stabilization of the long closed state of K_{ATP} channel (Tucker et al. 1998). With an increase in the cellular ATP concentration, Kir6.2 would stay longer in ATP-bound form. Therefore, it is believed that the activity of pancreatic β-cell K_{ATP} channels is determined by the balance of the action of ADP, stimulating the channel through SUR1, and the action of ATP, which stabilizes the long closed state by binding to Kir6.2 (Ueda et al. 1999a; Matsuo et al. 2000).

Each NBD contains a highly conserved Walker A (W_A) and Walker B (W_B) motif, and an intervening linker motif (LSGGQ), which is unique to ABC proteins. This is known as the ABC signature sequence. It is known that the W_A and W_B motifs are involved in nucleotide binding and hydrolysis, however, the function of the linker motif is not as clear (Matsuo et al. 2002). Since the linker motif is conserved throughout all ABC proteins, it is believed that it plays a critical role in their function.

Mutations within the Walker A motif in either of the NBDs of SUR1 eliminate MgADP-induced channel stimulation (Gribble et al. 1997). This suggests that both NBDs are essential for channel stimulation. By mutating the conserved serine to arginine in the linker of NBD1 (S1R) or NBD2 (S2R), it did not alter the ability of ATP or ADP (100 mM) to displace 8-azido-[^{32}P]ATP binding to SUR1, or abolish ATP hydrolysis at NBD2 (Matsuo et al. 2002). Kir6.2 was co-expressed with wild type or mutant SUR in Xenopus oocytes and then the resulting currents recorded from in inside-out macropatches (Matsuo et al. 2002). The S1R mutation in SUR1, SUR2A or

SUR2B decreased K_{ATP} current activation by 100 mM MgADP. While the S2R mutation in SUR1 or SUR2B (but not SUR2A) eliminated MgADP activation completely. The linker mutations also reduced (S1R) or eliminated (S2R) MgATP-dependent activation of Kir6.2 R50G co-expressed with SUR1 or SUR2B. With these results, it is suggested that the linkers are unnecessary for nucleotide binding, however might be involved in transducing nucleotide binding into channel activation (Matsuo et al. 2002).

Two additional residues were mutated, since these residues have been shown to interact with the ATP molecule in other ABC transporters: a highly conserved glutamine residue, which is located between the W_A and linker motifs, and a histidine residue that is located downstream of the W_B motif (Matsuo et al. 2002). When Q774A and H888A, which are located in NBD1 of SUR1, were mutated, they resulted in non-functional channels (Matsuo et al. 2002). The equivalent mutations of Q1426A and H1537A in NBD2 did not affect functional expression, although, both the Q1426A and H1537A mutations lessened the ability of 100 mM MgADP to stimulate channel activity. This resulted in a 50 ± 5.2% block of Kir6.2/SUR1 Q1426A currents and a 30 ± 2.6% block of Kir6.2/SUR1 H1537A currents. It is believed that these residues are possibly involved in nucleotide binding and/or transduction (Matsuo et al. 2002).

MgADP activation of Kir6.2/SUR1 and Kir6.2/SUR2B channels, but not that of Kir6.2/SUR2A channels was abolished when the invariant serine in the linker of NBD2 was mutated. It appears that this is a result principally from impaired transduction, since the ability of SUR1 to bind MgADP (at 100 µM) was not decreased. Other mutations (G1484D, G1484R and Q1485H) within the NBD2 linker of SUR1 are also believed to prevent MgADP activation of the K_{ATP} channel (Shyng et al., 1997). As shown for MgADP, binding of MgATP (at 100 µM) was unchanged by the S2R

mutation, still this nucleotide failed to activate Kir6.2 R50G/SUR1 S2R or Kir6.2 R50G/SUR2B S2R channels. It is believed that, this effect might arise from either defective MgATP hydrolysis and/or impaired transduction.

ATP has two effects on K_{ATP} channels, the first, an inhibition of the channel activity and the second, the maintenance of the channel in an activated state (Inagaki and Seino 1998). To maintain the channel in an operative state, hydrolysis of ATP or phosphorylation of the K_{ATP} channel is required (Nichols and Lederer 1991; (Furukawa et al. 1994). At the same time, the hydrolysis of ATP and phosphorylation of the K_{ATP} channel is unnecessary for the inhibition by the ATP, since nonhydrolyzable analogues of ATP, for example, AMP-PNP, AMP PCP and ATP in the absence of Mg^{2+} can inhibit the channel (Inagaki and Seino 1998; Nichols and Lederer 1991).

The gradual inactivation of the K_{ATP} channel is one important property, which follows patch removal in an ATP-free medium, and this process is called "channel rundown" (Findlay 1987; Trube and Hescheler 1984). MgATP can prevent a rundown of the K_{ATP} channel and also can reactivate channels that have already rundown (Findlay 1987; Ohno-Shosaku et al. 1987).

As mentioned in section 1.1.4, all Kir members are regulated by the membrane phospholipids and predominantly PIP2 (Rohacs et al. 2003). PIP2 binding to the K_{ATP} channels causes stabilizing of the channel in an active conformation and is essential for proper channel function, (Rohacs et al. 2003; S. L. Shyng and Nichols 1998). PIP2 appears to bind to both the N- and C-terminal of the pore forming Kir6.2 subunit of the K_{ATP} channels, such as F55, R54 in the N-terminal and R176, R 177, R 192, R206, R301, R314 in the C-terminal (Cukras et al. 2002b; Fan and Makielski 1999; Lin et al. 2006; Schulze et al. 2003; S. L. Shyng et al. 2000). Since, PIP2 activates the channel

by reducing the modulation of ATP inhibition, mutations at above mentioned residues reduced the PIP2 affinity and consequently caused a low open probability of the K_{ATP} channel (Baukrowitz et al. 1998; Cukras et al. 2002b; Fan and Makielski 1997; Lin et al. 2006; Schulze et al. 2003; S. L. Shyng and Nichols 1998; S. L. Shyng et al. 2000).

Together, at the present, many studies agree that PIP2 antagonizes the inhibitory effect of ATP by reducing the affinity of the binding site in K_{ATP} channels and since Kir6.2 Δ26 lacking SUR1 is still inhibited by ATP and stimulated by PIP2, the pore forming Kir6.2 subunit should be largely responsible for these interactions (Baukrowitz et al. 1998; Enkvetchakul et al. 2000; S. L. Shyng and Nichols 1998; Tucker et al. 1997).

Figure 1-6 shows the PIP2 binding site on an inward rectifier potassium channel (Kir2.2, (Hansen et al. 2012). This figure illustrates an X-ray crystal structure of a Kir2.2 channel in complex with short-chain derivative of PIP2 (Hansen et al. 2012). In their study, they found that PIP2 binds at an interface, which is located between the cytoplasmic domain and the transmembrane domain. The PIP2 binding site consists of conserved non-specific and specific phospholipid-binding regions. The non-specific region is in the transmembrane domain and the specific region is located in the cytoplasmic domain (Hansen et al. 2012).

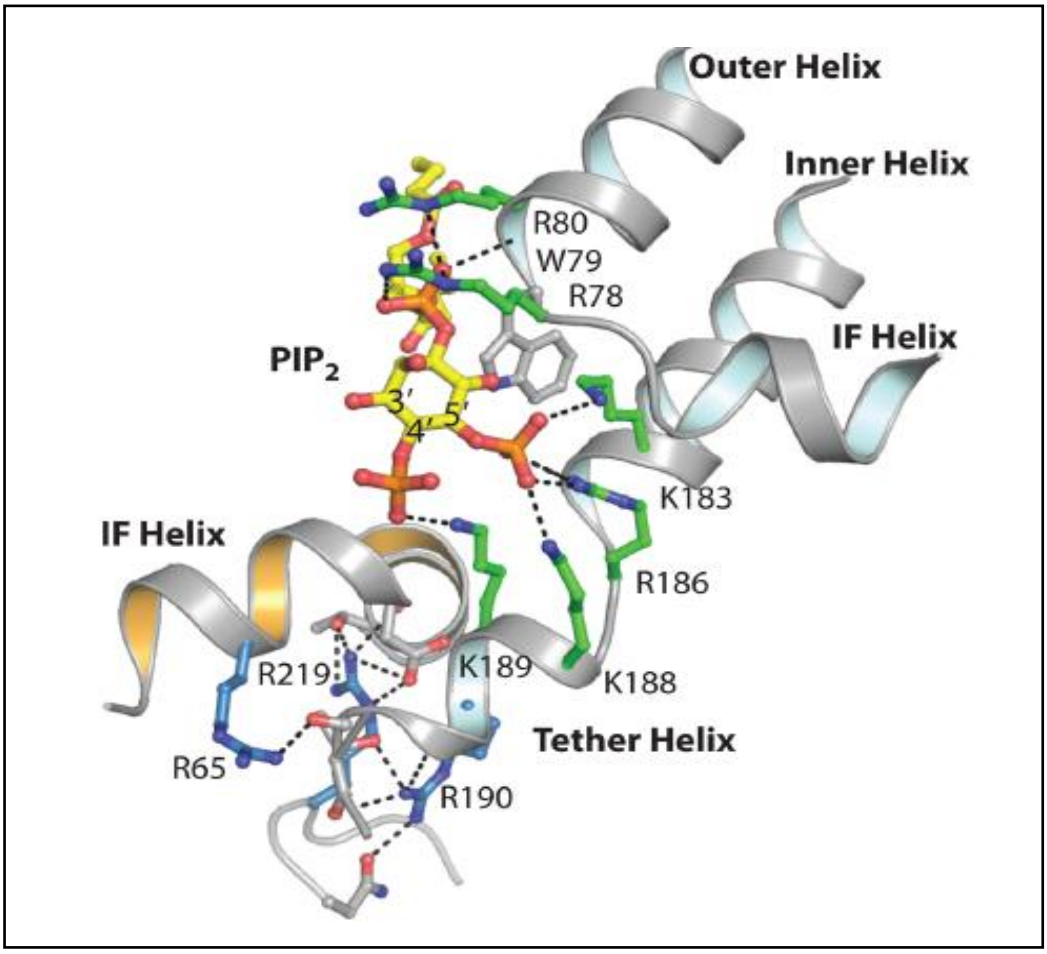

Figure 1-6 X-ray crystal structure of PIP2 binding site on inward rectifier potassium channel Kir2.2 (taken from Hansen et al. 2012).

One PIP2 molecule shown here as sticks and colored according to atom type: carbon, yellow; phosphorous, orange; and oxygen, red. Hydrogen bonding residues (dashed lines) which are interacting with PIP2 are in green colour and the blue colour represents the residues which have a role in stabilizing the PIP2 binding site in the cytoplasmic domain and have no direct contact with PIP2. The outer, inner, tether and interfacial (IF) helices which are shown in this figure as ribbon with colour interior orange or cyan.

1.7 Pharmacology

K_{ATP} channels are the major drug target and have the most therapeutic potential among potassium channels (Ashcroft and Ashcroft, 1990; Gopalakrishnan et al., 1993; Sheih et al. 2000). Pharmacological treatment of a number of clinical conditions such as angina and Type 2 diabetes are targeted on the K_{ATP} channel, although in different ways (tables 1-4 and 1-5). To treat angina, agonists such as potassium channel openers, KCOs, e.g. nicorandil are used to open the K_{ATP} channels in vascular smooth and cardiac muscle. In contrast to KCOs, antagonists such as sulphonylureas and related drugs are used to close K_{ATP} channels in pancreatic β-cells with, for example, tolbutamide and glibenclamide. Both types, agonists and antagonists, target the various SUR subunits to either open or close the channels.

It has shown that co-expression of Kir6.2/SUR2A, Kir6.2/SUR2B, and Kir6.1/SUR2B reconstitute cardiac, smooth muscle, and vascular smooth muscle K_{ATP} channels, respectively (Babenko et al. 1998; Seino 1999). These channels have different sensitivities to ATP (section 1.6.2, table 1-3). They also show different responses to sulphonylurea drugs and potassium channel openers (Inagaki et al. 1995; Isomoto et al. 1996; Matsuo et al. 2000) permitting a tissue selectivity in action of K_{ATP} channel directed therapies.

1.7.1 Sulphonylureas

Originally sulphonylurea compounds were intended as antibiotic agents during World War II. At that time, it was observed that a common side effect was hypoglycaemia,

now known to be due to the inhibition of pancreatic β-cell K_{ATP} channels. Today, sulphonylureas are used to treat Type 2 diabetes (table 1-4) (Proks et al. 2002)

The target of the sulphonylurea of drugs is the plasma membrane expressed K_{ATP} channel. At this site, the sulphonylurea causes channel closure, which results in depolarization of the β-cell membrane and stimulation of insulin secretion (Sturgess et al. 1985). Kir6.2/SUR1 K_{ATP} channels are inhibited by glibenclamide at K_i ~10 nM. Kir6.2/SUR2A, Kir6.2/SUR2B, and Kir6.1/SUR2B K_{ATP} channels are inhibited with K_i values in the low micromolar range (Inagaki et al. 1995; Isomoto and Kurachi 1996; Matsuo et al. 2000). The binding is isoform dependent; the β-cell isoform, SUR1 binds only tolbutamide and gliclazide and SUR2A and SUR2B bind all other types of sulphonylureas (Gribble et al. 1997; Gribble and Ashcroft 1999; Reimann et al. 2001; Sunaga et al. 2001).

1.7.2 Potassium Channel Openers (KCOs)

Potassium channel openers (KCOs) are a chemically diverse group of agents, which are exemplified by pinacidil, levcromakalin, aprikalim, and nicorandil. They activate K_{ATP} channels (Arena and Kass 1989; Edwards et al. 1993; Terzic et al. 1995). These agents possess high therapeutic potential in treating various clinical conditions including hypertension, acute and chronic myocardial ischaemia, or congestive heart failure, and also in managing bronchial asthma, urinary incontinence, and certain skeletal muscle myopathies (Edwards et al. 1993; Gopalakrishnan et al. 1993; Shieh et al. 2000). The effect of opening the K_{ATP} channel with KCOs is to cause a shift of the membrane

potential towards the reversal potential for potassium and, thereby, reduce to the cellular electrical excitability.

The K_{ATP} channel subtype, which is stimulated by diazoxide, is Kir6.2/SUR1 However, these channels are not stimulated by pinacidil or cromakalim (Gribble et al. 1997; Inagaki et al. 1995). In contrast, Kir6.2/SUR2A K_{ATP} channels are not stimulated by diazoxide but are stimulated by pinacidil and cromakalim (Isomoto and Kurachi 1996; Matsuo et al. 2000).

Similarly Kir6.2/SUR2B K_{ATP} channels are stimulated by both pinacidil and cromakalim (Isomoto and Kurachi 1996; Schwanstecher et al. 1998). Since nucleotide binding and/or hydrolysis at both NBDs of SUR subunits are believed to be crucial for the specific binding and action of these potassium channel openers (Gribble et al. 1997; Matsuo et al. 2000; Schwanstecher et al. 1998; S. Shyng et al. 1997) and for slowing the off-rate of pinacidil (Gribble et al. 2000), it is believed that the differences in sulphonylurea sensitivity between these channel subtypes may be caused partially by differences in nucleotide sensitivity of the different SUR isoforms (Matsuo et al. 2000).

The clinical use of potassium channel opening drugs has been limited due to the difficulty in developing tissue- and condition-selective K^+ channel-opening drugs (Schwanstecher et al. 1998). Different KCOs bind to different transmembrane polypeptide segments of the SUR. Within the 17 transmembrane polypeptide segments, the binding of pinacidil and cromakalim occurs at two domains within the helixes numbered 16 and 17, coloured green in figure 1-7 (Moreau et al. 2005), and in the cytoplasmic loop between, segments 13 and 14, green dashed circle in figure 1-7 (Babenko et al. 2000; Uhde et al. 1999). The binding site for diazoxide is not as well characterized. It is believed that diazoxide binding is nucleotide dependent (Moreau et

al. 2005). In SUR1, diazoxide binding has been mapped to bind between helixes 8 to 11, coloured pink in figure 1-7, and in the C-terminal region incorporating helix 17 and NBD2 (Moreau et al. 2005). This binding site was identified by using electrophysiological technique (patch clamp, explained in the next chapter) of SUR1-SUR2A/Kir6.2 chimeric constructs.

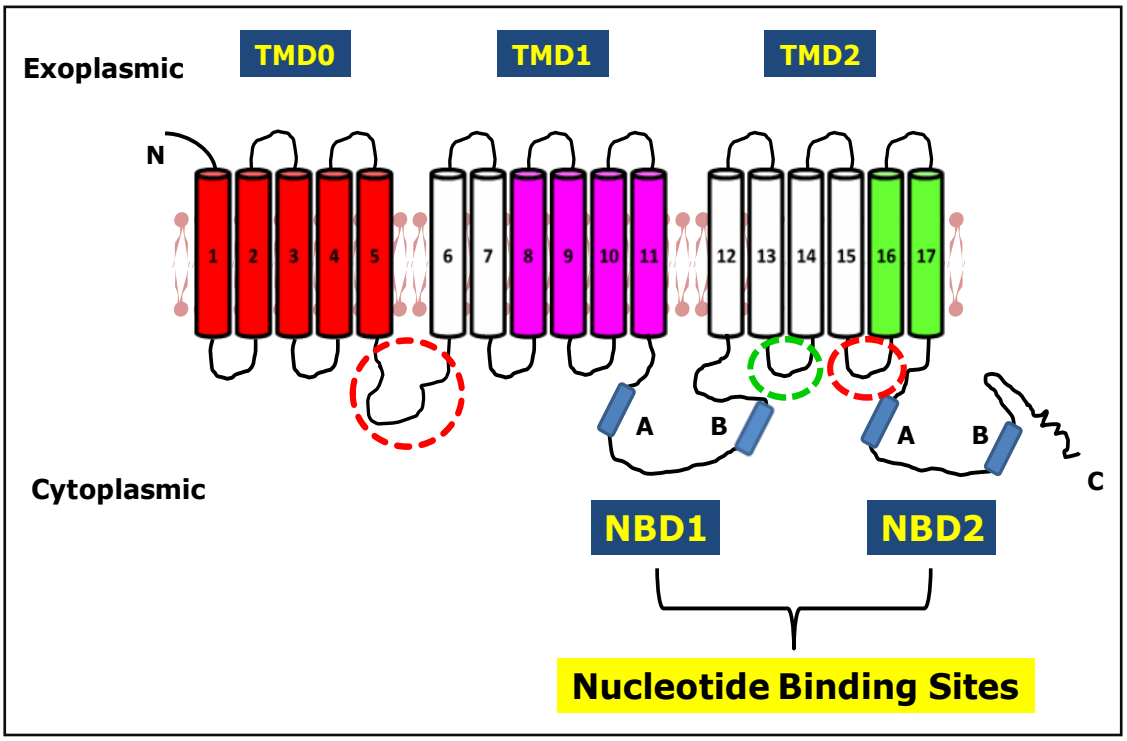

Figure 1-7 Pharmacological agent and nucleotide binding sites on regulatory sulphonylurea receptor (SUR) subunits.

Green shading represents the binding domains for the potassium channel openers (KCOs); pinacidil and cromakalim. Pink shading represents the binding domain for diazoxide, while the red represents the binding domains for the sulphonylureas (antagonist), glibenclamide. NBD1and NBD2 are the nucleotide binding sites (Babenko et al. 2000; Moreau et al. 2005; Uhde et al. 1999).

ATP-sensitive Potassium Channels Inhibitors				
Pharmacologic class			Mechanism of action	Clinical use
Sulphonylureas	First generation	e.g. Tolbutamide	Blocking K_{ATP} channels in pancreatic β-cells prevent K^+ efflux and causes depolarization of the plasma membrane, then opens Ca^+ channels, causing influx of Ca^+ and insulin release	Type 2 diabetes mellitus
	Second generation	e.g. Glibenclamide		
	Third generation	e.g. Glimepiride		

Table 1-4 The classification of sulphonylureas, the ATP-sensitive potassium channel antagonists.

Summary of the classification of sulphonylureas that are used in the treatment of type 2 diabetes mellitus (S. J. Ashcroft and Ashcroft 1990; Gribble and Reimann 2002; Hamaguchi 2004; Proks et al. 2002).

ATP-sensitive Potassium Channel Openers				
Agents	Pharmacologic class	Clinical use	As potential	Mechanism of action
Diazoxide	Potassium channel opener (KCO), Vasodilator	Hypertensive crises	Antihypertensive, and anti-asthmatic agents	Opening of K_{ATP} channels causing K^+ efflux, hyperpolarization of the cell membrane and smooth muscle relaxation which leads to vasodilation and drop in blood pressure
Minoxidil		Hair growth stimulant (Baldness), Severe hypertension		
Nicorandil		Angina pectoris		
Pinacidil		–		
Cromakalim		–		

Table 1-5 The potassium channel openers which target the ATP-sensitive potassium channels.

The table represents the summary of potassium channel openers (Aguilar-Bryan and Bryan 1999; S. J. Ashcroft and Ashcroft 1990; Dunne et al. 1997; Gribble and Reimann 2002; Hamaguchi et al. 2004; Mannhold 2004; Shieh et al. 2000; Terzic et al. 1995).

1.8 Do Interactions between the Two Heterologous Subunits of K_{ATP} Channels Mediate Allosteric Information Transfer?

More than two decades after the discovery of K_{ATP} channels, the transduction pathways for allosteric communication, which make the functional link between the pore forming Kir6 and the regulatory SUR subunits of K_{ATP} channels, remains poorly understood. In this section, the interaction between these two heterologous subunits will be discussed.

Lorenz and Terzic using co-immunoprecipitation found direct evidence of a physical association between Kir6.2 and SUR2A in cardiac K_{ATP} channel subunits. It was suggested that this association between the two heterologous subunits is necessary for full channel function to be expressed (Lorenz and Terzic 1999). Interestingly, the results represented in this study are consistent with the three-dimensional structure which is determined by single-particle electron microscopy at 18 Å resolution of the functional K_{ATP} channel complex $Kir6.2_4/SUR1_4$ (figure 1-8, Mikhailov et al. 2005). This structure, figure 1-8, is consistent with our initial work (Rainbow et al. 2004) and also with the results of this study that revealed the inter-subunit interactions are crucial for the assembly and function in hetero-octameric complex allostery of $Kir6_4/SUR2A_4$ of K_{ATP} channels.

In the light of the cytoplasmic location of NBD1 and NBD2 of SUR and the N- and C-termini of Kir6.2, a hypothesis was raised that the transfer of allosteric information between the two heterologous subunits occurs through the cytoplasmic domains rather than through the transmembrane domains; the transmembrane domains being required for the assembly of the channel. Thus, present study was undertaken to investigate the possible cytoplasmic allosteric communications between the two subunit types.

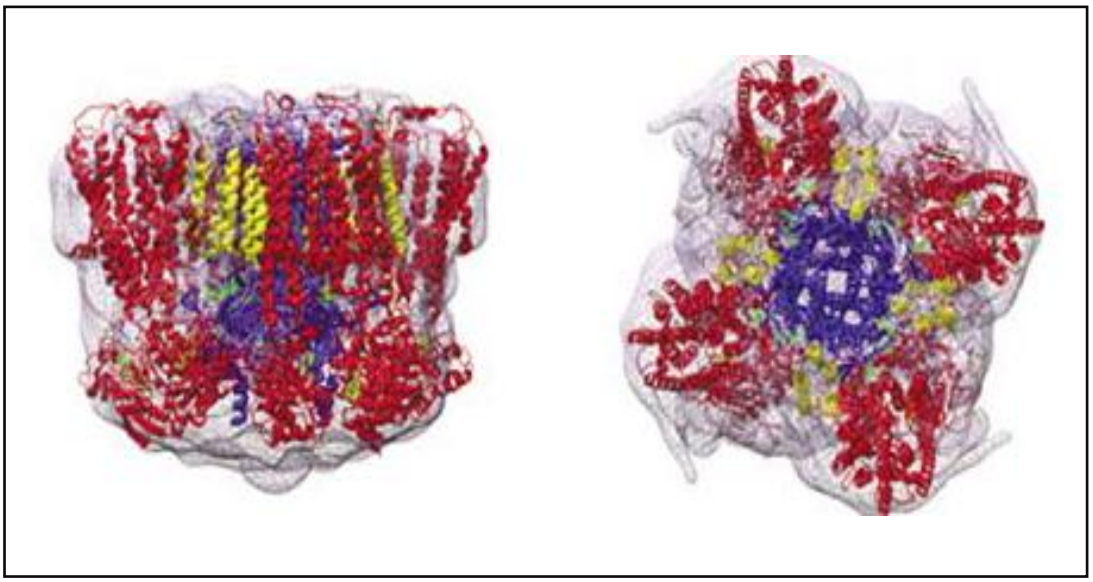

Figure 1-8 Three-dimensional structure of the functional K_{ATP} channel complex $Kir6.2_4/SUR1_4$ (taken from Mikhailov et al. 2005).

This figure shows the hetero-octameric functional complex of pancreatic K_{ATP} channel. The side view of the channel complex is shown to the left and a top view to the right. The colours represent as followed: (blue) Kir6.2 subunit, (red) SUR1 minus TMD0 and (yellow) TMD0 and (green) ATP molecules. As can be seen in the top view (right), the assembly of the functional pancreatic subtype K_{ATP} channel consists of four pore forming Kir6.2 subunits, which are surrounded by four SUR1. This structure (side view, left) is consistent with the results of this study, which revealed the cytoplasmic interactions between two heterologous subunits of Kir6 and SUR are physically (Chapter 5) and functionally (Chapter 6) important.

1.8.1 Sulphonylurea Receptor (SUR)

In response to nucleotides and pharmaceutical agonists and antagonists, SUR allosterically regulate K_{ATP} channel gating. The interactions of the transmembrane and the cytoplasmic domains of SUR with Kir6.X will be discussed in the next two sections.

1.8.1.1 Transmembrane Domains of SUR Subunits (TMD0, TMD1 and TMD2)

The sulphonylurea receptor consists of three transmembrane domains (TMD0, TMD1 and TMD2) (figure 1-3). Between TMD0 and TMD1 there is a linker named L0, which has large effects on the gating of K_{ATP} pores, which lack the C-terminal ER retention signal (Babenko and Bryan 2003). Studies have shown that if a truncated SUR lacks TMD0 then it fails to modulate the Kir. From this, it is believed that TMD0 is the domain that attaches SUR to the Kir pore (Babenko and Bryan 2003). When TMD0-L0 interacts with the outer helix and the N-terminus (M1) of Kir, inactive pores in K_{ATP} channels activate and surface expression is enhanced (Babenko and Bryan 2003).

1.8.1.2 Cytoplasmic Domains of SUR (NBD1 and C-terminal (NBD2))

To investigate possible interactions between cytoplasmic domains of heterologous K_{ATP} channel subunits, Rainbow et al. (Rainbow et al. 2004) undertook a co-immunoprecipitation study using full-length Kir6.2 subunits and MBP-tagged

fragments of SUR2A. This study identified an interaction between Kir6.2 and NBD2 of SUR2A and defined a minimal interacting fragment of 65 amino acids (SUR2A-CTE), amino acids 1294-1358, containing part of the Walker A motif of NBD2 (figure 1-9).

Furthermore, mutagenesis of conserved charged residues in SUR2A-CTE present in this domain in interacting SUR1, SUR2A and SUR2B subunits, to residues of the opposite charge in the equivalent domain of the non-interacting multidrug resistance protein 1 (MRP1), revealed three residues E1318, K1322 and Q1336, (figure 1-11), which when changed reduced the strength of the interaction and were, therefore, identified as likely to be key to the interaction, (Al-Johi PhD thesis, 2005).

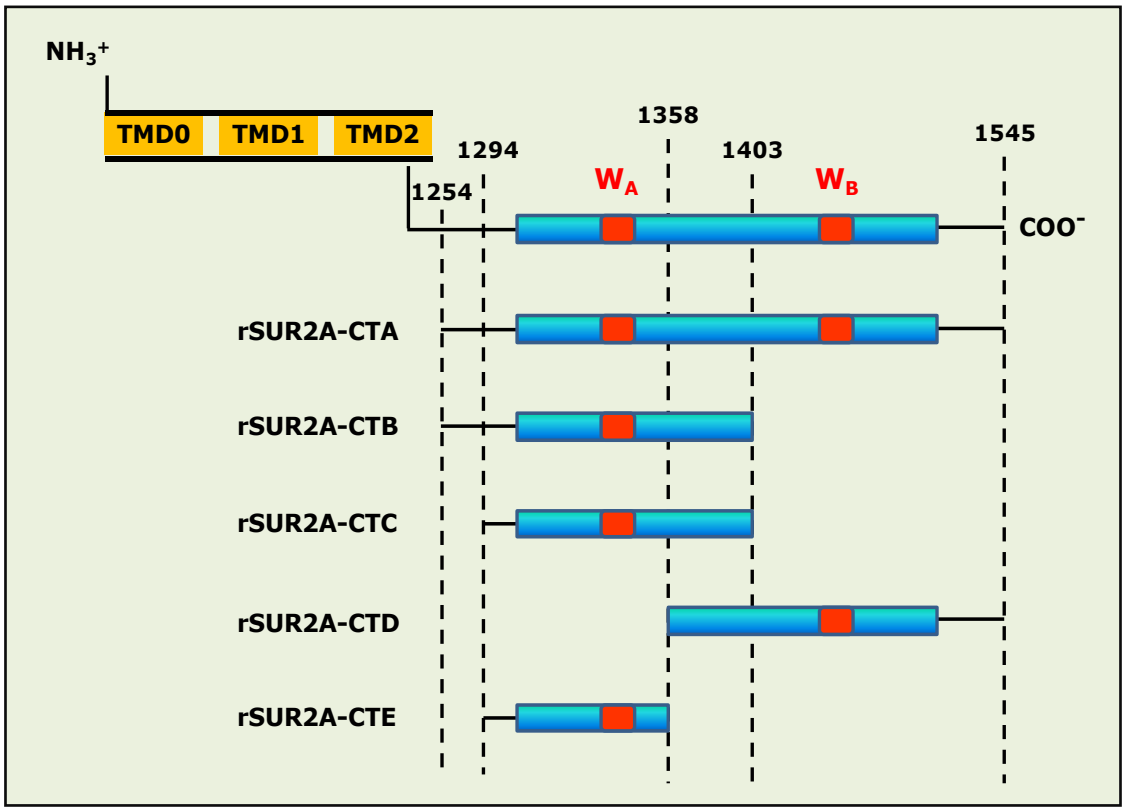

Figure 1-9 Schematic diagram of the SUR2A-CT fragments within the C-terminal domain of SUR2A used in subunit interaction studies.

Blue bar indicates NBD2 and red boxes represent Walker motifs A and B (numbering of residues positions, Rainbow et al. 2004). SUR2A-CTE represents a minimal interacting fragment of 65 amino acids (1294-1358) of NBD2 with full length Kir6.2, which was initially identified in our laboratory. Yellow colour represents the transmembrane domains (TMDs) 0, 1 and 2.

A)

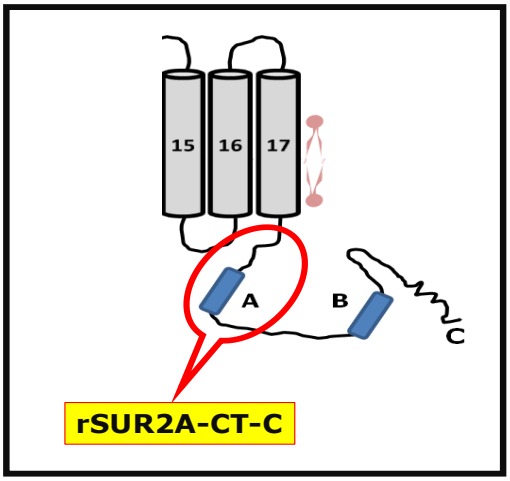

B)

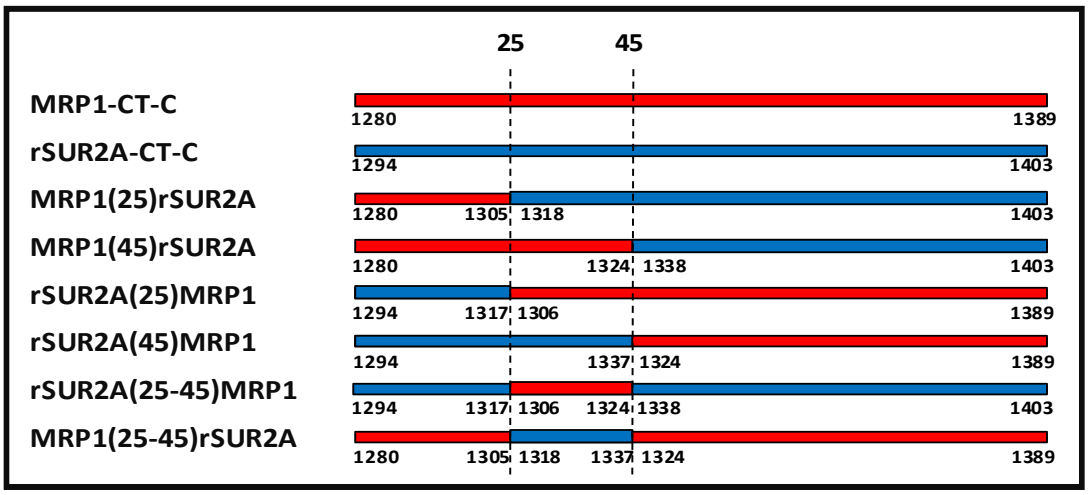

Figure 1-10 Characterization of SUR2A-NBD2 (1294-1403) and Kir6.2 interaction.

A) Schematic representation of SUR2A-CT-C fragment and (B) MRP1/SUR2A chimeras. Co-immunoprecipitation of maltose binding protein-tagged chimeric constructs with Kir6.2, suggest the amino acid sequence 1318-1337 of SUR2A to be the minimal interacting sequence with Kir6.2 (data not shown). Red colour represents non-interacting multidrug resistance protein 1 (MRP1) and the blue colour represents of SUR2A-NBD2 (1294-1403) that is located downstream of TM17, and includes the Walker A motif.

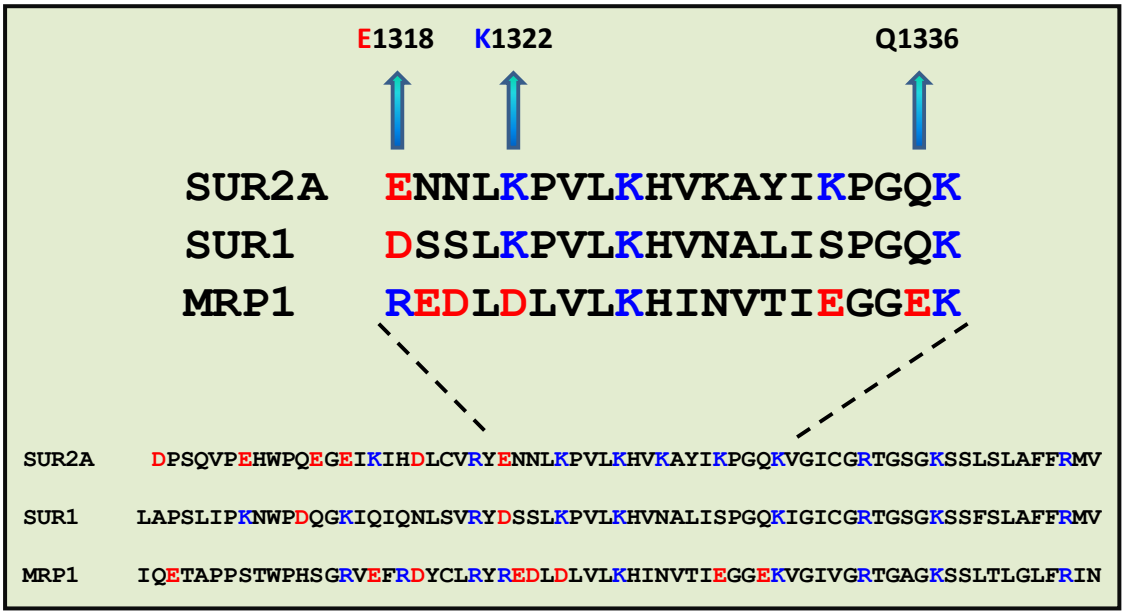

Figure 1-11 Sequence alignments for NBD2-CTE sequence from SUR2A (1318-1337), SUR1 and MRP1.

Mutagenesis and co-immunoprecipitation studies of the 20 amino acids of the minimal interacting fragment of SUR2A (1318-1337) with full length Kir6.2 revealed E1318, K1322 and Q1336 to be key for the interaction (Al-Johi PhD thesis, 2005). These residues lie just downstream of three residues in SUR2A, E1305, I1310 and L1313, which when mutated to those in non-interacting MRP1, were sufficient to remove pinacidil-stimulated channel activation, indicating a more extensive interacting surface in SUR2A (Dupuis et al. 2008). The arrows highlight the three residues as important for the interaction domain on regulatory SUR2A for the Kir6.2 subunit in Kir6.2/SUR2A channel. Residues coloured red and blue represent the negatively and positively charged amino acid groups, respectively.

Based on the above a study (Rainbow et al. 2004), Dupuis et al. (Dupuis et al. 2008) studied Kir6.2/SUR2A channel in more detail and they found that the proximal C-terminal of SUR2A within the cardiac K_{ATP} channel is a crucial link between potassium channel opener binding to SUR2A and Kir6.2 activation. Dupuis et al. (Dupuis et al. 2008) investigated a 65 residue fragment of SUR2A, which links TMD2 and NBD2 and had been shown to interacting with Kir6.2 (Rainbow et al. 2004). The 65 residue segment was replaced with the equivalent non-interaction segment from MRP1 to make a chimeric construct that was expressed in *Xenopus* oocytes and characterized by the patch-clamp technique. Results showed that activation by MgADP and synthetic openers was greatly weakened in this chimaera. Additional mutagenesis studies were performed resulting in the demonstration of three residues, E1305, I1310 and L1313 (rat numbering), which together were able to restore activation of K_{ATP} current by MgADP through SUR2A but which had no effects on the block of the channel by glibenclamide or by ATP. This study showed these three residues to have a role in activation not inhibition of the channels pore.

With these findings, Dupuis et al. (2008) suggested that one of the roles for these three residues may possibly be to form a part of an information transduction pathway, which functionally couples SUR2A and Kir6.2 subunits through the SUR2A cytosolic segment that interconnects transmembrane helix 17 to NBD2.

1.8.2 Kir6.2

1.8.2.1 Transmembrane Segments M1 and M2 of Kir6.2

The three-dimensional structure of Kir6 subunits is yet to be determined. A crystal structure study of the bacterial potassium channel KcsA indicated that M1 is exposed to the lipid membrane environment and does not directly contribute to the ion-conduction pathway and that M2 and the preceding pore domain (H5) from four subunits form the ion permeation pathway (Doyle et al. 1998).

Studies prior to Schwappach et al. (Schwappach et al. 2000) were all focused on the cytoplasmic domains and transmembrane segment M2 of Kir6.2 (Drain et al. 1998; Koster et al. 1999; Reimann et al. 2001; Trapp et al. 1998; Tucker et al. 1998). Schwappach et al. (2000) showed that the N-terminus of the Kir6.2 subunit and the transmembrane segment M1 are vital for specifying assembly with SUR1 and SUR2A. Various chimaeras between Kir6.2 and Kir2.1 were made in order to define the minimal structure in Kir6.2 in M1 required for the assembly. Schwappach et al. found the TMS (threonine-methione-serine) and FA (phenylalanine-alanine) residues at the beginning and at the end of the M1 helix were the most crucial for the interaction with SUR. An additional finding showed that the transmembrane domains and not the nucleotide-binding domains of SUR1 are necessary for interaction with Kir6.2 (Schwappach et al. 2000).

1.8.2.2 Cytoplasmic Domains (N- and C-terminal) of Kir6.2

A study done by Zerangue et al. disclosed that a novel endoplasmic reticulum (ER) retention sequence, RKR is present in both of the heterologous K_{ATP} channels subunits (Zerangue et al. 1999). In Kir6.2, RKR is located in the C-terminus and in SUR1, it is located upstream of the first nucleotide binding fold. With this finding, it is now understood why Kir6.2 does not form functional channels when expressed alone but does when co-expressed with SUR1 (Inagaki et al. 1995; Tucker et al. 1997). At the same time, when the RKR sequence was removed by truncating the C-terminus of Kir6.2 (Inagaki et al. 1995) functional expression of ATP sensitive K^+ currents was observed. Zerangue et al. concluded that, when both subunits are coexpressed, the RKR motifs on each are masked, allowing surface expression (Zerangue et al. 1999).

In 1996, Tinker et al. performed a deletion analysis, which showed that there is a possibility of removing the N-terminus but only a fraction of the C-terminus before biochemical and functional evidence of channel assembly is lost. Mutant Cδ333 represented a boundary for C-terminal deletion at which biochemical association, expression of current, and negative knockout of wild type current (replacement of GYG in the pore-forming loop, H5, with AAA) are decreased or lost (Tinker et al. 1996). Electrophysiological recordings from oocytes, injected with mRNA encoding a truncated form of Kir6.2, and in which the last 26 (Kir6.2 ΔC26) or 36 (Kir6.2 ΔC36) amino acids of the C-terminus were deleted resulted in functional expression of Kir6.2 in the absence of SUR1 (Tucker et al. 1997). In the same study, Kir6.2 ΔC26 and Kir6.2 ΔC36 were inhibited by ATP, which suggested that the Kir6.2 subunit has an intrinsic inhibitory ATP site.

Based on the assumptions of Lorenz and Terzic (Lorenz and Terzic 1999) described in section 1.8, Hough et al. (Hough et al. 2000) investigated the regions of Kir6.2 in addition to the RKR sequence that determine the dependency on SUR1 for cell surface expression. They expressed chimaeras between Kir6.2 and Kir2.1in *Xenopus* oocytes alone or together with SUR1 (figure 1-12, Rao 1, 2, 3 and 4). The results of this investigation confirmed previous studies that the ER retention sequence is located within the distal C-terminal segment (RKR) in Kir6.2 (Hough et al. 2000; Zerangue et al. 1999); and in addition to RKR that the M2/TM segment and the proximal C-terminal region of Kir6.2 also are responsible to the failure of Kir6.2 to traffic to the membrane independently of SUR1 subunit.

Tinker's laboratory (Tinker et al. 1996) were unable to produce functional expression with another set of chimaeras in Kir6.2/Kir2.1 oocytes (figure 1-12, Tin A, B, C, D, E, F). They concluded from their study that a domain in the proximal C-terminus (at least amino acids 208-279) in the Kir6.2 seems to largely determine biochemical interaction with SUR1 and it is necessary that both the Kir6.2 N- and distal C-terminus are present in order for a complete functional reconstitution of the K_{ATP} channels (Giblin et al. 1999). The positively charged residues R176 and R177 in the C-terminal of Kir6.2 are required for functional coupling to SUR1 (Fan and Makielski 1997; Ribalet et al. 2000).

To identify the cognate binding domain in Kir6.2 for the SUR2A-CTE sequence, binding of SUR2A-CTC to chimaeras of interacting Kir6.2 and non-interacting Kir2.1 subunits (figure 1-12) was investigated in a further series of co-immunoprecipitation experiments.

In this study, Rao 1, Rao 2, Rao 3, Rao 4, TinF and full length Kir2.1 were immunoprecipitated using anti-Kir2.1 as antibody. Likewise Tin A, Tin B, Tin C, Tin D, Tin E and full length Kir6.2 were immunoprecipitated with anti-Kir6.2 as expected. When the opposite antibody was used no immunoprecipitation was achieved due to the recognition of these antibodies of an epitope within the C-terminal tail (al-Johi 2005).

Figures 1-10 shows the five Kir6.2/Kir2.1 chimaeras and the full length Kir6.2, represented with a plus, which were able to co-immunoprecipitate with the SUR2A-CTC (amino acids 1294-1403) fragment. These chimaeras were as followed; Tin A, Tin B, Tin C, Tin D, Tin E and full length Kir6.2. The remaining Kir6.2/Kir2.1 chimaeras and full length Kir2.1, represented with a minus, were not able to co-immunoprecipitate with the SUR2A-CTC fragment. These chimaeras were as followed; Rao 1, Rao 2, Rao 3, Rao 4, Tin F and full length Kir2.1.

As a negative control for above mentioned co-immunoprecipitation, an equivalent amino acid sequence of non-interacting polypeptide MRP1 (amino acids 1280-1389, MRP1-CTC) to SUR2A-CTC (amino acids 1294-1403) was investigated with the Kir6.2/Kir2.1 chimaeras. The results showed no interaction between MRP1-CTC and Kir6.2/Kir2.1 chimaeras as expected.

Altogether, this study suggested that the interaction domain on Kir6.2 for NBD2 (1294-1358) of SUR2A is located within the 75 amino acids of the C-terminal tail beyond residue 315.

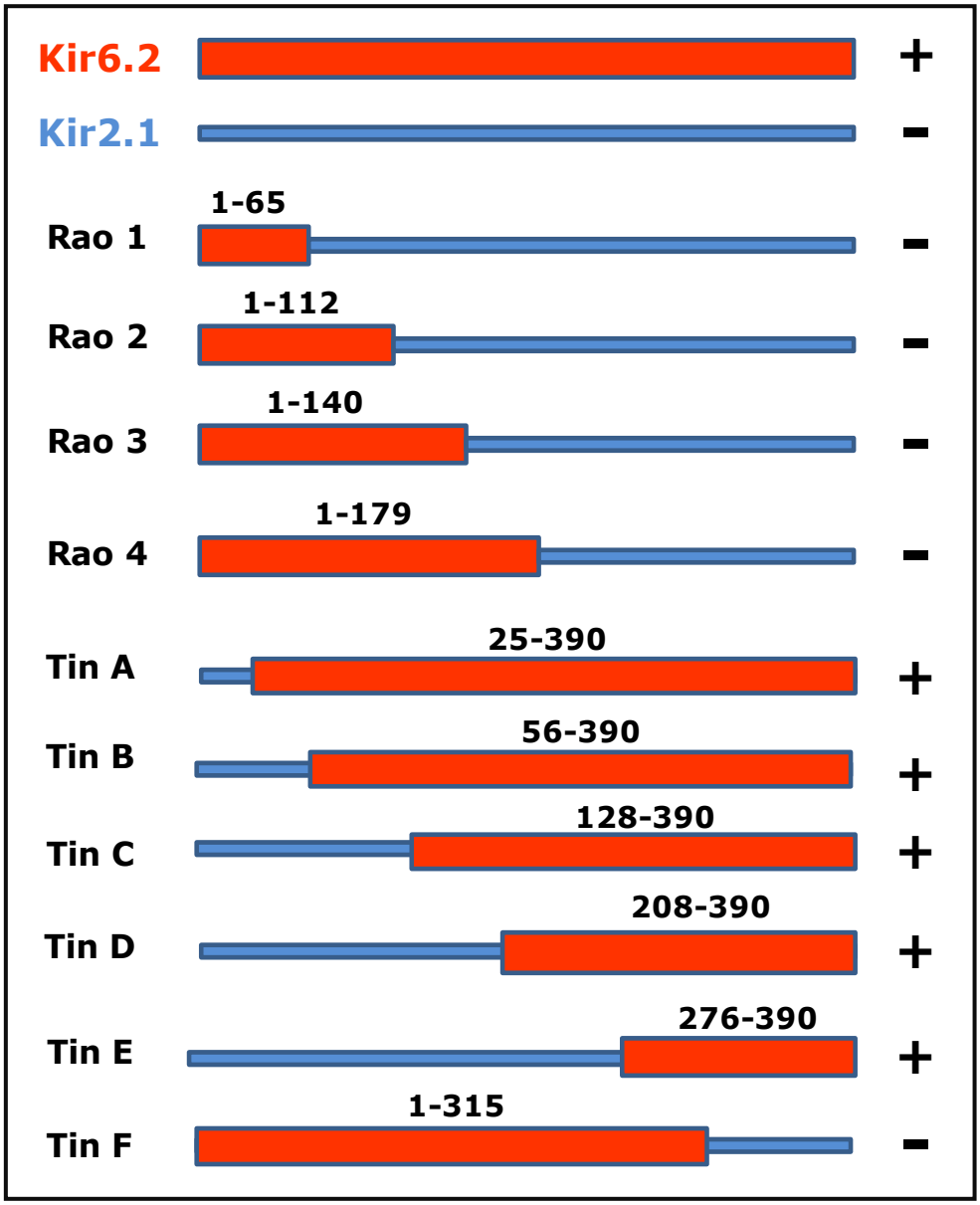

Figure 1-12 Schematic design of the Kir6.2/Kir2.1 chimaeras used in co-immunoprecipitation experiments with SUR2A-CTC fragment.

The full-length Kir6.2 subunit is presented in red and the non-interacting Kir2.1 in blue. The numbers indicate the amino acid sequence incorporated in each Kir6.2 chimaera. (+) represents the co-immunoprecipitation of maltose binding protein-SUR2A-CTC constructs with Kir6.2/2.1 chimeras and (-) represent the absence of co-immunoprecipitation. The results revealed the interaction domain on Kir6.2 to be located beyond residue 315 in Kir6.2, Tin F (Al-Johi PhD thesis, 2005).

1.9 Summary of aims

The general aim of this project was to study structure-function relationships in ATP-sensitive potassium channels. Specifically, characterization and identification of cytoplasmic interactions between the two heterologous subunits which are responsible for the assembly and allosteric communication were investigated (figure 1-13).

This study can be summarized by the three following aims:

1. To identify the cognate interaction domain on Kir6.2 for SUR2A using mutagenesis and co-immunoprecipitation.

2. To investigate allosteric information transfer between heterologous subunits using electrophysiological techniques.

3. To express and purify the cytoplasmic domains of Kir6.2 for structural analysis of the interaction between the two heterologous subunits.

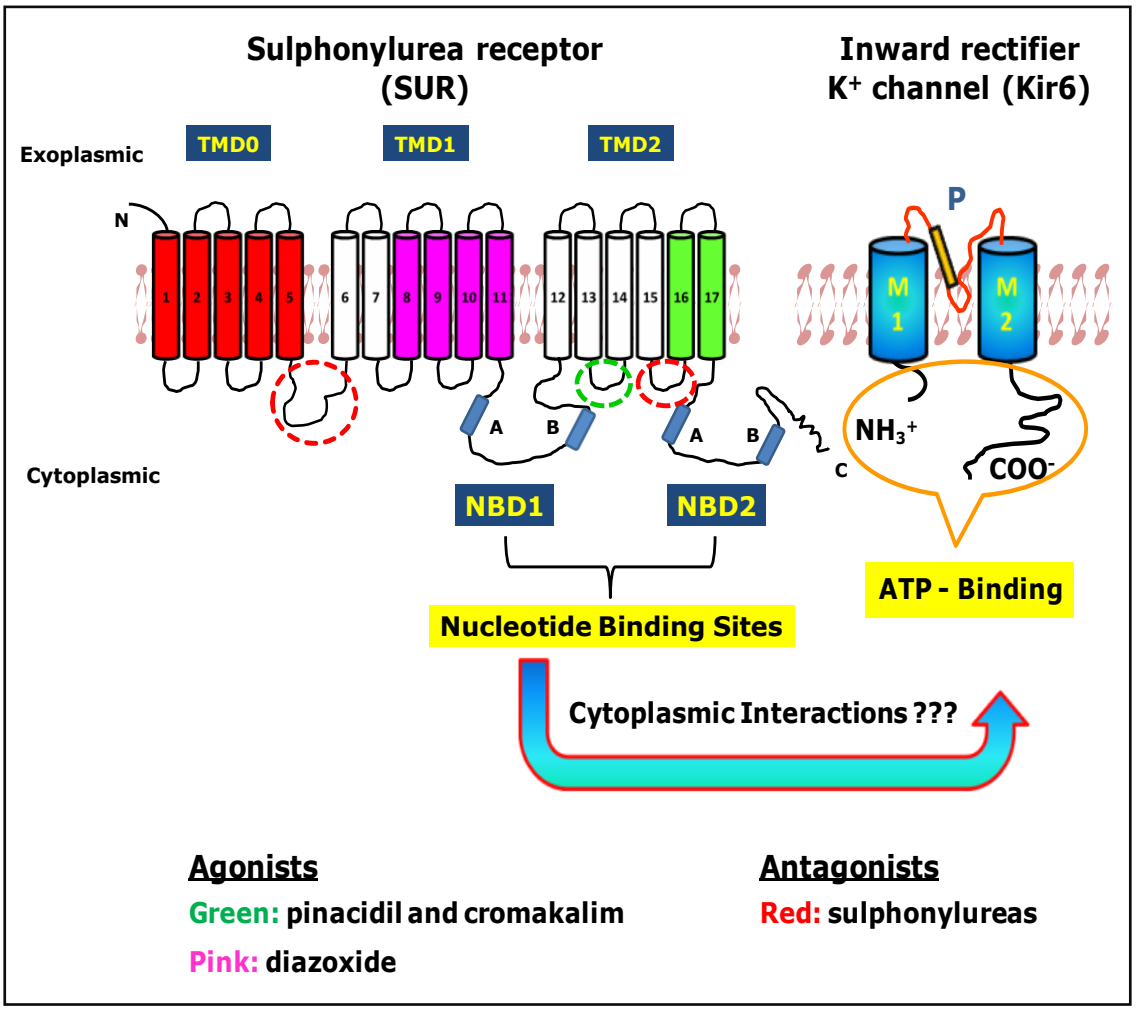

Figure 1-13 Allosteric information transfer through inter-subunit contacts in ATP-sensitive potassium channels.

K_{ATP} channels comprise hetero-octamers of four pore-forming Kir6 and four accessory SUR subunits. Inhibitory ATP binding occurs on the Kir6 subunits, while regulatory nucleotide and potassium channel drug binding is mediated by SUR subunits. The aim of this study was to characterize and identify possible cytoplasmic interactions between these two heterologous subunits which are involved in allosteric information transfer.

Chapter 2

Methods and Techniques

2.1 Biochemistry

2.1.1 Protein Expression

2.1.1.1 In Vitro

Wild type Kir6.2 and mutant constructs (provided by Dr Dave Lodwick, co-supervisor) were expressed *in vitro*, using the TNT® Quick Coupled Transcription/Translation System from (Promega). The reaction components were assembled in a 0.5 ml microfuge tube to a final volume of 50 µl as following; 40 µl TNT® Quick Master Mix, 6 µl plasmid cDNA templates (0.5µg/µl), 1 µl methionine (1mM), 2 µl [^{35}S]-Methionine (specific activity: > 1000 Curie (37 TBq, terabecquerel)/mmol, Perkin Elmer) and finally 1 µl canine pancreatic microsomal membranes. The reactions were mixed gently by pipetting and incubated at 30 ºC for 90 min. Following this, 1 µl of Protease Inhibitor Cocktail Set III (CALBIOCHEM®) was added to each reaction. These samples were used for co-immunoprecipitation (section 2.1.5)

2.1.1.2 In Vivo

For expression of TM1070-Kir6.2NC fusion protein, a heat shock transformation method (as described in 2.1.8) was used to transform the plasmid DNA (Pleics-05/6.2NT-TM1070-CT) in to the Arctic Express competent cells.

A single colony was inoculated to 3 ml Lysogeny Broth (LB, Appendix A)-ampicillin (1000:1, ampicillin stock solution is 100 mg/ml in dH_2O) medium. The culture was incubated at 37 °C with shaking at 230 rpm overnight. The next morning, the cells were subcultured in 20 ml tubes with 1:100 inoculation, 100 µl of starter culture to the new LB-ampicillin medium. The cultures were incubated at 37 °C with shaking at 230 rpm.

TM1070-Kir6.2NC fusion expression was induced with different concentrations of Isopropyl-beta-D-thiogalactopyranoside (IPTG) 0.1 mM, 0.3 mM and 1 mM, when the absorbance reached 0.8. Various concentrations of IPTG were used to optimise the induction and one incubation received no IPTG as a negative control. After induction the cultures were incubated at 13 °C with shaking at 230 rpm for 24 and 48 hrs to optimise the yield of expression. The cells were harvested by centrifugation at 4000 × g for 20 min at 4 °C. The medium were discarded and the pellets were stored at -20 °C. The expression was analysed by Coomassie blue staining and Western blot (section 2.1.4).

Fusion Protein Construct	Plasmid Vector	Amino Acid Numbers	Junctions	Linker Regions	Tag
MBP-SUR2A-CTC fragment (amino acids 1294-1403)	pMal-c2x	SUR2A 1294-1403	MBP 387	—	Maltose binding protein (MBP)
TM1070-Kir6.2 NC (C-terminal-His6 tag)	pLEICS 05	1. Kir6.2 1-73 (N-terminal) 2. TM1070 1-114 (without N- and C-terminal) 3. Kir6.2 167-390 (C-terminal)	—	TEV protease site (ENLYFQG) TEV protease site (ENLYFQG)	Polyhistidine-tag (hexa histidine-tag, His6 tag) placed on the C-terminal

Table 2-1 Plasmid vector information for the fusion protein constructs used for co-immunoprecipitation and structural studies.

The MBP-SUR2A-CTC construct was used for co-immunoprecipitation full length wild type and mutated Kir6.2 and TM1070-Kir6.2 NC (C-terminal-His6 tag) fusion protein for the structural study of the cytoplasmic domains of Kir6.2. The plasmid vector maps for these fusion protein constructs can be found in the Appendix B.

2.1.2 Bradford Protein Assay

Bradford protein assay was used to assess the protein concentration of samples. Coomassie brilliant blue (CBB) G-250 based reagent (Pierce) was used as dye and in response to various concentrations of protein a differential colour change was measured. Bovine serum albumin (BSA) (1 mg/ml stock) was used as a standard solution.

Absorbance of diluted BSA from stock solution with a range of 0 – 30 µg in a volume of 200 µl was measured at 595 nm wavelength using Ultrospec III Pharmacia as spectrophotometer to establish a standard curve. Samples with unknown protein concentrations were diluted with dH_2O to a volume of 200 µl (1:10, 1:100, 1:200). The spectrophotometer was warmed up (15 min) before use and all samples with known and unknown protein concentration were incubated with 1 ml CBB G-250 reagent at room temperature for 10 min before measurement. In order to measure the protein concentration of unknown samples the absorbance values of the unknown were read against the standard curve (figure 2-1).

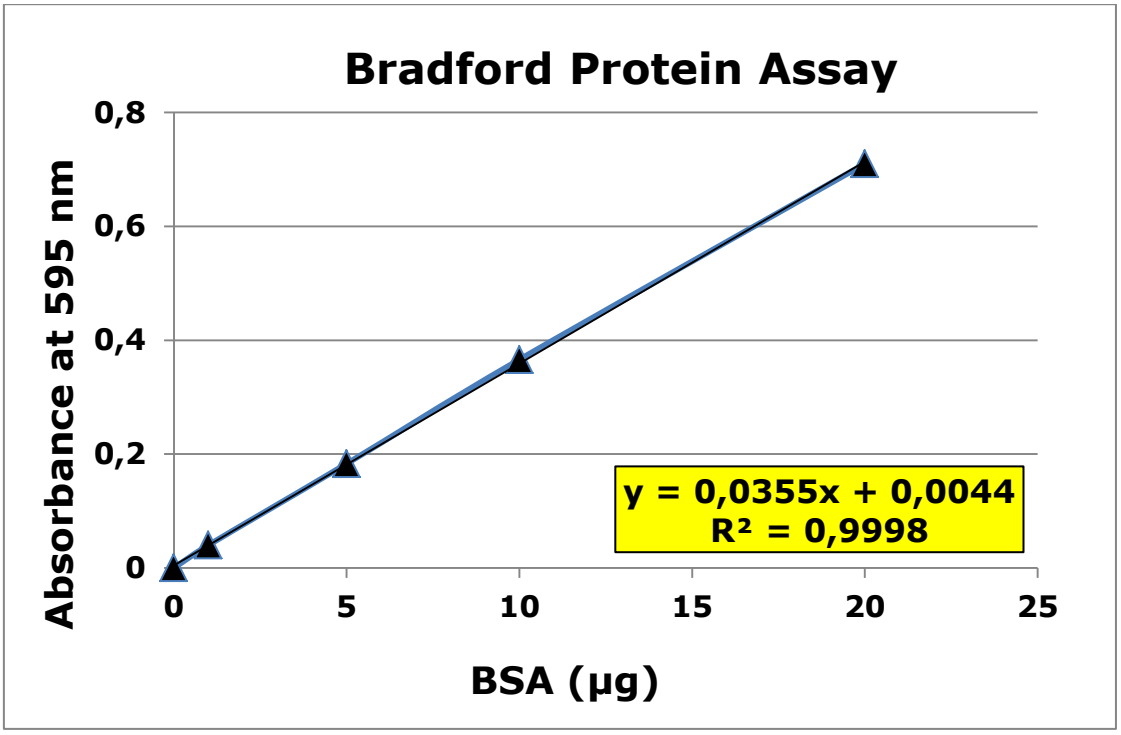

Figure 2-1 Bradford protein assay standard curve.

2.1.3 SDS-Polyacrylamide Gel Electrophoresis (SDS-PAGE)

Following determination of protein concentration by Bradford protein assay the protein mixtures were analysed by SDS-PAGE. Polyacrylamide (10%, 1.5 mm thick minigels were poured between two glass plates using Bio-Rad casting kit and allowed to polymerize; 10% resolving (separation) gel (see Appendix A) was polymerized for a minimum of 20 min and stacking gel (see Appendix A) of 10 min.

The samples were denatured after 20-30 min treatment with 4:1 of 4 x Laemmli sample buffer (10% w/v SDS, 1 M Tris-HCl (pH 7.5), 100 mM EDTA, 50% v/v glycerol, 0.3M dithiothreitol (DTT) and 0.05% w/v bromophenol blue dye) at room temperature. Then the samples were loaded into wells in the stacking gel. The gels were placed in the electrophoresis tank (Bio-Rad) and filled to the top with 1x SDS-PAGE running buffer (25 mM Tris-base, 192 mM glycine and 0.1% SDS (w/v)). The electrophoresis unit was connected to a power pack and the samples were migrated for about 80 min at 120 V at room temperature until the ion front reached the bottom of the gel.

2.1.4 Western Blot

Following SDS-PAGE, the Western blot technique was used to transfer the separated proteins from polyacrylamide gels to Amersham Hybond ECL nitrocellulose membrane (GE Healthcare) and the membrane was probed with specific antibody for antigen detection. The gel and the membrane were pre-wet with 1x transfer buffer (25 mM Tris (pH 8.3), 192 mM glycine and 10% v/v methanol) for 10 min. Then the electroblotting cassette was assembled and placed in the blotting unit. Protein transfer occurred at 4 ^{o}C at 100 V for 70 min or overnight at 30 V. Following transfer the membrane was

removed from the sandwich and blocked with blocking buffer (5% (w/v) nonfat milk in TBS-T (Tris-buffered saline: 10 mM Tris (pH 7.6), 150 mM NaCl and 0.1% v/v Tween 20) at room temperature for 2 hrs. Then the membrane was probed with desired antibody for each experiment (see below) and detected by Enhanced Chemiluminescence (ECL) detection system (see Appendix A).

The membrane was probed with primary antibody at room temperature for 2 hrs or in the cold room overnight with gentle agitation on a shaker. The incubation time for secondary and tertiary antibodies was 1 hr at room temperature with gentle agitation. The membrane was washed 6 x 5 min with 1x TBS-T buffer after each incubation with antibody.

2.1.5 Co-immunoprecipitation of MBP-rSUR2A-CT-C Fragment with Various Mutant Constructs of Kir6.2

Co-immunoprecipitation was used to identify interaction between MBP-rSUR2A-CT-C and the full length Kir6.2 subunit. A schematic illustration of co-immunoprecipitation between MBP-SUR2A-CTC fragment (as described previously in Rainbow et al. 2004) and various Kir6.2 mutant constructs is shown in figure 2-2. Mutant Kir6.2 polypeptides were expressed in vitro from cDNA cloned from rat and encoding mutant Kir6.2 subunits using the TNT® Quick Coupled Transcription/Translation Systems with procine microsomal membranes. The Kir6.2 polypeptides were solubilised in Triton X-100 solubilisation buffer and the protein-protein interaction with MBP SUR2A-CTC probed by co-immunoprecipitation with anti-Kir6.2 antibody and the immune-complex captured on protein A-Sepharose. The anti-kir6.2 used in this study was characterized in our laboratory (Singh et al. 2004) and also used in our initial work (Rainbow et al.

2004, Al-Johi PhD thesis, 2005). The polyclonal site-directed antiserum was raised to peptide corresponding to the C-terminal domain of rat Kir6.2 (accession number D86039), amino acid residues KAKPKFSISPDSLS (residues 377-390, Research Genetics Inc. Huntsville, AL, USA). To facilitate conjugation, cysteine residues of the C-terminal were added to the peptides Keyhole Limpet Haemocyanin carrier protein. Following, antiserum was raised against peptide carrier protein conjugates in New Zealand White Rabbits (Research Genetics Inc., Singh et al. 2004). Western blot analysis of the anti-Kir6.2 antiserum confirmed that the anti-Kir6.2 antiserum recognized its polypeptide and immunoprecipitation study revealed this antiserum to be specific to Kir6.2 isoform of K_{ATP} channel pore (Singh et al. 2004). It is worth mentioning the polyclonal anti-Kir6.2 was first tested and optimised against cardiomyocytes from adult rat (gift from Department of Cell Physiology and Pharmacology, University of Leicester) before use.

The immunoprecipitated complexes were analysed by Western blot using mouse, anti-MBP antibody to detect immunoprecipitated MBP-SUR2A-CTC and the bands were visualized using an ECL detection system. Blots were subjected to autoradiography to detect the presence of [^{35}S] Met-Kir6.2 polypeptides. The ECL immunodetection and autoradiography from the co-immunoprecipitation were quantified by densitometry. The amount of immunoprecipitation of MBP-SUR2A-CTC was normalised to the amount of [^{35}S] Met-Kir6.2 immunoprecipitated, to control for different levels of input of Kir6.2 mutants in each experiment. The normalised MBP-SUR2A-CTC immunoprecipitation was then expressed as a percentage of that obtained with the wild type [^{35}S] Met-Kir6.2 subunit to permit comparison.

The co-immunoprecipitation reactions were mixed in pyrex tubes (20 µl) and all solutions were made in 100 mM Tris-HCl (pH 7.4). Three microliters of wild type and

each mutant constructs which were expressed *in vitro* (section 2.1.1.1) was added to 5 ng of MBP-rSUR2A-CTC fragment (3 µl of 1.68 µg/ml) and 14 µl of 100 mM Tris-HCl (pH 7.4) to make a final volume of 20 µl for each reaction. A control reaction was made for each incubation. For control reactions MBP-rSUR2A-CT-C only was added to17 µl of Tris-HCl.

The pyrex tubes were placed in an ice-water bath and the samples were sonicated using a Soniprep 150 (MSE) at 4 ^{o}C, 8 times for 15 s with 20 s setting. After sonication the mixtures were incubated at 37 ^{o}C for 1 hr and then at room temperature for an additional hour. Twelve microliters of 3% Triton X-100 was added to the mixtures, which were transferred from pyrex tubes to 0.5 ml microfuge tubes and all mixtures were incubated at 4 ^{o}C for 30 min. The samples were centrifuged at 10,000 x g for 15 min at 4 ^{o}C. The supernatants were transferred to new 0.5 ml microfuge tubes and 4 µl of anti-Kir6.2 antibody were added to each tube and all samples were incubated at 4 ^{o}C with rolling for 30 min. Antibody bound protein complex was immobilized on protein A-Sepharose beads which were pre-blocked, as follows: Protein A-Sepharose (Sigma, from *Staphylococcus aurous*) was swelled with dH_2O, washed three times and equilibrated twice with 100 mM Tris-HCl (pH 7.4). The swollen Protein A-Sepharose (100 mg/ml) was then pre-blocked in 5% BSA, 0.5 M KCl and 100 mM Tris-HCl (pH 7.4) then incubated at room temperature with rolling for 2 hrs. Then the blocked protein A-Sepharose was washed 3 times with 100 mM Tris-HCl (pH 7.4) before adding 50 µl to co-immunoprecipitation reactions as a 1:1 slurry and incubated overnight at 4 ^{o}C with rolling.

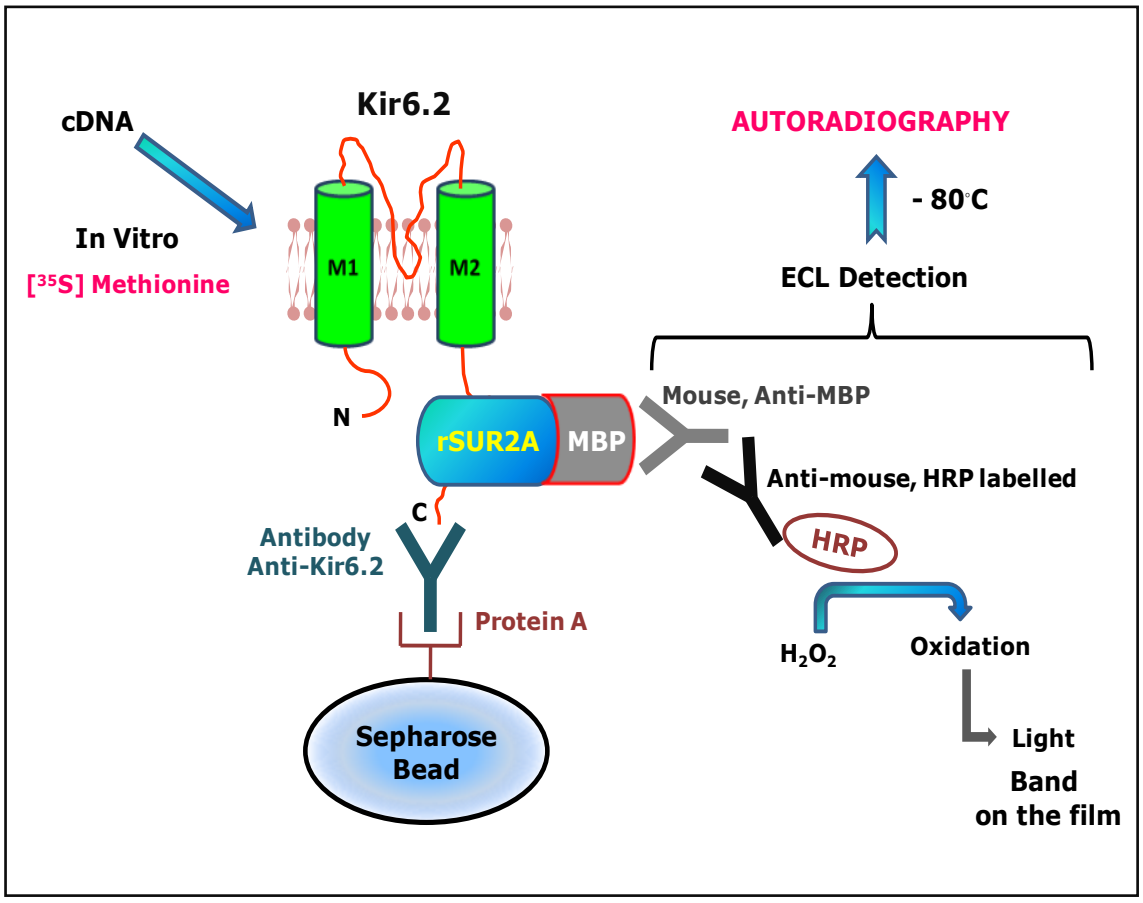

Figure 2-2 Schematic illustration of co-immunoprecipitation assay.

The various Kir6.2 mutant constructs were expressed in vitro and the MBP-SUR2A-CTC fragment-Kir6.2 construct complexes were probed by co-immunoprecipitation using anti-Kir6.2. The protein complex was captured by protein A-Sepharose. After washing to remove non-specifically adsorbed proteins, the MBP-SUR2A-CTC fragment-Kir6.2 construct complexes were eluted and analysed by SDS-PAGE followed by Western blot using mouse, anti-MBP antibody. ECL detection was used to visualize immunodetected bands. At the end of the experiment the membrane was exposed to the film at -80 ºC for autoradiography to normalize the results.

The next morning, samples were centrifuged at 10,000 x g for 1 minute at 4 ^{o}C; supernatants were removed with a syringe and discarded. Pellets were washed by centrifugation at 1,000 x g 4 times with 0.5 ml IP (immunoprecipitation) buffer (20 mM Tris-HCl (pH 7.4), 0.1% Triton X-100). Then samples were incubated with 20 µl of Laemmli denaturation buffer at room temperature for 30 min. Samples were centrifuged at 10,000 x g for 5 min and supernatants were electrophoresed by SDS-PAGE followed by Western blot. The membrane was probed with monoclonal anti-maltose binding protein (SIGMA) as primary antibody (1:5000) and then anti-mouse IgG horseradish-peroxidase conjugate (from sheep, Sigma, 1:2000) and detected using the enhanced chemiluminescence (ECL) detection system.

2.2 Molecular Biology

2.2.1 The Polymerase Chain Reaction (PCR)

Target DNA sequence was amplified using polymerase chain reaction (PCR). PCR is the most common method for the rapid amplification of a DNA fragment. Site-directed mutagenesis based on PCR was used in order to make a Kir6.2 D323K + K338E double mutant. In this method, any base difference between the amplification primer will be incorporated in the future template through PCR.

For construction of the Kir6.2 D323K + K338E double mutant four oligonucleotide sequences were used. Two of these primers were mutagenesis primers which were reverse complements of one another. They were designed to introduce the desired mutation and anneal to the same position on the template as one another but in different directions. Another two primers were designed to link the two fragments together to form the complete fragment with the mutation. Schematic drawing of Kir6.2 D323K + K338E double mutant construction by overlap PCR is shown in figure 2-3.

PCR	Primers	Sequence (5´ to 3´ Direction)
PCR1	62C1	GCGTCACAAGCATCCACTC
	DK2	TAGCGGCCCTTCTCCTCGGCCACGATGG
PCR2	DK3	GCCGAGGAGAAGGGCCGCTATTCTGTGGACT
	JR04	CGTAGAATTCCCCCAGCACTCTACATACCG
PCR3	62C1	GCGTCACAAGCATCCACTC
	JR04	CGTAGAATTCCCCCAGCACTCTACATACCG

Table 2-2 Sequences of PCR primers used for construction of Kir6.2 D323K + K338E double mutant.

In PCR 1, 62C1 primer was used as 5 prime terminus forward primer and DK2 as reverse mutagenesis primer and in PCR 2, DK3 as forward mutagenesis primer and JR04 as 3 prime terminus reverse primer. In overlap PCR (PCR3), 62C1 was used as 5 prime termini forward primer and JR04 as 3 prime terminus reverse primer.

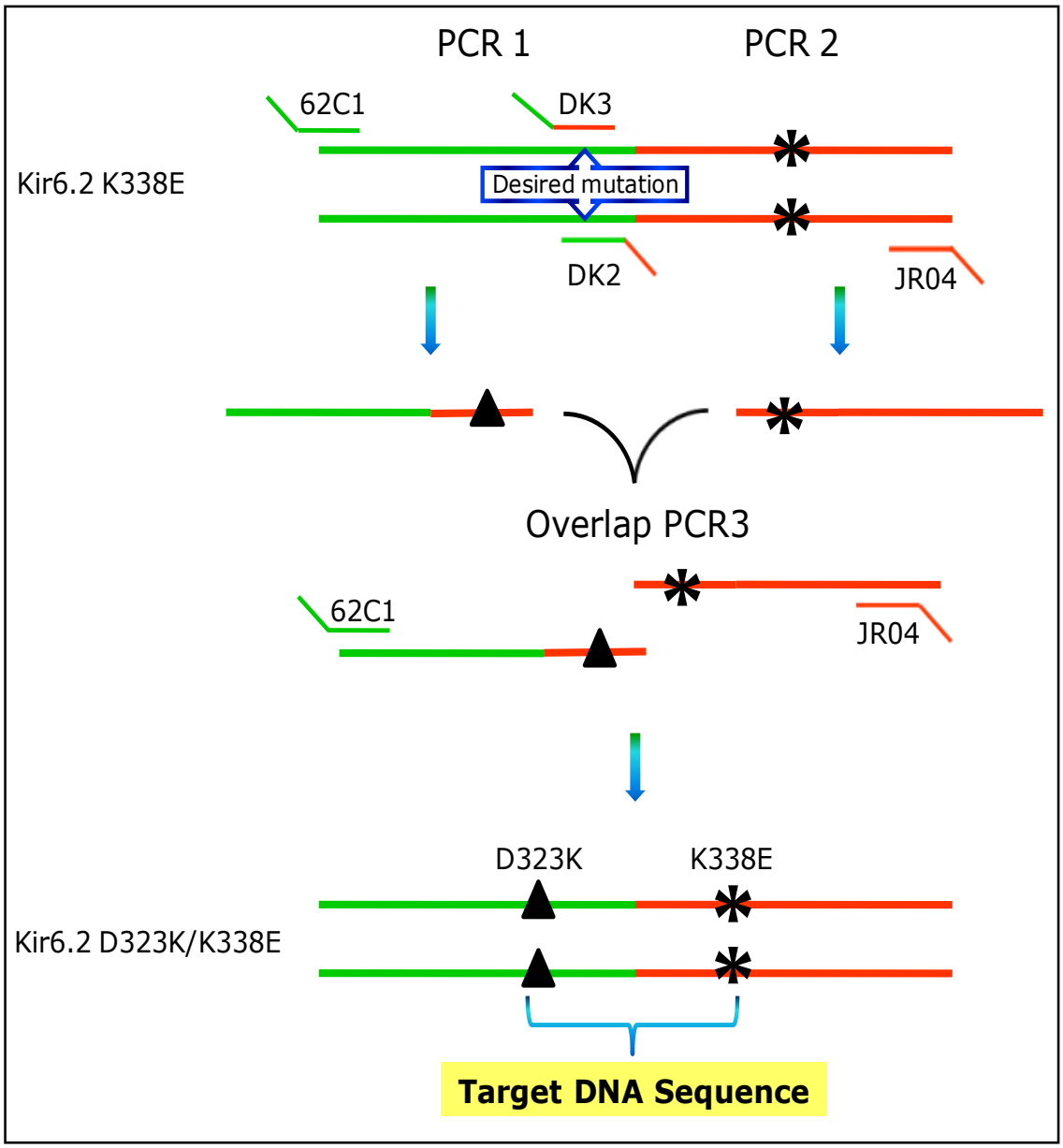

Figure 2-3 Schematic overview of Kir6.2 D323K + K338E double mutant construction by overlap PCR.

For construction of the Kir6.2 D323K + K338E double mutant, pcDNA3.1/myc/ HisA/rKir6.2 K338E was used as a template DNA for PCR1 and PCR 2. 62C1, DK2, DK3 and JR04 represent the primers used for amplifying the cDNA. Primers DK2 and DK3 were used to introduce the mutation and primers 62C1 and JR04 were used to introduce the overlap.

All PCR were performed using a PCR Sprint Thermal Cycler (Thermo Scientific) and all reagents which were used for PCR were from New England BioLabs. Every reaction was set up in a 0.5 ml tube with a total volume of 50 µl per reaction. For each reaction, 50 ng of template DNA and 12.5 pmol of each primer were used. PCR1 and PCR2 were set up with pcDNA3.1mycHisA/rKir6.2K338E (0.5 µg/µl) as a template and produced a ~ 600 bp and a 300 bp product respectively. Pipetting instruction in order to make a volume of 50 µl reaction for PCR1 and PCR2 were as follows; 32.5 µl nuclease-free H_2O, 10 µl 5x Phusion HF buffer, 1 µl dNTPs (10 mM), 2.5 µl of each primer (5 pmol/µl), 1 µl template DNA (50 ng/µl) and 0.5 µl Phusion DNA polymerase (0.02 U/µl).

A three step protocol (New England, BioLab) was used for thermal cycling conditions. Initial denaturation of the template DNA was done in first cycle at 98 ºC for 30 seconds. Following this, 30 cycles of: 98 ºC for 5 to 10 seconds (denaturation), about 54 ºC for 10 to 30 seconds (annealing) and 72 ºC for 15 to 30 seconds per 1kb (extension). A final extension was done at 72 ºC for 5 to 10 min.

Cycle Step	Temperature	Time	Cycles
Initial Denaturation	**98 °C**	**30 s**	**1**
Denaturation	**98 °C**	**5-10 s**	**25-30**
Annealing	**54 °C**	**10-30 s**	
Extension	**72 °C**	**15-30 /1kb**	
Final Extension	**72 °C**	**5-10 min**	**1**

Table 2-3 Three step PCR cycling instructions.

The overlap PCR reaction was performed, as described for PCR1 and PCR2, with 62C1 and JR04 as primers. For this reaction PCR1 and PCR2 products were used as template DNA to produce a ~ 929 bp product.

The products of PCR1, PCR2 and overlap PCR (PCR3) were analysed and visualized by agarose gel electrophoresis (section 2.2.2) and the result shown in Chapter 4, figure 4-1.

2.2.2 Agarose Gel Electrophoresis (AGE)

Agarose gel electrophoresis was used for many purposes; to analyse the product of PCR (mini-gel), to estimate the DNA concentration and for gel extraction (midi-gel). All PCR products were analysed on a 1% agarose mini-gel.

The comb and the tray were decided by the size of the required gel for experiments. The ends of the tray were taped with autoclave tape and the desired comb was set to an appropriate height. Appropriate gel volume (mini = 50 ml and midi = 100 ml) was made by adding 0.5 g for mini-gel or 1 g for midi-gel (1%) of agarose (Electrophoresis Grade Invitrogen) to 1x TAE in a flask and heating in the microwave for about 1-2 min at power-setting 3. Then the flask was placed on a shaker to cool, when the gel was lukewarm, 5 µl of ethidium bromide (10 mg/ml) was added.

The gel was poured onto the prepared tray and allowed to set for 30 min. Then the gel was placed in a tank containing 1x TAE with 5 µl/100ml ethidium bromide (10 mg/ml). The volume of 1x TAE was adjusted to cover the gel. 3 µl of loading buffer (0.05% (w/v) bromophenol, 5% (v/v) glycerol and desired volume of dH_2O) was added to each sample and the samples were loaded on the gel. The electrophoresis unit was connected

to a power pack (Bio-Rad) and the samples were migrated for 75 min at 100 V at room temperature. A MultiImage™ Light Cabinet and AlphaImager 1220 V5.5 software were used to visualize and analyse the agarose gel.

2.2.3 Gel Extraction

PCR1 and PCR2 were run on a midi gel for gel extraction to purify and elute the DNA. For gel extraction, a MinElute Kit Protocol (QIAGEN) using a microcentrifuge was used. The bands were detected in the dark room under UV light and then the gel slices were excised from the agarose gel with a clean scalpel under UV. The agarose fragment was placed into a 1.5 ml microfuge tube. Three volumes of buffer QG to 1 volume of agarose gel slice were added, assuming 100 mg = 100 µl. The 1.5 ml microfuge tube was incubated at 50 ºC for 10 min and the tubes were mixed by vortexing every 2 min during the incubation until the gel slices were completely dissolved. After the gel slices had dissolved completely, the colour of the mixture was checked, yellow (indicator dye), which is similar to QG buffer without dissolved agarose. Following this, 1 gel volume of isopropanol was added to the tubes and mixed by inverting the tubes several times.

A MinElute column was placed in a provided 2 ml collection tube and the sample was applied to the column and centrifuged for 1 min at 10,000 x g to bind the DNA. The flow-through was discarded and the columns were placed in the same collection tubes. Buffer PE (750 µl) was added to wash the columns and centrifuged for 1 min at 10,000 x g. The flow-through was discarded and the columns again centrifuged at the same speed for a further minute. The MinElute columns were placed into a clean 1.5 ml microfuge tube and 20 µl of buffer EB (10 mM Tris-HCl, pH 8.5) was added to the

centre of each column to elute the DNA and the column was allowed to stand for 1 min. Following this, the DNA was eluted by centrifugation of the MinElute columns for 1 min at 10,000 x g.

2.2.4 Purification of PCR Products

After PCR reaction, the products were purified by using the MinElute PCR Purification Kit Protocol using a microcentrifuge. Five volumes of PB buffer to 1 volume of the PCR reaction was added and mixed. Following this, the purification was performed as described in the previous section.

2.2.5 Restriction Enzyme Digestion

Appropriate enzymes were used according to New England, BioLabs recommendations to restrict digestion of DNA. Two restriction digest reactions of 20 µl as a total volume, one with 10 µl of PCR3 products and one with 10 µl of plasmid DNA/Kir6.2 K338E were set up. For each reaction, 0.1 volume of 10x buffer NEB3 (1X NEB 3 buffer; 100 mM NaCl, 50 mM Tris-HCl, 10 mM $MgCl_2$, 1 mM DTT, pH 7.9) was used. The reactions were incubated with the following restriction enzymes; first 1 µl EcoRI (20,000 U/ml) at 37 ^{o}C for 5 hrs and then with 1 µl Bst II (10,000 U/ml) overnight at 60 ^{o}C. Then the vector was treated with shrimp alkaline phosphatase as described in the next section.

2.2.6 Dephosphorylation of Vectors

Dephosphorylation is a necessary step prior to ligation to prevent the religation of the vectors by removing phosphate groups from both 5 prime termini. Dephosphorylation of Vectors step was done after restriction digestion. Six microliters of nuclease-free H_2O, 3 µl of 10x buffer for SAP (Fermentas) and 1 µl of Shrimp Alkaline Phosphatase (SAP, 1 U/µl) (Fermentas) were added to the 20 µl of plasmid DNA for a total volume of 30 µl. Then SAP treated plasmid DNA was incubated at 37 ^{o}C for 30 min.

2.2.7 Ligation

Following restriction enzyme digestion, the insert DNA was purified using MinElute PCR purification as described in section 2.2.4 and the vector was SAP treated (section 2.2.6). These two steps were carried out prior to ligation of insert and vector. The quantity of vector and insert DNA was estimated from the intensity of bands upon agarose gel electrophoresis compared to standards loaded. The reaction of ligation was comprised of a 1:3 molar ratio of vector: insert DNA.

With a total volume of 20 µl, the ligation reaction was set up in the following pipetting order: 12 µl nuclease-free H_2O, 4 µl ligase buffer (5X, Invitrogen), 1µl vector (30 fmol), 2µl insert (90 fmol), and 1µl T4 DNA ligase (1 U/µl Invitrogen). The ligation reaction was mixed and incubated at room temperature for 30 min and transformed into competent DHα *E. coli* cells (next section).

2.2.8 Transformation of Plasmid DNA to Host Cells

A heat shock method was used for transformation of plasmid DNA to the host cells. Fifty microliters of competent DHα *E. coli* cells, which were stored frozen in 14 ml polythene tubes, were thawed on ice. Four microliters of ligation mixture was added to 50 µl *E. coli* cells. The mixture was mixed and placed on ice for 30 min. Then the 14 ml polythene tube was placed at 42 ^{o}C in a water bath for 45 s (heat shocked) and placed on ice for 2 min. SOC medium (950 µl; Appendix A) was added to the tube and the tube was placed into an orbital incubator and incubated at 37 °C with shaking at 230 rpm for 1 hr. Following this, the cells were transferred to a 1.5 ml microfuge tube and centrifuged at 10,000 x g for 5 min, 800 µl of supernatant was removed and the pellet was resuspended with the remaining 200 µl supernatant. This liquid culture was plated out with a sterile glass spreader onto a prepared agar plate which contained LB medium with Amp. Then the agar plate was incubated at 37 °C with no humidification and no CO_2 using a Queue (CAMLAB) cell culture incubator for overnight. The colonies that grew were used for mini- and midi-preparation of plasmid DNA.

2.2.9 Mini-Preparation of DNA

A single colony was removed from the agar plate with a 10 µl micropipette tip and inoculated to 5 ml LB medium containing Ampicillin (Appendix A). In order to grow the inoculations, the liquid culture was placed in an orbital incubator and incubated overnight at 37 °C with shaking at 230 rpm. The following day, the liquid culture was centrifuged at 6000 x g, 4 °C for 20 min to collect the cells.

The buffers for these following steps were provided by the QIAGEN, Miniprep Kit. The pellet was completely resuspended in 250µl of buffer P1 (resuspension buffer; 50 mM Tris·Cl, pH 8.0, 10 mM EDTA, addition of 100 µg/ml RNase A). After being transferred to a microfuge tube, 250 µl of buffer P2 (lysis buffer; 200 mM NaOH, 1% SDS (w/v)) was added and mixed thoroughly by inverting the tube ten times. Buffer N3 (350 µl) was added and immediately afterwards mixed thoroughly by again inverting the tube ten times. The mixture was then was centrifuged for 10 min at 17,900 x g in a table-top microcentrifuge. The supernatant was applied to the QIAprep spin column by pipetting. A second centrifugation was done for 1 min. The flow-through was discarded and the QIAprep spin column was washed by adding 0.75 ml buffer PE followed by a further centrifugation for 1 min. The flow-through was discarded and a further 1 min of centrifugation was performed to remove residual wash buffer. The QIAprep column was placed in a clean 1.5 ml microfuge tube. 50 µl of buffer EB (10 mM Tris-Cl, pH 8.5) was added, to elute DNA, to the centre of each QIAprep spin column, which was left to stand then stood for 1 min, and finally centrifuged for 1 min.

2.2.10 Restriction Mapping Analysis of Miniprep DNA

Two restriction digest reactions for Miniprep products, colony 1 and 2 were set up in a final volume of 20 µl containing 10 µl of each colony. For each reaction 0.1 volume of 10x buffer NEB1 (New England, BioLabs) was used. The reactions were incubated with restriction enzyme (1 µl Kpn1, 10,000 U/ml, New England BioLabs) at 37 ^{o}C for 4 hrs. Following this, the products were analysed on a 1% agarose gel and the results

shown in Chapter 4. Both of the colonies were submitted to DNA sequencing (PNACL, at University of Leicester, section 2.2.13).

2.2.11 Midi-Preparation of DNA

A single colony was removed from the agar plate with a 10 µl micropipette tip and inoculated to 150 ml LB media containing Ampicillin (Appendix A). The liquid culture was placed in an orbital incubator and incubated overnight at 37 °C with shaking at 230 rpm. The following day, the liquid culture was centrifuged at 4000 g at 4 °C for 20 min to collect the cells. The supernatant was discarded and the pellets were completely resuspended with 6 ml of buffer P1 (resuspension buffer; 50 mM Tris·Cl, pH 8.0, 10 mM EDTA, addition of 100 µg/ml RNase A). The next step was to add 6 ml of buffer P2 (lysis buffer; 200 mM NaOH, 1% SDS (w/v)) and mix thoroughly by vigorously inverting the tube 10 times followed by incubation at room temperature for 5 min. During this time the QIAfilter Cartridge was prepared and placed into a convenient tube or a QIArack. Six millilitres of chilled buffer P3 (neutralization buffer; 3.0 M potassium acetate, pH 5.5) was added to the lysate and mixed immediately and thoroughly by vigorous inversion 10 times. The lysate was then poured into the barrel of the QIAfilter Cartridge and incubated at room temperature for 10 min. The HiSpeed Midi Tip was equilibrated by applying 4 ml QBT buffer (equilibration buffer; 750 mM NaCl, 50 mM MOPS, pH 7.0, 15% isopropanol (v/v) and 0.15% Triton® X-100 (v/v)) and the column was emptied by gravity flow. The cap of the QIAfilter outlet nozzle was then removed and the plunger was gently inserted into the QIAfilter Midi Cartridge. The cell lysate was filtered into the previously equilibrated HiSpeed Tip. The cleared

lysate was then loaded onto the resin by gravity flow. The HiSpeed Midi Tip was washed with 20 ml QC buffer (wash buffer; 1.0 M NaCl, 15–25°C, 50 mM MOPS, pH 7.0 and 15% isopropanol (v/v)). The DNA was eluted with 5 ml QF buffer (elution buffer; 1.25 M NaCl, 50 mM Tris·Cl, pH 8.5 and 15% isopropanol (v/v)). The DNA was precipitated by adding 3.5 ml of isopropanol at room temperature to the eluted DNA then mixed and incubated at room temperature for 5 min. During the incubation, the plunger was removed from a 20 ml syringe and the QIAprecipitator Midi Module was attached onto the outlet nozzle. The QIAprecipitator was placed over a waste bottle and the isopropanol mixture was transferred into the 20 ml syringe and the plunger inserted. The isopropanol mixture was then filtered through the QIAprecipitator using constant pressure. Afterwards the plunger was removed from a new 5 ml syringe and the QIAprecipitator was attached onto the outlet nozzle. The QIAprecipitator outlet was held over a 1.5 ml collection tube. One millilitre of TE buffer (10 mM Tris·Cl, pH 8.0 and 1 mM EDTA) was added to the 5 ml syringe, the plunger inserted and the DNA eluted into the collection tube using constant pressure. The QIAprecipitator was removed from the 5 ml syringe, the plunger was pulled out and then the QIAprecipitator was reattached to the 5 ml syringe. The elute was then transferred to the 5 ml syringe and then re-eluted for a second time into the same 1.5 ml tube.

2.2.12 DNA Quantification

A Qubit™ fluorometer (Invitrogen™) with the Quant-iT™ dsDNA BR Assay Kits was used to measure the DNA concentration. For each assay, a new calibration was performed by using Quant-iT™ dsDNA BR standard 1 and Quant-iT™ dsDNA BR standard 2 as standards for calibration. The standards 1 and 2 were prepared by adding 10 µl of each standard to 189 µl of Quant-iT™ dsDNA BR buffer. Samples were prepared by adding 1 µl of DNA to 198 µl of Quant-iT™ dsDNA BR buffer and finally 1 µl of Quant-iT™ dsDNA BR reagent was add to the each tube. The final volume of 200 µl for each standard and sample was added to a 0.5 ml Qubit™ assay tube, mixed by vortexing and incubated at 22 °C in a PCR Sprint Thermal Cycler for 2 min. After calculation of DNA concentration, the DNA was diluted with 10 mM Tris-HCl (pH 8.0) to the concentration of 0.5 µg/µl and stored at –20 °C.

2.2.13 DNA Sequencing

DNA sequencing was performed to confirm successful construction of the Kir6.2 D323K/K338E double mutant. Pure DNA 500 ng in volume of 8 µl with 100 µl of 62 C1 primer (1 pM/µl) was sent to sequencing service unit (PNACL, University of Leicester) and the products were analysed and confirmed using a 3730 automated sequencer. One microliter of DNA from the Miniprep was analysed on a 1% agarose gel to estimate the DNA concentration, before sending for DNA sequencing (Chapter 4, figure 4-3).

Constructs used in this study
Kir6.1 E332K
Kir6.1 R347E
Kir6.2 D323K
Kir6.2 K338E
SUR2A E1318R
SUR2A K1322D
SUR2A Q1336E
SUR2A K1322D + Q1336
MBP-SUR2A-CTC fragment (amino acids 1294-1403)
TM1070-Kir6.2 NC (C-terminal-His6 tag)

Table 2-4 List of the all constructs used in this study (Appendix B).

All plasmid vector maps (information) for the above listed constructs can be found in the Appendix B.

2.3 Cell Culture

2.3.1 Culture of Human Embryonic Kidney 293 (HEK-293) Cells

Human embryonic kidney 293 (HEK-293) a gift from the Department of Cell Physiology and Pharmacology (Leicester) were cultured at 37 ºC in a humidified atmosphere containing 5% CO_2 / 95% air. Minimum Essential Medium Eagle, alpha MEM (Sigma) was used with supplementation of 10% fetal bovine serum (FBS) and 1% glutamine. The cells were healthy and had greater than 90% viability before transfection. The culture medium was changed every 3-4 days until the cells were 70 - 80% confluent. For electrophysiological study the cells were used at passages 10 to 15 and the same seeding conditions were maintained between experiments.

2.3.2 Poly-L-lysine Coating of Glass Coverslips

Glass coverslips (Warner instruments) were sterilized by autoclaving and placed in a 6-well plate. One and a half millilitres of 1x Poly-L-lysine solution (from 10x Poly-L-lysine solution, Sigma) which was diluted with sterile phosphate buffered saline (PBS: 137 mM NaCl, 2.7 mM KCl, 8 mM Na_2HPO_4, and 2 mM KH_2PO_4, pH 7.4 from Invitrogen) was added to each well. After 10 to 15 min incubation in 1x Poly-L-lysine solution, the solution was discarded and the coverslips were washed three times with PBS. The coverslips were allowed to dry completely under a cell culture hood before the cells were plated out and seeded at 5 x 10^5 cells per well into 6-well plates and 2 ml of Alpha MEM media was added to each well. These cells were transfected (next section) and used for inside-out patch (Chapter 6).

Construct	Plasmid Vector	Insert	GFP Co-expression
Kir6.1 E332K	pcDNA3.1myc/hisA	Full length rat Kir6.1	—
Kir6.1 R347E	pcDNA3.1myc/hisA	Full length rat Kir6.1	—
Kir6.2 D323K	pcDNA3.1myc/hisA	Full length rat Kir6.2	—
Kir6.2 K338E	pcDNA3.1myc/hisA	Full length rat Kir6.2	—
SUR2A E1318R	pIRES2-EGFP-F	Full length rat SUR2A	+
SUR2A K1322D	pIRES2-EGFP-F	Full length rat SUR2A	+
SUR2A Q1336E	pIRES2-EGFP-F	Full length rat SUR2A	+
SUR2A K1322D + Q1336	pIRES2-EGFP-F	Full length rat SUR2A	+

Table 2-5 Plasmid vector, insert and green fluorescent protein co-expression information for the constructs used in electrophysiological study.

This table shows all the mutations used for patch clamp recording with information on the plasmid vector, insert and green fluorescent protein (GFP) co-expression. The GFP co-expression represented as plus and no co-expression as minus, respectively. The information for plasmid vector maps for the above constructs can be found in the Appendix B.

2.3.3 Transfection of Human Embryonic Kidney 293 (HEK-293) Cells with Kir6 and SUR2A Genes

As described in previous the section the HEK-293 cells were split and plated, 5 x 10^5 cells per well, in a 6-well culture dish 24 to 48 hrs before transfection in 2 ml of alpha MEM media. Next the cells (50 - 80% confluent) were transfected using a ratio of 7:2, microliters FuGENE® HD transfection reagent (Roche) to micrograms total cDNA (from a purified plasmid stock (0.5 µg/µl), respectively. The culture medium was removed from the 6-well plate and replaced with 2 ml/well fresh alpha MEM media (37 ºC). The transfection reaction was done in a 1.5 ml microfuge tube for each well and the following materials was added to the reaction; 100 µl of Ultra MEM (37 ºC), 1 µg rat cDNA for each subunit (Kir6 and SUR2A) which also contained the gene for the enhanced green fluorescent protein (EGFP) and finally 7 µl the FuGENE® HD transfection reagent. Transfection reactions were mixed vigorously by vortex and incubated at RT for 15 min.

Finally, the reactions were added to each well and the 6-well plate was incubated at 37 ºC in a 5% CO_2 (incubator) for 48-72 hrs before electrophysiological study (Chapter 6).

2.3.4 Preparation of Transfected Human Embryonic Kidney 293 (HEK-293) Cells for Electrophysiological Study

The growth medium was discarded from transfected HEK-293 cells and the cells were washed once with sterile PBS. After washing with PBS, the cells were treated with 2 ml

of 1x trypsin-ethylenediaminetetraacetic acid (EDTA) solution (0.5 g/l porcine trypsin and 0.2 g/l EDTA, Sigma) just long enough to detach the cells (1-2 min). Subsequently the cells were incubated for 5 min with 5 to 10 ml of alpha MEM medium in an incubator (37 ^{o}C with 5% CO2) to stop the trypsinization. After that, the cell suspension media was centrifuged at 100 x g for 3 min and the media was discarded and the cells were resuspended gently and washed two times with 5 ml and 1 ml extracellular solution (ECS, Tyrode's solution) respectively. The cell suspension (1 ml) was used for electrophysiological study by whole-cell recording (Chapter 6).

2.3.5 Preparation of Transfected HEK-293 Cells for Analysis of Total Surface Expression of Wild type and Mutated Kir6.2/SUR2A Channels

The Kir6.2/SUR2A channel subunits were co-transfected heterologously in HEK-293 cells as described in (section 2.3.3). The cells were washed three times by centrifugation in 20 mM Tris (pH7.5)/0.9% NaCl. Then 200 µl of 2% sodium dodecyl sulphate, SDS (in water) was added to solubilise the cells. Following that, the cells were scraped off in 2% SDS and pipetted into microfuge tubes. The cells were sonicated using a Soniprep 150 (MSE) at 4 ^{o}C, 3 times for 5 s with 20 s setting (rest). Finally the concentration of samples was determined by Bradford protein assay (described in section 2.1.2) and 10 µg protocol of each sample was loaded on a 10% polyacrylamide gel for Western blot analysis.

2.4 Electrophysiological Study of ATP-Sensitive Potassium Channel Subtypes

2.4.1 Introduction of Electrophysiology Study

Electrophysiological studies permit the measurement of ionic currents across the cell membrane from single cells or tissue. These techniques help understanding of the physiological and pathophysiological functions of excitable cells and tissue.

Intracellular measurements on animal cells were first achieved in 1939 by Hodgkin and Huxley (1952) at Plymouth and by Curtis and Cole (K. S. Cole 1949) at Woods Hole Massachusetts.

To study the function of wild type and mutated K_{ATP} channel subtypes, two patch clamp configurations were applied in this project, whole-cell and inside-out patch configurations.

2.4.2 The Basis of the Voltage Clamp Technique (Ohm's Law)

The voltage clamp technique was first invented by Marmont and Cole (1949) and intensely developed by Hogdkin and Huxley (1952). Generally, voltage clamp measures an electric current (ion flow across a cell membrane) while the membrane voltage is held constant (clamp) with a feedback amplifier. In more detail, the advantages of voltage clamp are that membrane ionic currents and capacitive currents are separated in this technique. Also, measuring the current when the voltage is controlled allows you to

study the channel behaviour much easier rather than having a freely changing voltage across the membrane (Halliwell et al. 1994). The voltage clamp is mainly convenient when investigating responses to membrane potential changes particularly the activation of voltage-gated channels.

The theory behind voltage clamp technique can be described as: to measure the total membrane current, I_m, two components are required, the ionic current, I_{ionic}, and the capacitance current, C_m.

$$\boldsymbol{I_m = I_{ionic} + C_m \, dV/dt}$$

The ionic current reflects the movements of ions through ion channels. The capacitance current is the accumulation of charge on one membrane side and its depletion on the other for a given voltage. Whenever, membrane potential is changed this charge stored on the membrane capacitor must be changed – giving rise to the capacitance current. With the voltage clamp techniques, once the voltage has been stepped to a new potential the membrane potential is held at a constant level, to create a zero value for d*V*/d*t*. This creates an initial capacitance transient that is brief (as voltage is changed) and then after that current can be measured that is completely ionic (Aidley and Stanfield 1996).

To investigate ion channel properties the voltage clamp technique is often performed with the help of native Xenopus Oocytes. Two microelectrodes are placed within the Oocyte. One is used to record the membrane voltage and the other passes a current to hold the cell membrane at a constant voltage (Ogden and Stanfield 1994). The data is used to calculate the voltage and time dependent kinetics of the ionic currents. Extensions of the voltage clamp method have been developed in order to investigate a single channel activity such as fluctuation analysis, usage of artificial lipid bilayers and

the patch clamp technique (Aidley and Stanfield, 1996; Ogden and Stanfield, 1994). The latter, the patch clamp technique, will be discussed in section 2.4.3.The measurement of ion channel current is based on Ohm's law.

Ohm's law: $I = V/R$ *or* $V = IR$

Here the movement of charged ions across the membrane is the current (I) and measured in amperes (A). Voltage (V) is the driving force needed for the charged ions to move through the channel and is measured in volts (V) and the resistance through the channel is represented as R and measured in ohms (Ω). From the equation, it can be seen that the current is inversely proportional to the resistance. Thus, when the voltage across a membrane is held constant, from Ohm's law, you can measure the current, the smaller the resistance, the larger the current and vice versa. For these studies, the gap free recording (continuous recording) was used, which gives the ability to measure the current by keeping the voltage constant during the recording.

2.4.3 Patch Clamp Technique

The patch clamp technique was invented in 1976 by Neher and Sackmann, for which they were awarded the Nobel Prize in 1991. Patch clamping is one of the very common electrophysiological techniques to study ion channel function. As described above, by clamping the voltage of an isolated excitable cell membrane, the currents that flow through ion channels may be measured. Very small currents, 10^{-12} A (pA) through ion channels can be measured by using the patch clamp technique.

In brief, for patch clamp recording a glass pipette containing intracellular solution and an electrode, which was connected to an amplifier, was lowered into the bath solution by a micromanipulator. The pipette was moved close to the cell in order to make a close contact with the cell membrane and form a tight seal. For whole-cell recording, when a gigaseal was achieved, a suction was applied to the pipette to rupture the cell membrane. For inside-out recording, when the gigaseal was formed without suction, the patch pipette was quickly withdrawn from the cell. Then the currents were measured through the electrode, which was connected via an electrical circuit to an amplifier.

The glass pipettes, which had seal resistances (Rt) of 3 to 6 mega-ohms (MΩ) were pulled using a vertical pull type with automated double mode electrode puller (Narishige model PC-10). The currents were amplified using an axopatch 200B amplifier (Axon Instruments) and the signals were converted from the amplifier into a digital signal on Axon Digidata 1440A (Molecular devices). For acquisition and analysis of patch-clamp data, Clampex 10.2 and Clamfit 10.2 version software (molecular devices) were used, respectively.

2.4.3.1 Technical Considerations

As described in previous section, in the patch clamp techniques an electrode is used, which is placed on the cell surface. By using an electrode, suction is applied to create a high resistance seal (gigaseal, derives from the range of the seal measured to a gigaohm) between the electrode and the surface of the cell creating an isolated area. There are two reasons for the need of a high seal resistance. First, if there is a high seal resistance then the membrane patch receives a more complete electrical isolation. Also,

if there is a high seal resistance then the current noise of the recording will be less. This allows single channel currents, with amplitude of 1 pA, to have a good time resolution (Ogden and Stanfield, 1994). In other words, the gigaseal reduces the noise level of the recording extremely effectively and with this it increases the single channel currents' resolution (Hamill et al. 1981). It is essential that there is minimal leakage between the cell membrane and the pipette otherwise the noise will increase and as stated no recording can be made of the current (Aidley and Stanfield, 1996; Ogden and Stanfield, 1994). Moreover, it is also crucial to have an equally low noise recording system. The most vital part is the current-to-voltage converter, the headstage, which receives the input directly from the patch electrode (Aidley and Stanfield, 1996).

There are four condition requirements for gigaseal formation. (1) The cell membrane surface ought to be clean and free of extracellular matrix and connective tissue. (2) Solutions should be filtered using 0.2 μm filters, detergent-free, and cell cultures should be washed several times to remove serum in order to get rid of any dust and macromolecules such as serum components in tissue culture media. (3) The tip of the pipette must be clean; this is mostly done by fire-polishing. (4) In order to keep the pipette free from debris, before seal formation a small positive pressure is applied to the pipette creating a solution outflow from the tip of the pipette (Ogden and Stanfield, 1994).

There are intrinsic limitations on the degree of time resolution, which can be received from patch clamp records of single channel activity. These records are commonly filtered to remove high frequencies of noise, which is an unavoidable consequence of the recording system. There is some frequency limit for all amplifiers and other electronic devices; a limit which the above frequency cannot respond (Aidley and Stanfield, 1996).

Whole cell recording is a useful technique for measuring a broad range of ionic currents. However, the series resistance (Rs) of the recording patch pipette limits this technique to study ion channels particularly when measuring rapid ionic currents (Aguilar-Bryan and Bryan 1999; Molecular 2008; Sherman et al. 1999). To overcome this limitation it is required to compensate for Rs by increasing the bandwidth.

The Rs generates two unwanted effects in whole cell voltage clamp recordings. First, the series resistance initiates a voltage error (IR) that causes the cell membrane voltage (Vm) to deviate from the wanted clamping voltage at any time the ionic current flows. Secondly, the Rs causes lowering of the temporal resolution of the voltage clamp, usually to a level, which does not allow the accurate measurement of the rapid physiologic processes.

In regards to whole cell patch clamp configuration (mainly used in this study), lowering of the temporal resolution of the voltage clamp by Rs makes the measurements very difficult (Molecular Devices 2008; Sherman et al. 1999). For that reason, the aim of Rs compensation is to decrease, and preferably eliminate, Rs errors from whole-cell voltage clamp recordings. It is worth mentioning, the liquid junction potential (bath potential minus the potential inside the pipette) can cause voltage error as a result of current flow through the grounding electrode (Molecular Devices 2008).

Data filtering frequencies and the signal conditioning are also very important subjects, which need to be considered when studying ion channels by using patch clamp technique. In other terms, one important question, which also needs to be answered, is, why should signals be filtered? Selected frequencies can be removed from the signal by a filter, which is a circuit. To remove undesired signals and noise from the data, filtering is frequently performed. Low-pass filtering is generally used to perform the

filtering, limiting the data bandwidth by removing signals and noise above the corner frequency of the filter. This is particularly important when studying single-ion channels (Molecular Devices 2008). In addition, the acquisition rate is very important when measuring currents from single-ion channels. Since, if your system for recording is not fast enough, you will loss information about the channel gating (opening). For that reason, acquisition rate can be vital for fast recordings (Molecular Devices 2008).

As a final point to be considered is the pipette properties in both whole cell and single-channel recording. Reducing the noise of the pipette is vital in both above mentioned recording, particularly in the single-channel recording is more important. As mention earlier, in whole cell recording the pipette resistance is the main source of noise. Therefore, the noise caused by the pipette is not as important as in single-channel recording. In whole cell recording, the resistance of a pipette must not exceed a few megohms, in order to limit the voltage errors. However, in single-channel recording this limitation of the pipette resistance is not necessary as much as in whole cell recording. In single-channel recording, a significant increase of the noise can occur when the pipette resistance reaches to several tens of megohms (Molecular Devices 2008).

2.4.4 Whole-Cell Patch Clamp Configuration

Whole-cell recording mode measures the currents of ion channels across the entire plasma membrane of a single cell. The patch pipette which contains the intracellular solution (pipette solution) and an electrode inside the pipette was used to achieve a high resistance seal (gigaseal) between the pipette and the cell membrane. When a gigaseal was achieved it was possible to measure the currents after rupturing the cell membrane

by applying suction. The voltage-clamping mode was used to keep the voltage produced on membrane constant, to permit the entire membrane current recording. Functional characterization of different subtypes and mutated isoforms of K_{ATP} channels were studied in the whole-cell configuration.

2.4.4.1 Whole-Cell Recording of Kir6.2/SUR2A Channels Currents

Wild type and mutated Kir 6.2 and SUR2A isoforms were co-expressed heterologously in HEK-293 cells using the Fugene transfection technique (section 2.3.3). After 48 to 72 hrs the currents of transfected cells were measured, which were prepared as a cell suspension (section 2.3.4). For whole-cell recording of Kir6.2/SUR2A channels the bath solution (electracellular solution, Tyrode's solution) contained (mM): 6 KCl, 135 NaCl, 0.33 NaH_2PO_4, 5 Na pyruvate, 10 glucose, 10 HEPES, 2 $CaCl_2$, 1 $MgCl_2$ and pH 7.4 with NaOH. The pipette solution (intracellular solution) contained (mM): 140 K^+ (30 KOH and 110 KCl), 10 EGTA, 10 HEPES, 0.1 $MgCl_2$, 1 ATP and pH 7.2 with KOH.

2.4.4.2 Whole-Cell Recording of Kir6.1/SUR2A Channels Currents

The function of the unique K_{ATP} channel isoform combination, Kir6.1 and SUR2A, was also studied by the whole-cell configuration. The wild type and mutated Kir6.1/SUR2A subunits were expressed in HEK-293 cell line by transfection and the currents were measured 48-72 hrs after transfection. The pipette solution contained (mM): 140 KCl, 10 EGTA, 10 HEPES, 2 $MgCl_2$, 1 $CaCl_2$, 0.1 NaADP, 0.1 GTP, 10 UDP, 1 ATP and

pH 7.2 with KOH (Kono et al. 2000, with modification). The bath solution was the same as that used for Kir6.2/SUR2A channel recording (previous section).

2.4.5 Inside-out Configuration (Excised Configuration)

To determine the ATP and ADP sensitivity of wild type and mutated K_{ATP} channel, inside-out configuration was used (these experiments were performed by Dr Richard Rainbow). Inside-out recording can be achieved by pulling the patch pipette quickly away from the cell membrane so a piece of the membrane attached to the pipette with the cytosolic side faces the bath solution. For that reason the bath and pipette solutions, which are used for inside-out patch have symmetrical K^+ concentration, 140 mM KCl, 1.2 mM $MgCl_2$, 2.6 mM $CaCl_2$ and 5 mM HEPES and pH 7.4 (Rainbow et al. 2004).

2.5 Structural Biochemistry

2.5.1 Protein Expression of TM1070-Kir6.2NC Fusion Protein

For expression of TM1070-Kir6.2NC fusion protein (a complex bacterial fusion construct which will be explained in Chapter 7), a heat shock transformation method (as described in 2.1.8) was used to transform the plasmid DNA (pLEICS-05/6.2NT-TM1070-CT) in to the Arctic Express competent cells. A single colony was inoculated to 3 ml LB-ampicillin (1:1000) medium. The culture was incubated at 37 °C with shaking at 230 rpm overnight. The next morning, the cells were subcultured in 20 ml

tubes with 1:100 inoculation, 100 µl of starter culture to the new LB-ampicillin (1:1000) medium. The cultures were incubated at 37 °C with shaking at 230 rpm. TM1070-Kir6.2NC fusion expression was induced with different concentrations of Isopropyl-beta-D-thiogalactopyranoside (IPTG) 0.1 mM, 0.3 mM and 1 mM, when the absorbance reached 0.8. Various concentrations of IPTG were used to optimise the induction and one incubation received no IPTG as a negative control. After induction the cultures were incubated at 13 °C with shaking at 230 rpm for 24 and 48 hrs to optimise the yield of expression. The cells were harvested by centrifugation at 4000 × g for 20 min at 4 °C. The medium were discarded and the pellets were stored at -20 °C. The expression was analysed by Coomassie blue staining and Western blot (as discussed in section 2.1.4).

2.5.2 Protein Purification by Immobilized Metal Ion Affinity Chromatography IMAC (Ni^{2+})

TM1070-Kir6.2 NC fusion protein was purified by immobilized metal ion affinity chromatography (IMAC) utilizing the polyhistidine-tag located either at the N- or C-terminals. All steps of purification were carried out in the cold room (4 ^{o}C) to minimize the risk of protein degradation.

Ni Sepharose 6 Fast Flow (GE Healthcare) was prepared as recommended manufacture before use. A 50% slurry of Ni Sepharose 6 Fast Flow was prepared by swelling with dH_2O and washing with binding buffer (pH 7.4, 20 mM sodium phosphate, 0.5 M NaCl and 20 mM imidazole) and finally adding binding buffer to make a 50% slurry. The

resin (0.5 ml) was washed with dH_2O before each experiment and equilibrated with 0.5 ml binding buffer and washed 5 ml x 2 with binding buffer.

The soluble fraction of TM1070-Kir6.2 NC fusion protein was applied to the pre-equilibrated column (0.5 ml) and the non-interacting proteins were collected in the flow-through. Following this, the column was washed 1 ml x 5 with binding buffer and the bound proteins were eluted with 1 ml x 5 of elution buffer (pH 7.4, 20 mM sodium phosphate, 0.5 M NaCl and 500 mM imidazole). Subsequently the concentration of proteins in fractions were quantified by Bradford assay (section 2.1.2) and analysed by SDS-PAGE (section 2.1.3).

2.5.3 Gel Filtration Chromatography (GFC) or Size-Exclusion Chromatography

Gel filtration chromatography (GFC) or size-exclusion chromatography is a technique, which separates the proteins on the basis of size. Following, the first step purification IMAC as described in section 2.5.2, GFC was used as a second step purification to enrich the TM1070-Kir6.2 NC fusion protein. The gel matrix, Superdex 200 (Amersham Biosciences), which is optimal for the separation of protein molecular weights in the range between 10,000 and 600,000 Daltons was used. Superdex 200 was swollen in an appropriate gel filtration buffer (pH 7.4, 20 mM sodium phosphate, 2 mM dithiothreitol and 0.5 M NaCl) overnight at 4 ^{o}C and degassed before the experiment.

Prior to performing the experiment, the column (diameter 15 mm, Pharmacia) was washed with 0.5 M NaOH and Milli-Q H_2O. In order to pack the bed (30 ml) and to

equilibrate the column with buffer, the column was washed with 2 to 3 bed volumes of gel filtration buffer (see above). The sample (0.4 µg/µl) in a buffer volume equal to 1% of the total bed volume of the column was applied on the top of gel. To achieve a better resolution the flow rate was kept low, about 0.3 ml/min. Individual chromatographic fractions (1 ml) were collected using an automated fraction collector (Pharmacia fraction collection LKB, FRAC-100). Next, the absorbance at 280 nm for each fraction (1 ml) was measured using a Nanodrop 1000 spectrophotometer (Thermo scientific) and the protein concentration for each fraction was measured using the Bradford assay as described in section 2.1.2. The purified TM1070-Kir6.2 NC fusion protein was analysed by Coomassie blue staining after SDS-PAGE.

2.6 Data Analysis

All data are presented as means ± standard error of the mean (SEM) and $P < 0.05$ considered statistically significant. Graph Pad Prism 5 software was used to analyse the results.

For co-immunoprecipitation data, one-way analysis of variance (ANOVA) followed by the Bonferroni multiple comparison test was used to calculate the p value. The K^+ currents recordings of recombinant wild type and point mutant subunit combinations of K_{ATP} channels were analysed by taking the peak current in the recording. For electrophysiological results, dose-response curve fitting was performed with nonlinear regression (curve fit) and sigmoidal dose-response variable slope with four parameters in Graph Pad Prism 5.

Chapter 3

Co-immunoprecipitation of MBP-SUR2A-CTC Fusion with Various Kir6.2 Subunit Mutant Constructs

3.1 Introduction

The aim of this sub-study was to investigate the protein-protein interaction between the cognate interaction domain (315-390 amino acids, figure 3-1) of the Kir6.2 subunit for the NBD2 in the proximal C-terminal of SUR2A (1294-1358 amino acids). In greater detail, the co-immunoprecipitation technique was used to identify specific charged residues in the distal C-terminal of the inwardly rectifying potassium channel Kir6.2 (beyond residue 315, figure 3-1) for NBD2 of sulphonylurea receptor SUR2A.

A similar strategy to that employed in the identification of interacting residues on SUR2A-CTC, as described in section 1.8.1.2, was employed for the Kir6.2 C-terminal domain. In this case, similarly charged residues present in both interacting Kir6.2 and Kir6.1 subunits but of opposite or no charge in the non-interacting Kir2.1 subunit were selected and changed to the corresponding residue in Kir2.1. In a separate mutant, the Kir6.2 endoplasmic retention sequence 369RKR371 was mutated to AAA (figure 3-1). Mutant Kir6.2 subunits were then tested for their ability to co-immunoprecipitated the MBP-SUR2A-CTC fragment.

It is noteworthy that the truncation of Kir6.2 Δ36 can be expressed independently of a SUR subunit with much of the ATP sensitivity preserved (Tucker et al. 1997) but, importantly retains sensitivity to regulation by SUR subunits when co-expressed. From this it was hypothesised that Kir6.2 RKR 369-371 AAA and K377A, were unlikely to be important in the interaction (figure 3-1).

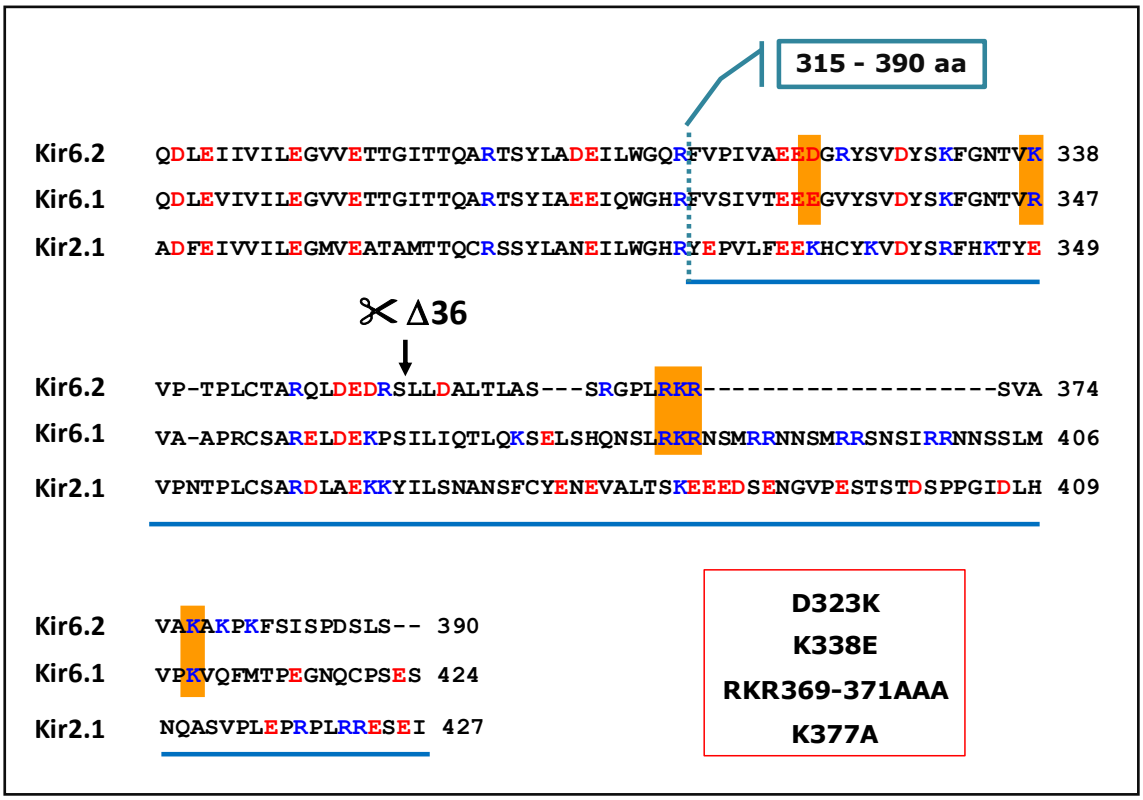

Figure 3-1 Sequence alignments of the C-termini of Kir6.2, Kir6.1 and Kir2.1.

The blue coloured underlining shows the cognate interaction domain (315-390 amino acids) on the distal C-terminal of Kir6.2 subunit for the NBD2 in the proximal C-terminal of SUR2A. Residues highlighted in orange, which were located in the interacting domain of Kir6.2 beyond residue 315 were selected for mutagenesis to the corresponding residue in Kir2.1 and co-immunoprecipitation with MBP-SUR2A-CTC. The red box shows the various mutant constructs of full length Kir6.2. Residues coloured red and blue represent the negatively and positively charged amino acid groups, respectively.

3.2 Results

Various experiments to study the interaction between the two heterologous subunits in Kir6.2/SUR2A channels were performed by co-immunoprecipitation of the MBP-SUR2A-CTC fragment with full length Kir6.2 wild type and mutant constructs (as described in section 2.1.5). The results of co-immunoprecipitation were analysed by Western blot using anti-MBP antibody as previously described (section 2.1.4).

Figure 3-2 is a representative result, showing lower co-immunoprecipitation of MBP-SUR2A-CTC (lower bands intensity on Western blot) with Kir6.2D323K and K338E respectively, (lane 4 and 6) compared to wild type (lane 2), with less change in Kir6.2 RKR369 371AAA (lane 8) and K377A (lane 10). MBP-SUR2A-CTC fragment loaded directly (lane 1) was used as a positive control for migration. Also, as a negative control for each Kir6.2 construct, Kir6.2 was omitted from each reaction (figure 3-2, lane 3, 5, 7, 9 and 11). Interestingly, these results confirmed the predications of the preliminary hypothesis that the Kir6.2 RKR 369-371 AAA and K377A, were unlikely to be important in the interaction (figure 3-1). Together, the figure (3-2) suggest that with single charge reversal point mutation, Kir6.2 D323K or K338E the physical interaction between full length Kir6.2 and the NBD2 of SUR2A were disrupted.

Figure 3-3 represents the autoradiography of Western blot analysis of co-immunoprecipitation. In figure 3-3, the bands, detected by autography, at ~ 40 kDa (molecular weight) represent the [^{35}S]-methionine labelled Kir6.2 subunit. The intensity of each band was measured by densitometry using Bio-Rad's image analysis systems (Multi-Analyst® software) and the amount of MBP-SUR2A-CTC immunoprecipitated was normalized to the amount of [^{35}S]-Kir6.2 in the precipitate as described previously.

The combined normalized data of co-immunoprecipitation experiments are represented in figure 3-4. As shown in the figure (3-4), there was a significant reduction of co-immunoprecipitation of MBP-SUR2A-CTC with Kir6.2 D323K (~ 50%, $P < 0.0009$) and K338E (~ 80%, $P < 0.0001$), while the Kir6.2 RKR369-371AAA or K377A mutants produced no change in the efficiency of co-immunoprecipitation. These results suggest that the negative charged aspartate at position 323 and positive charged lysine at position 338 in the distal C-terminal of Kir6.2 form part of the interaction domain with SUR2A-NBD2 raising the possibility that they may be possibly involved in allosteric communication between the two subunits and vital in the function of Kir6.2/SUR2A channels.

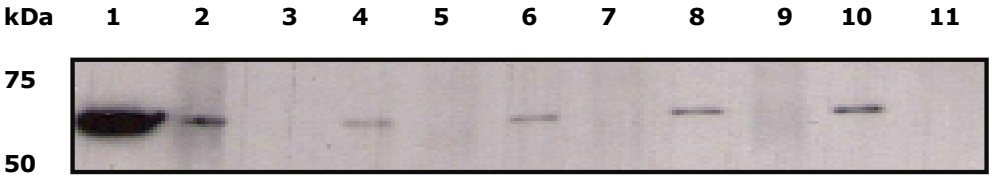

Co-IP	[^{35}S] - Kir6.2	MBP-SUR2A-CTC
1	—	Direct load (control)
2	WT	WT
3	—	WT
4	D323K	WT
5	—	WT
6	K338E	WT
7	—	WT
8	RKR369-371AAA	WT
9	—	WT
10	K377A	WT
11	—	WT

Figure 3-2 Co-immunoprecipitation assay of MBP-SUR2A-CTC fragment with various mutant constructs of Kir6.2 followed by Western blot analysis.

Immunodetection of MBP-SUR2A-CTC after co-immunoprecipitation, SDS-PAGE and Western blot. Lane 1, direct load of MBP-SUR2A-CTC as positive control for migration. Lanes 3, 5, 7, 9 and 11, co-immunoprecipitation performed in the absence of Kir6.2 and represents the negative control for each interaction. Lane 2: wild type, Lane 4: Kir6.2 D323K, Lane 6: Kir6.2 K338E, Lane 8: Kir6.2 RKR369-371AAA and Lane 10: Kir6.2 K377A. The intensity of the bands on Western blot in lane 4 (Kir6.2 D323K) and 6 (Kir6.2 K338E) are clearly lower compared to the wild type (lane 2) indicating the potential involvement of these two charged residues for the interaction with MBP-SUR2A-CTC fragment.

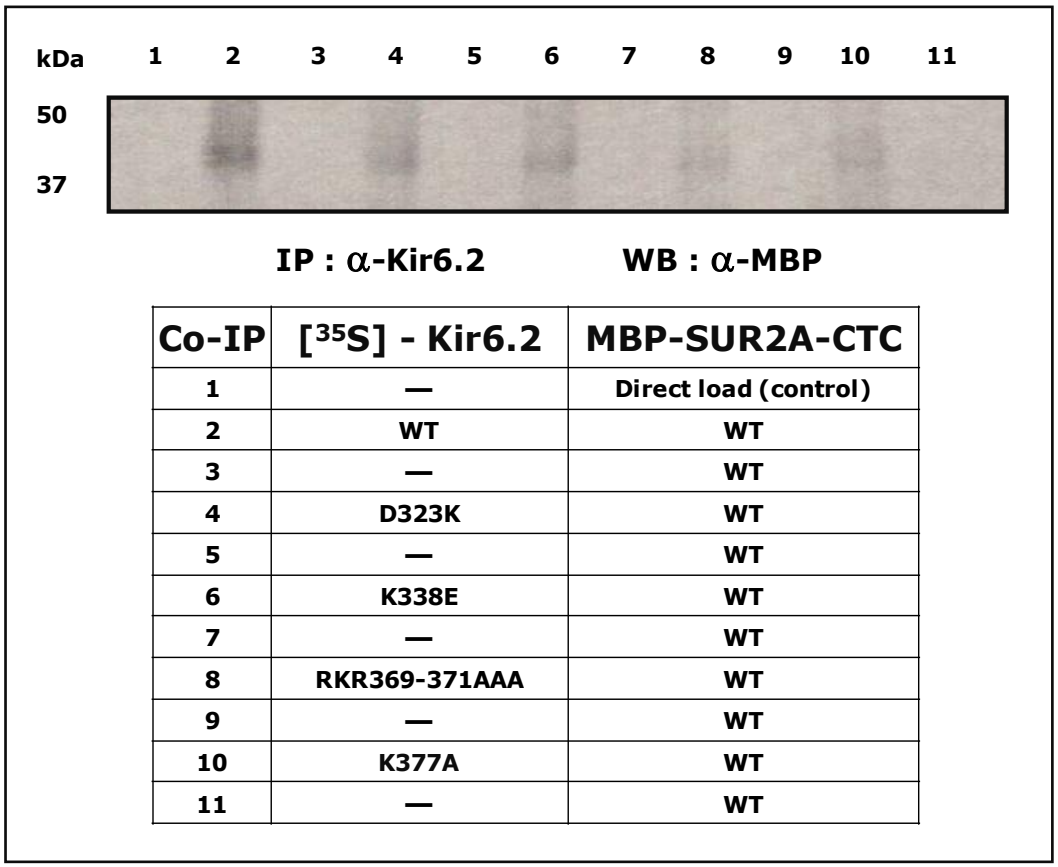

Co-IP	[^{35}S] - Kir6.2	MBP-SUR2A-CTC
1	—	Direct load (control)
2	WT	WT
3	—	WT
4	D323K	WT
5	—	WT
6	K338E	WT
7	—	WT
8	RKR369-371AAA	WT
9	—	WT
10	K377A	WT
11	—	WT

Figure 3-3 Autoradiography of co-immunoprecipitation of MBP-SUR2A-CTC fragment with various mutant constructs of Kir6.2.

Lane 1, direct load of MBP SUR2A-CTC as positive control for migration. Lane 2: wild type, Lane 4: Kir6.2 D323K, Lane 6: Kir6.2 K338E, Lane 8: Kir6.2 RKR369-371AAA and Lane 10: Kir6.2 K377A. In lanes 3, 5, 7, 9 and 11, the co-immunoprecipitation was performed in the absence of Kir6.2 and represents the negative control for each interaction Kir6.2. These mutants were electrophoresed through a 10% denaturing polyacrylamide mini gel and detected by autoradiography (X-ray) film of the Western blot. All full length Kir6.2 mutant constructs were labelled with [^{35}S]-methionine and expressed *in vitro.*

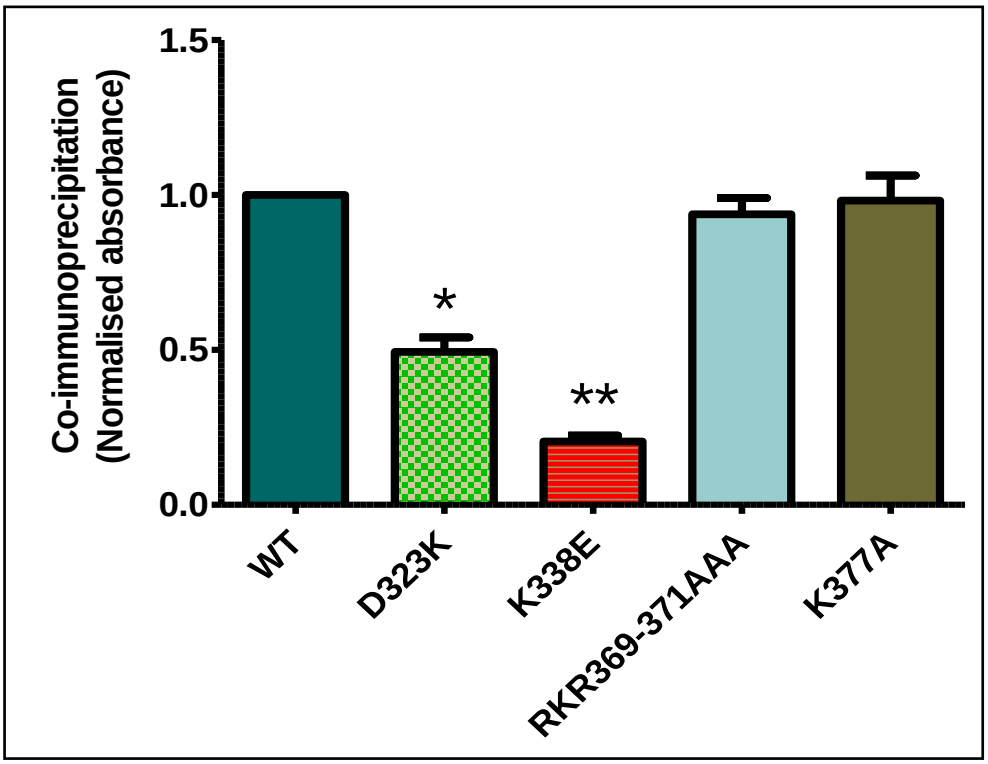

Figure 3-4 Co-immunoprecipitation of MBP-SUR2A-CTC normalized to the amount of Kir6.2 in the immunoprecipitate of that obtained with the wild type Kir6.2 subunit.

The results show significant reduction of co-immunoprecipitation of MBP-rSUR2A-CTC with Kir6.2 D323K (~ 50%, $P < 0.0009$) represented with *asterisk* and K338E (~ 80%, $P < 0.0001$) represented with *2 asterisks*, while the Kir6.2 RKR369-371AAA or K377A mutants produced no change in the efficiency of co-immunoprecipitation. Statistic analysis: bars indicate mean with SEM, using paired t test, two-tailed with 95% confidence interval, n = 5 experiments.

3.3 Summary and Conclusions

This biochemical sub-study, for the first time, reports on the identification of two charged residues D323 and K338 in the distal C-terminal of pore forming Kir6.2 that form part of interaction domain with the nucleotide binding domain 2 of SUR2A. These data indicate that the two mentioned residues may play a role in the Kir6.2/SUR2A channel assembly.

The aim of this study was to identify specific residues within the cognate interaction domain in the Kir6.2 subunit to further define the interaction with the SUR2A-CTC sequence. The co-immunoprecipitation assay of MBP-SUR2A-CTC fragment with various mutant constructs of the full length Kir6.2 subunit revealed that the negatively charged aspartic acid at position 323 (D323) and positively charged lysine at position 338 (K338) are required for the interaction with NBD2 in the proximal C-terminal of SUR2A. At the same time, these results reported the positively charged lysine at position 377 (K377) and the endoplasmic reticulum retention sequence (RKR369-371) are not necessary for the interaction with SUR2A-NBD2. These data are consistent with that truncated Kir6.2 (Kir6.2 ΔC26) can still co-assemble and be regulated by SUR subunit (Tucker et al. 1997). As described in Chapter 1 (section 1.6) Kir6 is blocked by direct ATP binding (in the presence or absence of Mg^{2+}) and activated allosterically by MgATP or MgADP binding to NBDs of the SUR (Nichols et al. 1996), Tucker et al. 1997, Drain et al. 1998 and Gribble et al. 1997). For this reason, the truncated Kir6.2 ΔC26 was considered for electrophysiological study (Chapter 6) to distinguish loss of SUR2A increase of ATP affinity from possible reduction in affinity resulting from mutation in Kir6.2 D323 or K338 directly.

In conclusion, the Kir6.2 D323 and K338 within the cognate interaction domain (315-390) of Kir6.2 subunit were identified as essential residues for the interaction with SUR2A-NBD2 (1294-1358). However, the most important question which remains to be answered is do these two charged residues (mentioned above) of Kir6.2 form cytoplasmic electrostatic interfaces with the previously identified three charged residues of SUR2A E1318, K1322 or Q1336 (Al-Johi, PhD thesis) in Kir6.2/SUR2A channels. The answer of this question will be discussed in chapter 5. Moreover, the final important point will be to investigate the effect of single charge reversal point mutation, Kir6.2 D323K and K338E, on the Kir6.2/SUR2A channel pharmacology (sensitivity to ATP, Mg^{2+}-ADP, K_{ATP} channel agonist and antagonists) by electrophysiological experiments. Since the effect of single residue mutations on function may be small, it was also important to study the combined effects of these mutations in a double mutant, Kir6.2 D323K + K338E, which may potentially augment disruption of interaction through the C-terminal domain of Kir6.2. The preparation of the Kir6.2 D323K + K338E construct is explained in the following chapter.

Chapter 4

Construction of Kir6.2

D323K + K338E Double Mutant

4.1 Introduction

In co-immunoprecipitation experiments, a significant reduction of co-immunoprecipitation of MBP-SUR2A-CTC fragment was observed with Kir6.2 D323E (~ 50%) and K338E (~80%) compared to wild type Kir6.2 (Chapter 3). These results were suggestive that these two charged residues may be involved in making interaction with the nucleotide binding domain 2 of SUR2A and, therefore, that they may be involved in stabilizing contacts between SUR2A and Kir6.2, which mediate allosteric information transfer.

It was proposed to study alteration of Mg^{2+}-ADP and KCO dependent channel activation and glibenclamide inhibition of K_{ATP} channel currents in the presence of each of these single mutations in the distal C-terminal of Kir6.2. Since a single mutation may produce no or only subtle changes to channel kinetics under these conditions, it was further proposed to prepare a Kir6.2 D232K + K338E double mutant to potentially augment disruption of interaction through the C-terminal domain of Kir6.2.

4.2 Results

To produce the Kir6.2 D323K + K338E double mutant construct, cDNA encoding the full length Kir6.2 containing a K338E single mutant already available in the laboratory was used as a template. This cDNA was cloned in pcDNA3.1/myc/HisA vector. The Kir6.2 D323K + K338E double mutant construct was made by overlap PCR using site-directed mutagenesis based on PCR method as described in section 2.2.1. The results of PCR1, PCR2 and overlap PCR are shown in figure 4-1 A and B respectively.

The 929 bp PCR product from the overlap PCR reaction was restriction digested, as described in section 2.2.5 to produce an 864 bp insert fragment, which was ligated into pcDNA3.1/myc/HisA vector. The results of restriction enzyme digestion were analysed on a 1% agarose gel (figure 4-2).

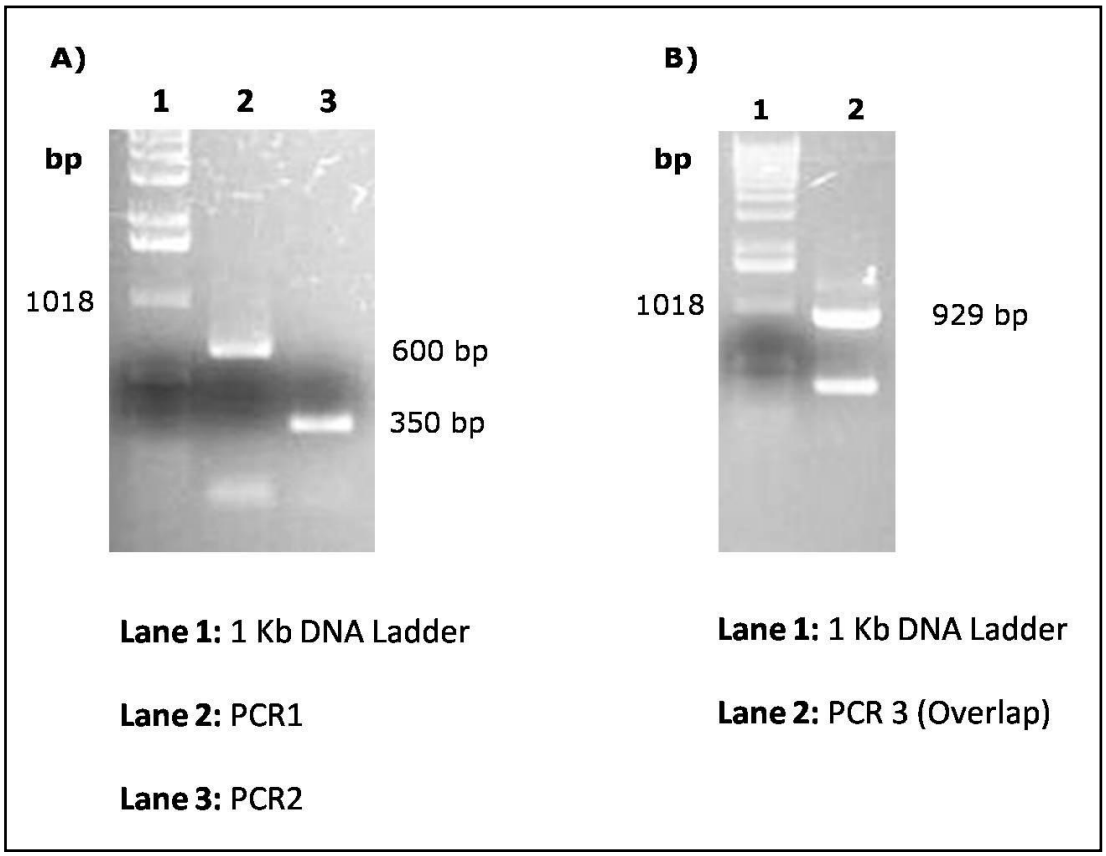

Figure 4-1 Agarose gel electrophoresis of polymerase chain reaction (PCR) products of Kir6.2 D323K + K338E double mutant construct.

(A) Gel of PCR1 product with expected 600 bp band and PCR2 product with expected 350 bp band. (B) Gel of the PCR3 product, which was produced by overlap of PCR1 and PCR2, with an expected size of 929 bp.

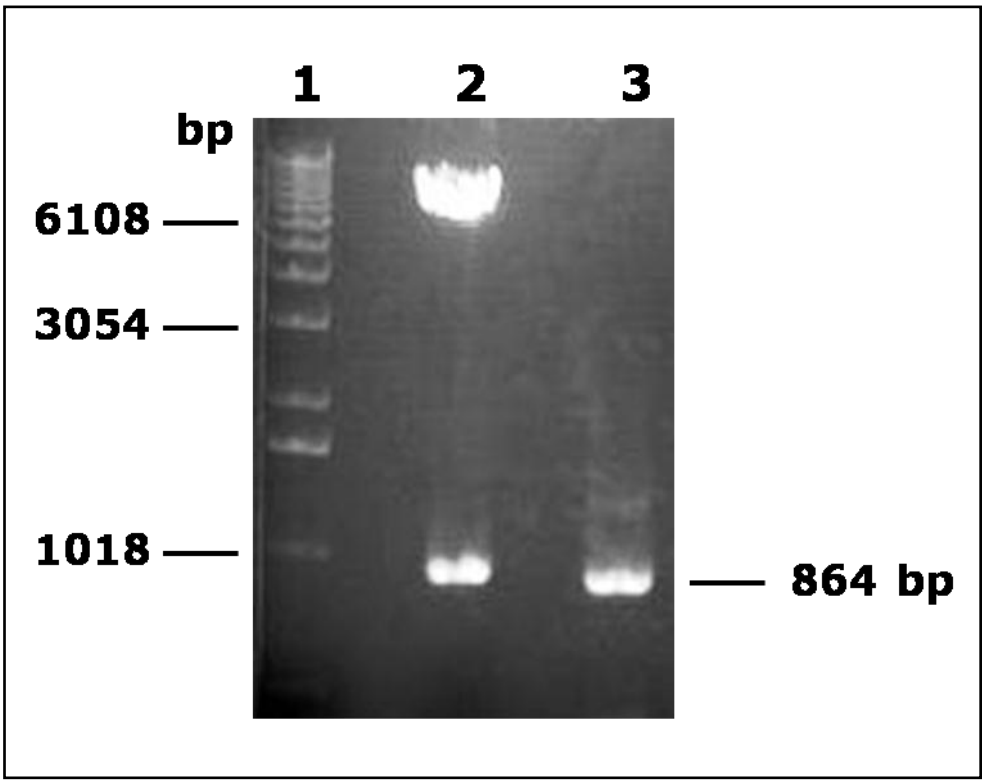

Figure 4-2 Restriction enzyme digestion analysis of the vector and the overlap PCR product with EcoRI and Bst II.

Restriction digestion products were analysed on a 1% agarose gel; *lane 1*: 1 Kb DNA Ladder, *lane 2*: restriction digest products of pcDNA3.1/myc/HisA vector with 864 bp insert and *lane 3*: restriction digest product of overlap PCR (929 bp), the 864 bp insert fragment.

Following quantification of DNA by Qubit™ fluorometer after Miniprep as described in section 2.2.12, 1µl of DNA was analysed on a 1% agarose gel to estimate the DNA concentration for DNA sequencing (figure 4-3). The construction of the Kir6.2 D323K + K338E double mutant was confirmed by DNA sequencing at the PNACL unit as previously discussed (section 2.2.13).

4.3 Summary and Conclusions

In conclusion, in this sub-study the Kir6.2 D323K + K338E double mutant was successfully constructed by using molecular biology techniques. This double charge reversal mutant construct was to be used for electrophysiology studies if the single charge reversal point mutations, Kir6.2 D323K or K338E, showed no significant disruption of the allosteric information transfer between Kir6.2 and SUR2A. In other words, generation of this double mutant in the distal C-terminal of the pore forming Kir6.2 perhaps will influence the sensitivity of ATP, ADP, K_{ATP} channels agonist or antagonist much more compared to the single point mutation Kir6.2 D323K or K338E in functional Kir6.2/SUR2A channels.

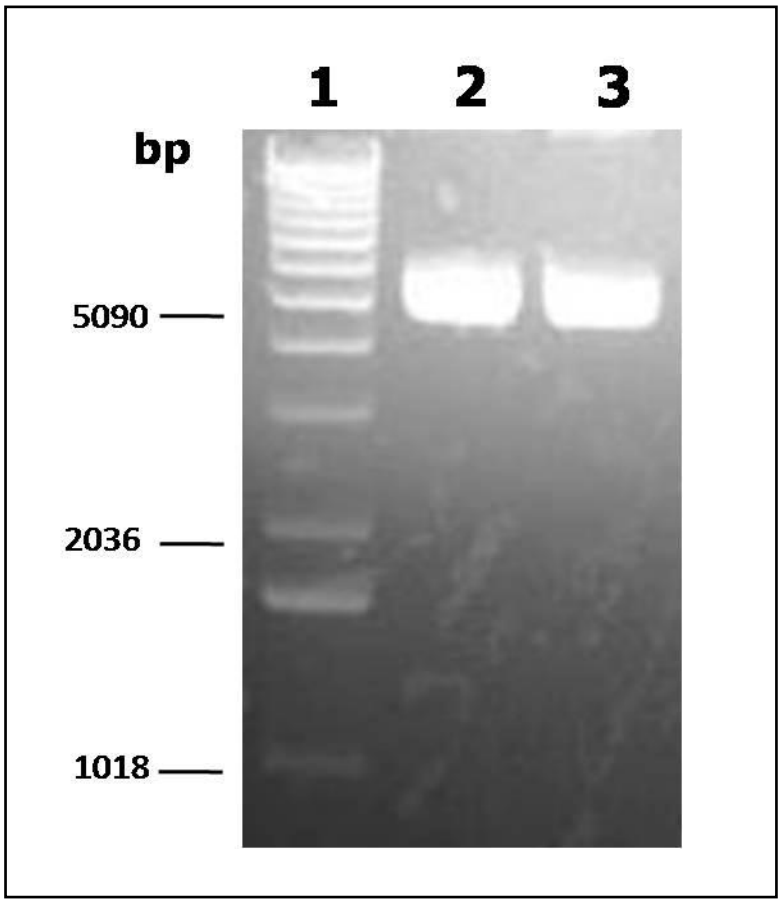

Figure 4-3 Estimation of DNA concentration.

Miniprep products were analysed on a 1% agarose gel to estimate the DNA concentration for DNA sequencing. The agarose gel photograph show; *Lane 1:* 1 Kb DNA Ladder and *Lane 2* and *Lane 3* represent 1 µl of DNA from Minipreps of colony 1 and colony 2, respectively.

Chapter 5

Identification of Salt Bridges between Cytoplasmic Domains of Heterologous Subunits in Kir6.2/SUR2A Channels

5.1 Introduction

Co-immunoprecipitation of chimaeric subunit constructs and point mutants revealed three charged residues of SUR2A (E1318, K1322 and Q1336) (Al-Johi, PhD thesis) and two in Kir6.2 (D323 and K338) (see Chapter 3) that are key to the interaction between these two heterologous subunits in Kir6.2/SUR2A subunit combination in K_{ATP} channels. In other words, single charge reversal mutation in either subunit, Kir6.2 D323K, K338E or SUR2A E1318R, K1322D or Q1336E (provided by Dr Dave Lodwick, co-supervisor) reduced the co-immunoprecipitation and disrupted the physical interaction of the cytosolic domains of the Kir6.2 and SUR2A subunits.

The results suggest that these cytoplasmic charged residues in the distal C-terminal of the pore forming Kir6.2 and the nucleotide binding domain 2 in the proximal C-terminal of the regulatory subunit SUR2A are possibly involved in electrostatic inter-subunit interactions that play a crucial role in the channel assembly in the functional $Kir6.2_4/SUR2A_4$ channel complex. Due to the lack of three-dimensional structures of these two minimal cytoplasmic regions in Kir6.2 and SUR2A, it was reasonably hypothesized that if the salt bridge formation was important, double charge reversal mutants in the Kir6.2 and SUR2A subunits should restore the co-immunoprecipitation and inter-subunit salt bridge interactions (figure 5-1).

Figure 5-1 represents the hypothesized interacting charged residues in the two minimal interaction motifs of SUR2A-NBD2 amino acids 1318 to 1338 and the distal C-terminus, amino acids 315-390 of Kir6.2 and three proposed inter-subunit salt bridges. As discussed above, single mutations of the targeted charged residues in either subunit disrupt the interaction (Chapter 3 and Al-Johi, PhD thesis).

The aim of this sub-study was to test the above hypothesis and identify possible electrostatic interactions between the cytoplasmic NBD2 of accessory SUR2A subunits and the distal C-terminus of the pore forming Kir6.2 subunits in Kir6.2/SUR2A channels.

To examine our hypothesis further, a three-dimensional model of SUR2A-NBD2 (1318-1337) sequence was modelled onto the crystal structure of the bacterial NBD dimer structure of MalK (MJ0796), figure 5-2 A. This model shows the three residues in SUR2A, E1318, K1322 and Q1336 mapped to the surface of the NBD in a three stranded β-sheet. Interestingly, in this model the SUR2A L1313 which is the equivalent residue to SUR1 L1350 can also be seen in this β-sheet structure. It is of interest that when the SUR1 L1350 residue was mutated to the glutamine (SUR1 L1350Q) this reduced the surface expression of the pancreatic β-cell K_{ATP} channel and resulted in congenital hyperinsulinism (Yan et al. 2007).

It is also worth mentioning that this model illustrates the three residues E1305, I1310 and L1313 as described in Chapter 1 (section 1.8.1.2) that have been shown to have a role in activation and not inhibition of the channel pore in Kir6.2/SUR2A channel (Dupuis et al. 2008). These residues lie just upstream of the three residues (SUR2A E1318, K1322 and Q1336) which were found to be the key for the interaction with full length Kir6.2 in this study (section 1.8.1.2).

Figure 5-2 B shows another three-dimensional model of SUR2A-NBD2, this time modelled onto the structure of the human cystic fibrosis transmembrane conductance regulator (CFTR) NBD2 structure docked with residues of the C-terminal domain of the pore forming Kir 6.2 subunit, based on the crystal structure of Kir3.1, (provided by Dr Mark Pfuhl, co-supervisor). This model illustrates the possible interaction between

the domains identified in each subunit but did not identify potential inter-subunit salt bridges between the SUR2A and Kir6.2 as identified in this study.

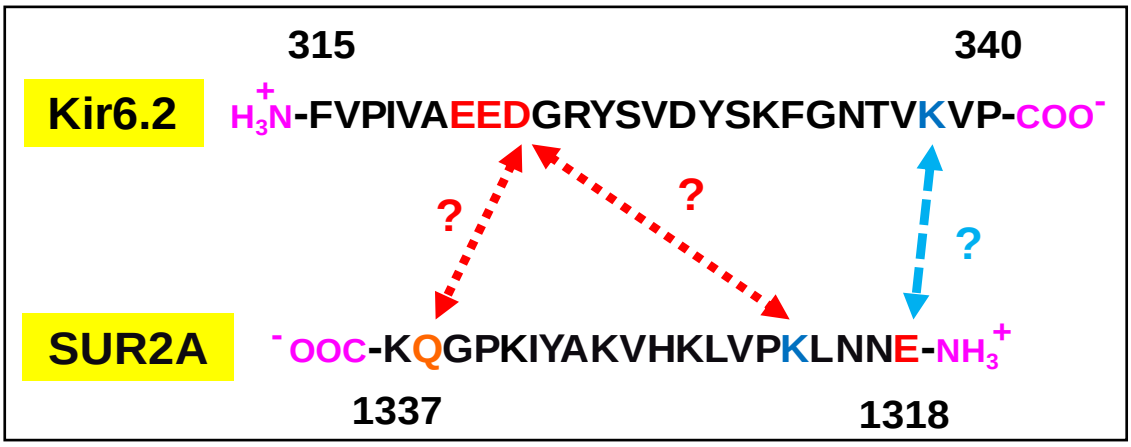

Figure 5-1 Model showing hypothesized interacting charged residues between two heterologous subunits in Kir6.2/SUR2A channels.

Linear sequences of the minimal interaction motifs of the Kir6.2 and SUR2A subunits showing predicted electrostatic interactions. It was hypothesized that single mutations in either subunit would disrupt, and double charge reversal mutants in Kir6.2 and SUR2A should restore, interaction and function.

A)

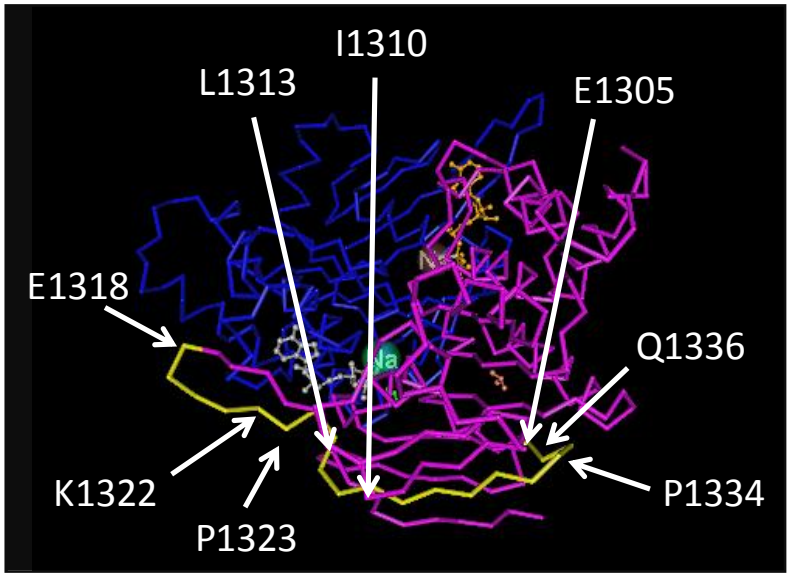

B)

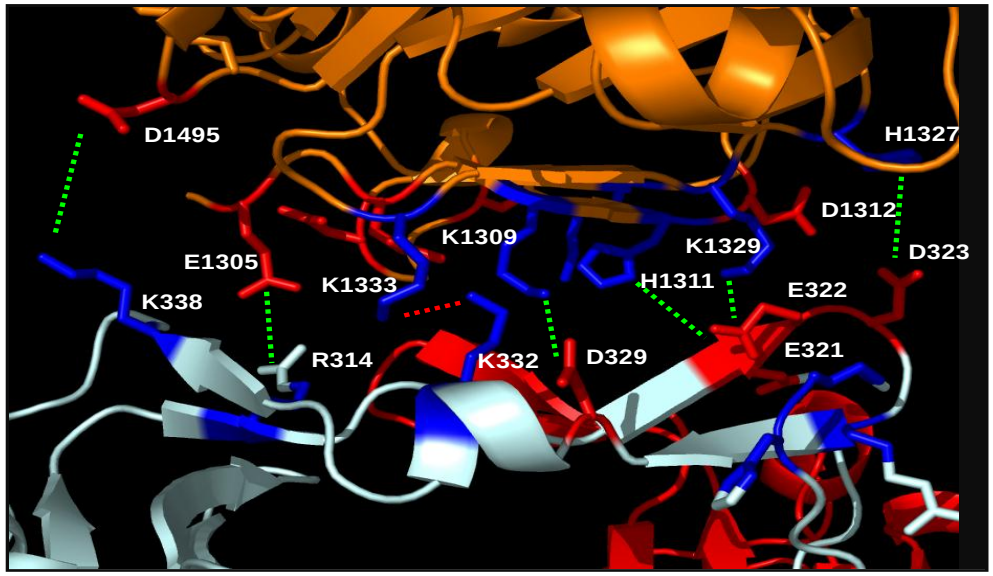

Figure 5-2 Three-dimensional structural model of the proposed inter-subunit interfaces between SUR2A and Kir6.2 in K_{ATP} channels.

A) Three-dimensional modelling of SUR2A-NBD2 (1318-1337, in yellow) primary sequence modelled onto the crystal structure of the bacterial NBD dimer structure of MalK (MJ0796). The blue colour represents one monomer of the dimer (MalK) and the magenta colour represents the other monomer with ATP molecule binding to each one. Clearly, this model illustrates the three residues in SUR2A, E1318, K1322 and Q1336 mapped to the surface of the NBD in a three stranded β-sheet. B) SUR2A-NBD2 residues modelled onto the human CFTR NBD2 structure docked with the C-terminal primary sequence of the Kir 6.2 subunit modelled onto the crystal structure of Kir3.1. This model (B) is inconsistent with the results of what was found in this study, which revealed the three residues, SUR2A E1318, K1322 and Q1336 to be the key for the interaction with full length Kir6.2 and formed inter-subunit salt bridges with Kir6.2 D323 and K338 as identified in this chapter.

5.2 Results

Co-immunoprecipitation between the mutated and the wild type, full length Kir6.2 and MBP-SUR2A-CT-C fragments was performed and the results of this study will be discussed in this section. The co-immunoprecipitation assay was performed (as described in section 2.1.5) to study protein-protein interaction and to test the hypothesis (figure 5-1) that double charge reversal mutants in Kir6.2 and SUR2A as illustrated should restore the interaction since, point mutants disrupted the interaction between two subunits compared to the wild type sequences (Chapter 3).

Prior to co-immunoprecipitation, the full length [^{35}S]-methionine labeled Kir6.2 WT, D323K and K338E subunits were expressed *in vitro* as described in Chapter 2 (section 2.1.1.1). The expression level was confirmed by autoradiography of wild type and other mutant constructs of the pore forming Kir6.2 subunit (figure 5-3).

The SDS-PAGE analysis of the SUR2A-CTC-C mutant constructs ran as double bands with charge reversal compared to the wild type possibly indicating alternative partially denatured species (figure 5-4). A simple experiment was done to confirm this and also to assess whether the interaction between two subunits or to the constructs of MBP-SUR2A-CTC fragments caused the running of the SUR2A-CTC-C mutant constructs as a double bands on SDS-PAGE. As shown in figure 5-4, the results suggest these double bands possibly can be explained due to the partial folding of fusion protein constructs of mutated MBP-SUR2A-CTC fragments.

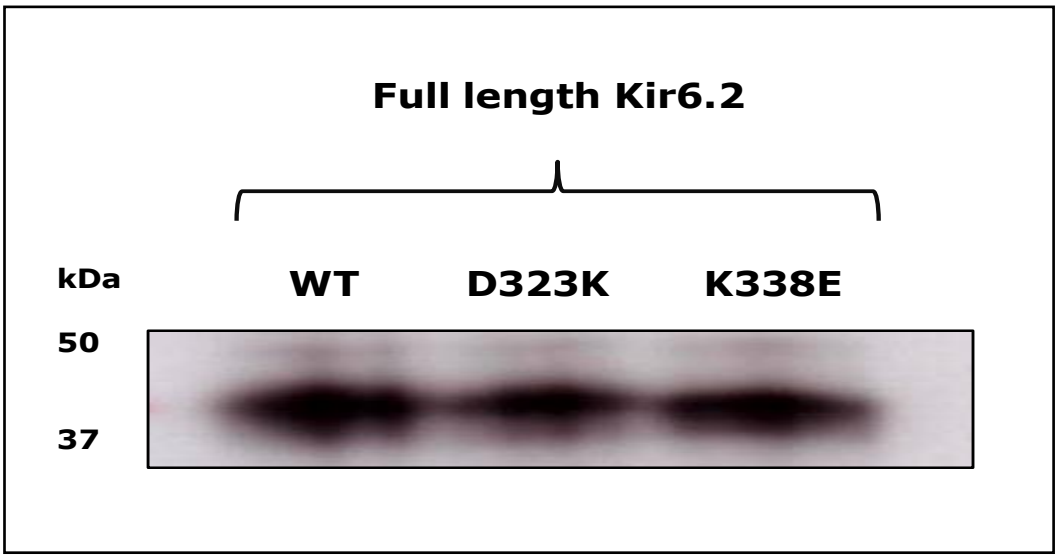

Figure 5-3 Autoradiography of *in vitro* expressed wild type and mutated full length [^{35}S] - Kir6.2.

Wild type full length Kir6.2 and mutant constructs were expressed *in vitro*, using the TNT® quick coupled transcription/translation system as described in Chapter 2 (section 2.1.1.1). The autoradiograph shows the expression level of [^{35}S]-methionine labeled Kir6.2 WT, D323K and K338E.

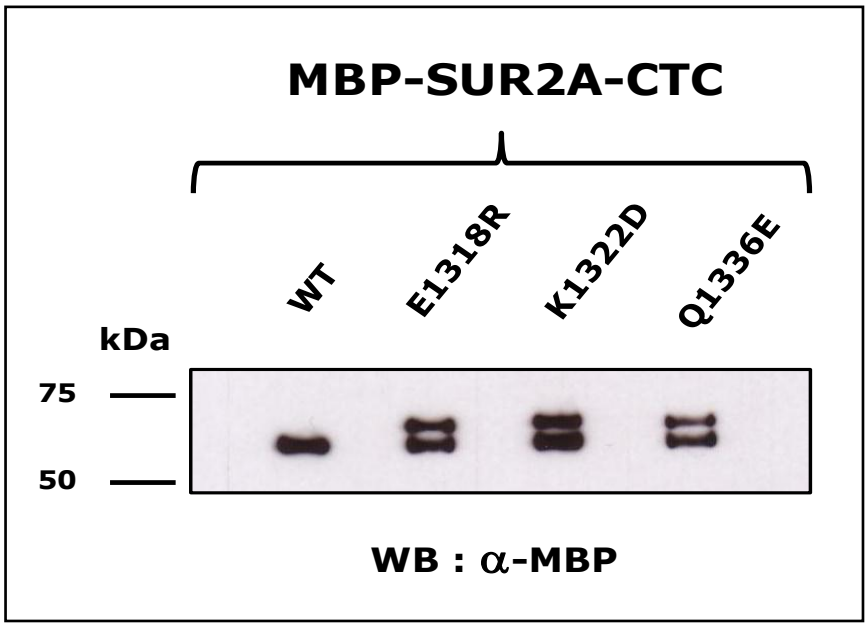

Figure 5-4 Western blot analysis of wild type and mutated MBP-SUR2A-CTC fragment.

The figure shows a Western blot of MBP-SUR2A-CTC constructs electrophoresed alone in 10% SDS-PAGE. The wild type MBP-SUR2A-CTC fragment ran as a single band, while the mutated MBP-SUR2A-CTC fragment ran as doublets. The blot was probed with monoclonal anti-maltose binding protein as the primary antibody.

Figure 5-5 represents the Western blot analysis of MBP-SUR2A-CTC co-immunoprecipitation with full length Kir6.2 or point mutant subunits. As shown in figure 5-5, replacing the negatively charged aspartic acid at position 323 (D323) with positive charged lysine (K, lane 4) and positively charge lysine at position 338 (K338) with negatively charged glutamic acid (E, lane 6) residues in full length Kir6.2 resulted in a noticeable reduction of co-immunoprecipitation with MBP-SUR2A-CTC-C fragment compared to the wild type (lane 2), as predicted (see Chapter 3). Once more, these results indicate that with single charge reversal point mutation, Kir6.2 D323K or K338E, the physical interaction between the two subunits was disrupted. Interestingly, the same figure (5-5) shows the co-immunoprecipitation was restored with charge swop mutants in both subunits, Kir6.2 K338E/SUR2A E1318R (lane 8), Kir6.2 D323K/SUR2A K1322D (lane 10) and Kir6.2 D323K/SUR2A Q1336E (lane 12) was restored. In other words, reinstatement of cytoplasmic electrostatic interfaces restored the interactions between the pore forming Kir6.2 and the accessory SUR2A subunit.

These results confirmed the hypothesis and identified three cytoplasmic salt bridges; Kir6.2 K338/SUR2A E1318, Kir6.2 D323/SUR2A K1322 and Kir6.2 D323/SUR2A Q1336 between the NBD2 of SUR2A and the distal C-terminus of Kir6.2, to be very important for the physical interaction in Kir6.2/SUR2A channel assembly (figure 5-5).

Figure 5-6 illustrates the autoradiography of Western blot analysis of the co-immunoprecipitations. The [^{35}S]-methionine labeled Kir6.2 subunits were detected by autoradiography and the intensity of each band was measured by densitometry using Bio-Rad's image analysis systems (Multi-Analyst® software). The results of Kir6.2 co-immunoprecipitation were normalized to the autoradiography of co-immunoprecipitation as described in Chapter 3. Since doublets of bands were observed on the gel electrophoresis of MBP-SUR2A-CT-C point mutants alone

(figure 5-4 and 5-5), both bands were considered when assuming co-immunoprecipitation of these constructs when results were normalized. The normalized results confirmed restoration of physical interaction between electrostatic partner residues; Kir6.2 K338E/SUR2A E1318R, Kir6.2 D323K/SUR2A K1322D and Kir6.2 D323K/SUR2A Q1336E (figure 5-7).

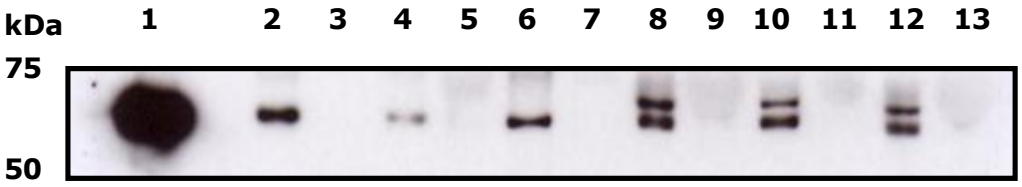

Co-IP	[^{35}S] - Kir6.2	MBP-SUR2A-CTC
1	—	Direct load (control)
2	WT	WT
3	—	WT
4	D323K	WT
5	—	WT
6	K338E	WT
7	—	WT
8	K338E	E1318R
9	—	E1318R
10	D323K	K1322D
11	—	K1322D
12	D323K	Q1336E
13	—	Q1336E

Figure 5-5 Restoration of co-immunoprecipitation between the charged swop mutants of the MBP-SUR2A-CTC fragment and full length Kir6.2 subunits.

The figure shows Western blot of MBP-SUR2A-CTC co-immunoprecipitation with full length Kir6.2 or point mutant subunits. As a positive control for migration, the MBP-SUR2A-CTC fragment was direct loaded (lane 1). The even numbered lanes represent the co-immunoprecipitation of MBP-SUR2A-CTC (amino acids, 1294-1403) constructs in the presence of full length Kir6.2 subunits and odd numbered lanes in the absence of full length Kir6.2 subunits (as control), respectively. The co-immunoprecipitation of wild type MBP-SUR2A-CTC-C with single point mutants, Kir6.2 D323K (lane 4) and K338E (lane 6) was clearly reduced, compared to the wild type (lane 2) indicating that the physical interaction between the two subunits was disrupted. Co-expression of the charged reversals residues in both subunits, Kir6.2 K338E/SUR2A E1318R (lane 8), Kir6.2 D323K/SUR2A K1322D (lane 10) and Kir6.2 D323K/SUR2A Q1336E (lane 12) reinstated the inter-subunit salt bridges and restored the co-immunoprecipitation.

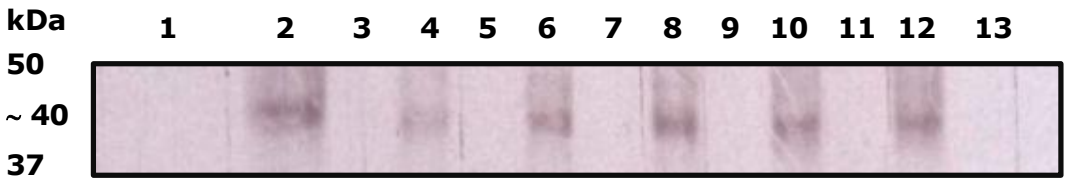

Co-IP	[^{35}S] - Kir6.2	MBP-SUR2A-CTC
1	—	Direct load (control)
2	WT	WT
3	—	WT
4	D323K	WT
5	—	WT
6	K338E	WT
7	—	WT
8	K338E	E1318R
9	—	E1318R
10	D323K	K1322D
11	—	K1322D
12	D323K	Q1336E
13	—	Q1336E

Figure 5-6 Autoradiography of co-immunoprecipitation of the charged swop mutants of MBP-SUR2A-CTC fragment and full length Kir6.2.

All full length Kir6.2 mutant constructs were labeled with [^{35}S]-Methionine and expressed *in vitro*. These mutants were electrophoresed through a 10% denaturing polyacrylamide mini gel and detected by autoradiography. The molecular weight (~ 40 kDa) of full length labelled-Kir6.2 confirmed the corresponding molecular weight of Kir6.2.

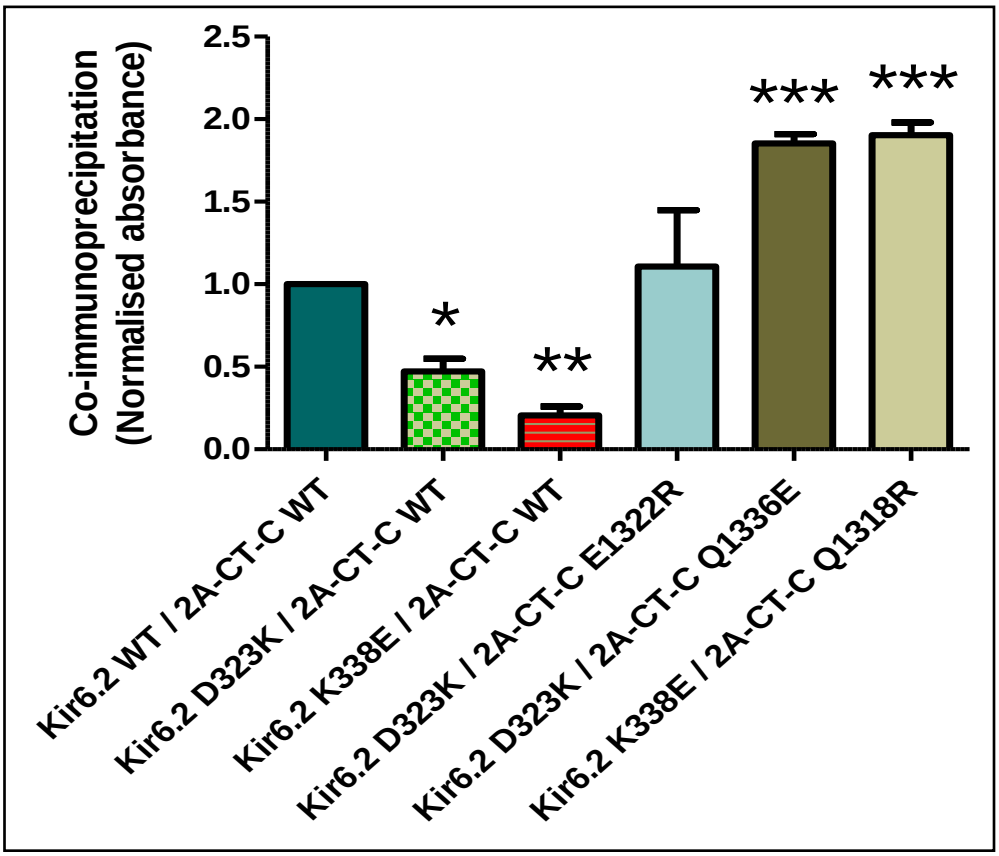

Figure 5-7 Restoration of co-immunoprecipitation between MBP-SUR2A-CTC mutant fragments and full length Kir6.2 subunit mutants confirmed three inter-subunit salt bridges.

The bar chart represents the normalized experimental data of co-immunoprecipitation and data in each bar shows the combination of wild type or mutated full length Kir6.2 subunit and the MBP-SUR2A-CTC fragments. The amount of MBP-SUR2A-CTC immunoprecipitated was normalized to the amount of [^{35}S] Kir6.2 in the precipitate and results expressed in comparison to that obtained with the wild type (positive control) Kir6.2 subunit. A single charge reversal point mutation, Kir6.2 D323K or K338E, significantly reduced the co-immunoprecipitation and reinstatement of the inter-subunit salt bridges by co-expression of the charged reversal residues in both subunits, Kir6.2 K338E/SUR2A E1318R, Kir6.2 D323K/SUR2A K1322D and Kir6.2 D323K/SUR2A Q1336E restored the co-immunoprecipitation. Mean data showing restoration of co-immunoprecipitation on charge reversal of target residues in both subunits confirmed the presences of three salt bridges (Kir6.2 K338/SUR2A E1318, Kir6.2 D323/SUR2A K1322 and Kir6.2 D323K/SUR2A Q1336) in both subunits, n = 5, *$p < 0.05$, **$p < 0.01$, *** $p < 0.0001$.

5.3 Summary and Conclusions

The main finding of this sub-study was the identification of the three inter-subunit salt bridges between the distal C-terminal of the pore forming Kir6.2 and the nucleotide binding domain 2 in the proximal C-terminal of the regulatory subunit SUR2A.
A single charge reversal mutation in either subunit, Kir6.2 and SUR2A, reduced the co-immunoprecipitation and disrupted the physical association between these two heterologous proteins.

In greater detail, the biochemical studies suggested that the charge residues D323 and K338 in Kir6.2 (this Chapter and 3) and E1318, K1322 and Q1336 in NBD2 of SUR2A (Al-Johi, PhD thesis) are key for the assembly in Kir6.2/SUR2A channels. The lack of three-dimensional structures of these cytoplasmic inter-subunit interactions raised the reasonable hypothesis, which was that; these charged residues should form ion pairs and stabilizing electrostatic interactions between the NBD2 of SUR2A and the distal C-terminal of Kir6.2 in functional $Kir6.2_4/SUR2A_4$ channel complex. Indeed, these predictions were confirmed by restoration of co-immunoprecipitation on single charge reversal in both subunits (Kir6.2 and SUR2A).These results revealed the Kir6.2 K338/SUR2A E1318, Kir6.2 D323/SUR2A K1322 and Kir6.2 D323/SUR2A Q1336 form inter-subunit salt bridges between the pore forming Kir6.2 and its partner SUR2A in Kir6.2/SUR2A channels.

In summary, for the first time this sub-study reports the identification of three cytoplasmic electrostatic interface interactions (mentioned above) between the regulatory sulphonylurea receptor SUR2A subunit and the inward rectifier potassium channel pore Kir6.2. Nevertheless, the most important question which remains to be answered is do these inter-subunit salt bridges mediate allosteric information transfer in

different isoform subunit combinations in functional hetero-octameric ($Kir6_4/SUR_4$) K_{ATP} channel complexes. To answer this question, electrophysiological study was undertaken to investigate if disruptions of the three proposed inter-subunit salt bridges alter the functional properties of Kir6.1/SUR2A or Kir6.2/SUR2A channels (Chapter 6).

Chapter 6

Allosteric Information Transfer through Inter-Subunit Salt Bridges between Kir6 and SUR2A

6.1 Introduction

Kir6.1 and Kir6.2 isoforms are highly homologous and share 71% amino acid identity with each other (Matsuo et al, 2000). With sulphonylurea receptors, these two isoforms form functional K_{ATP} channels (Matsuo et al, 2000). The biochemical study in Chapters 3 and 5 revealed that the two charged residues, D323 and K338, in the distal C-terminal of the pore forming Kir6.2 are key to the interaction with its regulatory partner, SUR2A subunit. In addition, these residues have been shown to form inter-subunit salt bridges with SUR2A E1318, K1322 and Q1336 (see Chapter 5). Since these contacts are close to residues involved in binding ATP in Kir6.2 and NBD2 in SUR2A, the next most important question was whether these residues and salt bridges are involved in allosteric communication between the two heterologous subunits in Kir6.2/SUR2A channels. Electrophysiological recording of various mutant subunits was undertaken to investigate the involvement of residues in equivalent positions in Kir6.1 and Kir6.2 (this Chapter), respectively. To investigate the hypothesis that the negatively charged aspartic acid residue at position 332 (E332) and positive charged arginine at position 347 (R347) in Kir6.1 represent residues found in the equivalent positions in Kir6.2 D323 and K338 were mutated to the opposite charge, Kir6.1 E332K and R347E, respectively (figure 6-1).

The major aim of this sub-study was to investigate whether allosteric information transfer occurs between NBD2 of SUR2A and the distal C-terminal of Kir6.1, via the equivalent residues in Kir6.1 to residues in the Kir6.2 315-390 and SUR2A 1318-1337 (figure 6-1) interactions which were characterized in Chapter 3 and 5, using the electrophysiological technique of whole-cell patch clamp, as described in Chapter 2.

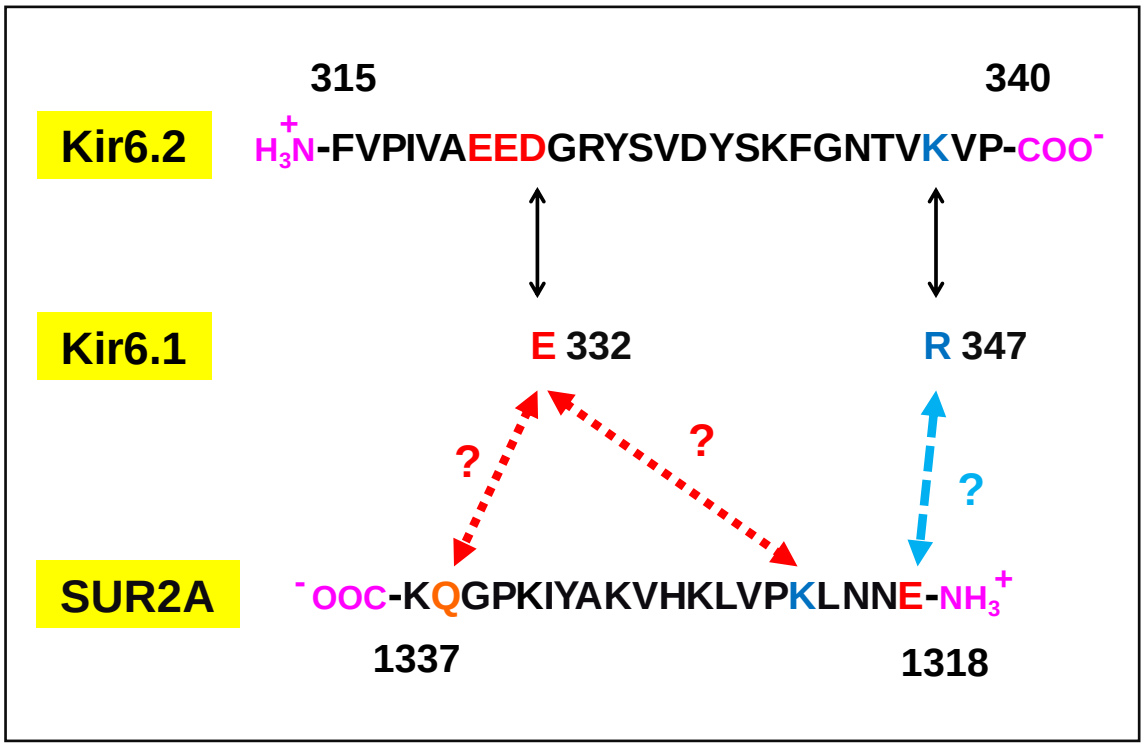

Figure 6-1 Model showing hypothesized cytoplasmic interacting charged residues between Ki6.1 or Kir6.2 and sulphonylurea receptor SUR2A in K_{ATP} channels.

Linear sequences of the minimal interaction motifs show the predicted cytoplasmic electrostatic interactions between the charged residues of the Kir6.2 D323 and K338 and the hypothesized equivalent negatively charged E332 and positive charged R347 in Kir6.1 to Kir6.2 with SUR2A subunits. It was hypothesized that single charge reversal mutations in either subunit of Kir6.1 with SUR2A would disrupt, and double charge reversal mutation in Kir6.1 and SUR2A should restore the interaction and the function in Kir6.1/SUR2A channels.

6.2 Results

6.2.1 Construction of Equivalents Charged and Conservative Residues on Kir6.1 to Kir6.2

PCR site directed mutagenesis, as described in Chapter 2 (similar strategy to construction of the Kir6.2 double mutant, section 2.2.1), was used to produce Kir6.1 E332K and Kir6.1 R347E mutants. The cDNA encoding the full length Kir6.1 was cloned in pcDNA3.1/myc/hisA vector. Table 6-1 represents the oligonucleotide sequences of specific primers, which were designed according to the fragment sequences of Kir6.1 and used for PCR reactions. The results of PCR1, PCR2 and overlap PCR for the Kir6.1 mutants are shown in figure 6-2. Figure 6-2 A represents the characteristics of PCR1 and PCR2 products and figure 6-2 B represents the products of overlap PCR for the Kir6.1 E332K and Kir6.1 R347E mutants.

Figure 6-3 represents the 1% agarose gel electrophoresis analysis of the restriction enzyme digestion of the inserts (672 bp) and vectors (pcDNA3.1/myc/hisA/Kir6.1, 6980bp), which were restriction digested (as described in section 2.2.5) with BspE1 and BstEII. Gel electrophoresis analysis confirmed the predicted bp sizes of the bands; the bands, the inserts (557 bp) and the vectors (6423 bp). These inserts and vectors had the same bp size for the both mutants (Kir6.1 E332K and Kir6.1 R347E). The products from restriction digestion were isolated from the agarose gel and the insert fragments were ligated to the digested vectors and analysed for ligation.

Following quantification of DNA by Qubit™ fluorometer after Miniprep (described in section 2.2.9), the Kir6.1 E332K and Kir6.1R347E mutants were confirmed by DNA sequencing at the PNACL unit as previously discussed (section 2.1.13). In the result section (this chapter), the electrophysiological study of these Kir6.1 mutants will be discussed.

PCR	Primers	Sequence (5′ to 3′ Direction)
Kir6.1-E332K	E332KF	GTGACTGAGGAGAAGGGAGTTACTCTGTGGACTATT
	E332KR	AGTACACTCCCTTCTCCTCAGTCACAATCGACAC
Kir6.1-R347E	R347EF	GGTAATACTGTGGAAGTGGCGGCGCCAAGATG
	R347ER	GCGCCGCCACTTCCACAGTATTACCAAATTTAGAATAGT
Overlap	61U	TCCGTAATGGCAAFCTGTG
	61D	ATGATTCTGATGGGCACTGG

Table 6-1 The oligonucleotide sequences of primers used for PCR reactions to prepare Kir6.1 point mutants.

The table represents the primers used to make the Kir6.1 mutants, which were synthesised by Eurofins MWG Operon. These primers were used to generate the Kir6.1 E332K and Kir6.1 R347E mutants. To generate the Kir6.1 E332K mutant, the E332KF and E332KR primers were used as forward and reverse primer respectively and for Kir6.1 R347E mutant, the R347EF as forward and R347ER as reverse primer. For overlap PCR 61U was used as forward primer and 61D as reverse primer.

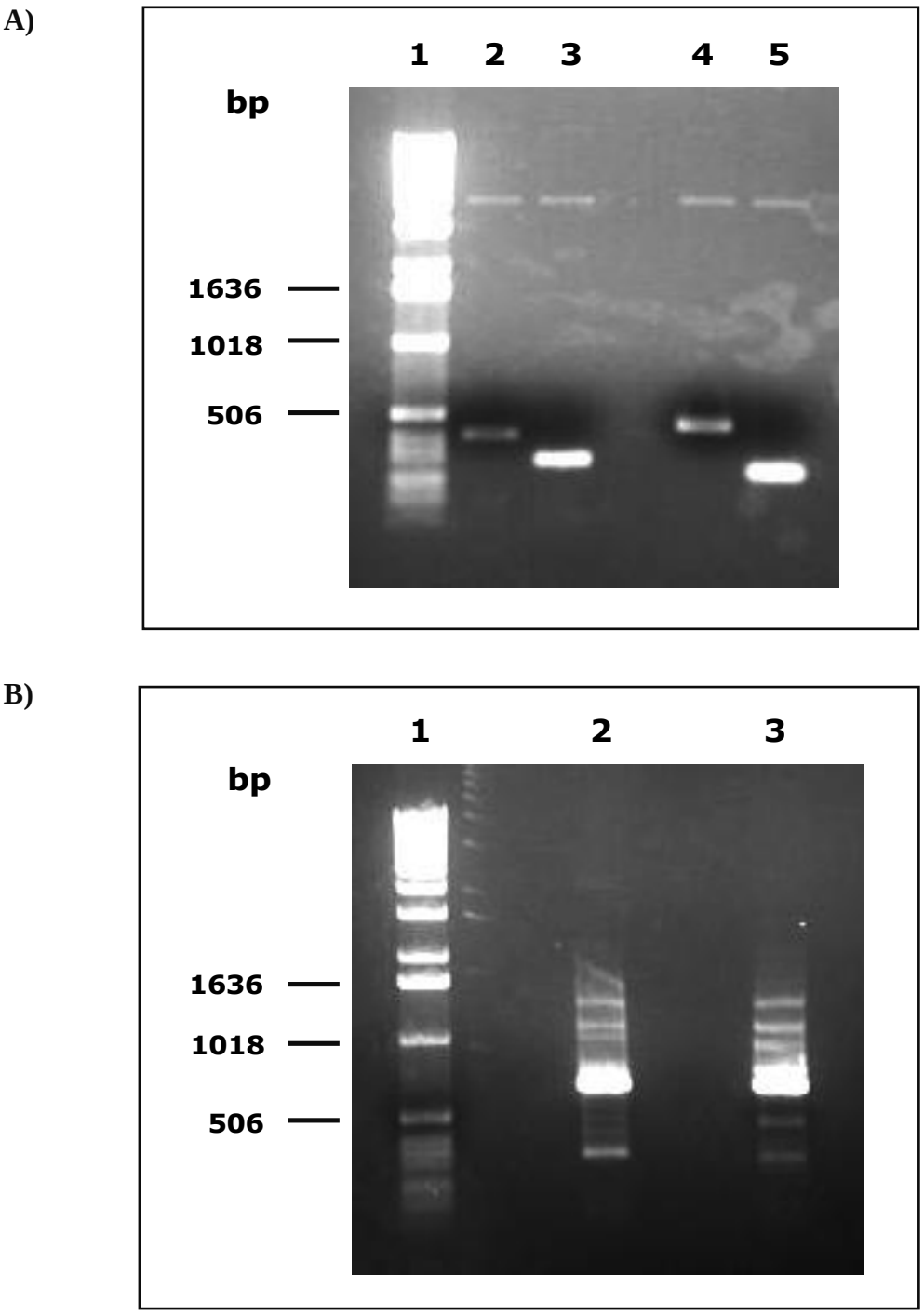

Figure 6-2 Agarose gel electrophoresis of PCR products of Kir6.1 point mutants.

A and B represent 1% agarose gel electrophoresis of PCR products, which were used to identify Kir6.1 mutants. The gels were stained with ethidium bromide and photographed under UV light. Lane 1 (A and B) represent the 1 Kb DNA ladder (molecular weight markers). A) Lanes 2 and 3 represent the PCR1 (405 bp) and PCR2 (292 bp) for Kir6.1 E332K, respectively; 4 and 5, the PCR1 (450 bp) and PCR2 (247 bp) for Kir6.1 R347E, respectively. B) Lane 2 and 3 represent the overlap PCR (672 bp) for Kir6.1 E332K and mutant Kir6.1 R347E respectively. All the bp size, which was mentioned here was as predicted.

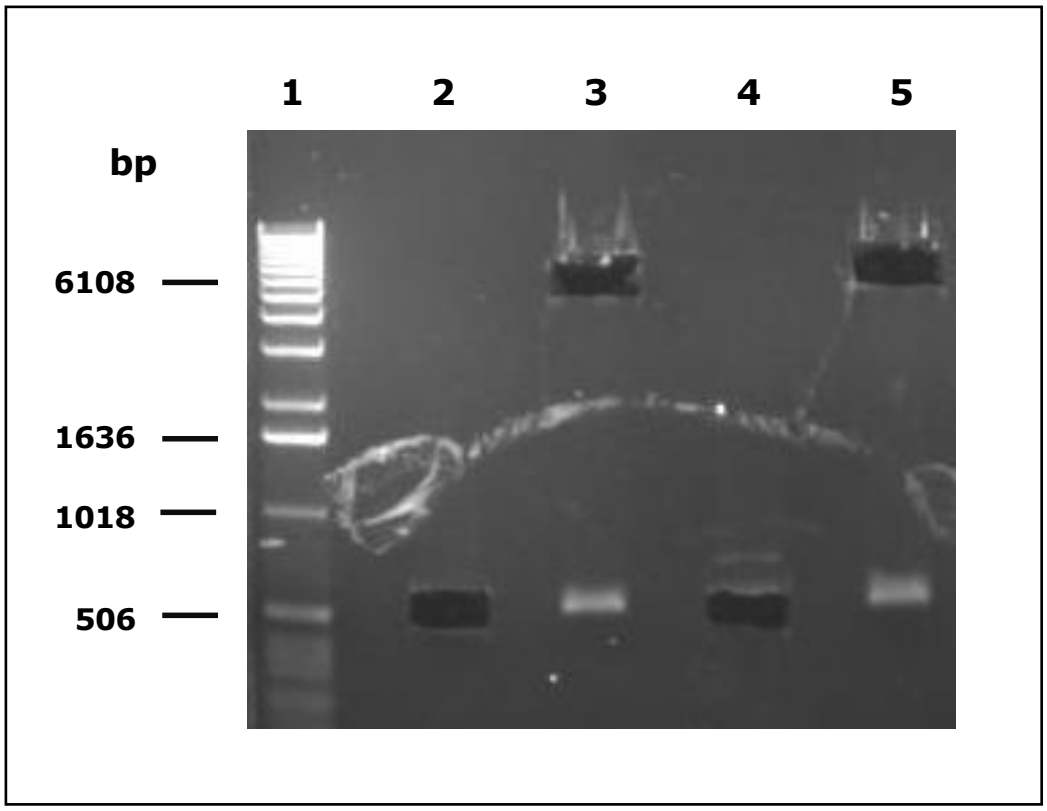

Figure 6-3 Agarose gel electrophoresis of restriction digest.

The figure represents the 1% agarose gel electrophoresis analysis of restriction digestion of Kir6.1, mutant vector constructs. The gel was stained with ethidium bromide and photographed under UV light. The pcDNA3.1/myc/hisA/Kir6.1 vector was digested by BspE1 at 37 ºC and BstEII at 60 ºC. Lane 1 represents the 1 Kb DNA ladder (molecular weight markers), lane 2; the insert (557 bp) and lane 3; the vector (6423 bp) for the Kir6.1 E332K mutant respectively, lane 4; the insert (557 bp) and lane 5; the vector (6423 bp) for the Kir6.1 R347E mutant, respectively. These products were excised (black rectangles) and used for ligation.

6.2.2 Functional studies of the cytoplasmic salt bridges in the $Kir6.1_4/SUR2A_4$ Channel Complex

The function of heterologously expressed wild type and mutated full length Kir6.1/SUR2A channel subunits was investigated in whole-cell patch clamp recording, 48-72 hrs after transfection in HEK-293 cells. The effects of single point mutations and reinstated proposed salt bridges (see Chapter 5) on the channel sensitivity to the potassium channel opener (pinacidil) and sulphonylurea (glibenclamide) were investigated.

The optimization of the co-expression of Kir6.1 and SUR2A subunits was performed as described in a previous study (Kono et al. 2000). Whole-cell patch clamp recording of wild type Kir6.1/SUR2A channels was performed (figure 6-4). Moreover, dose-response curves for the potassium channel opener, pinacidil, and the K_{ATP} channel sulphonylurea antagonist, glibenclamide, were carried out. The data from wild type Kir6.1/SUR2A channels was used as a control for that from channels containing single point mutations (Kir6.1 E332K and R347E) or reinstated inter-subunit salt bridges between Kir6.1 and SUR2A subunits.

The K_{ATP} channel currents for wild type and each mutated subunit combinations of Kir6.1/SUR2A and Kir6.2/SUR2A channel were acquired and analysed using Clampex 10.2 and Clamfit 10.2 version software (molecular devices), respectively. In order to establish dose-response curves for single point mutations and proposed salt bridges (see Chapter 5) on the channel sensitivity to potassium channel opener (pinacidil) and sulphonylurea (glibenclamide) a range of different concentrations of pinacidil and glibenclamide were used.

Prior to establishing the dose-response curves of K_{ATP} channel inhibition by glibenclamide, pinacidil concentration-response curves were performed and half-maximal effective concentrations (EC_{50}) value for wild type and each mutated subunit combinations of Kir6.1/SUR2A channel were measured. Pinacidil activated K_{ATP} channel currents in response to different concentrations for each subunit combinations were measured from HEK 293 cell line. To introduce pinacidil concentration-response curve, a large concentration range from nM (low concentration) to µM (highest concentration) were used. For accuracy and correctness close concentrations just 3 to 5 different concentrations were used in each recording. This was very important point to consider in single point mutated channel, Kir6.1 R347E/SUR2A, since this channel was very sensitive to pinacidil.

To make sure the current is a K_{ATP} channel current, glibenclamide which is a classical sulphonylurea K_{ATP} channel antagonist, was used in high concentration (10 to 100 µM) at the end of each recording to completely inhibit the channel. It is worth mentioning, the other reason to use glibenclamide in high concentration at the end to make sure if there is some leak current in the recording or not. Occasionally, when the glibenclamide (high concentration) inhibition current did not reached the zero, possibly about 2-5 pA, this current (leak current) was subtracted from the peak current as to obtain an accurate result. Moreover, if the leak current was bigger than 5 pA the recording was not included in the results.

The average of peak amplitude currents (pA) which was a response to each concentration of pinacidil was divided by cell capacitance (pF) to normalize the results to current density (pA/pF) then plotted against their pinacidil concentrations to introduce the pinacidil dose-response curve. The EC_{50} of pinacidil for each subunit combinations of Kir6.1/SUR2A or Kir6.2/SUR2A channel was used to activate the

channel to introduce dose-response curve of K_{ATP} channel inhibition by glibenclamide. The reason for using the EC_{50} and not maximum concentration of pinacidil to activate K_{ATP} channel current was that to distinguish between rundown and inhibition by glibenclamide. The fraction of glibenclamide-inhibited K_{ATP} channel current which was activated by EC_{50} of pinacidil was plotted against its concentration to establish glibenclamide dose-response curve.

In this sub-study, all whole-cell patch clamp recording was performed 48-72 hrs after cotransfection of HEK-293 cells with different Kir6.1/SUR2A subunit combinations (as described in Chapter 2).

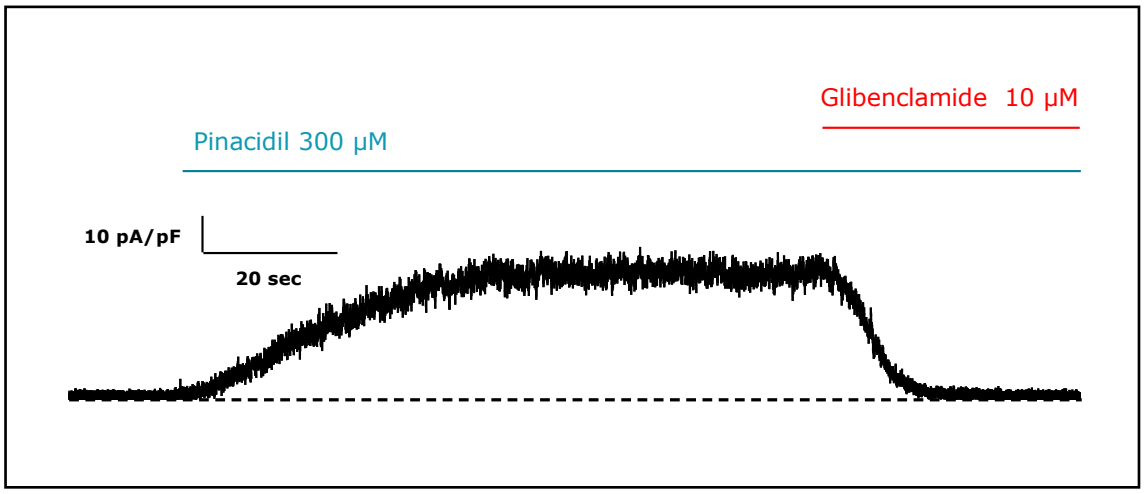

Figure 6-4 Representative trace of potassium channel opener activated current of wild type Kir6.1/SUR2A channel.

A typical pinacidil-activated potassium current recorded from the whole cell patch clamp configuration. The current was recorded 48-72 hrs after heterologous cotransfection of full length wild type Kir6.1 and SUR2A subunits in HEK-293 cells. The wild type Kir6.1/SUR2A channel was opened with 300 µM potassium channel opener, pinacidil, and inhibited with 10 µM K_{ATP} channel antagonist, glibenclamide. The current (pA) was normalized to the cell capacitance (pF) and the current data expressed as current density (pA/pF). The dashed line represents the zero current.

6.2.2.1 Single Point Mutation of R347 in the Distal C-Terminal of Kir6.1 Increased the Sensitivity to Potassium Channel Opener of Kir6.1/SUR2A Channels

The hypothesis in this sub-study was that disruption of the inter-subunit salt bridge Kir6.1 K347/SUR2A E1318 by single charge reversal mutation, Kir6.1 K347E, should impair the sensitivity of K_{ATP} channel opener, pinacidil. To test this hypothesis the sensitivity of pinacidil was measured in Kir6.2 K347E/SUR2A WT subunit combination channel. The single point mutation, R347E, in full length of the pore forming Kir6.1 expressed with wild type SUR2A increased significantly ($p < 0.006$) the sensitivity to activation by potassium channel opener of recombinant Kir6.1 R347E/SUR2A WT channels (EC_{50} = 0.71 ± 1.21 µM, n=6) versus the wild type Kir6.1/SUR2A channels (EC_{50} = 43.90 ± 1.28 µM, n=6) (figure 6-5, 6-8 A and table 6-2).

6.2.2.2 Inter-subunit Salt Bridge Formation Communicates Potassium Channel Opener Sensitivity in Kir6.1/SUR2A Channels

As described in the previous section, interruption of the cytoplasmic electrostatic interface, Kir6.1 R347/SUR2A E1318, by a single charge reversal mutation in the Kir6.1 R347E subunit caused increase in the pinacidil sensitivity in Kir6.1/SUR2A channel. To investigate whether pinacidil sensitivity could be restored by reestablishment of the Kir6.1 R347/SUR2A E1318 salt bridge, Kir6.1 R347E and SUR2A E1318R were coexpressed. When the charge reversals in both subunits were coexpressed heterologously to reform the inter-subunit salt bridge Kir6.1 R347E/SUR2A E1318R, the pinacidil sensitivity was significantly ($p < 0.028$) restored near to that of the wild type channel (EC_{50} = 23.50 ± 1.2 µM versus wild type EC_{50} = 43.90 ± 1.28 µM) compared to the Kir6.1 R347E/SUR2A WT channels (EC_{50} = 0.71 ± 1.21 µM, n=6) (figure 6-8 B and table 6-2).

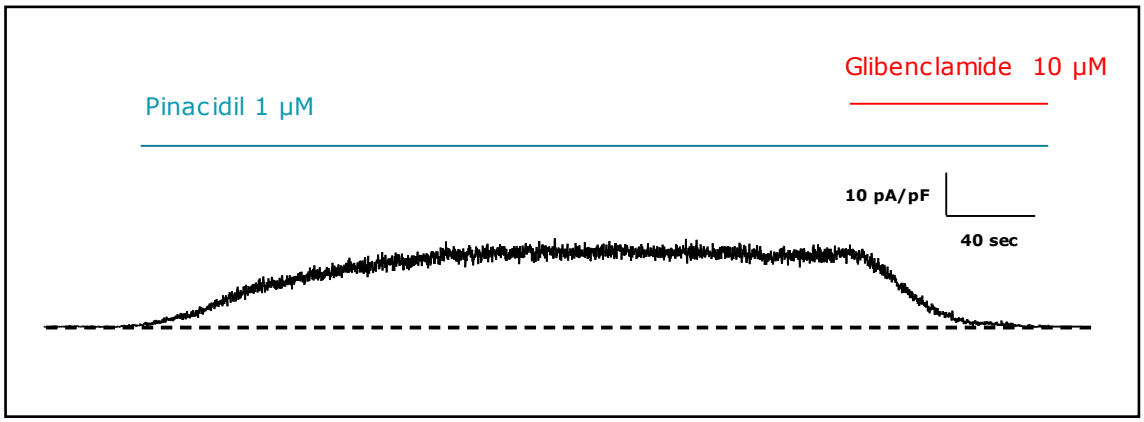

Figure 6-5 Representative trace of potassium channel opener activated current of Kir6.1 R347E/SUR2A WT channels.

A typical pinacidil activated potassium current of Kir6.1 R347E/SUR2A WT channels from the whole cell patch clamp configuration. This channel was sensitive to a low concentration (1µM) of potassium channel opener, pinacidil, while 10 µM of the K_{ATP} channel antagonist, glibenclamide, was sufficient to fully inhibit the channel. The current was recorded, 48-72 hrs after heterologous cotransfection of full length Kir6.1 R347E with SUR2A WT subunits in HEK-293 cells. The current (pA) was normalized to the cell capacitance (pF) and the current data expressed as current density (pA/pF). The dashed line represents the zero current.

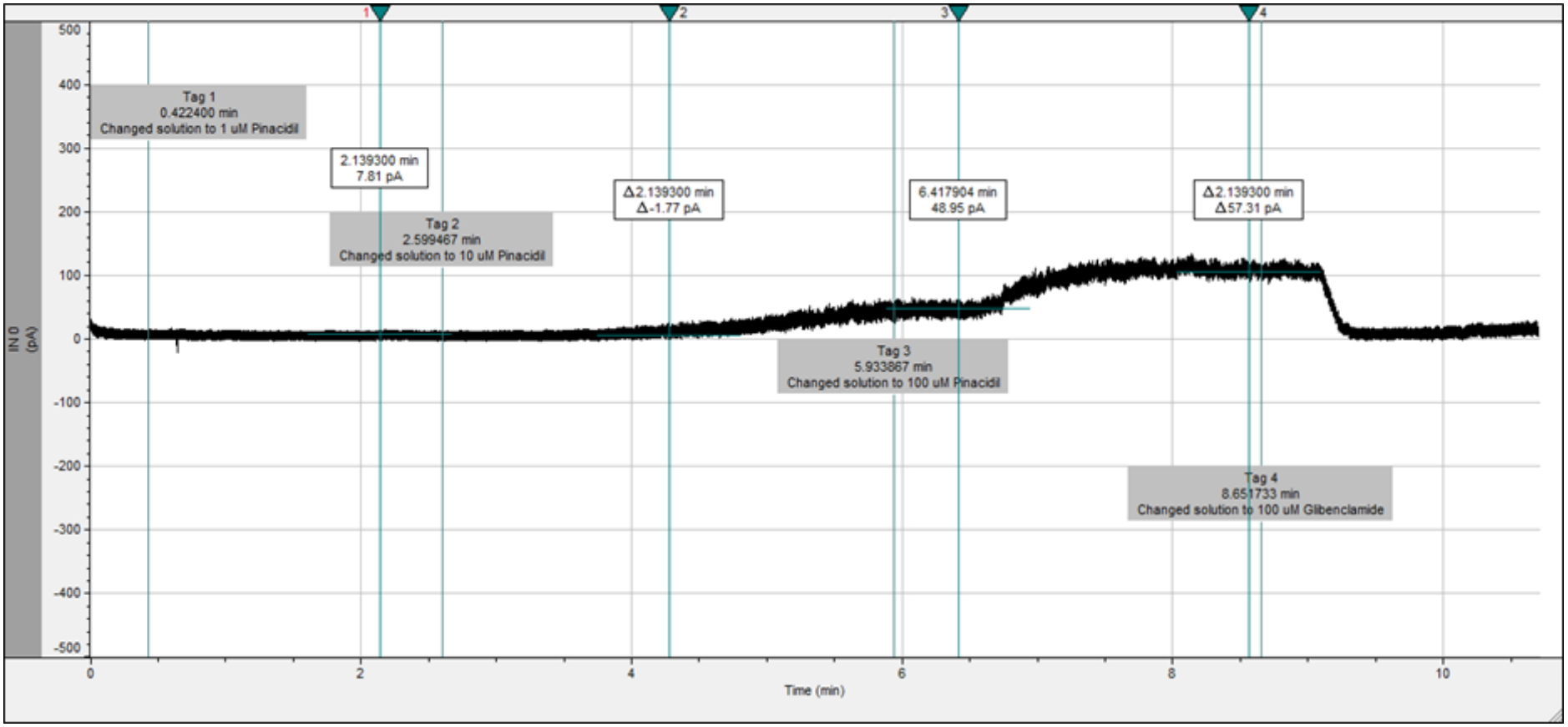

Figure 6-6 Representative current trace with different concentrations of K_{ATP} channel agonist pinacidil of wild type Kir6.1/SUR2A channel.

The figure illustrates a typical current trace from whole-cell patch clamp configuration in HEK-293 cells (48-72 hrs after cotransfection) of wild type Kir6.1/SUR2A channel. In order to make the pinacidil dose-response curve, different concentrations (in this recording; 1, 10 and 100 µM) of pinacidil were used to activate the channel and 100 µM glibenclamide (K_{ATP} channel antagonist) completely inhibited the pinacidil activated current of the wild type Kir6.1/SUR2A channel.

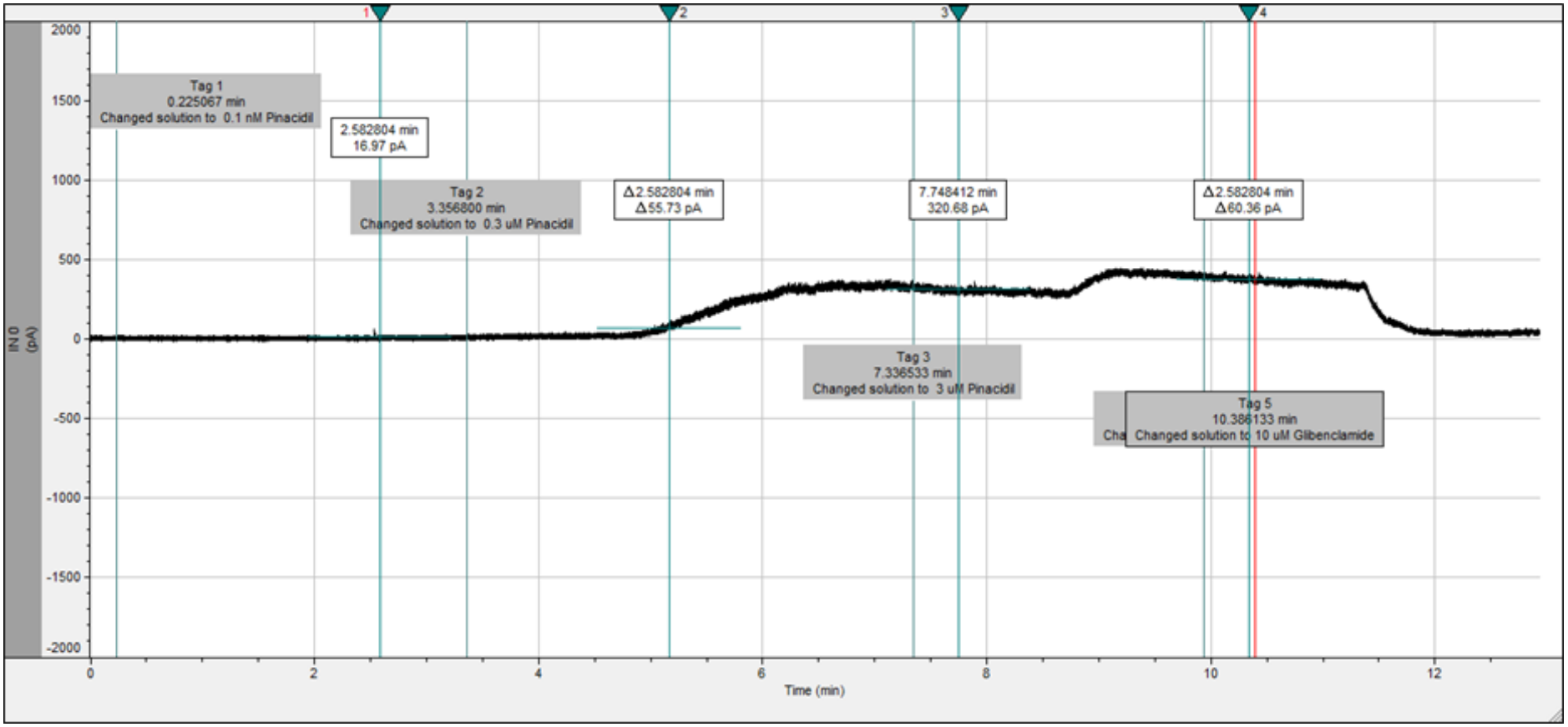

Figure 6-7 Representative current trace with different concentrations of K_{ATP} channel agonist pinacidil of Kir6.1 R347E /SUR2A WT channel.

The figure illustrates a typical current trace from whole-cell patch clamp configuration in HEK-293 cells (48-72 hrs after cotransfection) of Kir6.1 R347E/SUR2A WT channel. In order to make the pinacidil dose-response curve, different concentrations (in this recording; 0.1 nM, 0.3 µM and 3 µM) of pinacidil were used to activate the channel and 10 µM glibenclamide (K_{ATP} channel antagonist) inhibited the pinacidil activated Kir6.1 R347E/SUR2A WT channel current. Notably, just 0.3 µM of pinacidil induced a large current (> 300 pA) in this channel.

A) B)

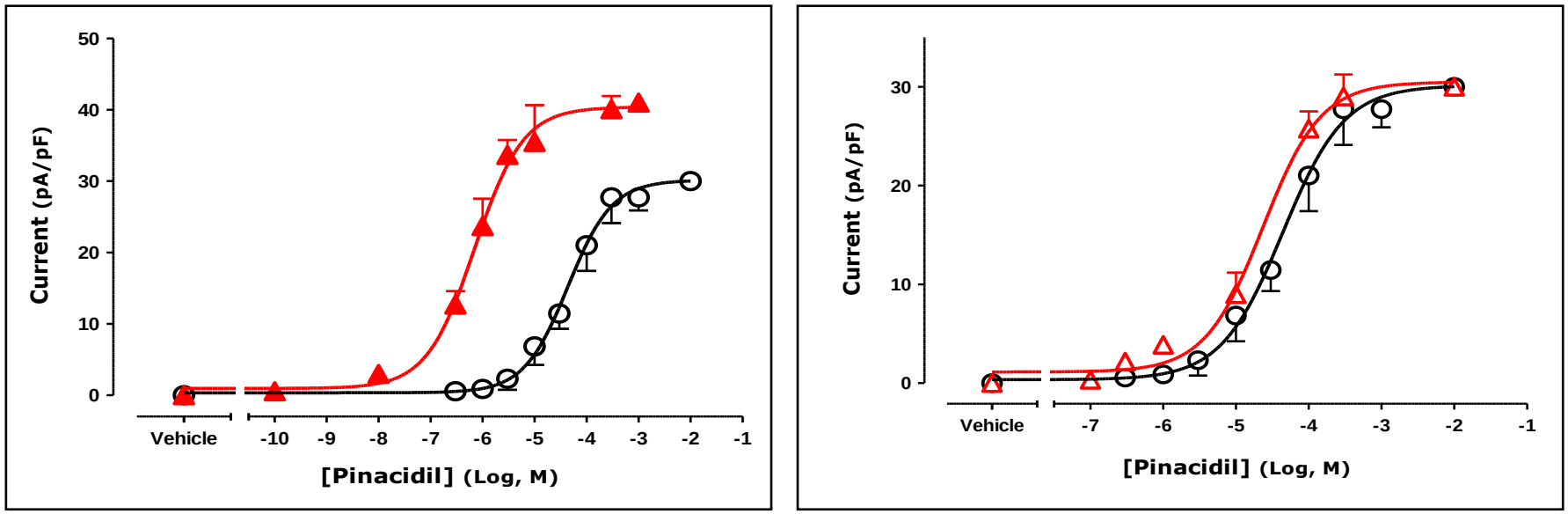

Figure 6-8 Dose-response curves for pinacidil activation of wild type Kir6.1/SUR2A, Kir6.1 R347E/SUR2A WT and Kir6.1 R347E/SUR2A E1318R channels.

Dose-response curves for current activation by pinacidil of wild type Kir6.1/SUR2A (circles, A and B), Kir6.1 R347E/SUR2A WT (filled triangles, A) and Kir6.1 R347E/SUR2A E1318R channel (empty triangles, B). A) The presence of the single point mutation of R347 in the distal C-terminal of Kir6.1 increased significantly ($p \langle 0.006$) sensitivity to the potassium channel opener, pinacidil (EC_{50} = 0.71 ± 1.2 µM, Hill slope = 0.94 ± 0.2) compared to the wild type Kir6.1/SUR2A channel (EC_{50} = 43.9 ± 1.3 µM, Hill slope = 1.03 ± 0.2). B) A single charge reversal of residues in both subunits for Kir6.1 R347E /SUR2A E1318R restored the pinacidil sensitivity (EC_{50} = 23.5 ± 1.3 µM, Hill = 1.09 ± 0.2) significantly ($p \langle 0.028$) near to that of wild type Kir6.1/SUR2A channel compared to the Kir6.1 R347E/SUR2A WT channels. For each point, a minimum 6 cells were recorded in the whole-cell patch clamp configuration, 48-72 hrs after transfection of HEK-293 cells. The dose-response curve fitting was performed with nonlinear regression (curve fit) and sigmoidal dose-response variable slope with four parameters. Statistic analysis: bars indicate mean with SEM, using paired t test, two-tailed with 95% confidence interval.

6.2.2.3 Single Point Mutation of E332 and R347 in the Distal C-Terminal of Kir6.1 Decreased the Sensitivity to Sulphonylurea in the Kir6.1/SUR2A Channel

The positive charged arginine at position 347 (R347) in Kir6.1was shown to be involved in influencing the pinacidil sensitivity between the two heterologous subunits, Kir6.1 and SUR2A, in Kir6.1/SUR2A channel (section 6.2.2.1). To assess the hypothesis that Kir6.1 E332 and/or R347 influence the glibenclamide sensitivity of the Kir6.1/SUR2A channel, whole-cell patch clamp recording of Kir6.1 E332K/SUR2A WT and Kir6.1 R374E/SUR2A WT channels was performed. The results revealed that both mutated channels, Kir6.1 E332K/SUR2A WT and Kir6.1 R374E/SUR2A WT, had significantly reduced sensitivity to antagonist, glibenclamide (IC_{50} = 318 ± 1.20 nM, $P < 0.043$ value and IC_{50} = 241 ± 1.09 nM, $P < 0.015$ value, respectively) compared to the wild type (IC_{50} = 6.14 ± 1.13 nM) (figure 6-11 A, figure 6-12 A and table 6-3).

6.2.2.4 Inter-subunit Salt Bridge Formation Communicates Sulphonylureas Sensitivity in Kir6.1/SUR2A Channels

A single charge reversal in the distal C-terminal of Kir6.1 of the residues involved in three putative salt bridges was sufficient to reduce significantly the sensitivity of pinacidil activated current to inhibition by sulphonylurea, glibenclamide (previous section). To investigate whether the sensitivity to the K_{ATP} channel antagonist,

glibenclamide, could be restored by reestablishing the proposed salt bridges, Kir6.1 R347E and SUR2A E1318R and Kir6.1 E332K/SUR2A E1322D were coexpressed.

Glibenclamide sensitivity was restored to near wild type when the charge reversals in both subunits were co-expressed heterologously to reform the proposed inter-subunit salt bridges, Kir6.1 R347E/SUR2A E1318R, (IC_{50} = 13.75 ± 1.11 nM, $p \langle 0.080$) and Kir6.1 E332K/SUR2A E1322D, (IC_{50} = 9.12 ± 1.12 nM, $p \langle 0.250$) versus wild type Kir6.1/SUR2A channel, (IC_{50} = 6.14 ± 1.13 nM) (figure 6-11 B, figure 6-12 B, table 6-3).

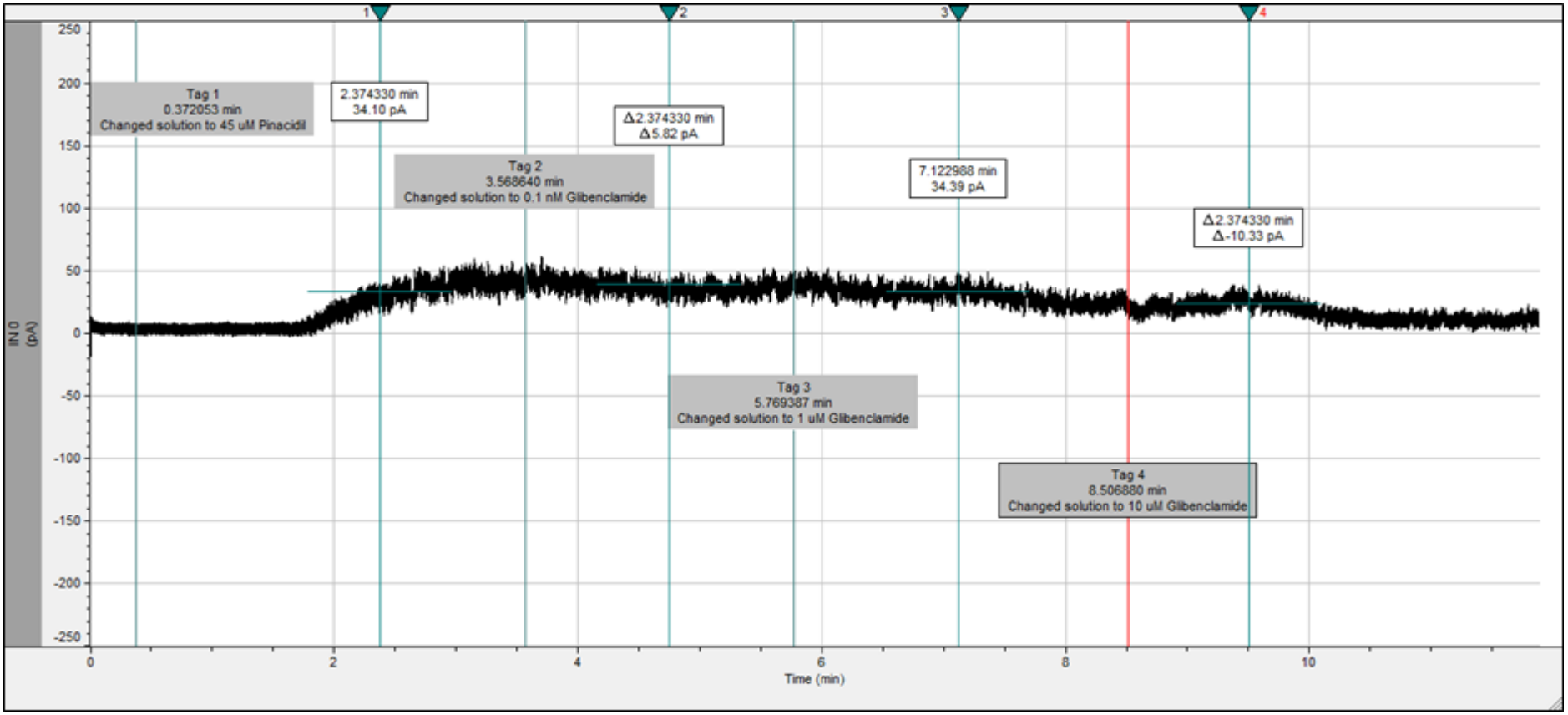

Figure 6-9 Representative current trace with different concentrations of K_{ATP} channel antagonist glibenclamide of wild type Kir6.1/SUR2A channel.

The figure illustrates a typical current trace from whole-cell patch clamp configuration in HEK-293 cells (48-72 hrs after cotransfection) of wild type Kir6.1/SUR2A channel. In order to make the glibenclamide dose-response curve, different concentrations (in this recording; 0.1 nM, 1 µM and 10 µM) of glibenclamide were used to inhibit the pinacidil activated K_{ATP} channel current. It is worth noting, to distinguish between rundown and inhibition by glibenclamide, just 45 µM (~ EC_{50}) of pinacidil was used to activate the wild type Kir6.1/SUR2A channel.

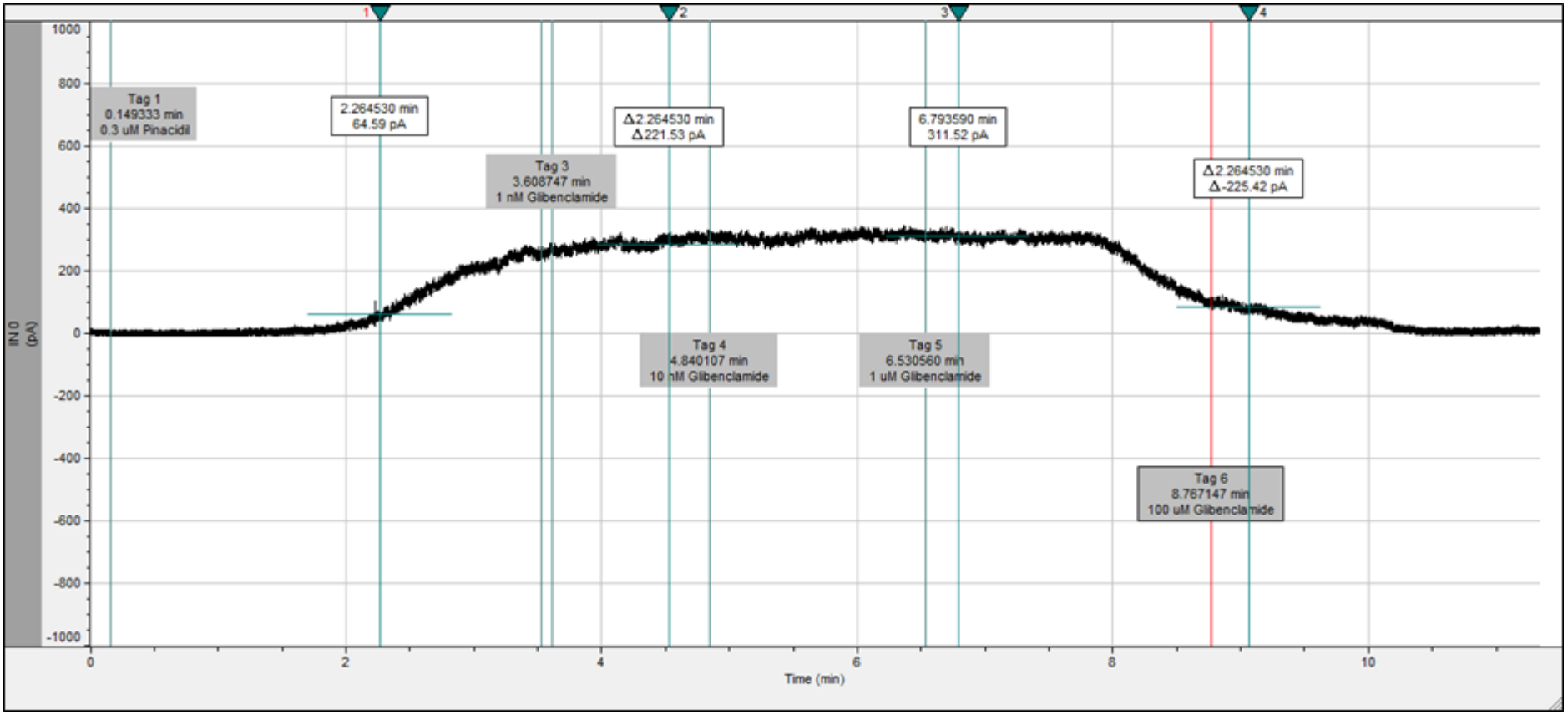

Figure 6-10 Representative current trace with different concentrations of K_{ATP} channel antagonist glibenclamide of Kir6.1 R347E/SUR2A WT channel.

The figure illustrates a typical current trace from whole-cell patch clamp configuration in HEK-293 cells (48-72 hrs after cotransfection) of Kir6.1 R347E/SUR2A WT channel. In order to make the glibenclamide dose-response curve, different concentrations (in this recording; 1 nM, 10 nM, 1 µM and 100 µM) of glibenclamide were used to inhibit the pinacidil activated K_{ATP} channel current. It is worth noting, to distinguish between rundown and inhibition by glibenclamide, just 0.3 µM (~ EC_{50}) of pinacidil was used to activate the Kir6.1 R347E/SUR2A WT channel.

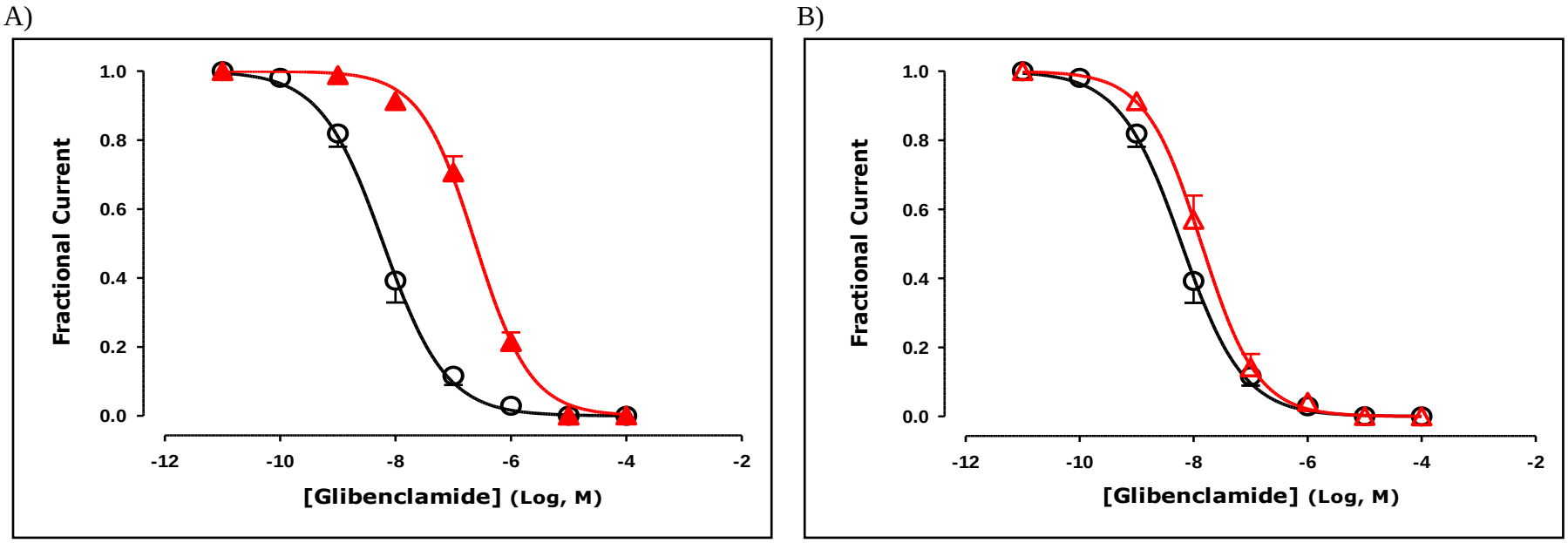

Figure 6-11 Dose-response curves for glibenclamide inhibition of wild type Kir6.1/SUR2A, Kir6.1 R347E/SUR2A WT and Kir6.1 R347E/SUR2A E1318R channels.

Dose-response curves for the inhibition of pinacidil activated current by glibenclamide of wild type Kir6.1/SUR2A (circles, A and B), Kir6.1 R347E/SUR2A WT (filled triangles, A) and Kir6.1 R347E/SUR2A E1318R channel (empty triangles, B). A) A single charge reversal point mutation R347E in the distal C-terminal of Kir6.1 decreased significantly ($p \langle 0.015$) the sensitivity to the K_{ATP} channel antagonist, glibenclamide, (IC_{50} = 241.60 ± 1.09 nM, Hill = 0.91 ± 0.06) compared to the wild type Kir6.1/SUR2A channel, (IC_{50} = 6.14 ± 1.13 nM, Hill slope = 0.80 ± 0.08). B) A single reversal of charged residues in both subunits for Kir6.1 R347E/SUR2A E1318R restored the glibenclamide sensitivity (IC_{50} = 13.75 ± 1.11 nM, Hill = 0.89 ± 0.07, $p \langle 0.080$) close to the wild type compared to Kir6.1 R347E/SUR2A WT channel. For each point, a minimum 6 cells were recorded in the whole-cell patch clamp configuration, 48-72 hrs after transfection of HEK-293 cells. The dose-response curve fitting was performed with nonlinear regression (curve fit) and sigmoidal dose-response variable slope with four parameters. Statistic analysis: bars indicate mean with SEM, using paired t test, two-tailed with 95% confidence interval.

A) B)

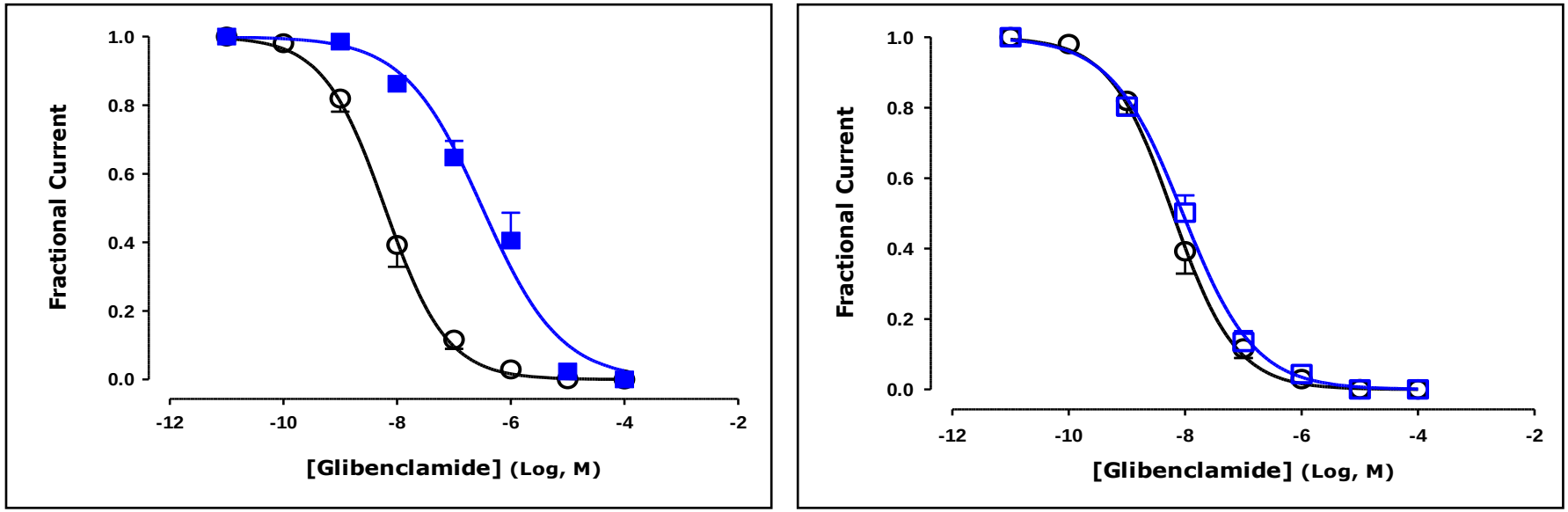

Figure 6-12 Dose-response curves for glibenclamide inhibition of wild type Kir6.1/SUR2A, Kir6.1 E332K/SUR2A WT and Kir6.1 E332K/SUR2A K1322D channels.

Dose-response curves for the inhibition of pinacidil activated current by glibenclamide of wild type Kir6.1/SUR2A (circles, A and B), Kir6.1 E332K/SUR2A WT (filled rectangles, A) and Kir6.1 E332K/SUR2A K1322D channel (empty rectangles, B). A) A single charge reversal point mutation E332K in the distal C-terminal of Kir6.1 decreased significantly ($p < 0.043$) the sensitivity to the K_{ATP} channel antagonist, glibenclamide, (IC_{50} = 318.40 ± 1.20 nM, Hill slope = 0.63 ± 0.06) compared to the wild type Kir6.1/SUR2A channel, (IC_{50} = 6.14 ± 1.13 nM, Hill slope = 0.80 ± 0.08). B) A single reversal of charged residues in both subunits for Kir6.1 E332K/SUR2A K1322D restored the glibenclamide sensitivity (IC_{50} = 9.12 ± 1.12 nM, Hill = 0.71 ± 0.06, $p < 0.250$) close to the wild type compared to the Kir6.1 E332K/SUR2A WT channel. For each point, a minimum 6 cells were recorded in the whole-cell patch clamp configuration, 48-72 hrs after transfection of HEK-293 cells. The dose-response curve fitting was performed with nonlinear regression (curve fit) and sigmoidal dose-response variable slope with four parameters. Statistic analysis: bars indicate mean with SEM, using paired t test, two-tailed with 95% confidence interval.

6.2.2.5 Single Point Mutation of E332 in the Distal C-terminal of Kir6.1 Resulted in Constitutive Opening of the Kir6.1/SUR2A Channel

Whole-cell patch clamp recording of a single mutation in full length Kir6.1, E332K expressed with SUR2A WT was performed to assess the hypothesis that E332 in the distal Kir6.1 C-terminal is involved in allosteric contact between the distal C-terminal of Kir6.1 and NBD2 of SUR2A. Whole-cell patch clamp recording revealed that this mutation (Kir6.1 E332K), in the absence of potassium channel opener, caused constitutive opening of the Kir6.1/SUR2A channel (figure 6-13 and 6-14 and table 6-2).

To investigate whether constitutive activation could be reversed or pinacidil sensitivity restored by reestablishment of the salt bridge(s) to Kir6.1 E332, the Kir6.1 E332K subunit was coexpressed with SUR2A Q1336E or K1322D (see Chapter 5). The whole-cell patch clamp recording of Kir6.1 E332K/SUR2A Q1336E and Kir6.1 E332K/SUR2A K1322D channels revealed continued disruption of channel properties in channel subunit combinations containing the single point mutation of E332 in the distal C-terminal of Kir6.1 (figure 6-9 B, 6-10 A and table 6-2). Furthermore, even double mutants in the NBD2 of SUR2A to restore both potential salt bridges did not restore the gated opening of the wild type channel (figure 6-14 B and table 6-2). The Kir6.1 E332K mutant, in addition to causing constitutive opening channels with SUR2A Q1336E or SUR2A K1322D + Q1336E, formed channels that were insensitive even to high concentrations of glibenclamide (100 µM) (figure 6-14 A and B, table 6-3).

The significant question remains to be answered is whether the residues in equivalent positions in Kir6.2 to Kir6.1 are also involved in allosteric regulation in Kir6.2/SUR2A channels. This is answered in the next section (6.2.3).

A)

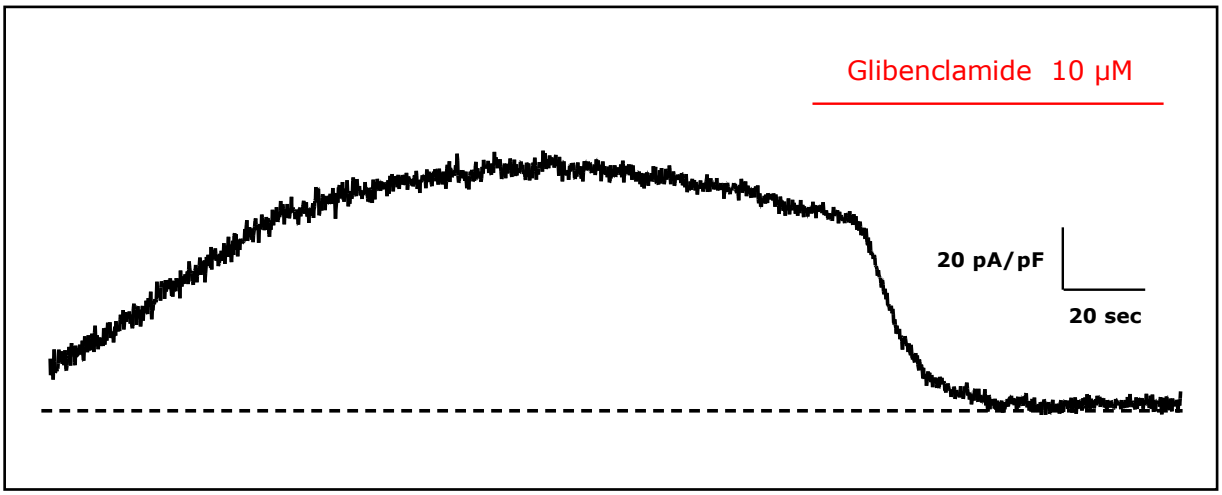

B)

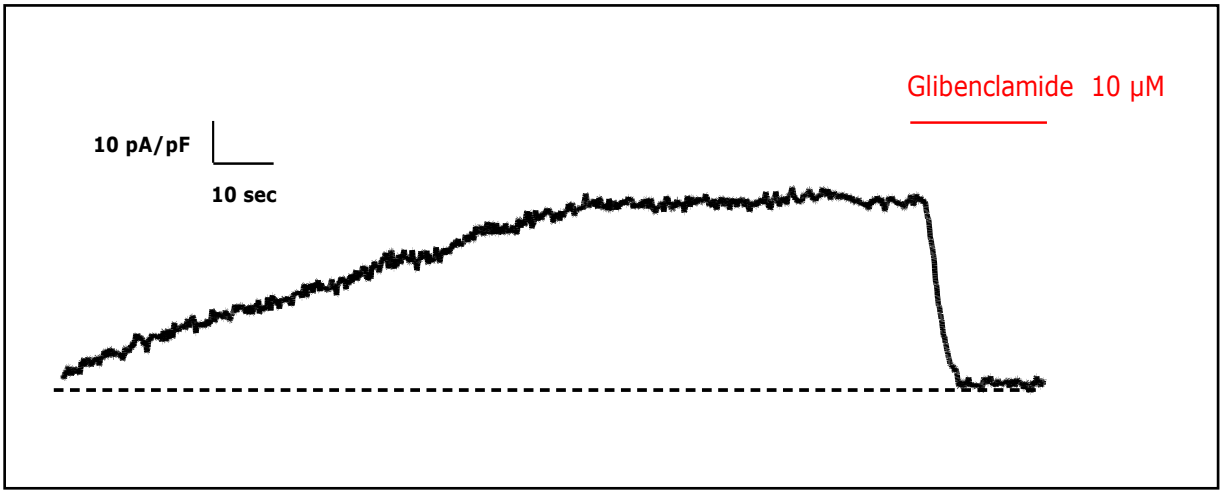

Figure 6-13 The Kir6.1 E332K mutant causes constitutive opening of the ATP-sensitive potassium channel.

The traces represent potassium currents in the absence of activation by pinacidil in the whole-cell configuration. A) A typical current for Kir6.1 E332K/SUR2A WT and (B) Kir6.1 E332K/SUR2A K1322D channel. The currents were recorded, 48-72 hrs after heterologous cotransfection of Kir6.1 and SUR2A subunits in HEK-293 cells. The current (pA) was normalized to the cell capacitance (pF) and the current data expressed as current density (pA/pF). The dashed line in (A) and (B) represents the zero current.

A)

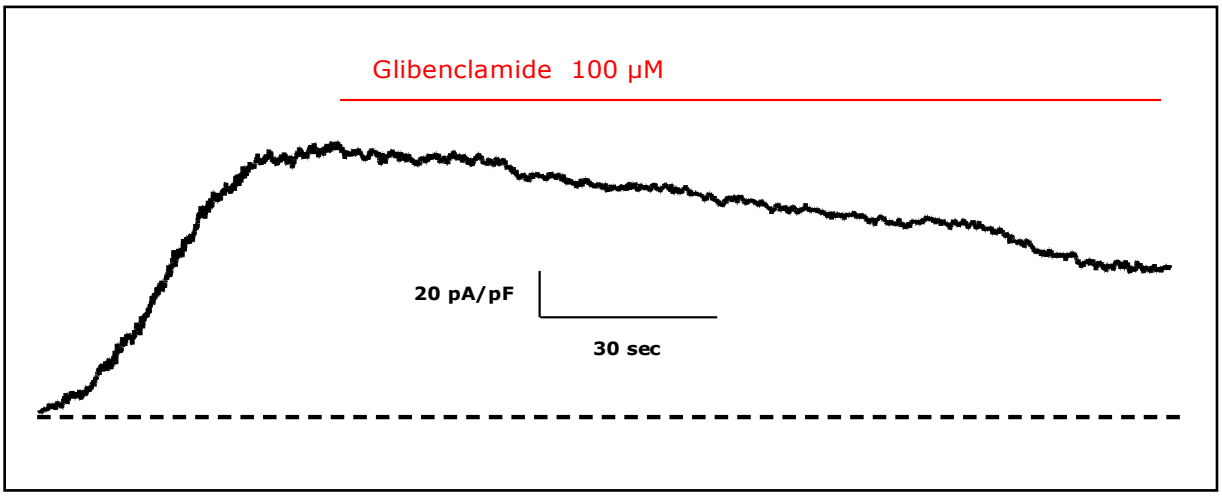

B)

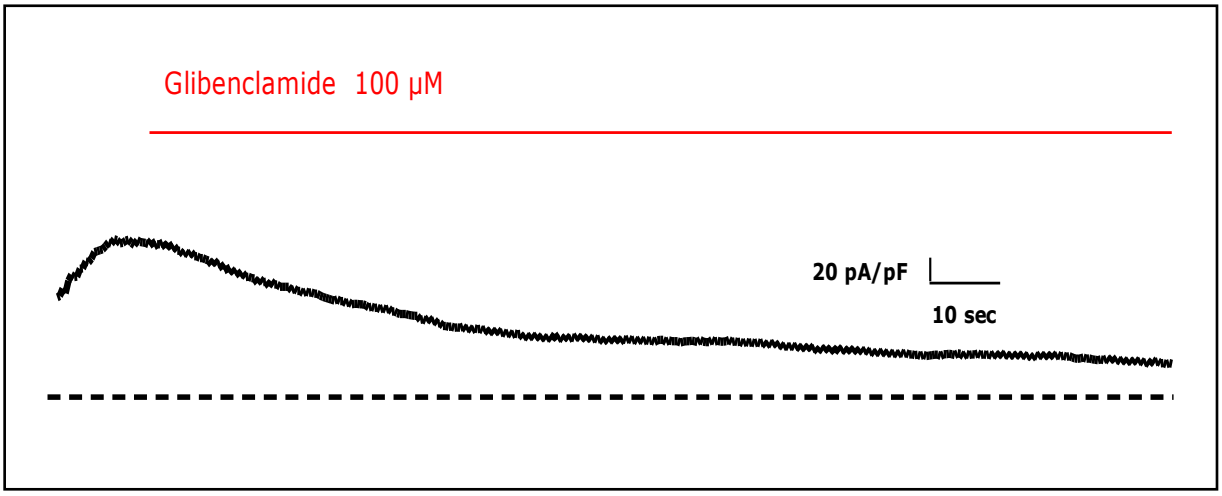

Figure 6-14 The Kir6.1 E332K mutant expressed with SUR2A Q1336E or SUR2A K1322D + Q1336E formed channels insensitive to sulphonylurea.

The traces represent potassium currents in the absence of activation by pinacidil in the whole-cell configuration. A) A typical current for Kir6.1 E332K/SUR2A Q1336E and (B) Kir6.1 E332K/SUR2A K1322D + Q1336E channels. These channels were insensitive to the K_{ATP} channel antagonist, glibenclamide, even at high concentration (100 µM). The dashed line in (A) and (B) represents the zero current.

Subunits						
Kir6.1	SUR2A	EC_{50} (μM)	SE	Hill	SE	P-value
WT	WT	43.90	1.28	1.03	0.23	—
R347E	WT	0.71	1.21	0.94	0.20	0.006
R347E	E1318R	23.50	1.26	1.09	0.20	0.028
E332K	WT	Constitutive				—
E332K	K1322D	Constitutive				—
E332K	Q1336E	Constitutive				—
E332K	K1322D + Q1336E	Constitutive				—

Table 6-2 Pinacidil sensitivity of Kir6.1/SUR2A channels is affected by cytoplasmic inter-subunit salt bridge formation.

The table represents the summary of the EC_{50} (μM) values determined for the potassium channel opener, pinacidil, on different Kir6.1/SUR2A subunit combinations. A single charge reversal point mutation in the distal C-terminal of Kir6.1, E332K, caused constitutive opening of the Kir6.1/SUR2A channel. The data was recorded from the whole-cell patch clamp configuration, 48-72 hrs after transfection of HEK-293 cells.

n = minimum 6 cells for each point. Statistic analysis: paired t test, two-tailed with 95% confidence interval (each mutated subunit combination of the Kir6.1/SUR2A channel, EC_{50}, was compared to the wild type, control).

Subunits						
Kir6.1	SUR2A	IC_{50} (nM)	SE	Hill	SE	P-value
WT	WT	6.14	1.13	0.80	0.08	—
R347E	WT	241.60	1.09	0.91	0.06	0.015
R347E	E1318R	13.75	1.11	0.89	0.07	0.080
E332K	WT	318.40	1.20	0.63	0.06	0.043
E332K	K1322D	9.12	1.12	0.71	0.06	0.250
E332K	Q1336E	Insensitive				—
E332K	K1322D + Q1336E	Insensitive				—

Table 6-3 Glibenclamide sensitivity of Kir6.1/SUR2A channels is affected by cytoplasmic inter-subunit salt bridge formation.

The table shows the summary of the IC_{50} (nM) values determined for the K_{ATP} channel antagonist, glibenclamide, on different Kir6.1/SUR2A subunit combinations. The Kir6.1 E332K/SUR2A Q1336 and Kir6.1 E332K/SUR2A K1322D + Q1336 channels were insensitive to glibenclamide. The data was recorded from whole-cell patch clamp configuration, 48-72 hrs after transfection of HEK-293 cells. n = minimum 6 cells for each point. Statistic analysis: paired t test, two-tailed with 95% confidence interval (each mutated subunit combination of the Kir6.1/SUR2A channel, IC_{50}, was compared to the wild type, control).

6.2.3 Functional studies of the cytoplasmic salt bridges in the $Kir6.2_4/SUR2A_4$ Channel Complex

Previous biochemical studies suggested that the Kir D323 and K338 are key residues for the Kir6.2/SUR2A channels assembly (see Chapter 3). In addition, these residues have been shown to form inter-subunit salt bridges with SUR2A E1318, K1322 and Q1336 (see Chapter 5). The main aim of this sub-study was to study the functional properties of mutated subunit combinations of these salt bridges in Kir6.2/SUR2A channels. In greater detail, to test the hypothesis of whether the C-terminal cytoplasmic interfaces, Kir6.2 D323/SUR2A K1322, Kir6.2 D323/SUR2A Q1336 and Kir6.2 K338/SUR2A E1318, influence the allosteric information transmission from SUR2A to the channel pore Kir6.2 in functional hetero-octameric complex $Kir6.2_4/SUR2A_4$ channels. All cell culture (transfection and cells preparation) in this section was done by me, Hussein N. Rubaiy, and the represented data shown in this section was measured by Dr Richard Rainbow (research fellow).

Whole-cell patch clamp data from HEK-293 cells revealed the inter-subunit Kir6.2 K338/SUR2A E1318 salt fridge formation communicates the sensitivity of the potassium channel opener, pinacidil, and blocker, glibenclamide of the Kir6.2/SUR2A channels. Disruption of this inter-subunit salt bridge by a single charge reversal mutation in either subunit caused an increase in the pinacidil sensitivity and decrease in the glibenclamide sensitivity, respectively (table 6-4 and 6-5). Co-expression of Kir6.2 K338E with SUR2A E1318R reinstates the inter-subunit interaction and restored the sensitivity of pinacidil and glibenclamide, respectively, near to the wild type Kir6.2/SUR2A channel (table 6-4 and 6-5).

Subunits		EC_{50} (μM)	SE	Hill	SE
Kir6.2	SUR2A				
WT	WT	39.6	13	1.5	0.5
K338E	WT	4.5	0.3	1.8	0.2
WT	E1318R	Very small current			
K338E	E1318R	46.7	4.9	1.1	0.1
D323K	WT	Constitutive			
WT	K1322D	Very small current			
D323K	K1322D	Constitutive			
WT	Q1336E	Some constitutive activity			
D323K	Q1336E	Some Constitutive			
WT	K1322D + Q1336E	Current too small to record			
D323K	K1322D + Q1336E	Constitutive			

Table 6-4 Pinacidil sensitivity of Kir6.2/SUR2A channels is affected by cytoplasmic inter-subunit salt-bridge formation.

The table represents the summary data of wild type and mutated pinacidil activated Kir6.2/SUR2A channel currents in whole-cell patch configuration. Pinacidil sensitivity was determined in the whole cell patch configuration for various Kir6.2/SUR2A combinations containing either targeted single point mutations or in charge reversal mutants in both subunits. Table shows EC_{50} ± SEM and Hill coefficient ± SEM. n = minimum 6 cells for each concentration in different subunit combinations.

Subunits		IC_{50} (nM)	SE	Hill	SE
Kir6.2	SUR2A				
WT	WT	3.1	0.8	1.9	0.1
K338E	WT	103	28	0.6	0.1
WT	E1318R	980	58	1	0.1
K338E	E1318R	6.4	0.9	1.1	0.2
D323K	WT	Insensitive			
WT	K1322D	Current too small to record			
D323K	K1322D	Insensitive			
WT	Q1336E	50600	8400	0.93	0.12
D323K	Q1336E	4.7	0.3	2.2	0.2
WT	K1322D + Q1336E	Current too small to record			
D323K	K1322D + Q1336E	Insensitive			

Table 6-5 Glibenclamide sensitivity of Kir6.2/SUR2A channels is affected by cytoplasmic inter-subunit salt-bridge formation.

The table represents the summary data of wild type and mutated glibenclamide inhibited Kir6.1/SUR2A channel currents in whole-cell patch configuration. Glibenclamide sensitivity was determined in the whole cell patch configuration for various Kir6.2/SUR2A combinations containing either targeted single point mutations or in charge reversal mutants in both subunits. Table shows EC_{50} ± SEM and Hill coefficient ± SEM. n = minimum 6 cells for each concentration in different subunit combinations.

In addition, the excised inside-out patch clamp data suggested this cytoplasmic electrostatic interface (Kir6.2 K338/SUR2A E1318) is not involved in determining the ATP sensitivity of the Kir6.2 pore or the ADP sensitivity from SUR2A to the channel pore Kir6.2 (table 6-6). Surprisingly, in the case of Kir6.2 D323/SUR2A K1322 or Q1336 or K1322 + Q1336 salt bridges, single charge reversal mutation on the pore forming Kir6.2 (D323K) resulted in constitutive channels activation in the absence of pinacidil. Additionally, reinstatement of the mentioned inter-subunit salt bridges did not fully or partially restore the channel properties near to the wild type Kir6.2/SUR2A. Conversely, reinstatement of the cytoplasmic electrostatic interface in Kir6.2 D323K/SUR2A Q1336E channel restored the decreased sensitivity of glibenclamide on single charge reversal in both subunits near to the wild type. These results suggest that the cytoplasmic Kir6.2 D323/SUR2A Q1336 salt bridge formation is involved in transmitting inhibitory information to the pore from antagonist binding to the SUR2A subunit. Inside-out patch clamp data revealed this salt bridge to be involved to some extent in determining the ADP sensitivity of Kir6.2/SUR2A channels (table 6-6).

It has been reported that association of SUR subunit enhances the affinity of ATP binding to Kir6 subunits in native K_{ATP} channels (Nichols et al. 1996, Tucker et al. 1997, Drain et al. 1998 and Gribble et al. 1997). The inhibition of current by ATP in channels formed from truncated Kir6.2 ΔC26 subunits was investigated to distinguish failure of SUR2A increase of ATP affinity in Kir6.2 D323 mutant which probably might cause reduction in affinity directly. Functional truncated Kir6.2 ΔC26 channels (provided by Dr Dave Lodwick, co-supervisor) were expressed alone without SUR2A subunit in HEK-293 cell lines. The results of excised inside-out patches revealed that the IC_{50} values for ATP inhibition of the wild type truncated Kir6.2 ΔC26 (120.0 ± 8.0 μM) and the mutated Kir6.2 ΔC26 D323K (129.0 ± 8.4 μM) are comparable (table 6-6). This evidence suggest that the single charge point mutation, Kir6.2 D323, might have little direct effect on ATP binding affinity within the pore forming Kir6.2

subunit. Furthermore, reinstatement of the salt bridge, Kir6.2 ΔC26 D323K/SUR2A Q1336 did not reduce the IC_{50} (123.0 ± 3.9 µM) for ATP inhibition near to the wild type Kir6.2/SUR2A channel (IC_{50} = 23.8 ± 1.7 µM, table 6-6).

Together, the ability of SUR2A to influence ATP binding to the Kir6.2 subunit was not restored sufficiently with the reinstated salt bridges with the Kir6.2 D323 (table 6-6), unlike the glibenclamide sensitivity which was restored in the Kir6.2 D323K/SUR2A Q1336E subunit combination (table 6-5).

In conclusion, the results of this electrophysiological sub-study provide evidence (for the first time) that inter-subunit salt bridges between the distal C-terminal of Kir6.2 and NBD2 of SUR2A mediate allosteric information transfer in Kir6.2/SUR2A channels. Moreover, this data of excised inside-out patch clamp recording shows that disruption of salt bridge did not disrupt Kir6.2 structure sufficiently to affect direct ATP_i binding and inhibition via the Kir6.2 subunit alone. Thus, the effect of breaking salt bridges must have been on the cross-talk between the two heterologous subunits. In addition, these results indicated that the inter-subunit Kir6.2 K338/SUR2A E1318 salt bridge do not necessarily play a crucial mediating role in allosteric modulation from SUR2A to the channel pore by ADP_i. Constitutive opening of the Kir6.2/SUR2A channel by single charge reversal point mutation of D323 in the distal C-terminal of the Kir6.2 possibly suggest that this negatively charged aspartic acid residue at position 323 to be important for stabilizing the assembly of functional channels of the Kir6.2/SUR2A subunit combinations in K_{ATP} channels.

Subunits		ATP, IC_{50} (μM)	SE	Hill	SE	ADP at 1 mM, Fraction	SE
Kir6.2	SUR2A						
WT	WT	23.8	1.7	1.8	0.2	0.34	0.06
K338E	WT	27.5	2	1.3	0.1	0.37	0.02
WT	E1318R	65.8	4.7	1.3	0.3	0.36	0.07
K338E	E1318R	27.7	1.5	1.8	0.2	0.34	0.05
D323K	WT	>10 mM				Not applicable	
WT	K1322D	Current too small to record				Not applicable	
D323K	K1322D	>10 mM				Not applicable	
WT	Q1336E	111.2	10	1.6	0.4	0.15	0.02
D323K	Q1336E	128.9	5.7	2.1	0.2	0.82	0.05
WT	K1322D + Q1336E	Current too small to record				Not applicable	
D323K	K1322D + Q1336E	>10 mM				Not applicable	
ΔC26	—	120	8	1.5	0.1	—	
ΔC26 - D323K	—	129	8.4	1.4	0.05	—	
ΔC26 - D323K	Q1336E	123	3.9	2.3	0.5	0.75	0.07

Table 6-6 Intracellular ATP and ADP sensitivity of Kir6.2/SUR2A channels is affected by cytoplasmic inter-subunit salt bridge formation.

The table represents the excised inside-out patch recording from HEK-293 cells of ATP and ADP sensitivity measurements of wild type and mutant recombinant channels, n = minimum 6 cells patches for each channel combination.

6.3 Summary and Conclusions

The major finding of this sub-study was that the proposed inter-subunit salt bridges mediate allosteric contacts between the two heterologous subunits in the Kir6.1/SUR2A channel. Single point mutation of E332 or R347 in the distal C-terminal of Kir6.1 impaired the properties of the Kir6.1/SUR2A channel and a single reversal charge residues in both subunits for Kir6.1 and SUR2A restored the function in some cases.

Biochemical study suggests that the Kir6.2 D323 and K338 are key residues for the Kir6.2/SUR2A channel assembly (see Chapter 3). Moreover, the same mentioned two residues in the distal C-terminus of Kir6.2 formed three cytoplasmic salt bridges (Kir6.2 K338E/SUR2A E1318K and Kir6.2 D323K/SUR2A K1322E, Kir6.2 D323K/SUR2A Q1336E) with NBD2 of SUR2A (see Chapter 5), indicating that these charged residues are very important for the physical interaction between the pore forming Kir6.2 and the regulatory subunit SUR2A in allostery $Kir6.2_4/SUR2A_4$ channel complex. This raised the hypothesis that equivalent residues in the same positions in Kir6.1 to Kir6.2 should play the same role and are crucial for the interaction between Kir6.1 and SUR2A subunits.

The major aim of this sub-study was to assess whether the negatively charged aspartic acid residue at position 332 (Kir6.1 E332) and positively charged arginine at position 347 (Kir6.1 R347) corresponding to Kir6.2 D323 and K338, are involved in making a functional interaction with NBD2 of SUR2A. These residues are of equivalent charge and position to Kir6.2 D323 and K338 but of opposite or no charge in the non-interacting Kir2.1 subunit and were selected and changed to the corresponding residue in Kir2.1.

Indeed, whole cell patch clamp results confirmed the hypothesis of this sub-study that the charged residues E332 or R347 in the distal C-terminal of Kir6.1 and E1318, K1322 and Q1336 of SUR2A-NBD2 are involved in determining the pinacidil and glibenclamide sensitivities of the regulatory SUR2A subunit to the ATP-sensitive potassium channel pore (Kir6.1). Due to the difficulty of recording Kir6.1/SUR2A channel currents, the inside out patch configuration to determine ATP and ADP sensitivity was not performed in this study. For this reason no data is presented relating to the ATP and ADP regulation of the mutated Kir6.1/SUR2A channels studied in this chapter.

When positively charged arginine, R347, in the distal C-terminal of Kir6.1was mutated to the oppositely charged glutamic acid, Kir6.1 R347E, this single mutation altered the properties of the Kir6.1 R347E/SUR2A WT channel. Disruption of the cytoplasmic salt bridge Kir6.1 R347/SUR2A E1318 by this single charge reversal mutation caused an increase and decrease of the sensitivity to the potassium channel opener, pinacidil and blocker, glibenclamide, respectively. Reinstatement of the cytoplasmic electrostatic interaction in Kir6.1 R347E/SUR2A E1318R subunit combination restored the sensitivity of pinacidil and glibenclamide, respectively, near to the wild type Kir6.1/SUR2A channel. The data of whole-cell patch clamp recording of mutated subunit combinations indicate that the Kir6.1 R347/SUR2A E1318 inter-subunit salt bridge plays a crucial role in mediating allosteric modulation from SUR2A to the channel pore Kir6.1 by K_{ATP} channel agonist and antagonist.

A single charge reversal mutation on the pore forming Kir6.1 (E332K) resulted in constitutive channels activation in the absence of pinacidil in Kir6.1 E332K/SUR2A WT subunit combination. In contrast to the above, reinstatement of the inter-subunit salt bridges in Kir6.1 E332K/SUR2A K1322D,

Kir6.1 E332K/SUR2A Q1336E or even Kir6.1 E332K/SUR2A K1322D + Q1336E did not fully or partially restore the channel properties near to the wild type Kir6.1/SUR2A. On the other hand, reinstatement of the cytoplasmic electrostatic interface in Kir6.1 E332K/SUR2A K1322D channel restored the decreased sensitivity of K_{ATP} channel antagonist, glibenclamide, in single charge reversal in the Kir6.1 E332K/SUR2A WT subunit combination near to the wild type. These data from whole-cell patch clamp recording demonstrate that the cytoplasmic negatively charge residue E332 of Kir6.1 form an ion-pair electrostatic interaction with the positively charged K1322 of SUR2A which is involved in transmitting inhibitory information to the pore (Kir6.1) from antagonist binding to the SUR2A subunit.

In brief, the cytoplasmic charged residues E332 and R347 in the distal C-terminal of Kir6.1 and E1318, K1322 and Q1336 in the proximal C-terminal in NBD2 of SUR2A formed ion-pair electrostatic interactions. Indeed, electrophysiological data (whole-cell patch clamp configuration) revealed these proposed inter-subunit salt bridges to be involved in determining the sensitivity of K_{ATP} channel agonist, pinacidil (Kir6.1 R347/SUR2A E1318) and antagonist, glibenclamide (Kir6.1 R347/SUR2A E1318, Kir6.1 E332/SUR2A K1322). Constitutive opening of the Kir6.1/SUR2A channel by single charge reversal point mutation of E332 of the Kir6.1 probably suggest that this negatively charged glutamic acid residue at position 332 to be important for stabilizing the assembly of functional channels of the allosteric $Kir6.1_4/SUR2A_4$ complex in K_{ATP} channels.

Finally, for the first time, electrophysiological data of Kir6.1/SUR2A and Kir6.2/SUR2A channels of these studies suggest that these inter-subunit electrostatic interactions are not just structural interactions for co-assembly between Kir6 isoforms and SUR2A, but that they are also crucial as functional interactions in K_{ATP} channels. In other words, these data provide evidence that the transmission of allosteric information through inter-subunit contacts mediate functional interactions between NBD2 in the proximal C-terminal of SUR2A and the distal C-terminal of the ATP-sensitive potassium channel pore, Kir6 isoforms.

Chapter 7

Expression of Kir6.2 Cytoplasmic Domains as Fusion Protein with Thermotoga Maritima 1070

7.1 Introduction

Membrane proteins are involved in various important cellular processes. Membrane proteins' communicative role between external and internal cellular metabolism make them very special as drug targets and for this reason they constitute targets for about 50% of the drug market (Hoag 2005). Membrane proteins are very stable in the cell membrane and extremely unstable outside this environment. For this reason expression of membrane proteins in soluble form is challenging due to insolubility in bacterial systems, inclusion bodies and toxicity to the host cells.

In attempts to express cytoplasmic domains of the Kir6.2 polypeptide for structural analysis, four constructs of Kir6.2 were made by Tezuka Takehiro; CT75 (residues 315-390), CT (residues 177-390), N30CT (residues 30-52/177-390) and N1CT (residues 1-51/177-390). The above constructs were expressed in the soluble fraction of *E.coli* both alone and as fusion proteins with thioredoxin. Although expressed, these domains aggregated and were not amenable to purification.

To improve solubility and potentially protein folding, a more complex bacterial fusion construct (TM1070-Kir6.2NC) was designed by Drs R I Norman and M Pfuhl (Department of Biochemistry at University of Leicester) and prepared by Tezuka Takehiro. For the expression of the combined cytoplasmic domains of Kir6.2, TM1070, the hypothetical bacterial protein from *Thermotoga Maritima* was used as the fusion partner with the N- and C-termini of Kir6.2 (figure 7-1). TM1070 is a soluble protein with N-and C-termini spaced at approximately the same distance apart as the membrane exit points of adjacent helical transmembrane domains in a membrane protein, e.g. M1 and M2 of Kir6.2 (NCBI 2009).

Fusion of the N- and C-terminal domains of Kir6.2 to the N- and C-termini or TM1070 may allow correct folding of the cytoplasmic domains against each other by mimicking their relative positioning in the native protein (figure 7-1). In this way, a properly folded cytoplasmic domain may be reconstructed to permit NMR spectroscopy and crystallisation for structural analysis. In addition, tobacco etch virus (TEV) cleavage sites were engineered at the junction between Kir6.2 and TM1070 sequence to facilitate release of potentially folded Kir6.2 cytoplasmic domain. Arctic Express competent *E.coli* cells were used to overcome protein misfolding, insolubility and inclusion bodies.

A His6-tag was placed either on the N- or C-terminal of the TM1070-Kir6.2NC fusion, which were named NT-His6 tag and CT-His6 tag respectively. The His-tag is widely used for detection, using monoclonal anti-polyhistidine antibody, and purification of recombinant expressed protein through its binding to the metal ion such as Ni^{2+} in immobilized metal ion affinity chromatography (IMAC).

7.2 Results

TM1070-Kir6.2NC fusion protein was expressed in *E coli* competent cells, which have a T7 expression system and total cell extract and a soluble protein fraction was prepared. Western blot analysis of expression using monoclonal anti-polyhistidine and anti-Kir6.2 antibodies showed no expression (results not shown).

TM1070-Kir6.2 NC (NT-His6 tag) and TM1070-Kir6.2NC (CT-His6 tag) were expressed *in vitro*, using the TNT® Quick Coupled Transcription/Translation System.

The results of this expression were analysed by Coomassie blue staining (figure 7-2) and Western blot (figure 7-3). The blots were probed with either anti-Kir6.2 (figure 7-3, panels A and B) or monoclonal anti-polyhistidine (figure 7-3 C). TM1070-Kir6.2NC (NT-His6 tag) expression was confirmed (~ 48 kDa) with anti-Kir6.2 antibody (figure 7-3 A). The anti-Kir6.2 antibody does not recognize the TM1070-Kir6.2NC (CT-His6 tag), as the C-terminal tag occludes the C-terminal epitope. Block with immunizing peptide (10 µg/ml) was used as a negative control. Possibly, due to misfolding or masking no immunoreactivity was seen with the anti-polyhistidine antibody (figure 7-3 C).

TM1070-Kir6.2NC (CT-His6 tag) fusion protein was expressed in Arctic Express using different concentrations of IPTG to optimise the induction of expression. The expression was analysed by Coomassie blue staining after SDS-PAGE (figure 7-4). Following successful expression of TM1070-Kir6.2NC (CT-His6 tag) fusion from Arctic Express, TM1070-Kir6.2 NC (CT-His6 tag) fusion was expressed with different incubation times after induction and different concentrations of IPTG to optimise the expression, after which the soluble fraction was prepared from each condition and analysed by Coomassie blue staining (figure 7-5) and by Western blot (figure 7-6). Optimal expression was observed after induction with 0.3 mM IPTG and 24 hrs incubation after induction.

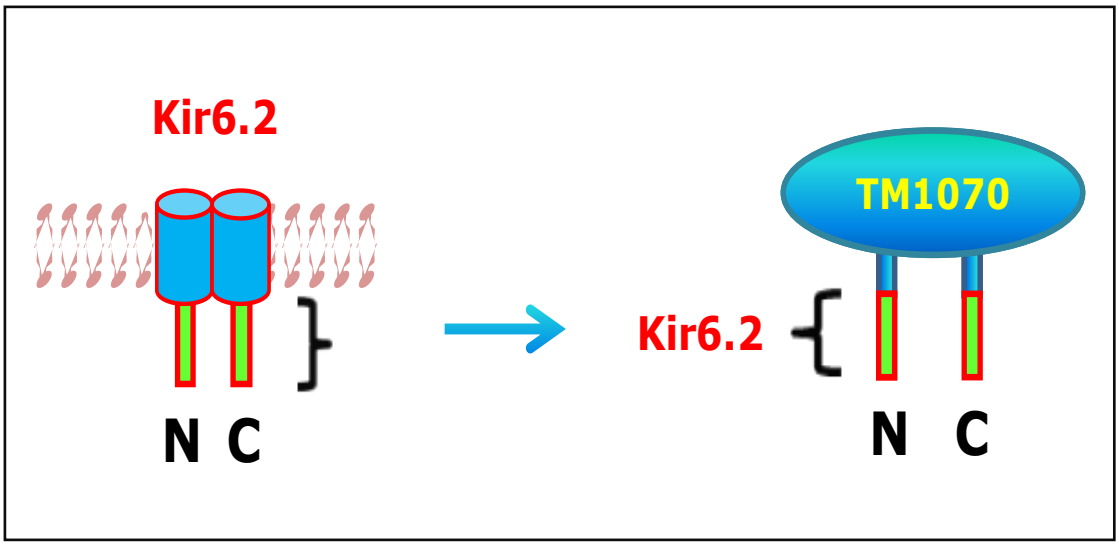

Figure 7-1 Illustration of *Thermotoga Maritima* (TM) 1070-Kir6.2NC fusion construct.

The figure demonstrates the design of construction for fusion protein TM1070-Kir6.2NC. To the left the pore forming Kir6.2 subunit and to the right the replacement of cytoplasmic domains of TM1070 with cytoplasmic N- and C-terminal of Kir6.2. To ease the crystallization for structural analysis the bacterial (*Thermotoga Maritima*, soluble protein) fusion protein constructs was designed to express the cytoplasmic domains of Kir6.2 in near native form.

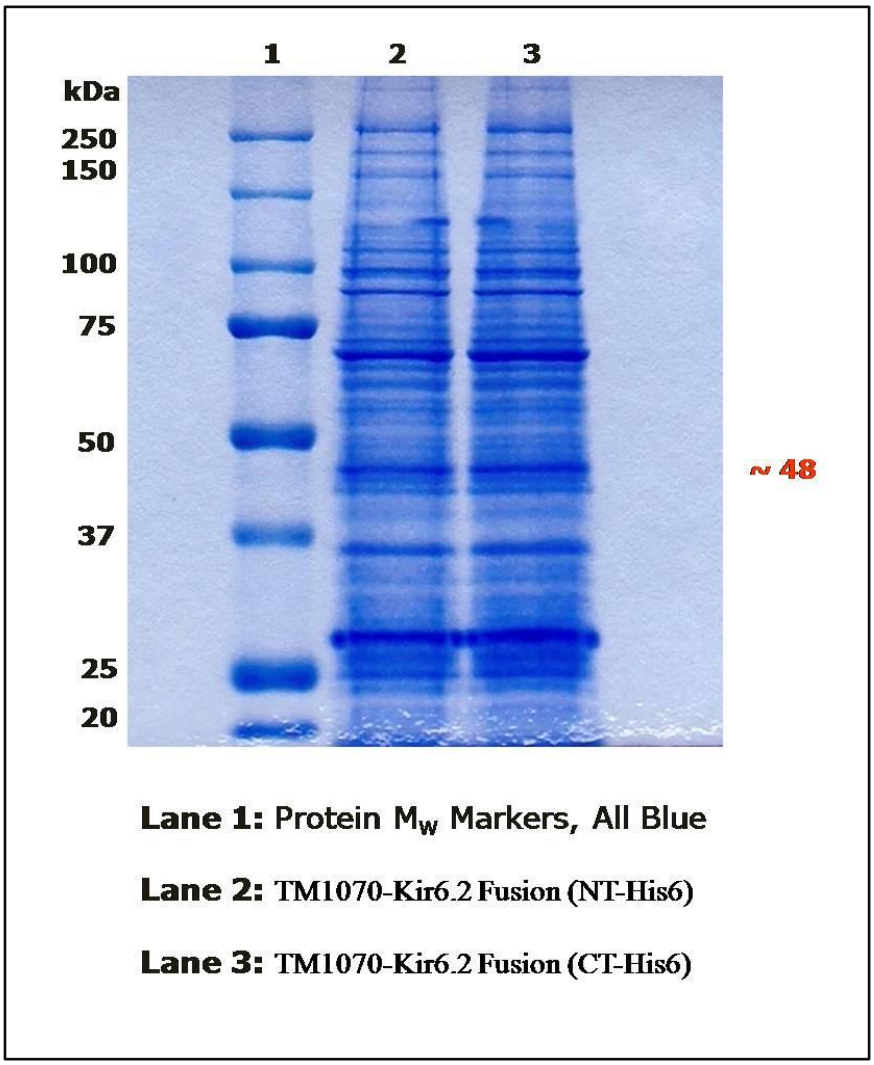

Figure 7-2 Coomassie blue staining of TM1070-Kir6.2NC fusion protein constructs expressed *in vitro*.

Coomassie blue stained polyacrylamide gel *in vitro* expressed TM1070-Kir6.2NC (NT-His6 tag) and TM1070-Kir6.2NC (CT-His6 tag) fusion proteins.

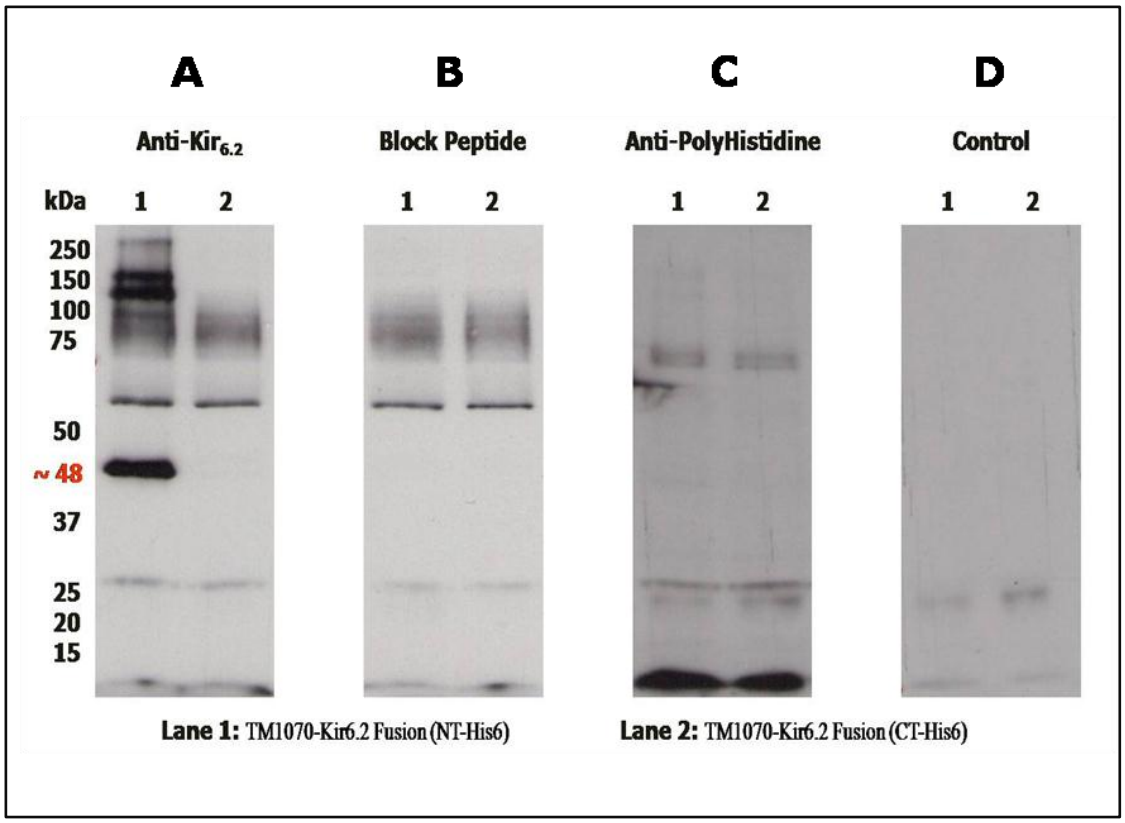

Figure 7-3 Expression (*in vitro*) analysis of TM1070-Kir6.2 NC (CT- and NT-His6 tag) fusion protein by Western blot.

Lane 1: TM1070-Kir6.2 NC (NT-His6 tag) fusion protein. *Lane 2*: TM1070-Kir6.2 NC (CT-His6 tag) fusion protein. (A) The blot was probed with anti-Kir6.2 antibody and as a negative control, blocking immunizing peptide preincubated with anti-Kir6.2 antibody (10 µg/ml) was used (B). (C) The blot was probed with anti-polyhistidine antibody. As a negative control the primary antibody (anti-polyhistidine) was omitted (D).

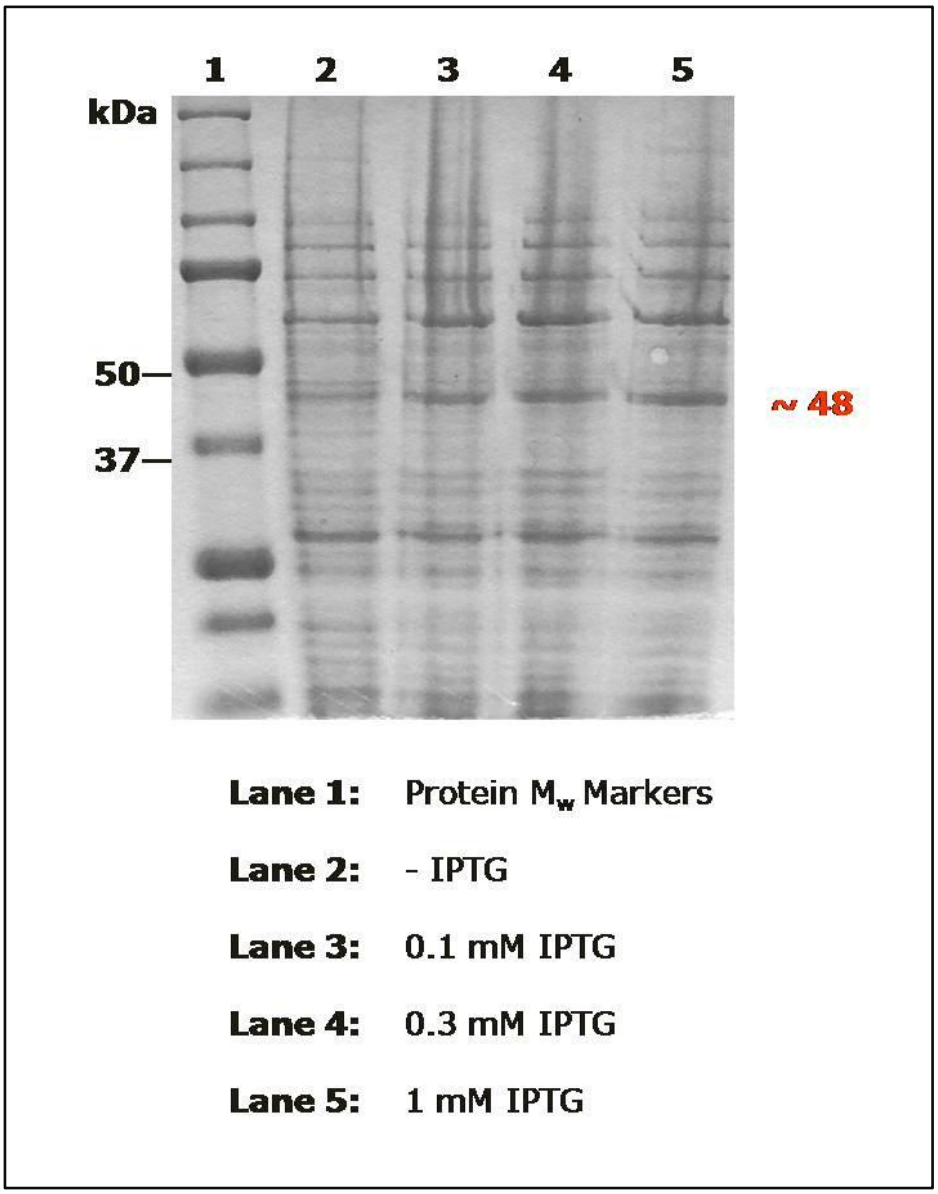

Figure 7-4 Coomassie blue staining of TM1070-Kir6.2NC (CT-His6 tag) fusion protein expressed in Arctic Express.

Different concentrations of IPTG were used to optimise the induction. Expression was detected in samples induced with IPTG (48 kDa, lanes 3, 4 and 5) compared to non-induced cells (lane 2). 10 µg protein was loaded in each well.

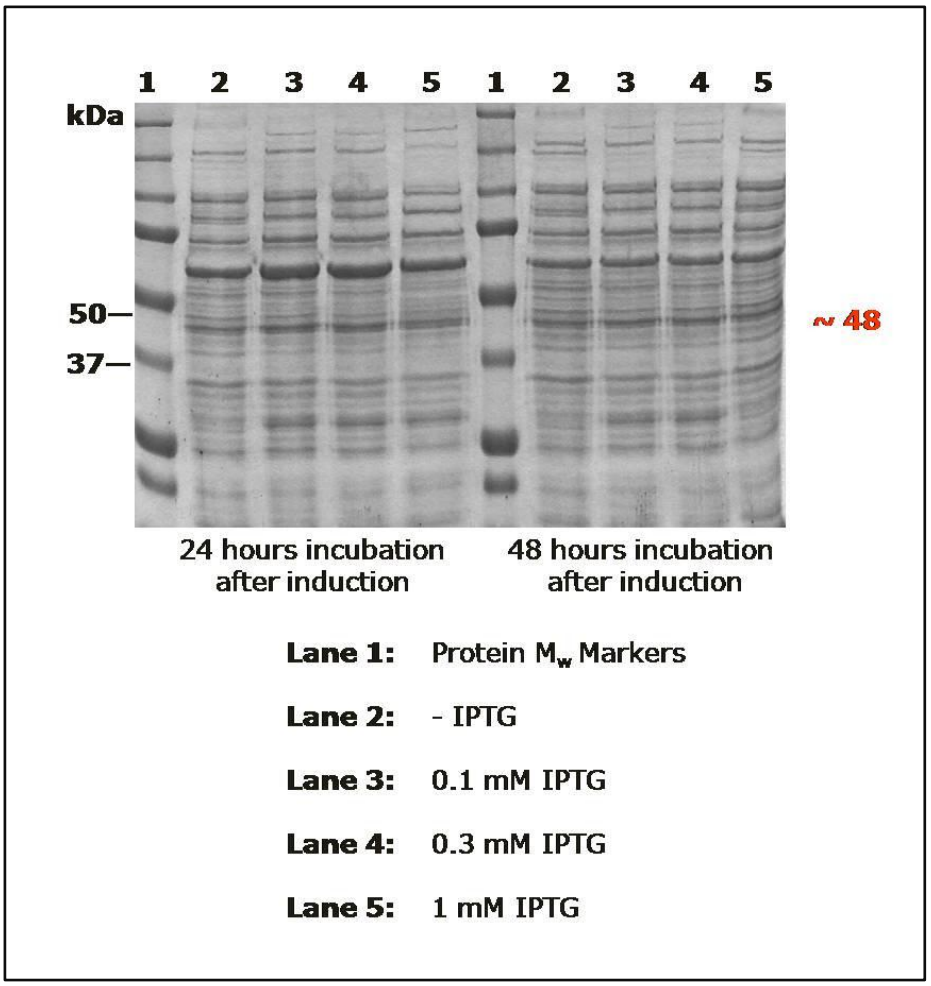

Figure 7-5 Protein expression analysis of TM1070-Kir6.2NC (CT-His6 tag) fusion protein in the soluble fraction prepared from Arctic Express.

10 µg protein was loaded in each well. Proteins were stained with Coomassie blue. Highest expression was observed on induction with 0.1 mM and 0.3 mM of IPTG and 24 hrs incubation after induction.

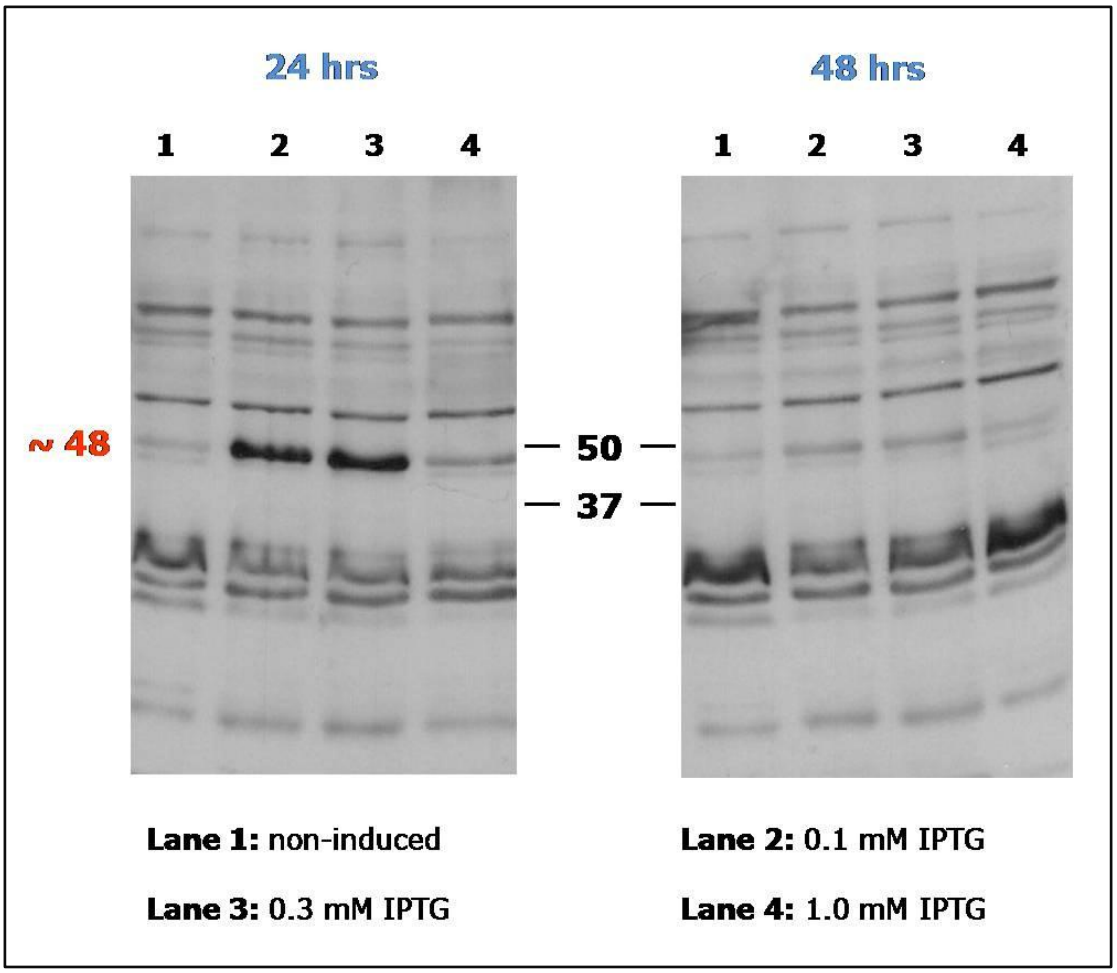

Figure 7-6 Western blot analysis of expression of TM1070-Kir6.2NC (CT-His6 tag) fusion protein in the soluble fraction prepared from Arctic Express.

TM1070-Kir6.2NC (CT-His6 tag) fusion protein expression was analysed by Western blot and the blots probed with monoclonal anti-polyhistidine antibody. Optimal expression was observed after induction with 0.3 mM IPTG and 24 hrs incubation after induction. 10 µg protein was loaded in each well.

To reconfirm the higher efficiency of expression of TM1070-Kir6.2NC (CT-His6 tag) fusion protein in Arctic Express, the conditions of expression were re-analysed by Western blot and compared with *E.coli* which has the T7 expression system (figure 7-7) and *in vitro* expression (figure 7-3 and 7-7, lane 3 and 4). In this experiment the blot was probed with monoclonal anti-polyhistidine antibody and 10 µg protein was added in each well. No expression was observed with T7 expression system (figure 7-7, lane 2) and *in vitro* expression (figure 7-7, lanes 3 and 4) compared to the successful expression in Arctic Express competent cells, cell culture (figure 7-7, lanes 6, 7 and 8) and soluble fraction (figure 7-7, lanes 10, 11 and 12). Following the expression of TM1070-Kir6.2NC (CT-His6 tag) fusion protein, this was purified by IMAC, which will be discussed in the next chapter.

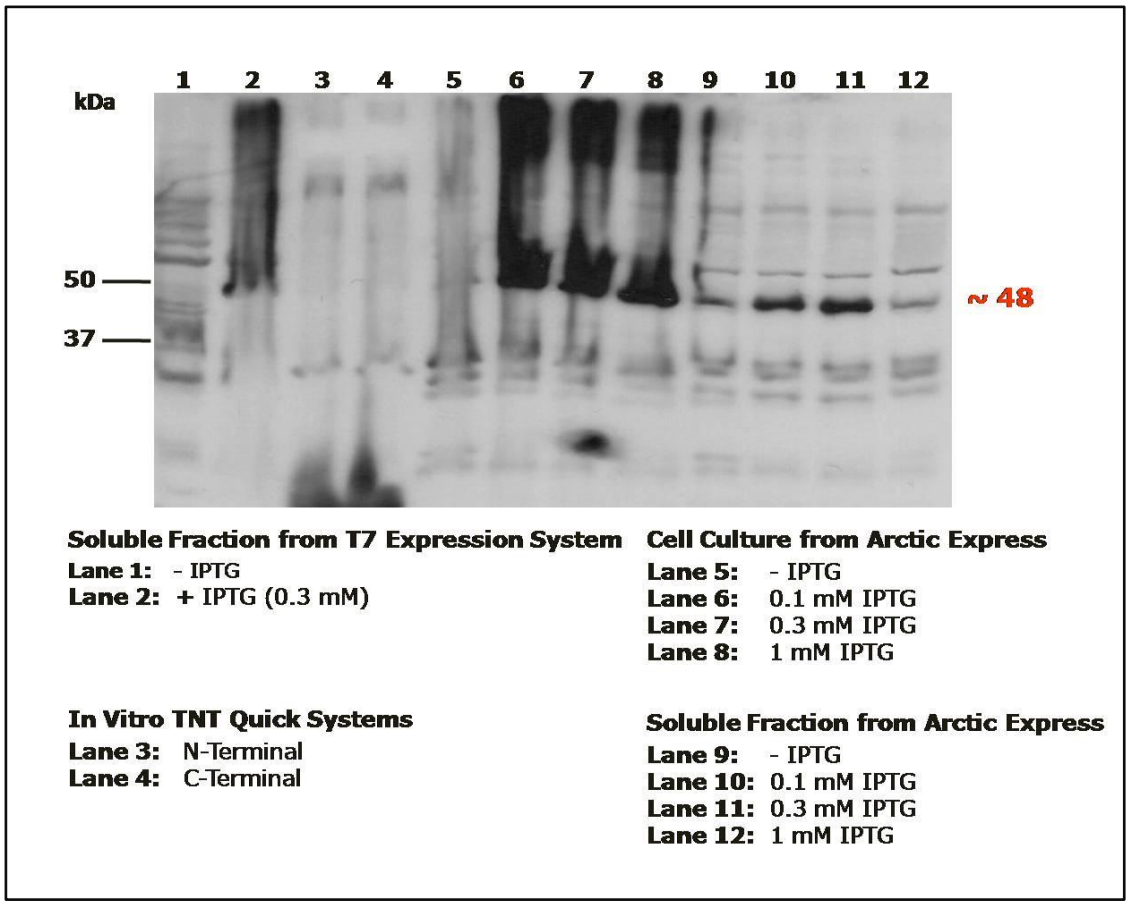

Figure 7-7 Comparison of TM1070-Kir6.2NC (CT-His6 tag) fusion protein expression using different expression systems by Western blot.

10 µg of protein was loaded in each well. The blot was probed with monoclonal anti-polyhistidine antibody. The blot shows successful expression of cell culture (lane 6, 7 and 8) and soluble fraction (lane 10 and 11) from Arctic Express.

7.3 Summary and Conclusions

The main aim of this sub-study was to express the cytoplasmic domains of the pore forming Kir6.2 subunit as fusion partner with *Thermotoga Maritima* (soluble bacterial protein) for structural analysis. Indeed, the more complex bacterial fusion construct, TM1070-Kir6.2NC (CT-His6 tag) as describe in the introduction (section 7.1), improved the protein folding and allowed the expression of the cytoplasmic domains of Kir6.2 in near native form.

No expression was observed with T7 system and *in vitro* expression was not a good alternative due to low yield and expensive. Thus, to overcome protein misfolding, insolubility and inclusion bodies the recombinant fusion protein was expressed in Arctic Express competent *E.coli* cells and the results revealed promising and successful expression. Coomassie blue staining SDS-PAGE and Western blot analysis revealed that the induction with 0.3 mM IPTG and 24 hrs incubation after induction to be the optimal expression of TM1070-Kir6.2NC (CT-His6 tag) fusion protein from Arctic Express.

In summary, for the first time the cytoplasmic domains of the Kir6.2 was expressed successfully (soluble form) as fusion protein with the bacteria *Thermotoga Maritima* in Arctic Express competent *E.coli* cells. High level of expression and improvement of solubility and protein folding of the heterologous proteins, Kir6.2 and TM was noticed from Arctic Express. Finally, how this recombinant fusion protein, TM1070-Kir6.2NC (CT-His6 tag), is to be purified remains to be answered in the next chapter.

Chapter 8

Purification of Kir6.2 Cytoplasmic Domains

8.1 Introduction

The field of structural analyses of membrane protein is growing rapidly in order to understand their structure-function relationships. The purification step is quite essential prior to performing structure studies due to the requirement of high purified protein. For protein purification, IMAC is a favoured method due to the ease and the single step, and because it is inexpensive and produces a high yield purification (Jiang et al. 2009). Generally for affinity tag purification, a His-tag can be placed on the N- or C-terminal of recombinant proteins (Loughran et al. 2006). The aim of this sub-study was to purify the cytoplasmic domains of Kir6.2 for structural analyses.

Following expression of TM1070-Kir6.2NC (CT-His6 tag) fusion protein, purification was performed by IMAC. The His-tag within the protein of interest binds to the metal ion, in this case Nickel (Ni^{2+}), which is the preferred metal ion for purification. IMAC is a very common method for single step purification of polyhistidine-tagged proteins. Two constructs of TM1070-Kir6.2NC fusion protein have been constructed previously in the laboratory (Tezuka Takehiro); one with the His6-tag attached to the N-terminal (NT-His6 tag) and the other one with His6-tag attached to the C-terminal (CT-His6 tag). For structural analysis highly purified, 1 – 2 mg protein is required. Purification of TM1070-Kir6.2NC (CT-His6 tag) fusion protein by IMAC (Ni^{2+}) in this study was confirmed by Western blot, and showed IMAC to be a promising first step in the purification. Further improvements to the purification will be required.

8.2 Results

The purification of TM1070-Kir6.2NC (CT-His6 tag) fusion protein by IMAC was analysed by Coomassie blue staining and Western blot. The blot was probed with monoclonal anti-polyhistidine antibody and confirmed the molecular weight of monomer for this His-tagged fusion protein at 48 kDa as predicted. Figure 8-1shows the Coomassie blue staining of the purification of TM1070-Kir6.2NC (CT-His6 tag) fusion protein by IMAC (Ni^{2+}) which revealed a substantial enrichment of a 48 kDa polypeptide in this single step (figure 8-1, Lane 7). The identity of this enriched polypeptide was confirmed by Western blot analysis with monoclonal anti-polyhistidine antibody. The result of Western blot also confirmed the enrichment of the fusion protein within the elution fraction (figure 8-2 B, lane 6) compared to the starting material (figure 8-2 A). Coomassie blue staining analysis indicated a substantial purification of the target fusion protein (~48 kDa) with some remaining contaminating polypeptides. Further purification steps will be required to remove the trace of contaminating proteins trace (figure 8-1, lane 7).

To improve this single step, IMAC, purification for structural study, due to the presence of contaminating proteins, the binding, washing and elution buffers were optimised. In the previous experiment just two buffers was used for IMAC (see section 2.5.2) but using three buffers and optimizing each buffer; binding buffer (pH 7.4, 20 mM sodium phosphate, 0.5 M NaCl and 10 mM imidazole), washing buffer (pH 7.4, 20 mM sodium phosphate, 2 M NaCl and 20 mM imidazole) and elution buffer (pH 7.4, 20 mM sodium phosphate, 0.5 M NaCl and 500 mM imidazole) increased the yield and improved the purification about 10 fold (figures 8-3, 8-4 and 8-5). Coomassie blue stained SDS-PAGE and Western blot analysis of the purification of TM1070 Kir6.2NC

(CT-His6 tag) fusion protein after optimization of IMAC (Ni^{2+}) buffers revealed the improvement of one step purification with IMAC (figures 8-3 and 8-4). Furthermore, evaluation of protein level by densitometry measurements of intensity of each band of Western blot films confirmed the improvement of IMAC to be about 10 fold (figure 8-5).

Optimization of IMAC (Ni^{2+}) buffers and improvement of this one step purification did not remove the remaining contaminating polypeptides. On that account, it was thought that the contamination in elution was due to containments in the use of Laemmli sample buffer. Although, using new Laemmli sample buffer, the pattern of elution in Coomassie blue stained SDS-PAGE analysis of the purification of TM1070 Kir6.2NC (CT-His6 tag) fusion protein was not changed (data not shown). Figure 8-6 A and B show that the TM1070 Kir6.2NC (CT-His6 tag) fusion protein was still contaminated, even with longer washes and using a different range of imidazole concentration (50 mM to 200 mM) in the washing buffer. For that reason, gel filtration chromatography (GFC) was performed as a second purification step after trying all possible ways to remove the contamination of elution fraction with IMAC (Ni^{2+}).

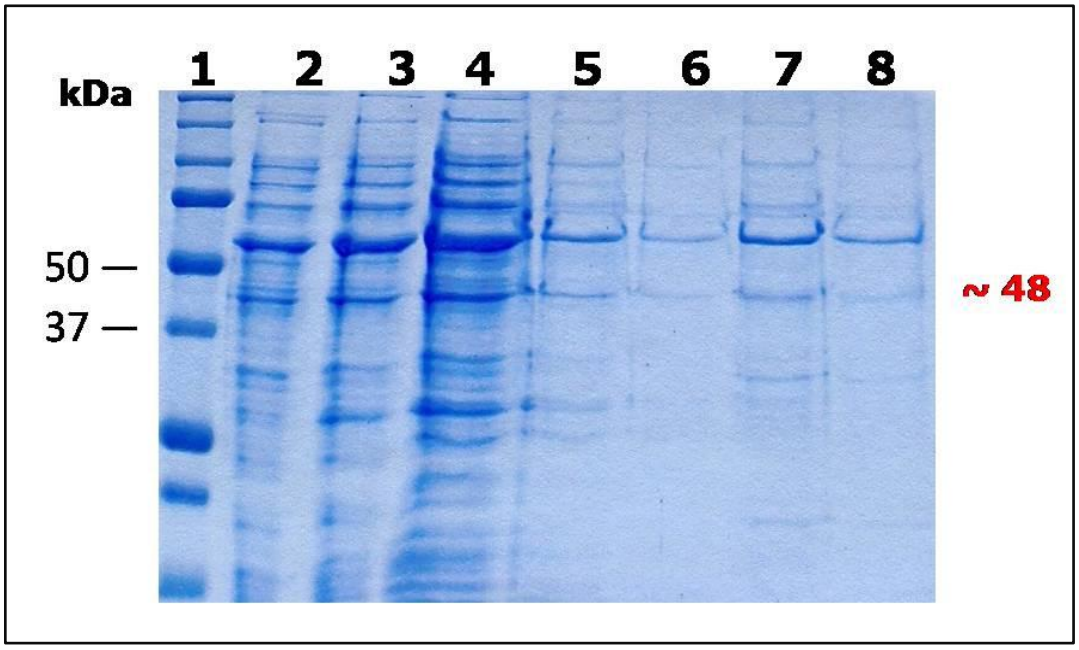

Lane	µg loaded
1. Protein Mw Markers	-
2. Non-induced	10
3. Breakthrough	10
4. Wash 1	7.8
5. Wash 2	2.5
6. Wash 3	0.9
7. Elution 1	2.8
8. Elution 2	1.7

Figure 8-1 Coomassie blue stained SDS-PAGE analysis of the purification of TM1070-Kir6.2NC (CT-His6 tag) fusion protein by IMAC (Ni^{2+}).

TM1070-Kir6.2NC (CT-His6 tag) fusion was purified from the soluble protein fraction after expression in Arctic Express, subjected to purification by IMAC and analysed in a Coomassie blue stained SDS-PAGE.

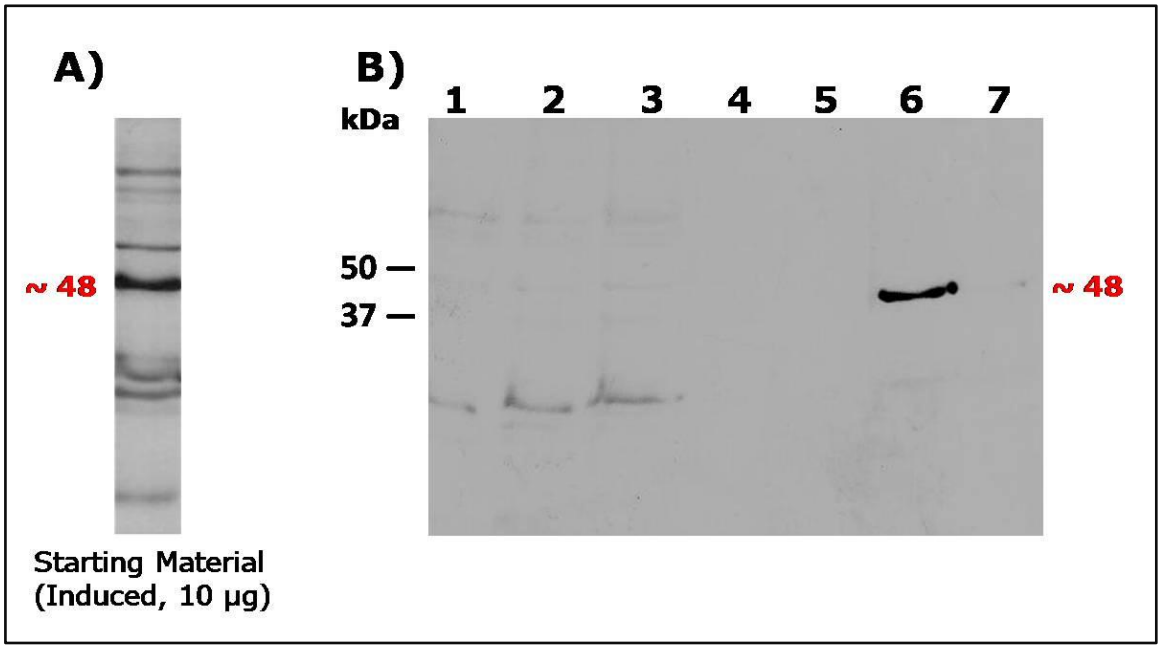

Lane	µg loaded
1. Non-induced	10
2. Breakthrough	10
3. Wash 1	7.8
4. Wash 2	2.5
5. Wash 3	0.9
6. Elution 1	2.8
7. Elution 2	1.7

Figure 8-2 Western blot analysis of the purification by IMAC (Ni^{2+}) of TM1070-Kir6.2NC (CT-His6 tag) fusion protein from the soluble fraction.

The Western blot analysis in (A) 10 µg of TM1070-Kir6.2NC (CT-His6 tag) fusion protein. Weak staining within the starting material (A, 10 µg) compared to the elution (lane 6, 2.8 µg) revealed a high degree of purification.

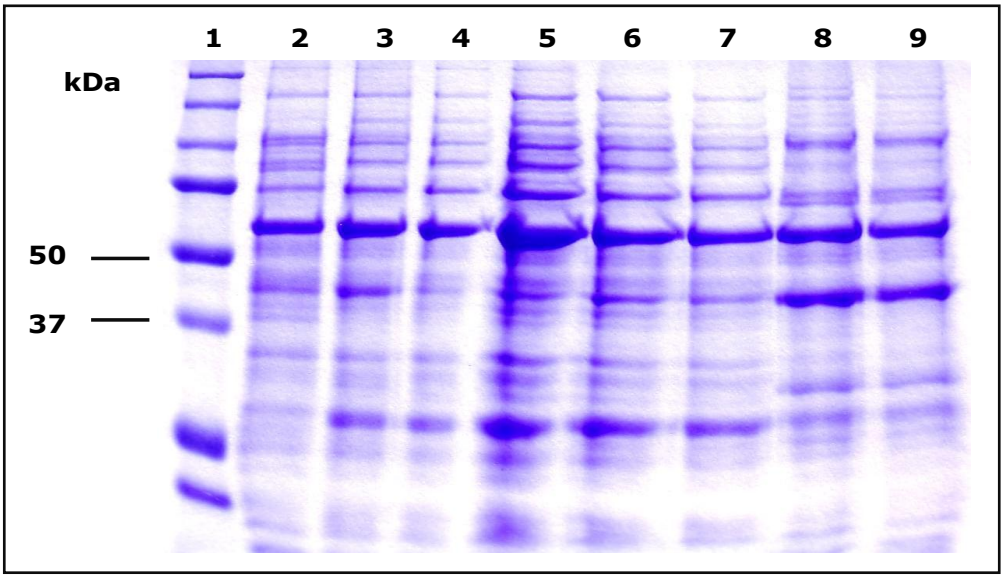

Lane	µg loaded
1. Protein Mw Markers	-
2. Non-induced	10
3. Induced	10
4. Breakthrough	10
5. Wash 1	10
6. Wash 2	10
7. Wash 3	10
8. Elution 1	10
9. Elution 2	9

Figure 8-3 Coomassie blue stained SDS-PAGE analysis of the purification of TM1070-Kir6.2NC (CT-His6 tag) fusion protein after optimization of IMAC (Ni^{2+}) buffers.

TM1070-Kir6.2NC (CT-His6 tag) fusion was purified from the soluble protein fraction after expression in Arctic Express, subjected to purification by IMAC and analysed in a Coomassie blue stained SDS-PAGE.

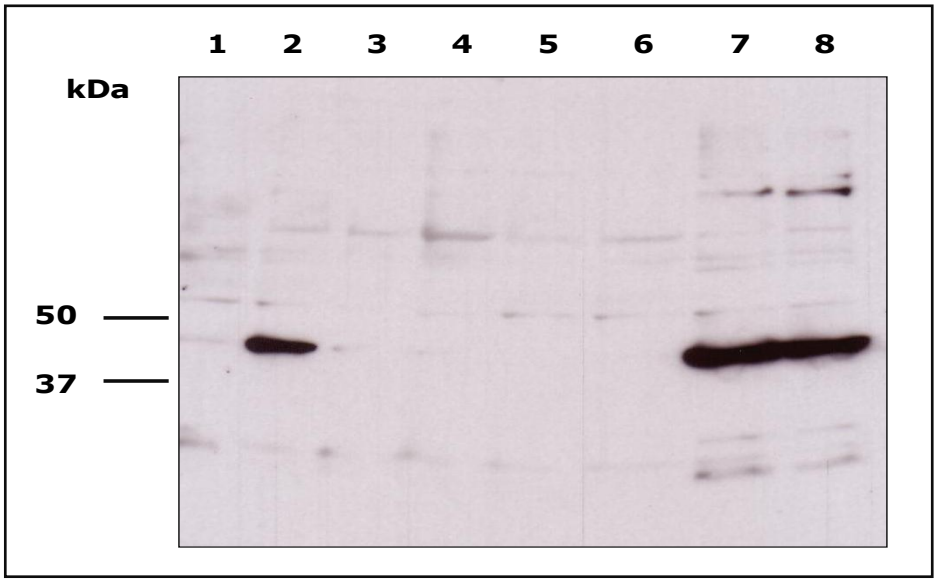

Lane	µg loaded
1. Non-induced	10
2. Induced	10
3. Breakthrough	10
4. Wash 1	10
5. Wash 2	10
6. Wash 3	10
7. Elution 1	10
8. Elution 2	9

Figure 8-4 Western blot analysis of the purification of TM1070-Kir6.2NC (CT-His6 tag) fusion protein after optimization of IMAC (Ni^{2+}) buffers.

The blot represents the soluble fraction of TM1070-Kir6.2NC (C-terminal His6 tag) fusion protein which was purified by IMAC (Ni^{2+}). Western blot analysis with monoclonal anti-polyhistidine antibody revealed this enriched polypeptide, lane 7 and lane 8 (elution) compared with lane 2 at 48 kDa.

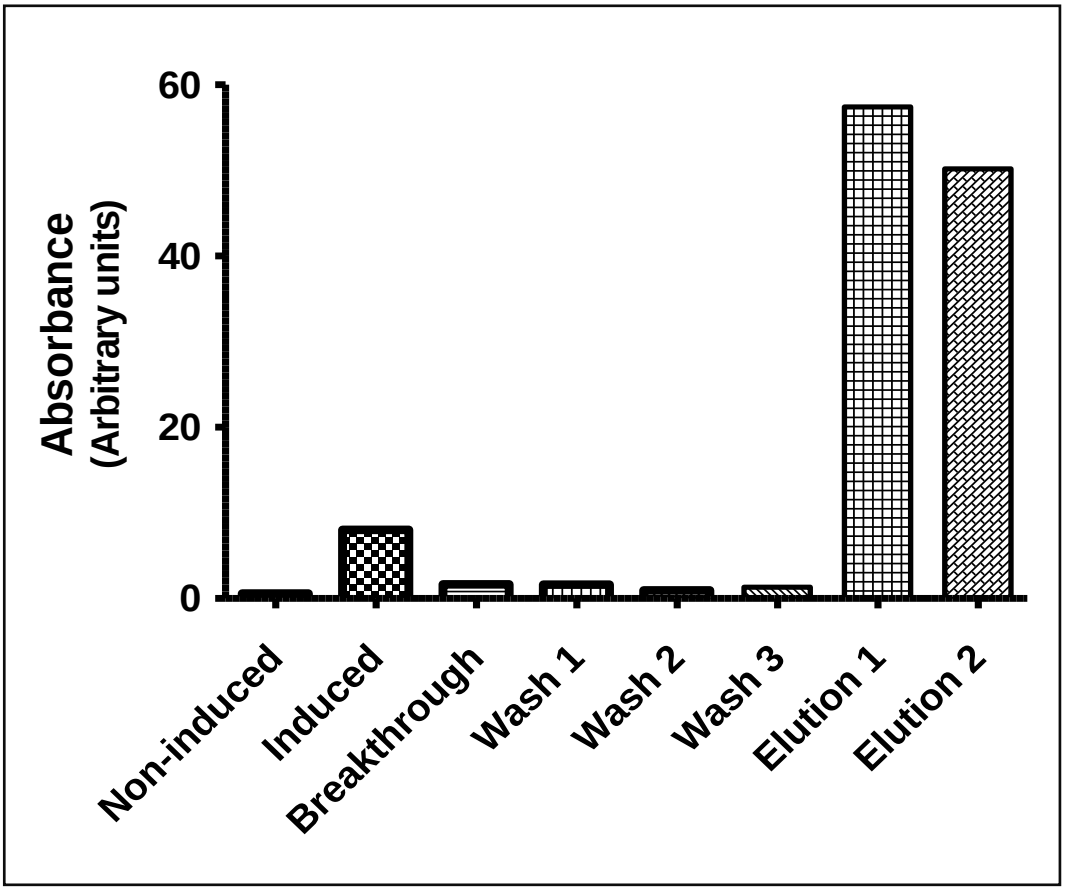

Figure 8-5 Diagram represents the purification fold of TM1070-Kir6.2NC (CT-His6 tag) fusion protein by IMAC (Ni^{2+}).

The bar diagram shows the densitometry measurements (Western blot) of the purification of TM1070-Kir6.2NC (CT-His6 tag) fusion protein by IMAC (Ni^{2+}). Elution 1 and 2 are about 10 fold compared with the induced.

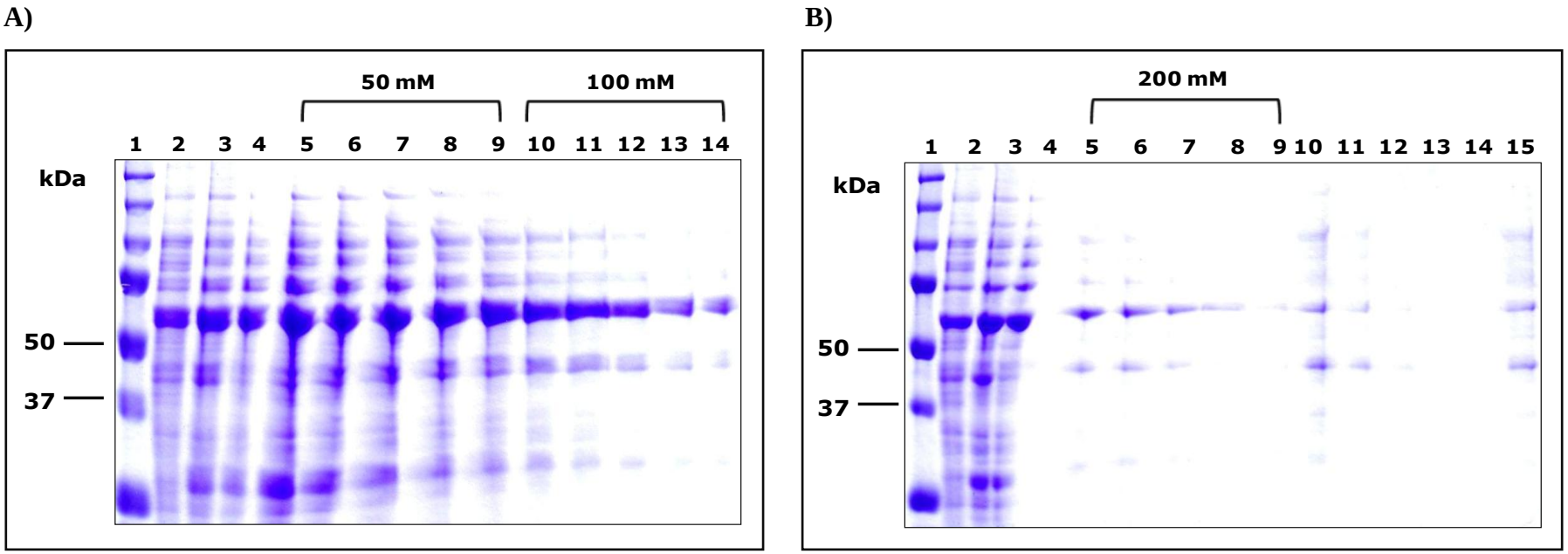

Figure 8-6 Coomassie blue stained SDS-PAGE analysis of the purification of TM1070-Kir6.2NC (CT-His6 tag) fusion protein by IMAC (Ni^{2+}) with different concentration of imidazole.

A representative result of the soluble protein fraction of TM1070-Kir6.2NC (CT-His6 tag) fusion purified by IMAC (Ni^{2+}) after expression in Arctic Express and analyses in a Coomassie blue stained SDS-PAGE. The IMAC was performed with different concentrations of imidazole (50 mM to 200 mM) to optimise the purification. In A and B: lane 1 represents the protein Mw markers, lane 2; non-induced, lane 3; induced, lane 4; breakthrough. A) lane 5 to 9 represent wash 1 to 5 with 50 mM imidazole and lane 10 to 14 wash 1 to 5 with 100 mM imidazole. B) lane 5 to 9 represent wash 1 to 5 with 200 mM imidazole, lane 10 to 14 represent elution 1 to 5 and lane 15; elution 1 was heated at 95 ºC for 5 minutes.

GFC or size exclusion chromatography (SEC) separates the proteins on the basis of size (see section 2.5.3). The elution profile from GFC of TM1070-Kir6.2NC (CT-His6 tag) fusion protein was very promising and as expected (figure 8-7). Small peaks which supposed to represent the contamination (large molecules) and the sharp peak were assured to be TM1070-Kir6.2NC (CT-His6 tag) fusion protein (48 kDa). But, results of Bradford assay for protein concentration of all fractions revealed no presence of proteins in fractions and also Coomassie blue stained SDS-PAGE analysis of the GFC purification confirmed no presence of any bands in the gel (data not shown). In addition, investigation of GFC column explained that the TM1070-Kir6.2NC (CT-His6 tag) fusion protein was aggregated on the top of column and the peaks probably represents the imidazole in buffer (figure 8-7).

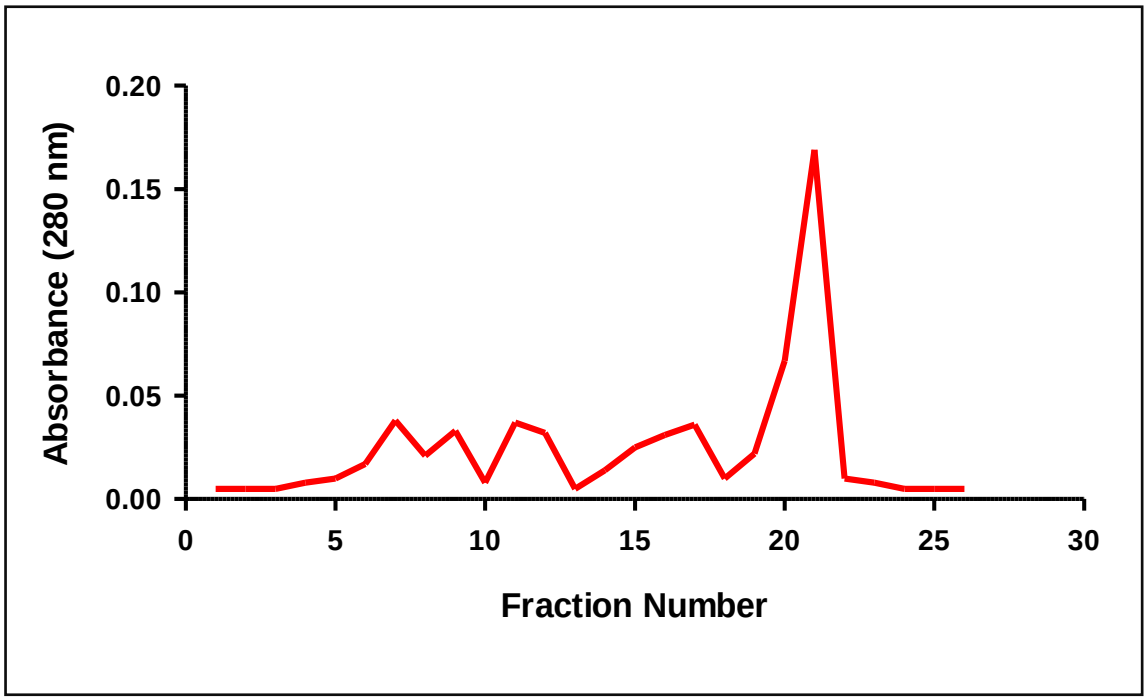

Figure 8-7 Elution profile from gel filtration chromatography of TM1070-Kir6.2NC (CT-His6 tag) fusion protein expressed in Arctic Express.

The figure represents the chromatographic elution profile of TM1070-Kir6.2NC (CT-His6 tag) fusion protein which was obtained by measuring the absorbance at 280 nm (in arbitrary units). Individual chromatographic fractions were collected in a volume of 1 ml.

8.3 Summary and Conclusions

The main aim of this sub-study was to purify the *Thermotoga Maritima* 1070-Kir6.2NC (C-terminal His6 tag) fusion protein in one or multiple steps. IMAC (Ni^{2+}) was performed as one step purification subsequently of the expression of TM1070-Kir6.2NC (CT-His6 tag) fusion protein. Coomassie blue stained SDS-PAGE analysis of the purification of this histidine-tagged fusion protein revealed some remaining contamination of the polypeptides and one step purification by IMAC should be optimised and improved. Optimization of IMAC by changing the condition of buffers, flow rates and longer washes increased slightly the yield and improved the purification fold but did not remove the contamination. For this reason the GFC was performed as a secondary purification step to remove the remaining minor contaminants.

The elution profile of GFC column shows small peaks and a sharp peak. Small peaks were assumed to represent the contamination and the sharp peak was expected to be the TM1070-Kir6.2NC (CT-His6 tag) fusion protein. But no bands were observed with Coomassie blue stained SDS-PAGE analysis of the purification and Bradford assay on all fractions revealed no protein concentration suggesting the peaks possibly represent the imidazole in buffer. Further investigation of GFC column revealed the TM1070-Kir6.2NC (CT-His6 tag) fusion protein was aggregated on the top of the GFC column.

In conclusion, TM1070-Kir6.2NC (CT-His6 tag) fusion protein was purified with two steps IMAC and GFC. IMAC purification resulted in high yield and about 10 fold purification with remaining contamination and why TM1070-Kir6.2NC (CT-His6 tag) fusion protein was aggregated on the top of GFC column remains to be answered and resolved.

Chapter 9

Overall Discussion

9.1 Introduction

K_{ATP} channels are composed of a hetero-octamer of two subunits types, a pore forming Kir6 subunit, which is a member of the inwardly rectifying potassium channel family (Xie et al. 2007), and a sulphonylurea receptor (SUR), a regulatory subunit, which is a member of the ATP-binding cassette family of proteins (Dean et al. 2001). In response to nucleotides and pharmaceutical agonists and antagonists, SUR allosterically regulates channel gating (Dupuis et al. 2008). The allosteric inter-subunit communication pathways in K_{ATP} channels are still today poorly understood after more than two decades of research. Given that K_{ATP} channels are present in various tissues and cell types and are involved in vital and various mechanisms, K_{ATP} channels are now considered a major drug target among potassium channels and have become an extremely interesting target for pharmaceutical companies.

The aim of this project was to understand the structural basis for allosteric information transfer through inter-subunit contacts in K_{ATP} channels by application of multidisciplinary techniques. To explain in greater detail, to study the structure-function relationships in K_{ATP} channels this project can be divided into three major sub-projects and aims: 1) The application of site directed mutagenesis and biochemical techniques to identify the cognate interaction domain on Kir6.2 for SUR2A-NBD2. 2) The employment of electrophysiological techniques to investigate the allosteric information transfer between heterologous subunits Kir6 and SUR2A. 3) The utilization of recombinant fusion protein to express and purify the cytoplasmic domains of Kir6.2 for structural information of the interaction between two subunits. The accomplishments of the three aims will be discussed in the following sections.

9.2 Identification of Inter-subunit Salt Bridges between Nucleotide Binding Domain 2 of SUR2A and the Pore Forming Kir6 in ATP-sensitive Potassium Channels

The major finding of this sub-study was that first identification of D323 and K338 on the distal C-terminal of Kir6.2 as residues involved in interaction with SUR2A-NBD2 in Kir6.2/SUR2A channels and also identification of salt bridges between cytoplasmic domains of heterologous subunits, Kir6.2 and SUR2A, in ATP-sensitive potassium channel.

As discussed in the introduction chapter (section 1.8.1.2), Rainbow et al. (2004) identified a Kir6.2 interaction domain within the MBP-SUR2A-CTC fragment in NBD2 of the SUR2A subunit in K_{ATP} channels. The next step was to identify the cognate interaction domain on the Kir6.2 subunit. In this regard, an earlier study by M. Al-Johi in our laboratory suggested that the interaction domain on Kir6.2 for SUR subunit is located within the distal C-terminal, beyond residue 315.

In this sub-study, the biochemical interactions between Kir6.2 and SUR2A subunits were investigated by co-immunoprecipitation. The analysis of the results demonstrated a significant reduction of co-immunoprecipitation of MBP-SUR2A-CTC fragments with the following Kir6.2 single amino acid substitution mutants, Kir6.2 D323K (~ 50%) and K338E (~ 80%), while mutants Kir6.2 RKR369-371AAA (endoplasmic reticulum retention sequence) or K377A had no significant effect on the efficiency of co-immunoprecipitation.

Hence, electrophysiological studies were necessary to explore the possibility from this finding, which suggested that the negative charged aspartic acid at position 323 and positive charged lysine at position 338 may be potentially involved in allosteric information transfer between subunits in Kir6.2/SUR2A channels. It has been reported that the 334 GNTI 337 region of Kir6.2 is part of the inhibitory ATP-binding site (Drain et al. 1998). Interestingly, the residues identified in this study on Kir6.2 with the SUR2A-NBD2 interaction domain are located close to or possibly within the ATP inhibitory domain on Kir6.2 subunit. This places the interaction close to the regulatory ATP binding site on Kir6.2 and is suggestive that Kir6.2 residues D323 and K338 residues are possibly critical for Kir6.2/SUR2A association and the transfer of regulatory information from the SUR2A subunit to the Kir6.2 pore. The most important question arising from this finding which will be discussed in the next section was: does this interaction relate to the allosteric communication between heterologous K_{ATP} channel subunits and to what extent is the function of the channel affected?

Single point mutation of the charged cytoplasmic residues in either subunit (Kir6.2 and SUR2A) resulted in reduction of the co-immunoprecipitation and disruption of the assembly of the K_{ATP} channel (Chapter 3). The lack of three-dimensional structural information of this inter-subunit interface forced the hypothesis that these cytoplasmic charged residues should form three electrostatic interactions between SUR2A and Kir6.2. To test these predictions, further co-immunoprecipitation of hypothesised residue pairs (Kir6.2 D323/SUR2A K1322, Kir6.2 D323/SUR2A Q1336 and Kir6.2 K338/SUR2A E1318) was performed and the results supported these predictions (Chapter 5). In other words, the co-immunoprecipitation was restored with the single charge reversals in both subunits (Kir6.2 and SUR2A) in the proposed salts bridges.

In summary, interpretation of the results of this biochemical study is that the charge residues E1318, K1322 and Q1336 on the proximal C-terminal of SUR2A which are parts of NBD2 and D323 and K338 on the distal C-terminal of Kir6.2 form cytoplasmic electrostatic interactions. Furthermore, these salt bridges at inter-subunit interfaces contribute to the stability and contribute to the assembly of K_{ATP} channels.

The demonstration of the involvement of these inter-subunit electrostatic interactions in hetero-octameric complex allostery of $Kir6_4/SUR2A_4$ will be discussed in the next section.

9.3 Sulphonylurea Receptor (SUR2A) Regulates the ATP-sensitive Potassium Channel Pore (Kir6) Allosterically via Inter-subunit Salt Bridges

The electrophysiological results of K_{ATP} channels in this sub-study, for the first time, provides new information on the inter-subunit electrostatic interactions between the pore forming Kir6 isoforms and the regulatory SUR2A subunits, which are involved in determining the sensitivity to the agonist, pinacidil, and antagonist, glibenclamide and in some extend ADP. These novel findings indicate that the proposed inter-subunit salt bridges mediated allosteric contacts between the two heterologous subunits in the Kir6.1/SUR2A and Kir6.2/SUR2A channels.

Biochemical study identified three putative inter-subunit salt bridges, the Kir6.2 K338/SUR2A E1318, Kir6.2 D323/SUR2A K1322 and Kir6.2 D323/SUR2A Q1336,

between the Kir6.2 and SUR2A-NBD2 (Chapter 5). Thus, the hypothesis in this sub-study was that these C-terminal electrostatic interactions (mentioned above) in the intracellular domains of two heterologous subunits are possibly involved in allosteric contacts and are functionally critical in K_{ATP} channel.

It was thought that residues in the equivalent position in the Kir6.1 (E332 or R347) subunit to those of the Kir6.2 (D323 and K338) should also be important for the cytoplasmic interaction between Kir6.1and SUR2A in K_{ATP} channel. In other words, the proposal was that this region including D323 and K338 of Kir6.2 or E332 or R347 of Kir6.1 in the distal C-terminal of Kir6 isoforms is key to the interaction with NBD2 of SUR2A. To assess this hypothesis, electrophysiological study in the whole cell and inside-out patch clamp configuration was performed to test the sensitivities to potassium channel opener and sulphonylurea, in mutated Kir6.2/SUR2A and Kir6.1/SUR2A channels compared to the control (wild type) channel and in addition the sensitivities of ADP and ATP in the Kir6.2/SUR2A channel.

Single point mutation of E332 or R347 in the distal C-terminal of Kir6.1 impaired the properties of the Kir6.1/SUR2A channel and a single reversal of charged residues in both subunits for Kir6.1 and SUR2A restored the function in some cases. Indeed, whole cell patch clamp results confirmed the hypothesis of this sub-study that the charged residues E332 or R347 in the distal C-terminal of Kir6.1 and E1318, K1322 and Q1336 of SUR2A-NBD2 are involved in determining the pinacidil and glibenclamide sensitivities of the regulatory SUR2A subunit to the ATP-sensitive potassium channel pore (Kir6.1).

When positively charged arginine, R347, in the distal C-terminal of Kir6.1 was mutated to the oppositely charged glutamic acid, Kir6.1 R347E, this single mutation altered the

properties of the Kir6.1 R347E/SUR2A WT channel. Disruption of the cytoplasmic salt bridge between Kir6.1 and SUR2A by this single mutation caused an increase of the sensitivity to the potassium channel opener pinacidil (figure 6-8 A). Expression of SUR2A E1318R with Kir6.1 R347E restored the pinacidil sensitivity nearly to the wild type (figure 6-8 B). In other words, the sensitivity to the potassium channel opener depends on the inter-subunit electrostatic interaction between R347 and E1318 of the distal C-terminal of Kir6.1 and the NBD2 of SUR2A, respectively. The same single point mutations in Kir6.1 in the Kir6.1 R347E/SUR2A WT channel also resulted in alteration of the glibenclamide sensitivity and modified the cross-talk between the regulatory subunit SUR2A and the channel pore (Kir6.1) in K_{ATP} channels (figure 6-11 A).

Similar results were found when Kir6.1 E332K was co-expressed with the wild type SUR2A. In other words, in the Kir6.1 R347E/SUR2A WT or Kir6.1 E332K/SUR2A WT channel, the dose-response curves for glibenclamide inhibition were shifted to the right compared to the wild type Kir6.1/SUR2A channel (figure 6-11 A and figure 6-12 A). This indicates that the positively charged arginine, R347, and negatively charged glutamine acid, E332, in the distal C-terminal of Kir6.1 are not just key for the physical interaction between heterologous subunits but that, they are also crucial for the determination of the sulphonylurea sensitivity mediated from binding to SUR2A to the channel in K_{ATP} channel. The co-expression of Kir6.1 R347E with SUR2A E1318R and Kir6.1 E332K with SUR2A E1322D reestablished these two proposed inter-subunit salt bridges and restored the sensitivity to the K_{ATP} channel antagonist, glibenclamide, close to that of the wild type Kir6.1/SUR2A channel (figure 6-11 B, figure 6-12 B and table 6-3). These results suggested that cytoplasmic electrostatic interactions between these ion pairs are involved in transmission of allosteric information and the Kir6.1

R347/SUR2A E1318R or Kir6.1 E332/SUR2A E1322 salt bridges specifically are required for the cross talk (glibenclamide sensitivity) between the two heterologous subunits in the K_{ATP} channel. Another explanation could be that the allosteric regulation depends on these salt bridges, which determine the glibenclamide sensitivity of SUR2A, and the information may be transmitted through other contacts between two subunits.

The single mutation in Kir6.1, E332K, resulted in constitutive channel opening of Kir6.1 E332K/SUR2A WT channel. This subunit combination was activated in the absence of potassium channel opener pinacidil (figure 6-13 and figure 6-14). The effect of the mutation of the negatively charged glutamic acid, E332, in the distal C-terminal of Kir6.1 was very confusing and it was more difficult to interpret the role of this residue in the structure-function terms.

The co-expression of Kir6.1 E332Kwith SUR2A K1322D or SUR2A Q1336E and even with the double mutant SUR2A K1322D + Q1336E did not restore the pinacidil activated property of the WT channel that was impaired by single mutation E332K in Kir6.1 (figure 6-13 B, figure 6-14 and table 6-2). It is worth emphasizing that the Kir6.1 E332/SUR2A E1322 salt bridge was involved in determining the inhibitory regulation to the pore from antagonist binding to the SUR2A but not activation by pinacidil since Kir6.1 E322K/SUR2A E322D channels restored the glibenclamide but not the pinacidil sensitivity (table 6-2 and 6-3). Due to the difficulty of performing inside out patch clamp, this was an impediment to further understand the possible transmission of functional information from SUR2A involving Kir6.1 E332 and Kir6.1 R347 residues in terms of ATP and ADP regulation of the Kir6.1/SUR2A channel.

Interestingly, in the case of Kir6.2/SUR2A channel, the electrophysiological results revealed similar changes in the sensitivity to pinacidil and glibenclamide in the

equivalent salt bridges in Kir6.2/SUR2A to Kir6.1/SUR2A channels. These data suggest that the transmission of allosteric information via these inter-subunit interfaces is similar between sulphonylurea receptors, SUR2A and Kir6 isoform combinations in K_{ATP} channels. An exception was that the D323 of Kir6.2, which is equivalent to E332 of Kir6.1, formed a salt bridge with SUR2A Q1336 to mediate glibenclamide sensitivity, however, in Kir6.1 isoform E332 formed a salt bridge with SUR2A K1322.

Initially, it was thought that the Kir6.2 K338 may be part of the ATP binding site or involved in ATP regulation since the 334 GNTI 337 region of Kir6.2 is part of the inhibitory ATP binding site (Drain et al. 1998). In other words, the K338 might contribute to the Kir6.2 inhibitory binding site directly and the Kir6.2 K338E mutation might have a direct effect on inhibition by ATP. Conversely, the inside-out patch results revealed that the ATP sensitivity was unchanged in the Kir6.2 K338E/SUR2A WT compared to the wild type Kir6.2/SUR2A channel, eliminating the possibility that the K338 contributes to the Kir6.2 inhibitory binding site directly. In summary, the ATP and ADP sensitivities were unaffected by mutation in Kir6.2 K338E or SUR2A E1318R, or charge reversal in both subunits (Kir6.2 K338E/SUR2A E1318R) indicating that the Kir6.2 K338/SUR2A E1318 salt bridge does not play a critical role in mediating the ATP and ADP sensitivities, unlike pinacidil and glibenclamide sensitivities.

In congential hyperinsulinaemia, the residue F1388 in SUR1 was identified, and if deleted, it results in defective stimulatory responses to MgADP and diazoxide and disrupted trafficking of channels to the cell surface (Cartier et al. 2001). For correct trafficking, substitutions of single amino acids in this region revealed that hydrophobicity is important. However, the residue in this position has a detailed architecture, more importantly, to determine the sensitivity to MgADP and the drugs

which target the K_{ATP} channels. In SUR2A and SUR2B at position 1351, the conservative substitution of leucine was suggested to explain some of the pharmacological differences between SUR isoforms (Cartier et al. 2001).

The study of Dupuis et al (2008), which was based on our lab work (Rainbow et al. 2004) revealed that the proximal C-terminal of SUR2A within the Kir6.2/SUR2A channels is a crucial link between potassium channel opener binding to SUR2A and Kir6.2 activation. A summary of their results was that they identified three residues, E1305, I1310 and L1313, which when mutated to those in non-interacting MRP1, were sufficient to remove the pinacidil-stimulated channel activation. The conclusion of their study was that these residues probably have a role in activation but not inhibition of the channels pore. In other words, with these findings, Dupuis et al. suggested that these three residues are involved in forming a part of an information transduction pathway, which functionally couples SUR2A and Kir6.2 subunits through the SUR2A cytosolic segment that interconnects transmembrane helix 17 to NBD2.

This interface SUR2A-NBD2 (1294-1358) studied herein lies just downstream of three above mentioned residues in SUR2A in Dupuis' study. Hence, Cartier's, Rainbow's, Dupuis' studies and the present study indicate that this region of SUR is important for mediating allosteric information transfer between two heterologous subunits in ATP-sensitive potassium channels.

The three-dimensional structural model of the proposed inter-subunit interfaces between SUR2A and Kir6.2 in ATP-sensitive potassium channels (figure 5-2 B) was inconsistent with the finding of this study. In other words, this three-dimensional structural model was not in agreement with the biochemical and electrophysiological findings in this study and did not confirmed our initial hypothesis that the three residues of SUR2A

E1318, K1322 or Q1336 and two charged residues in Kir6.2 D323 or K338 form three cytoplasmic salt bridges; Kir6.2 K338/SUR2A E1318, Kir6.2 D323/SUR2A K1322 and Kir6.2 D323/SUR2A Q1336 between the NBD2 of SUR2A and the distal C-terminus of Kir6.2.

Failure of this initial attempt to dock the two structural domains to identify the inter-subunit salt bridges characterised in this study was likely due to too many assumptions being made in modelling the amino acid sequences of both subunits onto homology models (figure 5-2 B). Indeed, it was perhaps surprising that the in silico docking brought the two interacting domains together at all. Given this preliminary result, it will be of interest to continue in silico docking by further constraining the model by imposing the characterised inter-subunit salt bridges identified herein.

Interestingly, the results represented in this study are consistent with the three-dimensional structure which is determined by single-particle electron microscopy at 18 Å resolution of the functional K_{ATP} channel complex $Kir6.2_4/SUR1_4$ (figure 1-8, Mikhailov et al. 2005). This structure, figure 1-8, shows there are cytoplasmic interactions between two heterologous subunits of Kir6 and SUR which are physically (Chapter 5) and functionally (Chapter 6) important. In other words, this structure is consistent with our initial work (Rainbow et al. 2004) and also with the results of this study that revealed the inter-subunit interactions are crucial for the assembly and function in hetero-octameric complex allostery of $Kir6_4/SUR2A_4$ of K_{ATP} channels.

Taken together, electrophysiological data of Kir6.1/SUR2A and Kir6.2/SUR2A channels of these studies suggest that these inter-subunit electrostatic interactions are not just structural interactions for co-assembly between Kir6 isoforms and SUR2A, but that they are also crucial as functional interactions in K_{ATP} channels. In other words,

these data provide evidence that the transmission of allosteric information through inter-subunit contacts mediate functional interactions between NBD2 in the proximal C-terminal of SUR2A and the distal C-terminal of the ATP-sensitive potassium channel pore, Kir6 isoforms.

9.3.1 Single Point Mutations in the Distal C-Terminal of Kir6 Effect the K_{ATP} Channels Kinetics

The functional evidence results suggest that single point mutation of the two charged residues, E332K or R347E on the pore forming Kir6.1 and the D323K or K338E on the Kir6.2 favour the activation of the Kir6.1/SUR2A and Kir6.2/SUR2A channels gating by potassium channel opener pinacidil. In other terms, these residues, which were found in this substudy, altered the stabilization of the closed state of K_{ATP} channel kinetics. Therefore, the sensitivity of K_{ATP} channel agonist pinacidil increased and the EC_{50} decreased which caused a shift of the dose-response curve to the left (Kir6.1 R347E/SUR2A WT) relative to that of wild-type Kir6.1/SUR2A channel. Thus, the potassium channel opener, pinacidil, activated this mutated channel easier compared to the wild type.

In the case of Kir6.1 E332K/SUR2A WT channel, it appeared to be constitutively opened, possibly due to the conformational changes of closed channel state. In other terms, the single charged residue Kir6.1 E332 is involved in the stability of the closed state and mutation to opposite charged residue (E332K) disrupted the kinetics of closed state in this subunit combination of K_{ATP} channel and caused relaxation. Whereas the

antagonist, glibenclamide, had no effect on the Kir6.1 E332K/SUR2A Q1336E and Kir6.1 E332K/SUR2A K1322D + Q1336E channels and these subunit combinations were insensitive to the glibenclamide. Moreover, the glibenclamide sensitivity was decreased (IC_{50} increased) in Kir6.1 R347E/SUR2A WT and Kir6.1 E332K/SUR2A WT channels and the glibenclamide dose-response curves for these mutated subunit combinations were shifted to the right compare to the wild type Kir6.1/SUR2A channel.

These data once more confirmed that these two charged residues (E332 and R347) on the distal C-terminal of the pore forming Kir6.1 involved in stabilizing the closed state of K_{ATP} channel kinetics. Hence, mutations in mentioned charged residues favoured the activation of the mutated subunit combinations, Kir6.1 R347E/SUR2A WT and Kir6.1 E332K/SUR2A WT channels by pinacidil but not the inhibition by glibenclamide.

9.4 Structural Studies of Kir6.2 Cytoplasmic Domains as Fusion Protein with Thermotoga Maritima 1070 (TM1070)

The main outcome of this sub-study was the report for the first time of expression and purification of Kir6.2 cytoplasmic domains as fusion protein with *Thermotoga Maritima* 1070. As discussed in Chapter 7, the purification of four constructs of the Kir6.2 polypeptide expressed in *E.coli* by Tezuka Takehiro was unsuccessful due to protein aggregation. To express and purify the cytoplasmic domains of Kir6.2 as a soluble fraction *Thermotoga Maritima* 1070 was used as fusion partner with the N- and C-termini of Kir6.2 to improve solubility and potentially protein folding. The results of

protein expression indicate that the more complex bacterial fusion construct, TM1070-Kir6.2NC (CT-His6 tag) improved the protein folding and solubility. These results support our initial hypothesis that the soluble protein, TM1070, should improve the expression of cytoplasmic domains of the Kir6.2 polypeptide for structural analysis. Enhanced expression of TM1070-Kir6.2NC (CT-His6 tag) was observed from Arctic Express compared to other expression systems. Further investigation revealed the optimal expression was observed after induction with 0.3 mM IPTG and 24 hrs incubation after induction from Arctic Express.

To purify the polyhistidine-tagged TM1070-Kir6.2NC (CT-His6 tag) fusion protein immobilized metal ion affinity chromatography (nickel column) was used as single-step purification. Coomassie blue stained SDS-PAGE and Western blot analysis of the purification of TM1070-Kir6.2NC (CT-His6 tag) fusion protein revealed that IMAC (Ni^{2+}) to be a promising first step in the purification. An enrichment of the target fusion protein (~ 48 kDa) with some remaining contaminating polypeptides within the elution fraction was observed. Thus, to remove the protein contamination, the IMAC was optimised by changing such as the condition of buffers, flow rates and longer washes.

Interestingly, optimization of IMAC increased slightly the yield and improved the purification fold. Since, the single-step IMAC did not remove the protein contamination an additional purification step, gel filtration chromatography, was considered necessary to remove the trace contaminants. Furthermore, Bradford assay on all fractions (GFC column) revealed no protein concentration indicating the absence of proteins in all fractions and that the peaks in elution profile probably represent the imidazole in buffer. A more detailed analysis of the GFC column showed the recombinant fusion protein, TM1070-Kir6.2NC (CT-His6 tag), was aggregated on the top of the column.

In summary, successful expression of TM1070-Kir6.2NC (CT-His6 tag) fusion from Arctic Express was obtained and it is clear that Arctic Express competent cells enhanced the protein folding and solubility of expressed recombinant fusion proteins. Single step purification by IMAC (Ni^{2+}) of TM1070-Kir6.2NC (CT-His6 tag) purification resulted in high yield and about 10 fold purification with remaining contamination. As secondary purification step GFC was performed, however, what still remains unanswered and unclear is why TM1070-Kir6.2NC (CT-His6 tag) fusion protein was aggregated on the top of GFC column.

9.5 Conclusions

In conclusion, multidisciplinary techniques (molecular biology, biochemistry, electrophysiology, pharmacology) were used to study the allosteric regulation between the two heterologous subunits, the pore forming Kir6, which is a member of the inwardly rectifying potassium channels family and a regulatory sulphonylurea receptor (SUR2A) in ATP-sensitive potassium channels. This study reports on the identification of three cytoplasmic electrostatic interfaces between Kir6 and SUR2A involved in determining the sensitivity of K_{ATP} channel agonist, pinacidil, and antagonist, glibenclamide, from SUR2A to the Kir6 channel pore. Also, the C-terminal cytoplasmic interfaces are functionally crucial in Kir6.1/SUR2A and Kir6.2/SUR2A channels.

The biochemical study, for the first time, reports on the identification of two charged residues D323 and K338 in the distal C-terminal of pore forming Kir6.2 that form part of interaction domain with the nucleotide binding domain 2 of SUR2A. These data indicate that the two mentioned residues play a role in the Kir6.2/SUR2A channel

assembly. In addition, these results revealed the Kir6.2 K338/SUR2A E1318, Kir6.2 D323/SUR2A K1322 and Kir6.2 D323/SUR2A Q1336 form inter-subunit salt bridges between the pore forming Kir6.2 and its partner SUR2A in Kir6.2/SUR2A channels. In other words, the Kir6.2 D323 and K338 with SUR2A E1318, K1322 and Q1336 formed ion pairs that stabilized the electrostatic interactions between the NBD2 of SUR2A and the distal C-terminal of Kir6.2 in functional $Kir6.2_4/SUR2A_4$ channel complex.

The electrophysiological study revealed the three putative inter-subunit salt bridges mediate allosteric contacts between the two heterologous subunits in the Kir6.1/SUR2A and Kir6.2/SUR2A channels. Single point mutation of E332 or R347 (equivalent residues in the same positions in Kir6.1 to Kir6.2) in the distal C-terminal of Kir6.1 impaired the properties of the Kir6.1/SUR2A channel. Moreover, a single reversal charge residues in both subunits for Kir6.1 and SUR2A restored the function in some cases. Similar changes in the sensitivity to K_{ATP} channel agonist, pinacidil and antagonist, glibenclamide were measured for the equivalent salt bridges in Kir6.2/SUR2A to Kir6.1/SUR2A channels indicating that the transmission of allosteric information via these inter-subunit interfaces is similar between sulphonylurea receptors, SUR2A and Kir6 isoform combinations in K_{ATP} channels. The identification of the cytoplasmic salt bridges perhaps can provide data and also contribute to validate a future three-dimensional structural model of these inter-subunit interfaces in K_{ATP} channels.

The cytoplasmic domains of the pore forming Kir6.2 subunit were expressed as fusion partner with *Thermotoga Maritima* (soluble bacterial protein) for structural analysis. Indeed, the complex bacterial fusion construct, TM1070-Kir6.2 NC (CT-His6 tag),

expressed in Arctic Express competent cells permitted successful expression of folded cytoplasmic domains of Kir6.2 in near native form. Subsequently, immobilized metal ion affinity chromatography, IMAC (Ni^{2+}), purification resulted in high yield and about 10 fold purification with remaining contamination and gel filtration chromatography (GFC) column as second purification step needs to be improved to purify this recombinant protein for structural analysis.

As a final point, possibly the therapeutic importance of this new information on channel function may contribute to the design of novel and more effective drugs to change the activity of this channel for the treatment of diabetes, high blood pressure and/or as a cardioprotective agent in heart attack or cardiac surgery.

9.6 Future Directions

9.6.1 Biochemical and Electrophysiological Study

Re-examination of the primary sequences (figure 3-1) at the distal C-termini of Kir6.2, Kir6.1 and Kir2.1 revealed further residues with potential interest in making inter-subunit interactions; these residues are shown in table 9-1. The basic local alignment search tool (BLAST) search of sequences that align with the Kir6.2 C-terminal domain revealed residue variation in non-conserved positions. The same criteria as described in Chapter 3 was used to select conserved only in Kir6 or conserved in Kir6 and renal outer medullary potassium channel (ROMK1 or Kir1.1), the latter of which also makes an allosteric interaction with the ABC cassette protein,

cystic fibrosis transmembrane conductance regulator (CFTR). Using these criteria, it was possible to restrict residues on the distal C-terminal of Kir6.2 for mutagenesis as shown in table 9-1 farthest to the right (ticked). Potentially these residues can undergo mutagenesis for co-immunoprecipitation and electrophysiological analyses. Single Kir6.2 mutants of the above mentioned residues expressed with wild type SUR2A should be screened for pinacidil activated K^+ current in whole cell recordings. If allosteric activation is absent, a metabolic poisoning should be produced to activate the K_{ATP} current. Where the current is absent, a consideration needs to be made for surface labeling to establish surface expression of the channels. Where pinacidil activated current is still present, a dose-response curves should be performed for pinacidil and ADP activation in whole-cell and inside-out patch clamp configurations. K_{ATP} channel inhibitor, such as glibenclamide, should be used for these Kir6.2 mutant constructs to investigate the inhibition response of the channel. In addition, ATP inhibition-response curves for the potential residues (table 9-1) need to be done to consider if these residues are involved in ATP binding or in ATP regulation. Since, a study has shown that the 334 GNTI 337 region of Kir6.2 is part of the inhibitory ATP binding site (Drain et al., 1998).

9.6.2 Structural Study

For structural analysis, such as Nuclear magnetic resonance (NMR) spectroscopy and X-ray crystallography, it will be required to prepare highly purified proteins in 1 - 2 mg amounts and the purification of TM1070-Kir6.2NC fusion protein should be improved to remove contaminating proteins. A crystal structure of this interaction is essential to comprehend the allosteric information transfer through inter-subunit contacts in K_{ATP}

channels. Given the latter, a model structure, which may inform the rational design of novel drugs to either strengthen or weaken the interaction to achieve a pharmacological endpoint, such as augmented sensitivity to Mg^{2+}-ADP for tissue protection, will be highly informative.

Finally, there is no doubt much work needs to be done to clarify the allosteric communications and the structure-function relationship between K_{ATP} channels subunits, which induce the conformational changes and the channel gating.

Kir6.2 residue	Kir6.2	Kir6.1	ROMK1	Kir2.1	Kir2.3	Kir3.1	Kir3.3	GIRK1	Kir6 not others	Kir6 + ROMK1	Kir6 + ROMK1 not others	Mutagenesis
295	G	G	S	A	A	G	G	G				
296	I	I	A	M	M	M	M	M	✓			✓
300	A	A	V	C	A	A	A	A				
307	D	E	E	N	S	D	D	D		✓		
315	F	F	F	Y	F	F	F	F		✓		
316	V	V	V	E	E	L	M	F		✓	✓	✓
318	I	I	I	V	V	V	V	V		✓	✓	✓
319	V	V	V	L	V	M	L	I		✓		
323	D	E	E	K	K	E	D	E		✓		**Done**
324	G	G	E	H	G	G	G	G				
327	S	S	R	K	K	R	E	K	✓			✓
332	K	K	N	R	R	Q	C	Q	✓			✓
333	F	F	F	F	F	F	F	F				
334	G	G	G	H	H	H	H	H		✓		✓
335	N	N	K	K	K	N	Q	A				
337	V	V	V	Y	Y	F	L	F		✓	✓	✓
338	K	R	E	E	E	E	E	E	✓			**Done**
350	D	D	N	A	A	D	A	E				
354	S	S	A	Y	K	S	A	-				

Table 9-1 Potential residues on the distal C-terminal of Kir6.2 for future study.

The red and blue colours represent the negative respectively positive charged residues. The Kir6.2 D323 and K338 residues were studied in this project and farthest to the right (ticked) column represent the potential residues, which can undergo mutagenesis for co-immunoprecipitation and electrophysiological analyses. Rat sequences where used when there was a choice. Abbreviations: ROMK1 (renal outer medullary potassium channel, Kir1.1) and GIRK1 (G protein activated inwardly rectifying potassium channel).

Appendix A:

Solutions, Buffers and Reagents

SDS-PAGE

The size of the protein of interest determines the SDS-polyacrylamide gels percentage. For casting two 10%, 1.5mm minigels the following solutions and volumes were used (Bio-Rad casting Kit).

Resolving gel

dH_2O	6.5 ml
30% Acrylamide/Bis	5.32 ml
1.5 M Tris-HCl (pH 8.8)	4 ml
10% SDS	160 µl
10% APS	160 µl
TEMED	20 µl

Stacking gel

dH_2O	5.55 ml
30% Acrylamide/Bis	1.7 ml
0.5 M Tris-HCl (pH 6.8)	2.5 ml
10% SDS	100 µl
10% APS	100 µl
TEMED	10 µl

10 X SDS-PAGE Running Buffer (1 L)

Tris-base	30 g
Glycine	144 g
SDS	10 g

Agarose Gel Electrophoresis (AGE)

50X TAE (1L)

Tris-base	242 g
Glacial acetic acid	57.1 ml
EDTA (0.5 M, pH 8.0)	100 ml
dH_2O	up to 1 L

Gel Staining and Destaining

Coomassie blue stain

Acetic acid	10% v/v
Isopropanol	25% v/v
Coomassie blue	280 g
dH_2O	up to 1 L

Destain of Coomassie blue

Acetic acid	10% v/v
Methanol	5% v/v
Glycerol	3% v/v

Western Blotting

10x Transfer buffer, 1 L (pH 8.3)

Tris-base	250 mM
Glycine	1.92 M

1X Transfer buffer (1L), (25 mM Tris, 192 mM Glycine, pH 8.3)

10x Transfer buffer	100 ml
Methanol	100 ml (final 10 % methanol)
dH_2O	800 ml

10x TBS (Tris-buffered saline) pH 7.6, 1L

Tris-base	100 mM
NaCl	1.50 M

Enhanced Chemiluminescence (ECL)

0.1 M Tris pH 7.6	50 ml
Solution A:	22 µl
(90mM p-coumaric acid in DMSO, Sigma)	
Solution B:	50 µl
(250 mM Luminol in DMSO, Sigma)	
6 % H2O2	3 µl

Culture Medium

Liquid media

Lysogeny Broth (LB) Medium (1 litre, autoclave)

Bacto tryptone	10 g
Bacto yeast extract	5 g
NaCl	10 g

SOC medium: Super optimal broth with Catabolite repression

Peptone	2%
Yeast extract	0.5%
NaCl	0.05%
250 mM KCl	1 ml
2 M $MgCl_2$	0.5 ml
1M glucose	2 ml
dH_2O	up to 100ml

Antibiotic Solutions

LB + Ampicillin

Amp Stock (made in dH_2O)	100 mg/ml
Amp final concentration	100 µg/ml

LB + Kanamycin

Kana Stock (made in dH_2O)	50 mg/ml
Kana final concentration	50 µg/ml

Appendix B:

Plasmid Vector Maps for All Constructs

Plasmid Vector Map for Kir6.1 E332K Construct

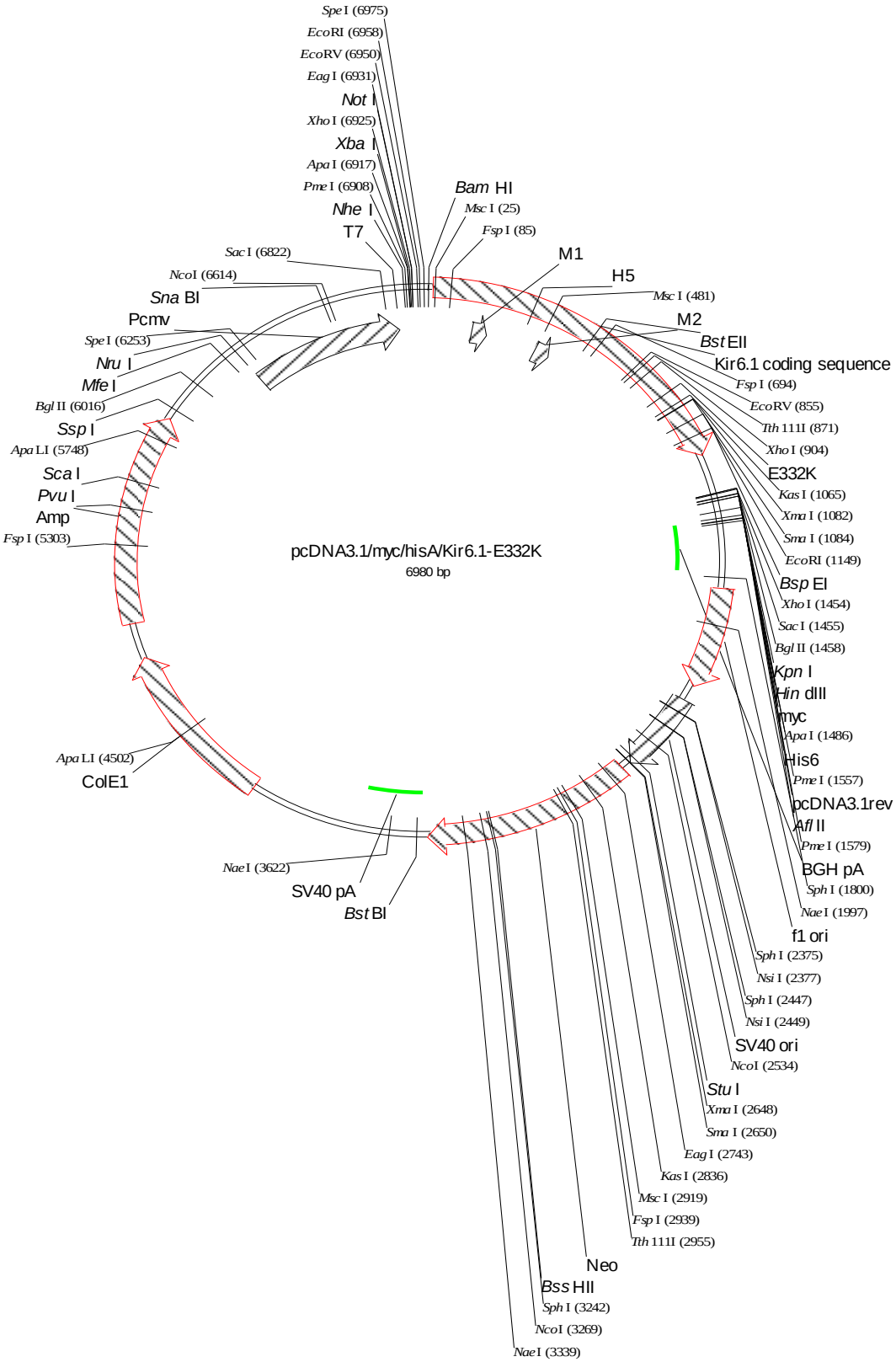

Plasmid Vector Map for Kir6.1 R347E Construct

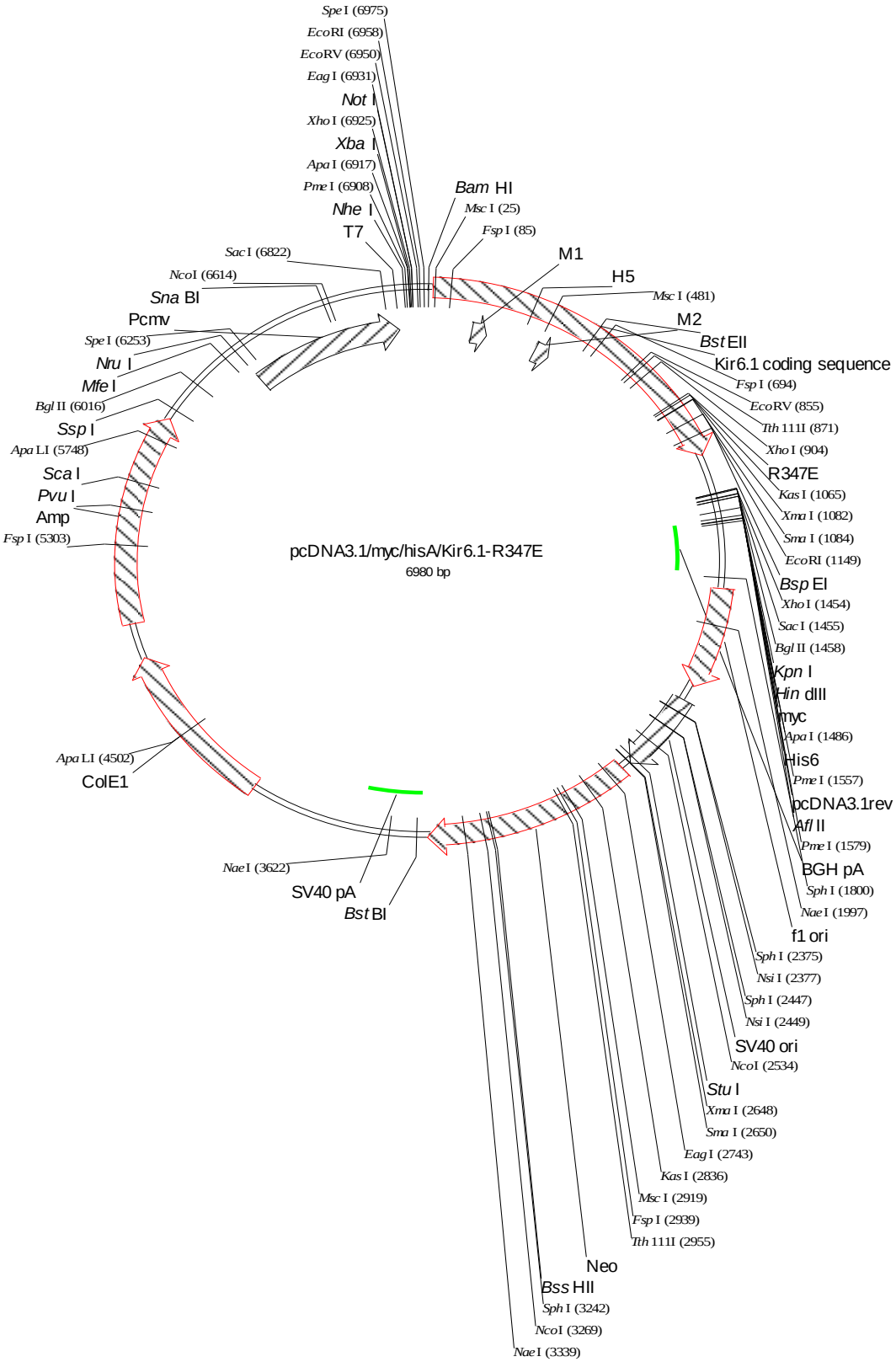

Plasmid Vector Map for Kir6.2 D323K Construct

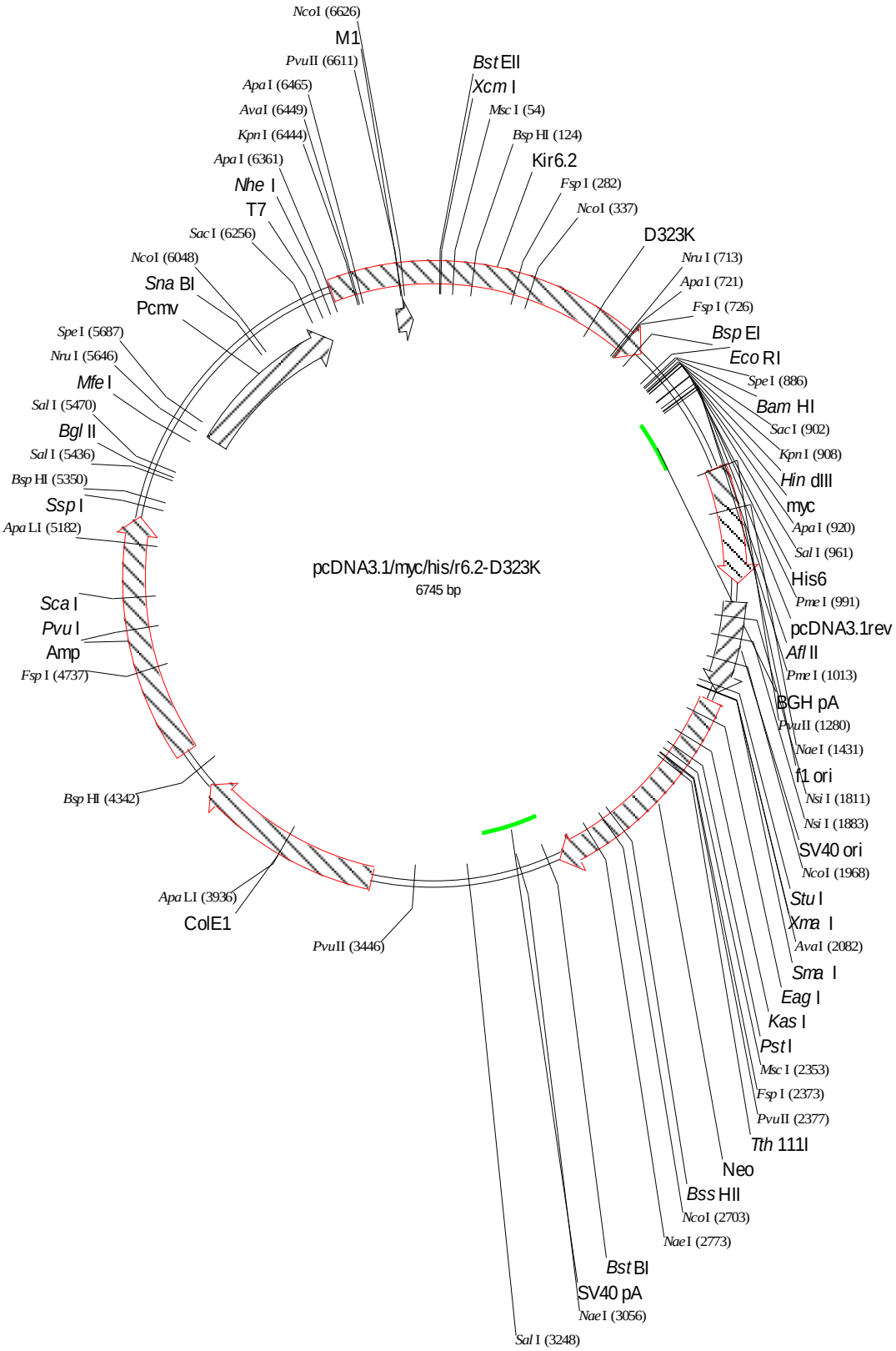

Plasmid Vector Map for Kir6.2 K338E Construct

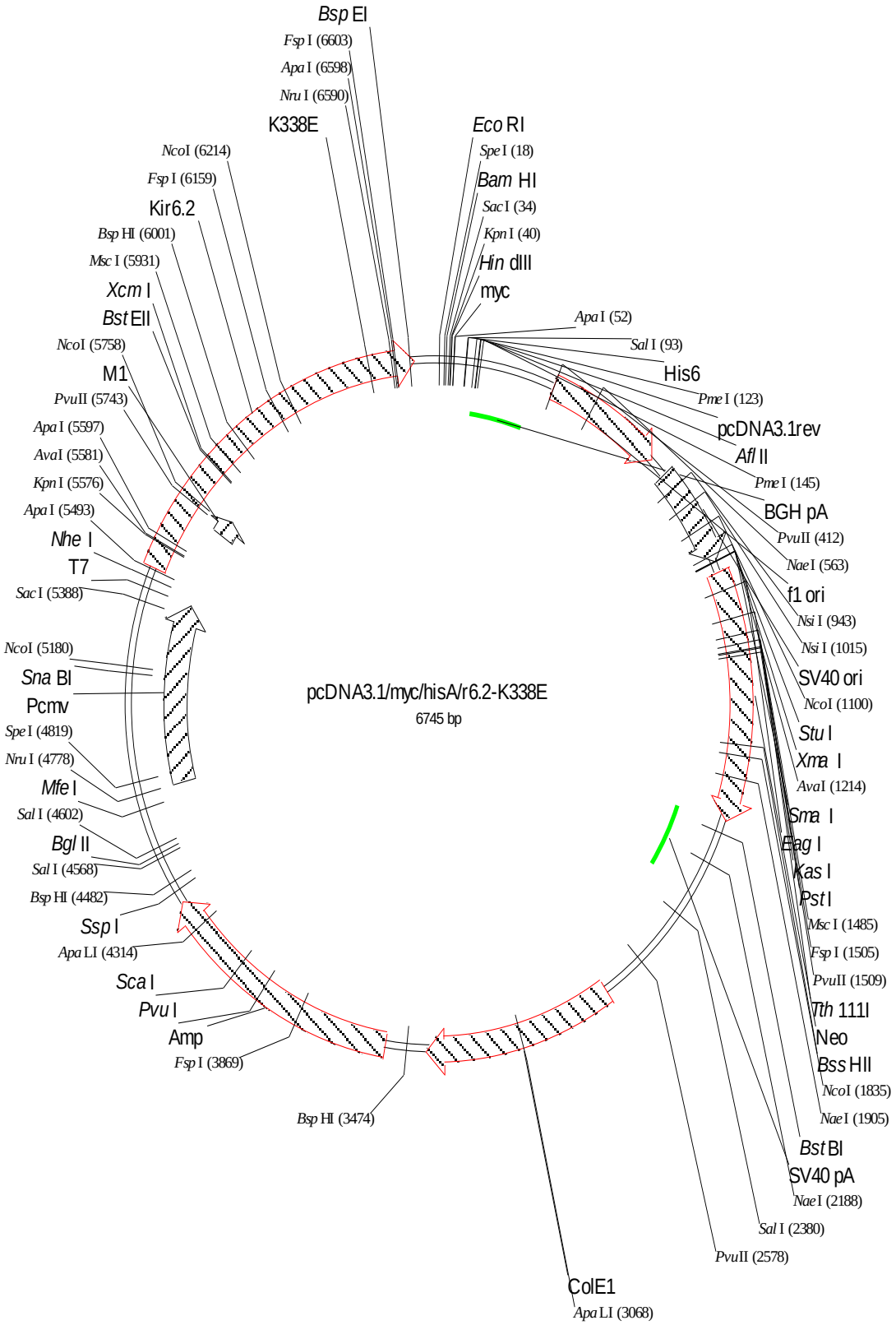

Plasmid Vector Map for SUR2A E1318R Construct

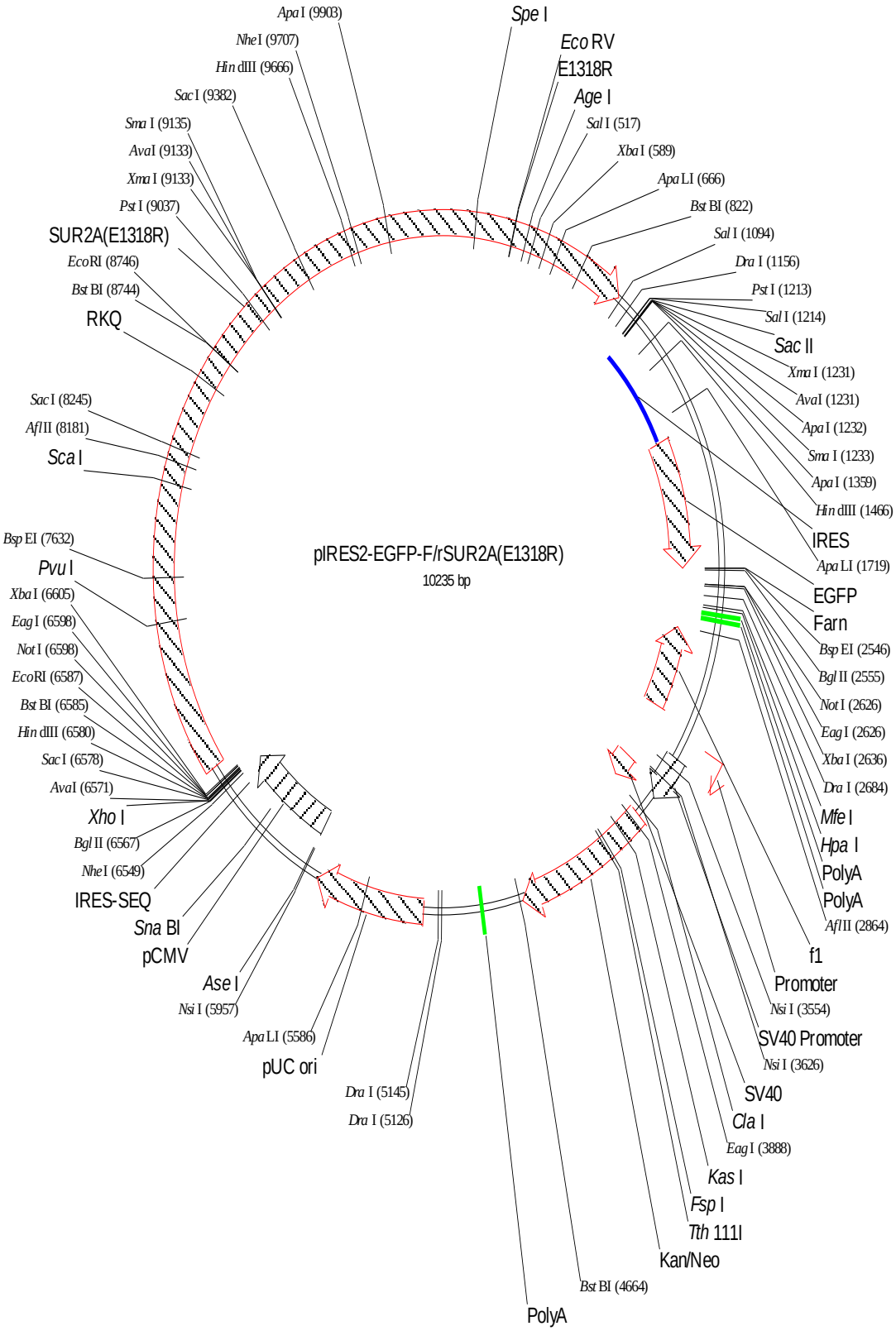

Plasmid Vector Map for SUR2A K1322D Construct

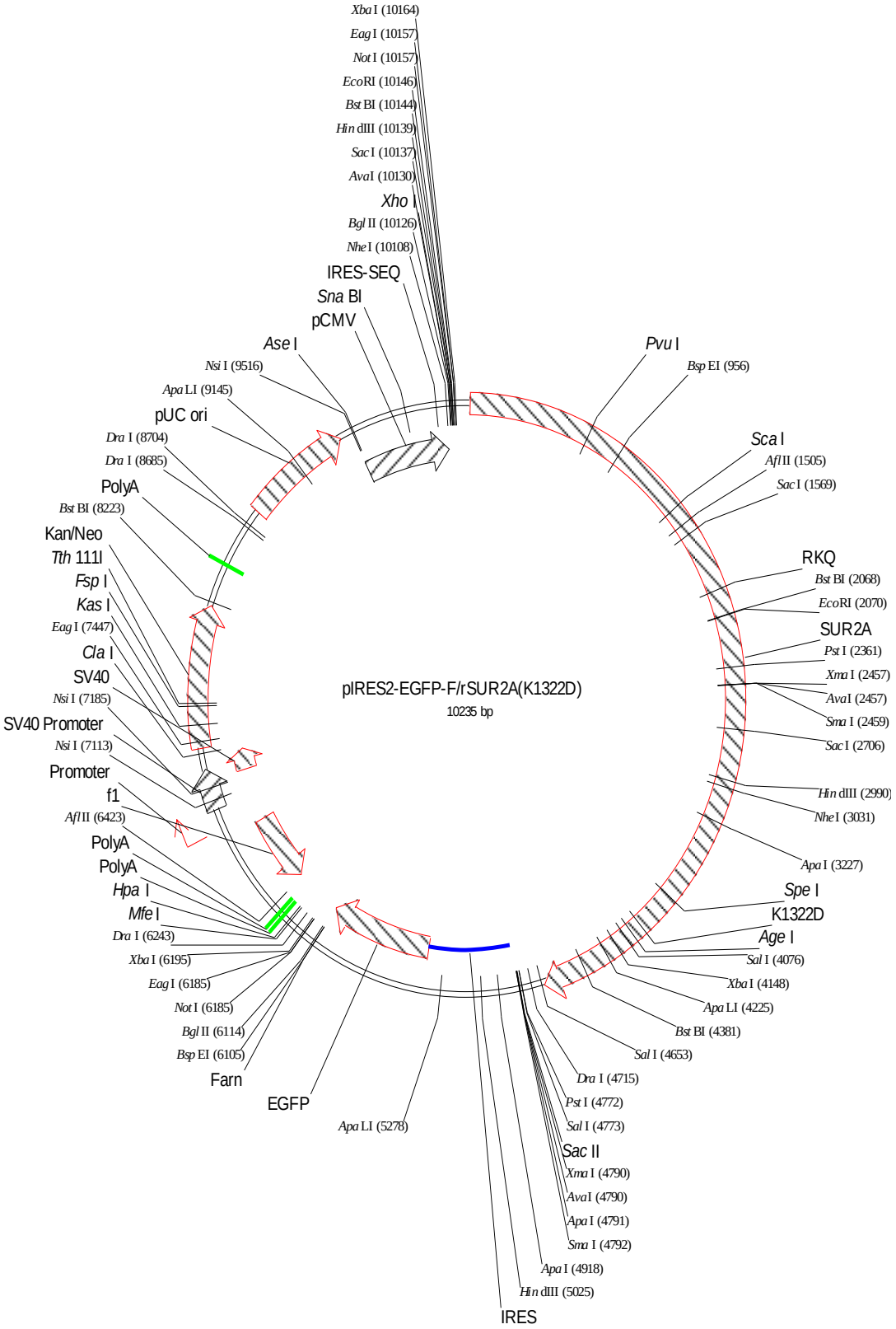

Plasmid Vector Map for SUR2A Q1336E Construct

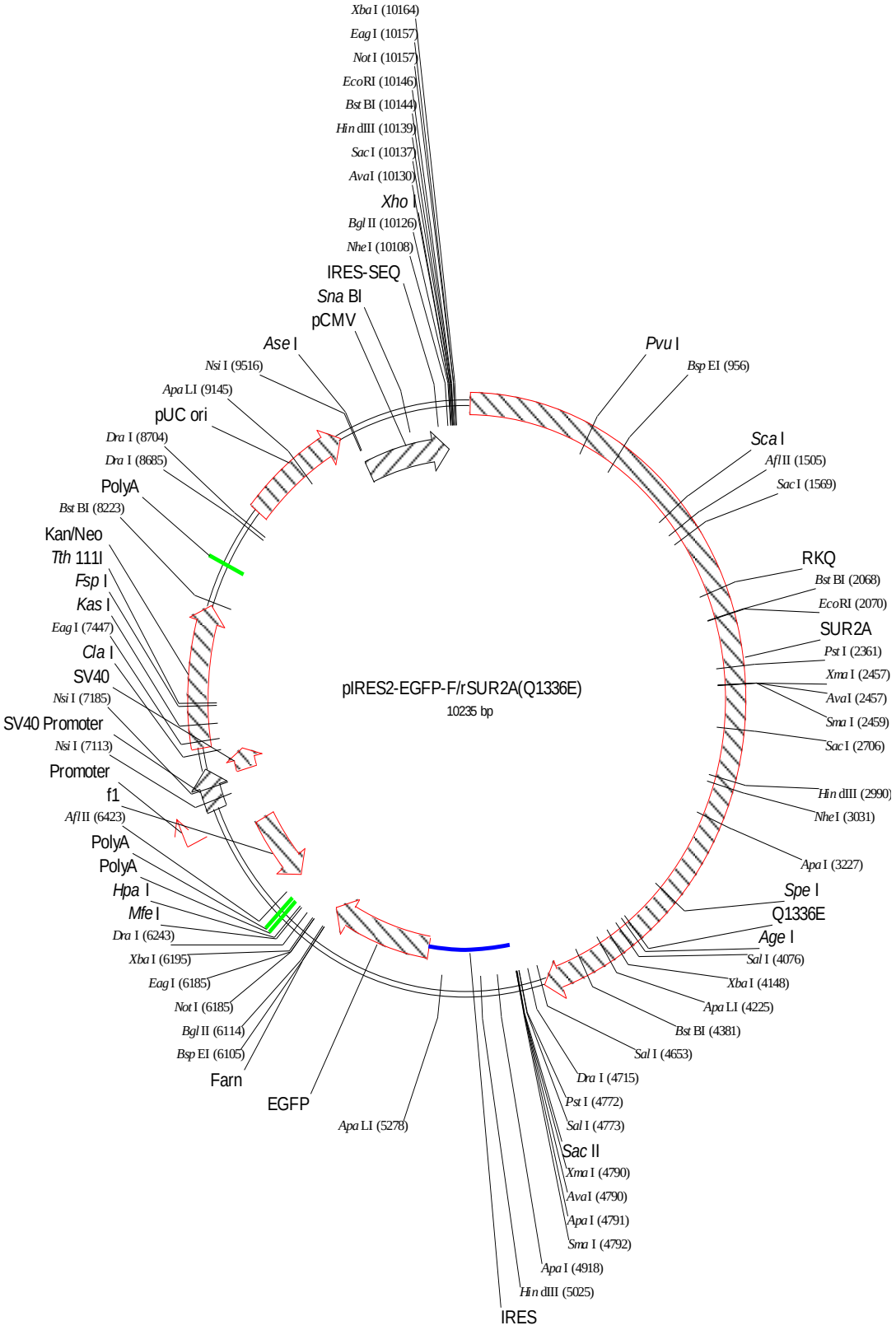

Plasmid Vector Map for SUR2A K1322D + Q1336 Construct

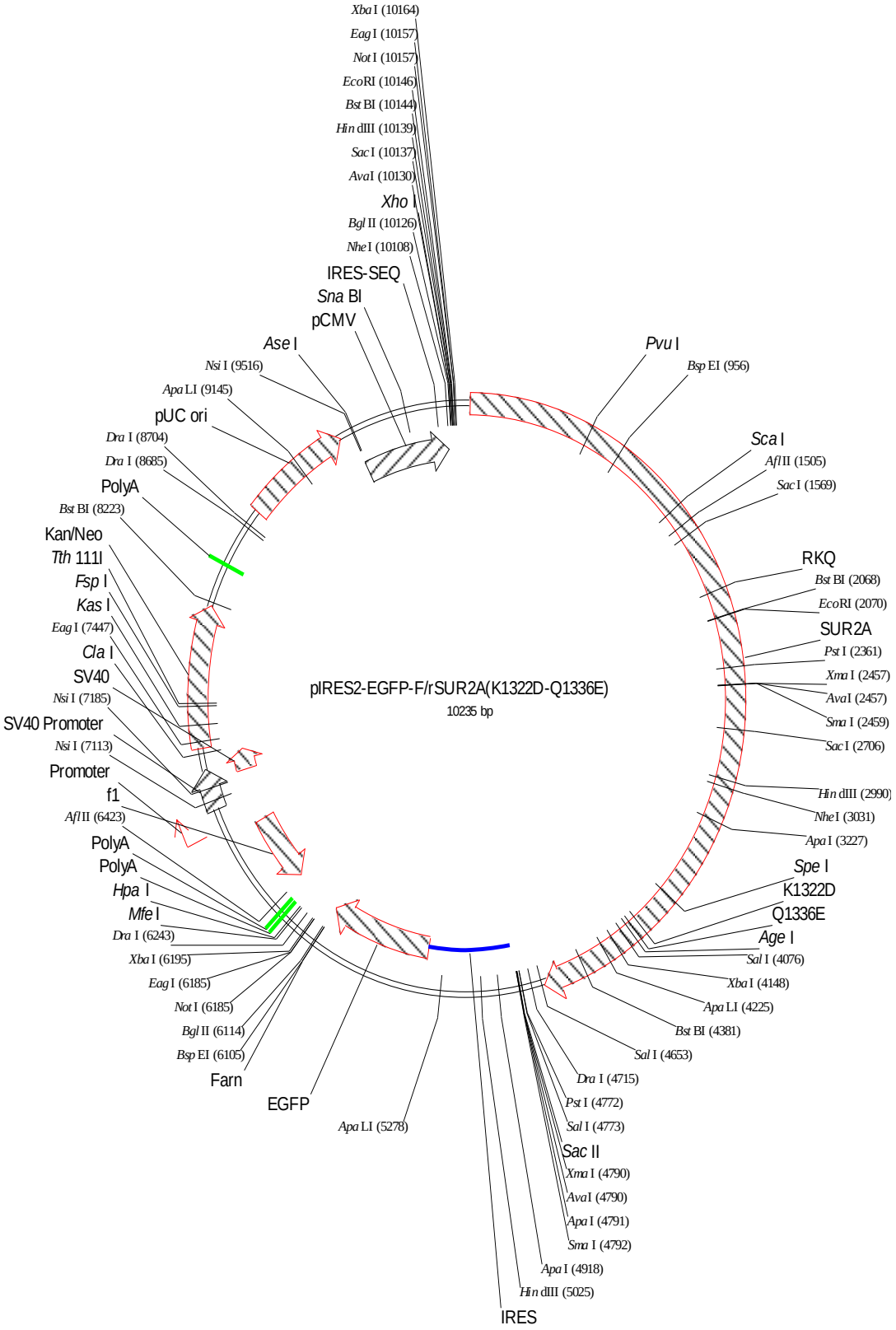

Plasmid Vector Map for MBP-SUR2A-CTC fragment Construct

(amino acids 1294-1403)

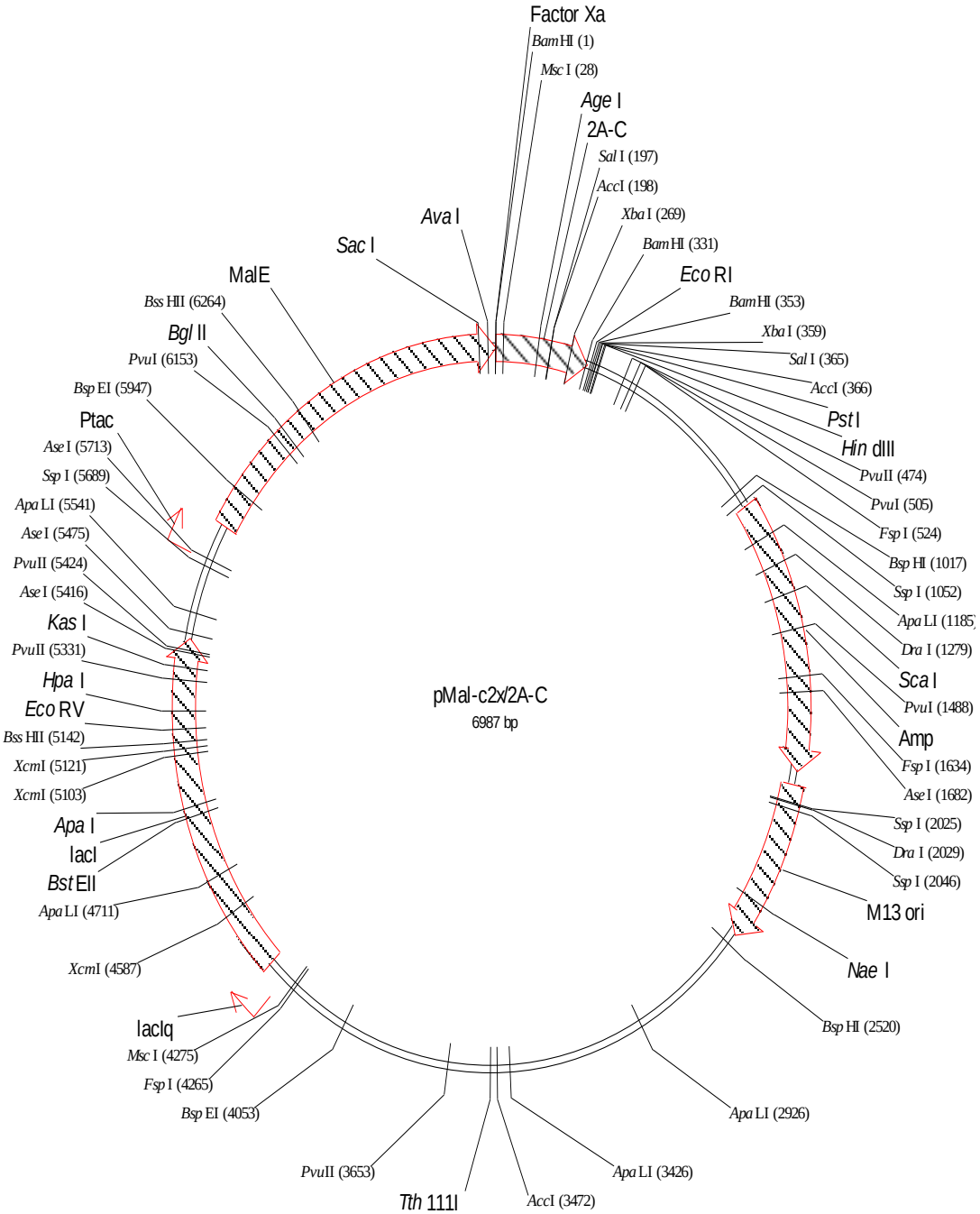

Plasmid Vector Map for TM1070-Kir6.2 NC (C-terminal-His6 tag) Construct

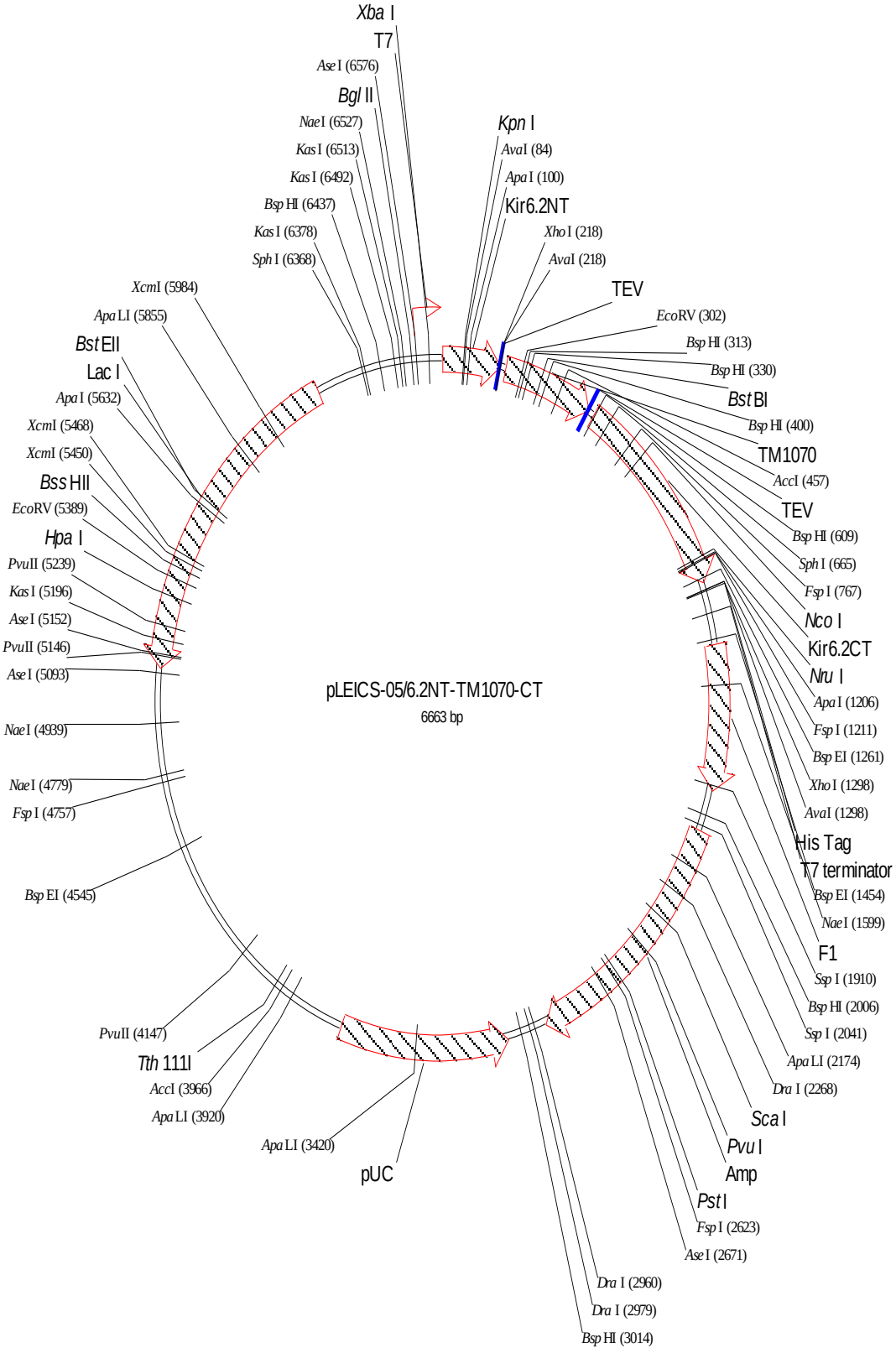

Appendix C:

Functional Studies' Results of the Cytoplasmic Salt Bridges in the $Kir6.2_4/SUR2A_4$ Channel Complex

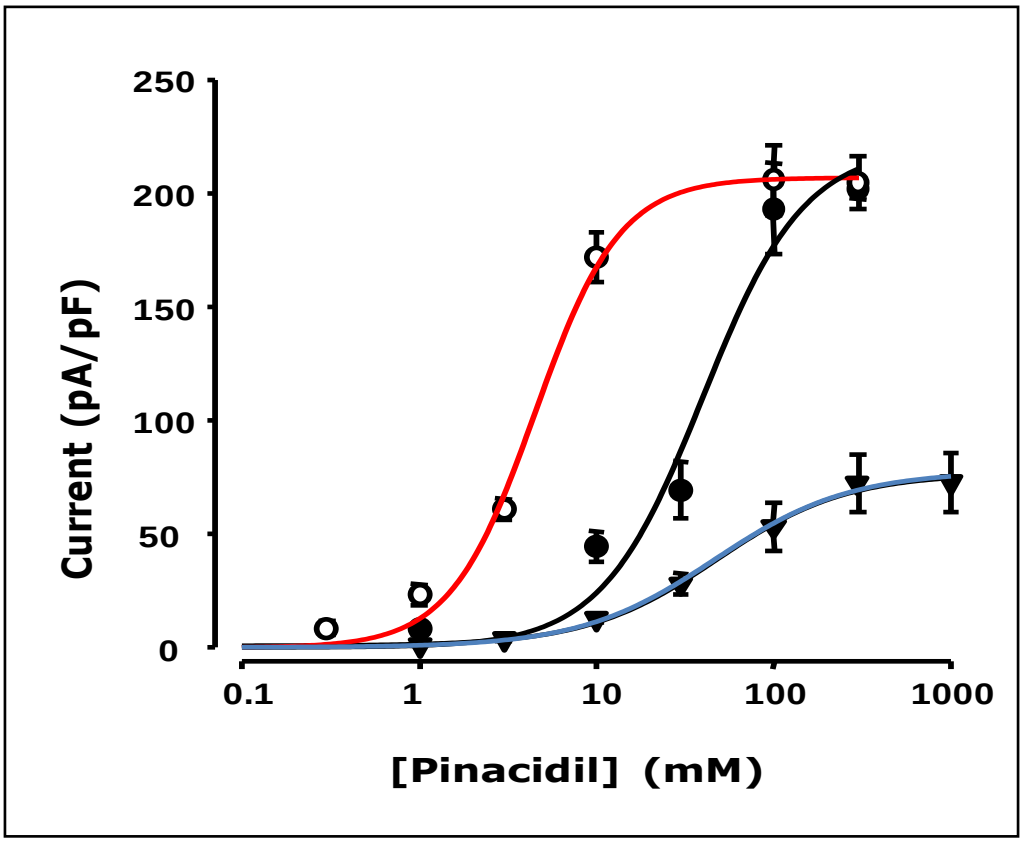

Pinacidil sensitivity from the SUR2A subunit to Kir6.2 channel is mediated via an inter-subunit salt bridge between Kir 6.2 K338 and SUR2A E1318.

Dose-response curves for current activation by pinacidil for different Kir6.2 and SUR2A subunit combinations. A single mutation of Kir6.2 K338E (red curve) increased the sensitivity to the agonist, pinacidil, compared to the wild type Kir6.2/SUR2A channel (black curve) in whole-cell patch clamp, 48-72 hrs after co-transfection of HEK-293 cells with Kir6.2 and SUR2A. Co-expression of Kir6.2 K338E with SUR2A E1318R (blue curve) reinstated the inter-subunit salt bridge and restored the EC_{50}. n = minimum 6 cells per point and the statistical data analysis: $P \langle 0.0309$, one-way ANOVA and post test; Bonferroni with 95% confidence intervals.

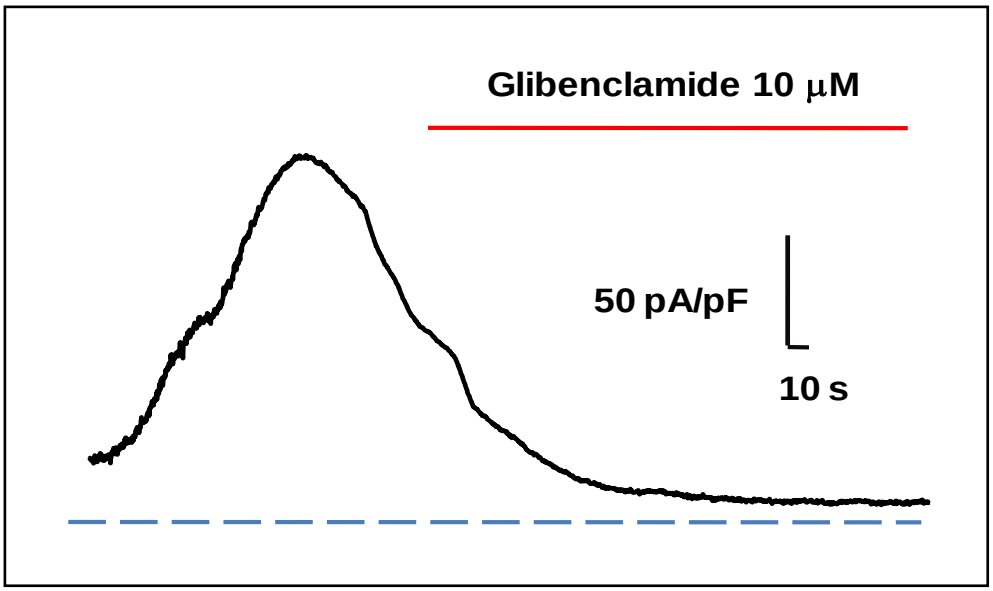

The Kir6.2 D323K mutant expressed with SUR2A WT causes constitutive opening of the ATP-sensitive potassium channel.

The trace represents potassium current in the absence of activation by pinacidil in the whole-cell configuration. The current of the Kir6.2 D323K/SUR2A WT channel was relatively insensitive to the K_{ATP} channel antagonist glibenclamide with block occurring only at relatively high glibenclamide concentration in the micromolar range.

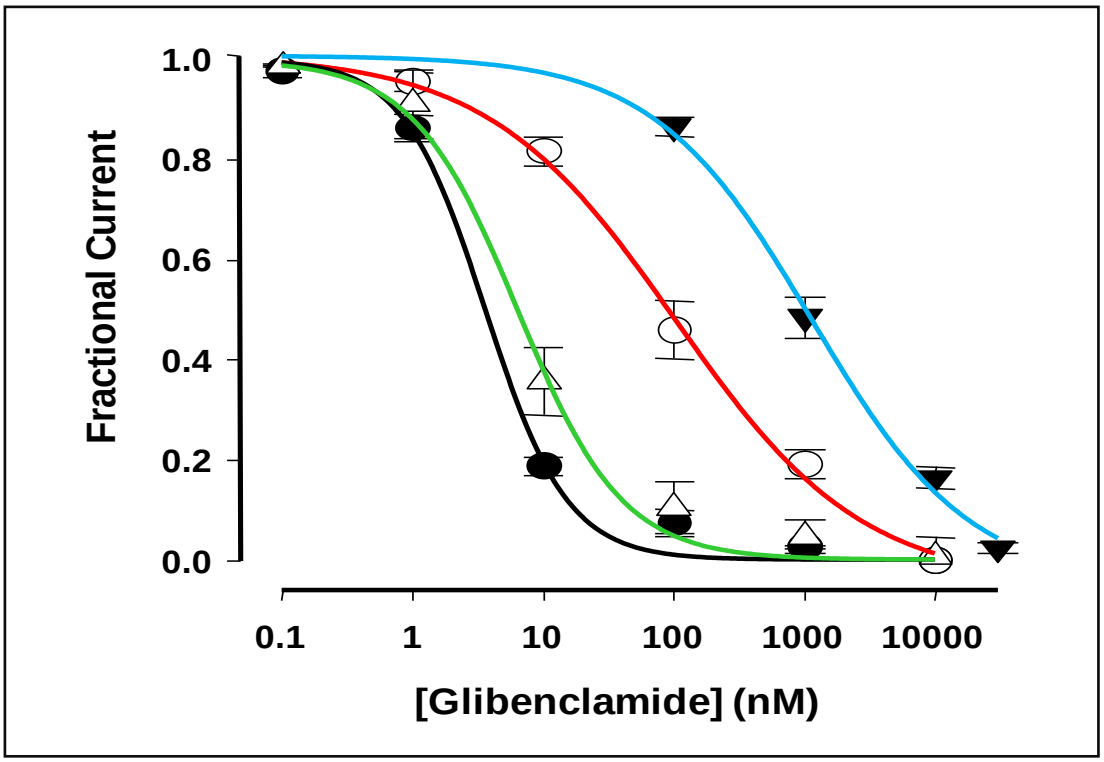

Glibenclamide sensitivity from drug binding to the SUR2A subunit to the Kir6.2 channel is mediated via an inter-subunit salt bridge between Kir6.2 K338 and SUR2A E1318.

Dose-response curves for current inhibition by glibenclamide for different Kir6.2/SUR2A combinations. A single mutation in either subunit Kir6.2 or SUR2A reduced the sensitivity to antagonist, glibenclamide, in whole-cell patch clamp, 48-72 hrs after transfection of HEK-293 cells. The glibenclamide sensitivity was reduced in Kir6.2 K338E/SURA WT (red curve) and Kir6.2 WT/SUR2A E1318R (blue curve with filled triangles) compared to the wild type Kir6.2/SUR2A channel (black). The green curve with empty triangles represents the restoration of the glibenclamide sensitivity in the proposed salt bridge reinstatement in Kir6.2 K338E/ SUR2A E1318R. n = minimum 6 cells per point and the statistical data analysis: $P \langle 0.6738$, one-way ANOVA and post test; Bonferroni with 95% confidence intervals.

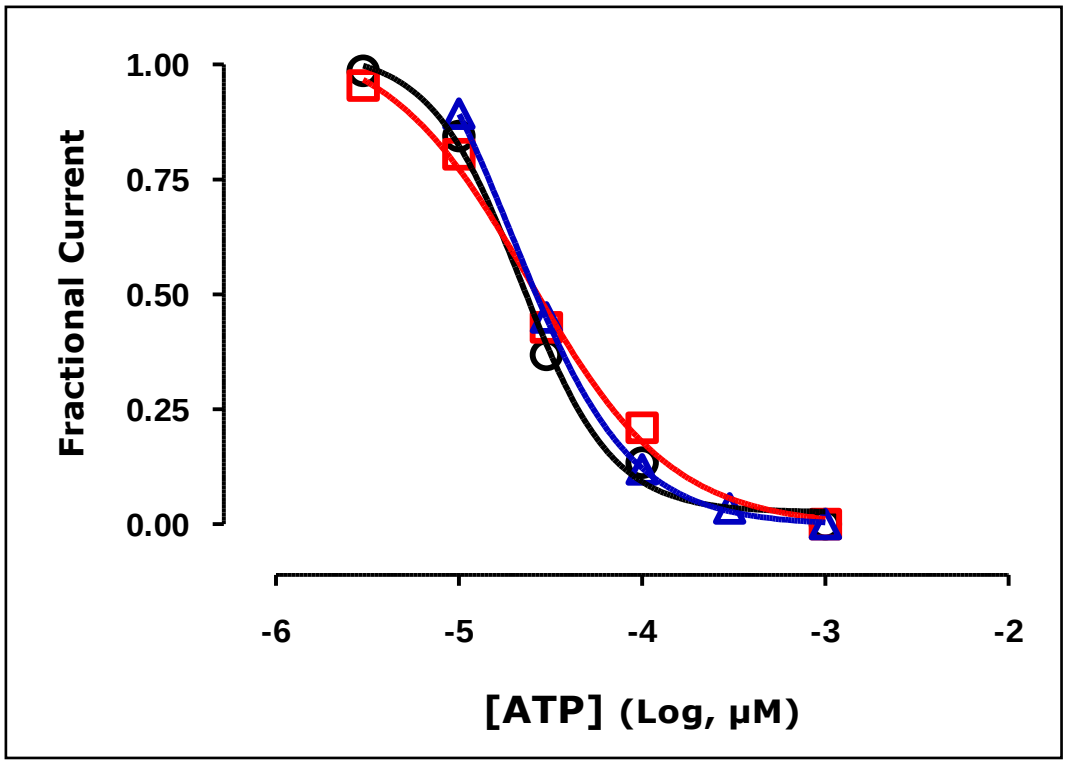

The inter-subunit Kir6.2 K338/SUR2A E1318 salt bridge is not involved in determining ATP sensitivity of Kir6.2/SUR2A channels.

The concentration-inhibition curves for excised inside-out patch clamp recording of wild type (black curve), Kir6.2 K338E/SUR2A WT (red curve) and Kir6.2 K338E/SUR2A E1318R (blue curve) channels, 48-72 hrs after transfection from HEK-293 cells. ATP concentration-inhibition curves show that the ATP sensitivity of the Kir6.2 K338/SUR2A WT and Kir6.2 K338E/SUR2A E1318R mutated channels was essentially unmodified, n = minimum 6 cells patches for each point and the statistical data analysis: $P \langle 0.80$, one-way ANOVA and post test; Bonferroni with 95% confidence intervals. Fractional current means the data were normalized to the maximum current.

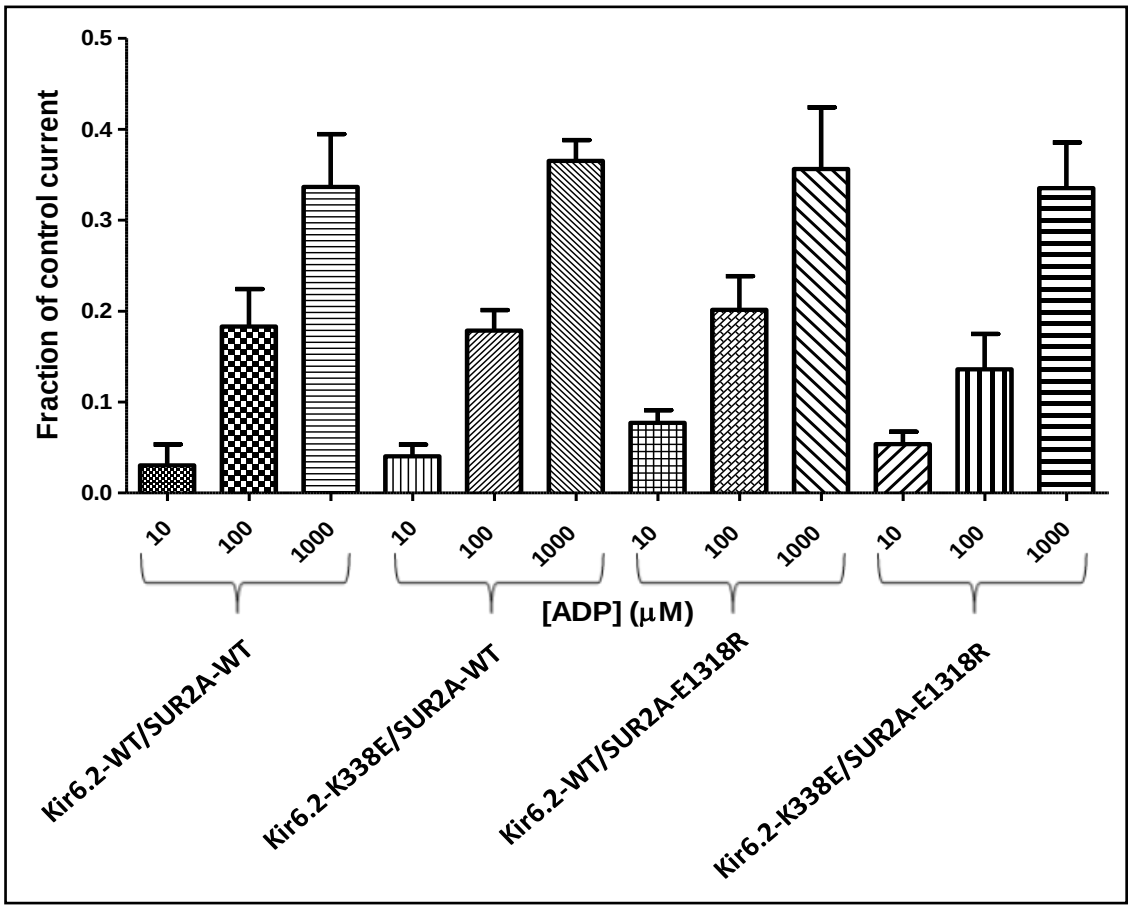

The inter-subunit Kir6.2 K338/SUR2A E1318 salt bridge is not involved in determining ADP sensitivity of Kir6.2/SUR2A channels.

The figures represent the summary results of excised inside-out patch clamp recording of wild type and different mutated subunit combination channels, 48-72 hrs after transfection from HEK-293 cells. The ADP sensitivity was unmodified on disruption of the Kir6.2 K338/SUR2A E1318 salt bridge by single charge reversal mutation in Kir6.2 K338E or SUR2A E1318R, or charge reversal mutations in both subunits Kir6.2 K338E/SUR2A E1318R compared to the wild type Kir6.2/SUR2A channel.

n = minimum 6 cells patches for each point and the statistical data analysis: $P \langle 0.0001$, one-way ANOVA and post test; Bonferroni with 95% confidence intervals. Fractional current means the data were normalized to the maximum current.

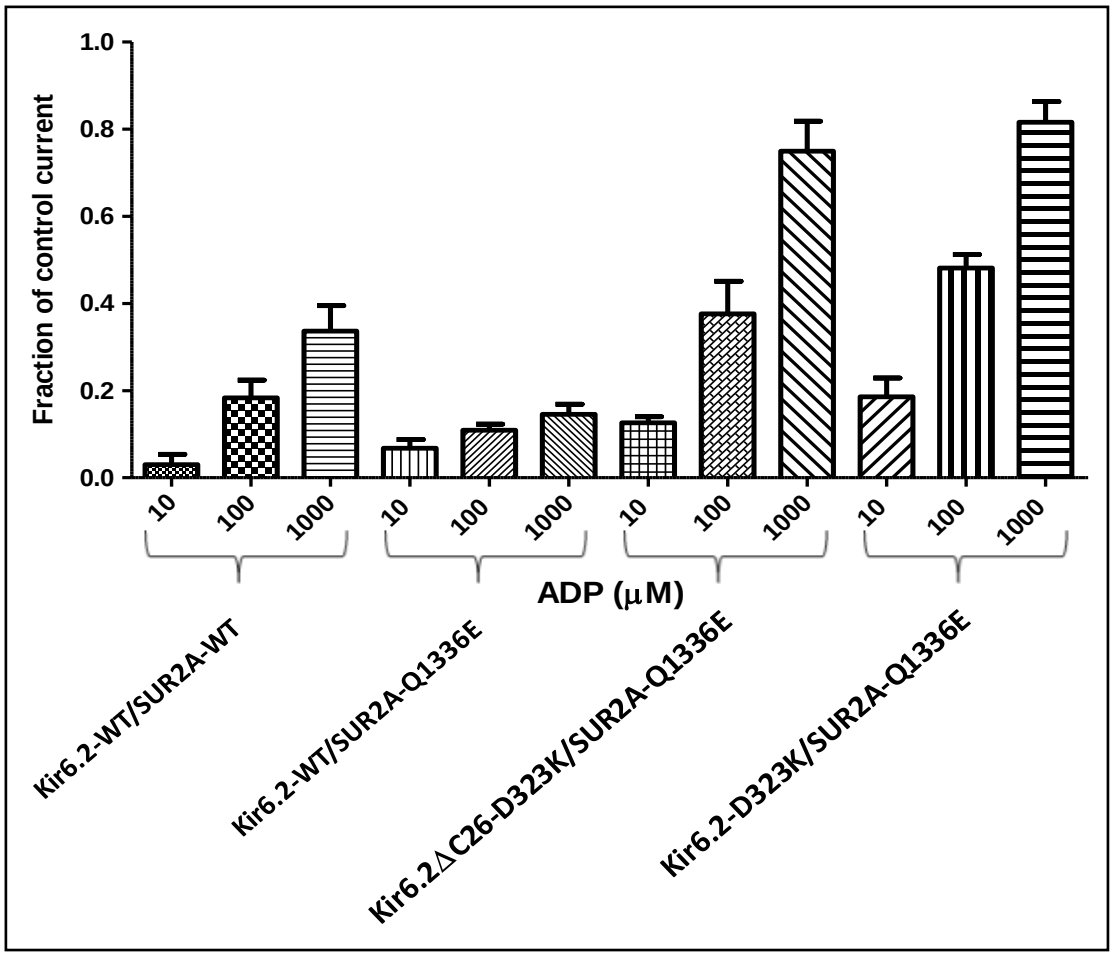

The inter-subunit Kir6.2 D323/SUR2A Q1336 salt bridge is involved in determining ADP sensitivity of Kir6.2/SUR2A channels.

The figures represents the summary results of excised inside-out patch clamp recording of wild type and different mutated subunit combination channels, 48-72 hrs after transfection from HEK-293 cells. To measure the ADP sensitivity, different concentrations of ADP were used to relieve the fraction of ATP-inhibited current. n = minimum 6 cells patches for each point and the statistical data analysis: $P \langle 0.0001$, one-way ANOVA and post test; Bonferroni with 95% confidence intervals. Fractional current means the data were normalized to the maximum current. Kir6.2 ΔC26 represents the truncated isoform of Kir6.2, in which the last 26 amino acids of the C-terminal were deleted.

Appendix D:

Abstracts, Posters

and

Press Release

Inter-subunit salt bridges communicate glibenclamide sensitivity to the ATP-sensitive potassium channel pore

Hussein N. Rubaiy, Richard D. Rainbow, Mohamed Al-Johi, David Lodwick and Robert I. Norman

Cardiovascular Sciences, University of Leicester, Leicester, UK

ATP-sensitive K^+ channels couple metabolic status to membrane potential in many tissues. They comprise subunit hetero-octamers of $Kir6_4/SUR_4$. A minimal Kir6.2 binding domain in SUR2A (residues 1294-1358, Rainbow et. al. Biochem. J. 2004; 379:173-181) was further refined to residues 1318-1337 by co-immunoprecipitation with Kir6.2 of chimaeras of SUR2A (1294-1358) containing non-interacting multi-drug resistance protein-1 (MRP1) sequence. Mutagenesis of charged residues in SUR2A, E1318R, K1322D or Q1336E, conserved in SUR1 but not MRP1, reduced co-immunoprecipitation. Co-immunoprecipitation of a maltose binding protein (MBP)-tagged SUR2A(1294-1358) polypeptide by chimaeras of Kir6.2/Kir2.1 identified the cognate binding domain in Kir6.2 (residues 315-390). Mutagenesis of charged residues in Kir6.2, D323K or K338E, conserved in Kir6.1 but not Kir2.1, was alone sufficient to significantly reduce co-immunoprecipitation of MBP-SUR2A (1294-1358). Single charge reversals in both subunits restored co-immunoprecipitation and identified putative salt bridges Kir6.2 D323/SUR2A K1322, Kir6.2 D323/SUR2A Q1336 and Kir6.2 K338/SUR2A E1318. Glibenclamide sensitivity of pinacidil-activated currents was reduced on charge reversal of single residues in either the Kir6.2 or SUR2A subunit. Near wild type glibenclamide sensitivity was restored by single charge reversal in both subunits of proposed salt bridges involving SUR2A E1318 and Q1336, establishing a novel inter-subunit interaction that transmits inhibitory information to the pore from antagonist binding to the SUR subunit.

Inter-subunit Salt Bridges Communicate Glibenclamide Sensitivity to the ATP-Sensitive Potassium Channel Pore

Hussein N. Rubaiy, Richard D. Rainbow, Mohamed Al-Johi, David Lodwick, Robert I. Norman

University of Leicester

Department of Cardiovascular Sciences, University of Leicester, Robert Kilpatrick Clinical Sciences Building, Leicester Royal Infirmary, Leicester LE2 7LX, U.K.

Introduction

ATP-sensitive potassium (K_{ATP}) channels are regulated by the ATP/ADP ratio and this unique property forms a link between cellular metabolism and membrane excitability in many tissues. K_{ATP} channels comprise subunit hetero-octamers of $Kir6_4/SUR_4$[1,2]. The aim of this study was to further characterise an intersubunit interaction[3] (SUR2A NBF2(1294-1358)/Kir6.2) involving cytoplasmic domains between these two heterologous subunits (Fig. 1).

Fig. 1. Subunit Structure of K_{ATP} Channels.

(A) K_{ATP} channels comprise hetero-octamers of four pore-forming Kir6 and four accessory SUR subunits. Inhibitory ATP binding occurs on the Kir6 subunits, while regulatory nucleotide and potassium channel drug binding is mediated by SUR subunits[2,4,5]. (B) Top view of $Kir6_4/SUR_4$ hetero-octamer.

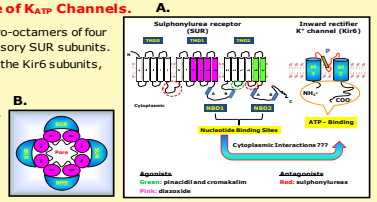

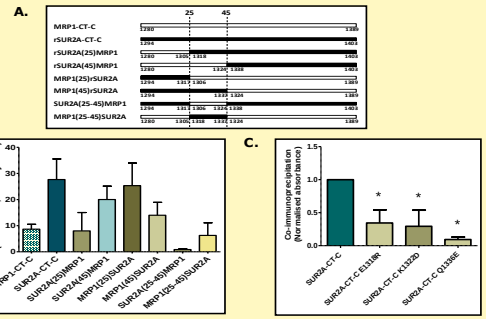

Fig.2. Characterization of SUR2A-NBD2(1294-1358) and Kir6.2 interaction. (A) Schematic representation of MRP1/SUR2A chimaeras. (B) Co-immunoprecipitation of maltose binding protein-tagged constructs with Kir6.2, suggest the amino acid sequence 1318-1337 of SUR2A to be the minimal interacting sequence for Kir6.2. (C) Three charged residues E1318, K1322 and Q1336, present in SUR2A but not in non-interacting MRP1, are key to the interaction, *p < 0.05.

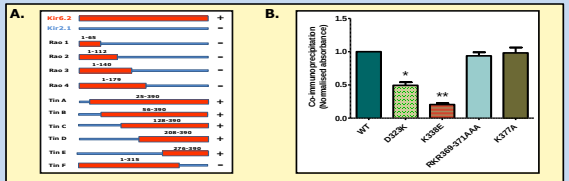

Fig. 3. Identification of Kir6.2 D323 and K338 as Residues Involved in Interaction with SUR2A(1294-1358). Co-immunoprecipitation of maltose binding protein-SUR2A(1294-1358) constructs with Kir6.2/2.1 chimaeras revealed the interaction domain on Kir6.2 to be located beyond residue 315 (data not shown). (B) Co-immunoprecipitation of wild type and mutant Kir6.2 in which conserved charged residues were mutated to equivalent residues in non-interacting Kir2.1 subunits. n = 5, *p<0.05, ** p<0.001.

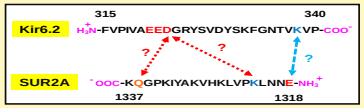

Fig. 4. Model Showing Hypothesized Interacting Charged Residues.

Linear sequences of the minimal interaction motifs between Kir6.2 and SUR2A showing predicted electrostatic interactions. It was hypothesized that single mutations in either subunit would disrupt, and double charge reversal mutants in Kir6.2 and SUR2A should restore, interaction and function.

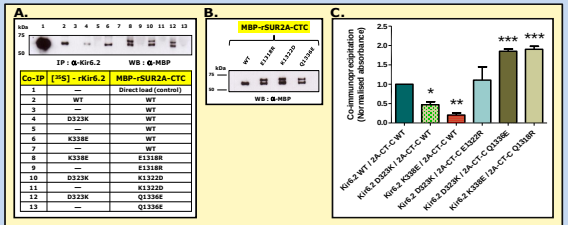

Fig. 5. Identification of Salt Bridges between Cytoplasmic Domains of Heterologous Subunits. (A) Co-immunoprecipitation of MBP-SUR2A(1294-1358) constructs in the absence (odd numbered lanes) and presence (even numbered lanes) of Kir6.2 subunits. (B) Western blot of expressed wild type and mutant MBP-SUR2A(1294-1358) constructs. (C) Pooled data showing restoration of co-immunoprecipitation on charge reversal in both subunits, n = 5, *p < 0.05, **p < 0.01, *** p < 0.0001.

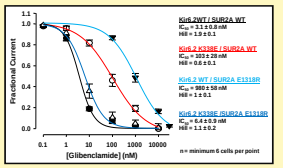

B.

Subunits		Glibenclamide (nM)			
Kir6.2	SUR2A	IC50	SE	Hill	SE
WT	WT	3.1	0.8	1.9	0.1
K338E	WT	103	28	0.6	0.1
WT	E1318R	980	58	1	0.1
K338E	E1318R	6.4	0.9	1.1	0.2
D323K	WT	Insensitive			
WT	K1322D	Current too small to record			
D323K	K1322D	Insensitive			
WT	Q1336E	50600	8400	0.93	0.13
D323K	Q1336E	4.7	0.3	2.2	0.2
WT	K1322D + Q1336E	Current too small to record			
D323K	K1322D + Q1336E	Insensitive			

Fig. 6. Kir6.2-K338/SUR2A-E1318 and Kir6.2-D323/SUR2A-Q1336 Salt Bridges Determine Glibenclamide Sensitivity of the K_{ATP} Channel Pore.

(A) Dose-response curves for current inhibition by glibenclamide. Single mutations in either subunit reduced sensitivity to antagonist, glibenclamide, in whole cell patch clamp, 48-72 hrs after transfection of HEK 293 cells with Kir6.2 and SUR2A. On co-expression of targeted charge reversal mutants in both Kir6.2 and SUR2A, the IC_{50} was restored close to that of wild-type (WT). (B) IC_{50} values.

Conclusions

Co-immunoprecipitation of chimaeric and mutant MBP-SUR2A(1294-1358) constructs with wild type, chimaeric and mutated Kir6.2 subunits identified three putative inter-subunit salt bridges (Fig. 5). Glibenclamide sensitivity of pinacidil-activated currents was reduced on charge reversal of single residues in either the Kir6.2 or SUR2A subunit. Near wild type glibenclamide sensitivity was restored by single charge reversal in both subunits of proposed salt bridges involving SUR2A E1318 and Q1336, establishing a novel inter-subunit interaction that transmits inhibitory information to the pore from antagonist binding to the SUR subunit. This interface lies just downstream of three residues in SUR2A, E1305, I1310 and L1313, which when mutated to those in non-interacting MRP1, were sufficient to remove the pinacidil-stimulated channel activation[6].

References

1. Clement JP. et. al. Neuron 1997; Vol. 18, 827–838
2. Shyng S-L. and Nichols CG. The J. General Physiology 1997; 110, 655-664.
3. Rainbow RD et. al. Biochemical Journal 2004; 379:173-181
4. Aguilar-Bryan L. et. al. Science. 1995;268:423– 426.
5. Ashcroft FM. Neuroscience 1998; 11: 97-118
6. Dupuis JP. et. al. The Journal of Physiology 2008; 586, 3075-3085.

Acknowledgements:

- British Heart Foundation
- PhD Studentship funded by TH Wathes

British Heart Foundation

Hussein N. Rubaiy: Tel, +44 (0)116 252 3191; e-mail, hnr1@le.ac.uk

Sulphonylurea Receptors Regulate Kir6.2 Subunits Allosterically via a Salt Bridge in Cardiac K_{ATP} Channels

H. N. Rubaiy, R. D. Rainbow, D. Lodwick, R. I. Norman

Department of Cardiovascular Sciences, University of Leicester, Robert Kilpatrick Clinical Sciences Building,

Leicester Royal Infirmary, Leicester LE2 7LX, U.K.

ATP sensitive potassium (K_{ATP}) channels play important roles in many tissues, coupling metabolic status to membrane potential. In heart, they comprise subunit hetero-octamers of $Kir6.2_4/SUR2A_4$.

A minimal sequence (residues 1294-1358) in nucleotide binding domain-2 of SUR2A has been identified previously by us to bind Kir6.2 (Rainbow et. al. Biochem. J. 2004;379:173-181). Co-immunoprecipitation of chimaeras of Kir6.2/Kir2.1 with maltose binding protein (MBP)-tagged SUR2A (1294-1358) fragments identified the cognate binding domain in Kir6.2 (residues 315-390). Mutagenesis of charged residues in Kir6.2, D323K and K338E, conserved in Kir6.1 but not Kir2.1, was alone sufficient to significantly reduce co-immunoprecipitation of MBP-SUR2A (1294-1358) by ~50 % ($P<0.0009$) and ~80% ($P<0.0001$), respectively. Similarly, co-immunoprecipitation with Kir6.2 of chimaeras of SUR2A (1294-1358) containing multi-drug resistance protein-1 (MRP1) sequence further refined the SUR2A binding motif to residues 1318-1337. Mutagenesis of charged residues in SUR2A, E1318R, K1322D and Q1336E, conserved in SUR1 but not MRP1, reduced co-immunoprecipitation.

Whole cell patch clamp of Kir6.2 K338E/SUR2A WT channels 48-72 h after transfection in HEK 293 cells revealed increased sensitivity to agonist, pinacidil (EC_{50} = 4.5 ± 0.3 versus 39.6 ± 13 µM with Kir6.2 WT), and reduced sensitivity to antagonist, glibenclamide (IC_{50} = 103 ± 28 versus 3.1 ± 0.8 nM with Kir6.2 WT). Expression of the double mutant Kir6.2 K338E/SUR2A E1318R restored wild-type properties (EC_{50} pinacidil = 46.7 ± 4.9 µM; IC_{50} glibenclamide = 6.4 ± 0.9 nM). Similar results were observed for the equivalent residue on Kir6.1 R347. Furthermore, inside-out patch clamp

revealed that the IC_{50} for ATP was unaffected in Kir6.2K338E/SUR2A channels (27.5 ± 2.0 versus 23.8 ± 1.7 μM with Kir6.2 WT, P>0.5).

Together, these data provide evidence for the transmission of allosteric information via a salt bridge between SUR2AE1318 and Kir6.2K338 in cardiac K_{ATP} channels, while ATP-sensitivity remains unaltered.

University of Leicester

Sulphonylurea Receptors Regulate Kir6.2 Subunits Allosterically via a Salt Bridge in Cardiac K_{ATP} Channels

Hussein N. Rubaiy, Richard D. Rainbow, David Lodwick, Robert I. Norman

Department of Cardiovascular Sciences, University of Leicester, Robert Kilpatrick Clinical Sciences Building, Leicester Royal Infirmary, Leicester LE2 7LX, U.K.

Introduction

ATP-sensitive potassium (K_{ATP}) channels are ubiquitously expressed and link metabolic state to electrical excitability. These channels are hetero-octameric in structure comprising, in cardiac ventricular tissue, $Kir6.2_4/SUR2A_4$[1,2].

The aim of this study was to further characterize an intersubunit interaction[3] (SUR2A NBD2(1294-1358)/Kir6.2) involving cytoplasmic domains between these two heterologous subunits (Fig. 1).

Fig. 1. Subunit Structure of K_{ATP} Channels. (A) K_{ATP} channels comprise hetero-octamers of four pore-forming Kir6 and four accessory SUR subunits. Inhibitory ATP binding occurs on the Kir6 subunits, while regulatory nucleotide and potassium channel drug binding is mediated by SUR subunits[2,4,5]. (B) Top view of $Kir6_4/SUR_4$ hetero-octamer.

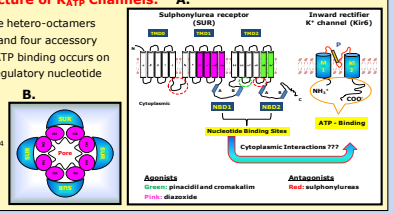

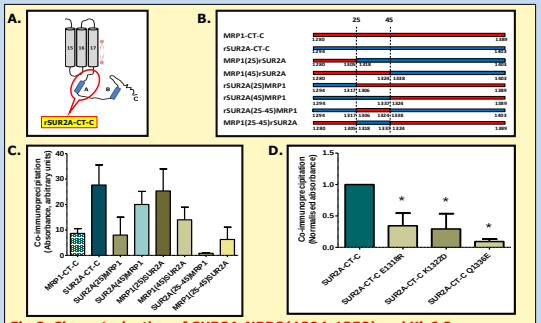

Fig.2. Characterization of SUR2A-NBD2(1294-1358) and Kir6.2 interaction. Schematic representation of rSUR2A-CT-C fragment (A) and MRP1/SUR2A chimeras (B). (C) Co-immunoprecipitation of maltose binding protein-tagged chimeric constructs with Kir6.2, suggest the amino acid sequence 1318-1337 of SUR2A to be the minimal interacting sequence with Kir6.2. (D) Three charged residues, E1318, K1322 and Q1336, present in SUR2A but not in non-interacting MRP1, are key to the interaction, *p < 0.05.

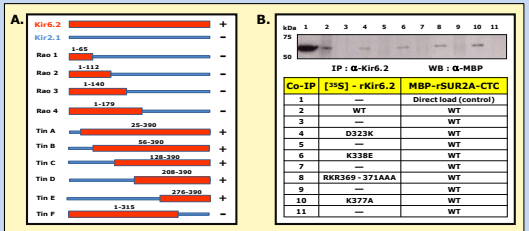

Co-IP	[35S] - rKir6.2	MBP-rSUR2A-CTC
1	—	Direct load (control)
2	WT	WT
3	—	WT
4	D323K	WT
5	—	WT
6	K338E	WT
7	—	WT
8	RKR369-371AAA	WT
9	—	WT
10	K377A	WT
11	—	WT

Fig. 3. Identification of Kir6.2 D323 and K338 as Residues Involved in Interaction with SUR2A(1294-1358). Co-immunoprecipitation of maltose binding protein-SUR2A(1294-1358) constructs with Kir6.2/2.1 chimeras (A) revealed the interaction domain on Kir6.2 to be located beyond residue 315 (data not shown). (B) Co-immunoprecipitation of wild type and mutant Kir6.2 in which conserved charged residues were mutated to equivalent residues in non-interacting Kir2.1 subunits. n = 5, *p<0.05, ** p<0.001 (C).

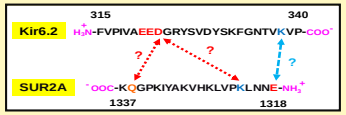

Fig. 4. Model Showing Hypothesized Interacting Charged Residues. Linear sequences of the minimal interaction motifs between Kir6.2 and SUR2A showing predicted electrostatic interactions. It was hypothesized that single mutations in either subunit would disrupt, and double charge reversal mutants in Kir6.2 and SUR2A should restore, interaction and function.

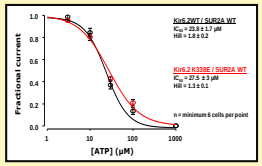

Fig. 5. Kir6.2 K338 is not Involved in Determining ATP Sensitivity of K_{ATP} Channels. Excised inside-out patch clamp recording of wild type and Kir6.2(K338)/SUR2A channels 48-72 hrs after transfection of HEK 293 cells. ATP concentration-response curves show that ATP sensitivity of the Kir6.2(K338)/SUR2A mutant channel was essentially unmodified.

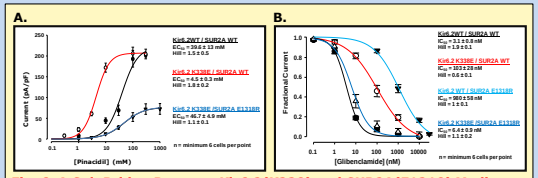

Fig. 6. A Salt Bridge Between Kir6.2(K338) and SUR2A(E1318) Mediates Allosteric Communication in Cardiac K_{ATP} Channels. Concentration-response curves for current activation by pinacidil and inhibition by glibenclamide of cardiac K_{ATP} channels. Whole cell patch clamp of Kir6.2(K338E)/SUR2A WT channels 48-72 hrs after transfection in HEK 293 cells revealed increased sensitivity to agonist, pinacidil (A), and reduced sensitivity to antagonist, glibenclamide (B). Expression of the double mutant Kir6.2(K338E)/SUR2A(E1318R) restored wild-type properties (A and B). Although the double swap mutant did not functionally express to the same density as the WT channel, the proportion of pinacidil activated current was similar when compared to total current activated by metabolic poisoning in both WT and double mutant channels. Similar results were obtained for the equivalent residue on Kir6.1(R347).

Conclusions

Co-immunoprecipitation of SUR2A-MRP1 chimeras and mutant MBP-SUR2A(1294-1358) constructs with wild type, chimeric and mutated Kir6.2 subunits identified three putative inter-subunit salt bridges (Fig. 4). The data presented provide evidence that the transmission of allosteric information between heterologous K_{ATP} channel subunits is dependent on a salt bridge between SUR2A(E1318) and Kir6.2(K338) in cardiac K_{ATP} channels, while ATP-sensitivity remains unaltered. SUR2A(E1318) lies just downstream of three residues in SUR2A, E1305, I1310 and L1313, which when mutated to those in non-interacting MRP1, were sufficient to remove the pinacidil-stimulated channel activation indicating a more extensive interacting surface in SUR2A[6].

References

1. Clement JP. et. al. Neuron 1997; Vol. 18, 827–838
2. Shyng S-L. and Nichols CG. The J. General Physiology 1997; 110, 655-664.
3. Rainbow RD et. al. Biochemical Journal 2004; 379:173-181
4. Aguilar-Bryan L. et. al. Science. 1995;268:423– 426.
5. Ashcroft FM. Neuroscience 1998; 11: 97-118
6. Dupuis JP. et. al. The Journal of Physiology 2008; 586, 3075-3085.

Acknowledgements:

- British Heart Foundation
- PhD Studentship funded by TH Wathes

British Heart Foundation

Hussein N. Rubaiy: Tel, +44 (0)116 252 3191; e-mail, hnr1@le.ac.uk

Dissecting Mechanisms of Information Transfer within a Cardiac Potassium Channel

Hussein N. Rubaiy, David Lodwick, Richard D. Rainbow, Robert I. Norman

Department of Cardiovascular Sciences, University of Leicester, Robert Kilpatrick Clinical Sciences Building,

Leicester Royal Infirmary, Leicester LE2 7LX, U.K.

Ion channels are pore-forming proteins, which are located on the surface of all living cells. They make connection between inside and outside environments by selectively allowing ions (charged metal atoms, e.g. potassium ion (K^+)) to move through the channel pore. Opening and closing of ion channels is involved in vital electrical signaling processes, e.g. heart rhythm and cell-to-cell communication in the nervous system, and without them life would be impossible.

This study focused on one channel type that acts as an energy sensor in cells by monitoring the molecular energy currency (ATP). Activity of the channel translates falling energy levels into reduced electrical excitability in the cell. These channels, known as ATP-sensitive potassium channels, are a major drug target for the treatment of Type 2 diabetes.

K_{ATP} channels comprise of two different protein components, a pore-forming protein and a second accessory protein, which regulates the channel. Both proteins are required to provide sensitive monitoring of energy levels and, therefore, there needs to be efficient molecular communications between them.

Cross-talk between these two partner proteins regulates the opening or closure of the channel pore. The aim of this study was to identify and characterize regions in these proteins, which are responsible for information transfer between them. This study used molecular fishing techniques in mixtures of unmodified and modified channel pieces to dissect out structural features of the interaction site between the partners. Structural features of the partners were then charged by genetic mutation and the function of the channel was measured and analysed.

Results of the study showed that cross-talk between the channel proteins depends on at least three charge-charge bonds between them. This information contributes to the understanding of normal channel function and also to the action of antidiabetic drugs that act on these channels.

University of Leicester

PhD Studentship funded: by TH Wathes

Dissecting Mechanisms of Information Transfer within a Cardiac Potassium Channel

Hussein N. Rubaiy

Supervisor: Dr. R.I. Norman, Co-supervisors: Dr. D. Lodwick and Dr. R.D. Rainbow

Department of Cardiovascular Sciences, Leicester Royal Infirmary

Introduction

Ion channels are pore-forming proteins, which are located on the surface of all living cells. They are involved in vital processes, such as heart rhythm and nerve impulse conduction. This study focuses on ATP-sensitive potassium (K_{ATP}) channels that have important functions in tissue protection and are a major drug target for Type 2 Diabetes[1,2,3] (Fig. 1).

Aim

Cardiac K_{ATP} channels comprise of two different proteins, a pore-forming Kir6.2 and an accessory SUR2A, which regulates the channel[1,2]. The aim of this study was to understand the cross-talk between these two partners, which regulates the opening or closure of the channel pore (Fig. 2C and D).

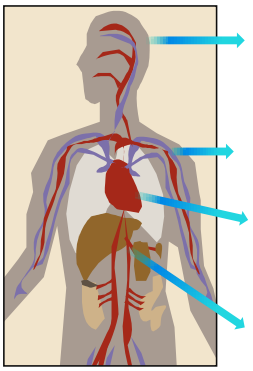

Fig. 1. K_{ATP} Channels in the Human Body in Health and Disease.

Results

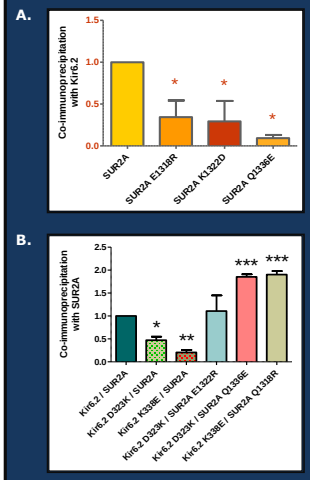

Fig. 3. Identification of Charged Amino Acids, which are Key to the Assembly of Cardiac K_{ATP} Channels.

Mutation and biochemical interaction studies between the pore-forming Kir6.2 and the regulatory SUR2A revealed three charged amino acids E1318, K1322 and Q1336 in SUR2A (A) and two amino acids D323 and K338 in Kir6.2 along with charge-charge bonds that are key for the interaction between these two different proteins (B). Reduced co-immunoprecipitation indicates reduced interaction.

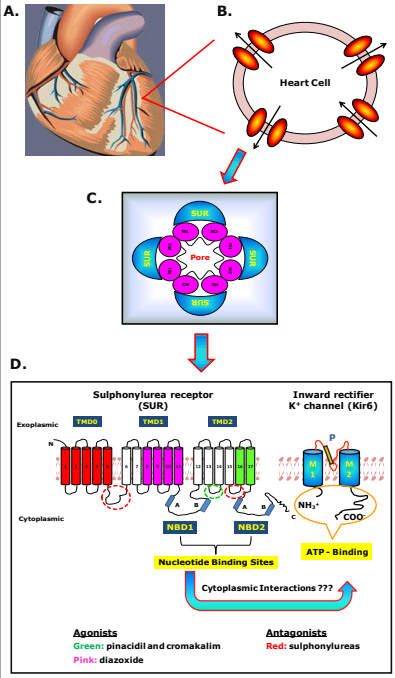

Fig. 2. Functional K_{ATP} Channel Structure in Heart Cells. Diagrammatic representation (top view) of the assembly of the two constituent protein components ($Kir6_4/SUR_4$) to form a functional K_{ATP} channel (panel C) in heart cells (panel A and B). Regulatory binding sites on K_{ATP} channel components that control the channel pore (D).

Results

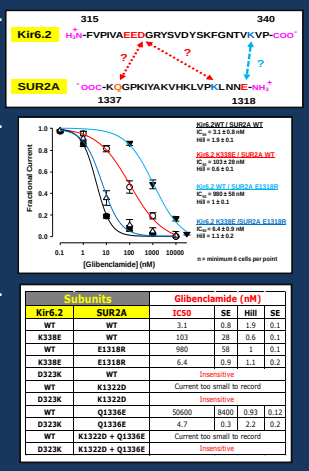

Subunits		Glibenclamide (nM)			
Kir6.2	SUR2A	IC50	SE	Hill	SE
WT	WT	3.1	0.8	1.9	0.1
K338E	WT	103	28	0.6	0.1
WT	E1318R	980	58	1	0.1
K338E	E1318R	6.4	0.9	1.1	0.2
D323K	WT	Insensitive			
WT	K1322D	Current too small to record			
D323K	K1322D	Insensitive			
WT	Q1336E	50600	8400	0.93	0.12
D323K	Q1336E	4.7	0.3	2.2	0.2
WT	K1322D + Q1336E	Current too small to record			
D323K	K1322D + Q1336E	Insensitive			

Fig. 4. Cross-talk between the Channel Proteins depends on Three Charge-charge Bonds.

A) Model showing the three charge-charge bonds between Kir6.2 and SUR2A subunits. B) Dose-response curve for channel inhibitor glibenclamide. Single mutations on both proteins disrupt the effect of the drug and charge reversal mutations in both proteins restore the effect confirming that the charge-charge bond mediates information transfer. C) The half maximal inhibitory concentration (IC_{50}) values.

Conclusions

This study identified three charge-charge interactions between component proteins (Kir6.2 and SUR2A) in the K_{ATP} channel that play a role in permitting information transfer between component parts (Fig. 4A).

General Public Benefits

This new information on channel function may contribute to the design of novel and more effective drugs to change the activity of this channel for the treatment of diabetes, high blood pressure and/or as a cardioprotective agent in heart attack or cardiac surgery.

References

1. Clement JP. et. al. Neuron 1997; Vol. 18, 827–838
2. Aguilar-Bryan L. et. al. Science. 1995;268:423– 426.
3. Ashcroft FM. Neuroscience 1998; 11: 97-118

Hussein N. Rubaiy: Tel, +44 (0)116 252 3191; e-mail, hnr1@le.ac.uk

New treatment hope for diabetes and cardiovascular diseases

New research at the University of Leicester to contribute to more effective drug design

Issued by University of Leicester Press Office on 03 June 2011

A cutting-edge research project at the University of Leicester is aiming to improve the treatment of diabetes and cardiovascular diseases.

Figures show that cardiovascular diseases remain the number one killer in Western countries, particularly heart attacks, and most recently a warning has been issued by the World Health Organization (WHO) that Type 2 diabetes, the most common form of diabetes, will increase by as much as 80% in some regions throughout the world in the near future.

A PhD student with the Department of Cardiovascular Sciences, Hussein Rubaiy, has uncovered new information from his study, which has the potential to contribute to the design of novel and more effective drugs for the treatment of diabetes and cardiovascular diseases, e.g. high blood pressure and heart attack.

In his study, Rubaiy analysed the mechanisms of a cardiac potassium channel and its component parts, which play an important role in such vital processes as heart rhythm and tissue protection. His work has thrown more light on how the channel works and how information from drug interaction is converted into modified function.

Rubaiy commented:

"This research provides important foundations of understanding on which to build future research and development of more targeted drug design. I am very optimistic that my detailed findings will find application in the pharmaceutical industry in the design or improvement of drugs for the treatment of Type 2 diabetes and cardiovascular diseases."

Dr Bob Norman, Senior Lecturer at the Department of Cardiovascular Sciences, added:

"Modulation of the properties of the channel has wider potential as a target for therapies to protect tissues from damage resulting from low blood flow, as in heart attack or cardiac surgery, and possibly as a treatment for high blood pressure. Hussein Rubaiy's findings add significantly to our understanding of how these channels work and hopefully should contribute in the future to the more rational design of drugs to modify the properties of this important drug target."

- This research is being presented at the Festival of Postgraduate Research on Thursday, 16 June. The annual one-day exhibition of postgraduate research offers organisations and the public the opportunity to meet the next generation of innovators and cutting-edge researchers. More than 50 University of Leicester students will explain the real world implications of their research in an

engaging and accessible way. The event is open to the public and free to attend. More information at http://www2.le.ac.uk/offices/ssds/sd/pgrd/fpgr.

Note to Newsdesk:

For more information/interviews/pictures and filming opportunities contact **Hussein N. Rubaiy** on: Tel: 0116 252 3191; Fax: 0116 252 3173; e-mail: hnr1@le.ac.uk

Violetta Mertins

References

Aguilar-Bryan, L. and Bryan, J. (1999), 'Molecular biology of adenosine triphosphate-sensitive potassium channels', *Endocr Rev,* 20 (2), 101-35.

Aguilar-Bryan, L., Clement, J. P. th, Gonzalez, G., Kunjilwar, K., Babenko, A., and Bryan, J. (1998), 'Toward understanding the assembly and structure of KATP channels', *Physiol Rev,* 78 (1), 227-45.

Aidley, David J., Stanfield, Peter R. (1996), *Ion channels: Molecules in action* (Cambridge University Press).

al-Johi, Mohammed (2005), 'Characterization of interaction sites between Kir6.0 and SUR subunits of ATP-sensitive potassium (KATP) channels', (University of Leicester).

Antcliff, J. F., Haider, S., Proks, P., Sansom, M. S., and Ashcroft, F. M. (2005), 'Functional analysis of a structural model of the ATP-binding site of the KATP channel Kir6.2 subunit', *EMBO J,* 24 (2), 229-39.

Arena, J. P. and Kass, R. S. (1989), 'Activation of ATP-sensitive K channels in heart cells by pinacidil: dependence on ATP', *Am J Physiol,* 257 (6 Pt 2), H2092-6.

Ashcroft, F. M. (2005), 'ATP-sensitive potassium channelopathies: focus on insulin secretion', *J Clin Invest,* 115 (8), 2047-58.

--- (2010), 'New uses for old drugs: neonatal diabetes and sulphonylureas', *Cell Metab,* 11 (3), 179-81.

Ashcroft, F. M. and Gribble, F. M. (1998), 'Correlating structure and function in ATP-sensitive K+ channels', *Trends Neurosci,* 21 (7), 288-94.

Ashcroft, S. J. and Ashcroft, F. M. (1990), 'Properties and functions of ATP-sensitive K-channels', *Cell Signal,* 2 (3), 197-214.

Ashford, M. L., Boden, P. R., and Treherne, J. M. (1990), 'Tolbutamide excites rat glucoreceptive ventromedial hypothalamic neurones by indirect inhibition of ATP-K+ channels', *Br J Pharmacol,* 101 (3), 531-40.

Babenko, A. P. and Bryan, J. (2003), 'Sur domains that associate with and gate KATP pores define a novel gatekeeper', *J Biol Chem*, 278 (43), 41577-80.

Babenko, A. P., Aguilar-Bryan, L., and Bryan, J. (1998), 'A view of sur/KIR6.X, KATP channels', *Annu Rev Physiol*, 60, 667-87.

Babenko, A. P., Gonzalez, G., and Bryan, J. (2000), 'Pharmaco-topology of sulfonylurea receptors. Separate domains of the regulatory subunits of K(ATP) channel isoforms are required for selective interaction with K(+) channel openers', *J Biol Chem*, 275 (2), 717-20.

Baukrowitz, T., Schulte, U., Oliver, D., Herlitze, S., Krauter, T., Tucker, S. J., Ruppersberg, J. P., and Fakler, B. (1998), 'PIP2 and PIP as determinants for ATP inhibition of KATP channels', *Science*, 282 (5391), 1141-4.

Bernardi, H., De Weille, J. R., Epelbaum, J., Mourre, C., Amoroso, S., Slama, A., Fosset, M., and Lazdunski, M. (1993), 'ATP-modulated K+ channels sensitive to antidiabetic sulfonylureas are present in adenohypophysis and are involved in growth hormone release', *Proc Natl Acad Sci U S A*, 90 (4), 1340-4.

Bernardo, N. L., D'Angelo, M., Okubo, S., Joy, A., and Kukreja, R. C. (1999), 'Delayed ischemic preconditioning is mediated by opening of ATP-sensitive potassium channels in the rabbit heart', *Am J Physiol*, 276 (4 Pt 2), H1323-30.

Bichet, D., Haass, F. A., and Jan, L. Y. (2003), 'Merging functional studies with structures of inward-rectifier K(+) channels', *Nat Rev Neurosci*, 4 (12), 957-67.

Billman, G. E. (2008), 'The cardiac sarcolemmal ATP-sensitive potassium channel as a novel target for anti-arrhythmic therapy', *Pharmacol Ther*, 120 (1), 54-70.

Brayden, J. E. (2002), 'Functional roles of KATP channels in vascular smooth muscle', *Clin Exp Pharmacol Physiol*, 29 (4), 312-6.

Brejc, K., van Dijk, W. J., Klaassen, R. V., Schuurmans, M., van Der Oost, J., Smit, A. B., and Sixma, T. K. (2001), 'Crystal structure of an ACh-binding protein reveals the ligand-binding domain of nicotinic receptors', *Nature*, 411 (6835), 269-76.

Burke, M. A., Mutharasan, R. K., and Ardehali, H. (2008), 'The sulfonylurea receptor, an atypical ATP-binding cassette protein, and its regulation of the KATP channel', *Circ Res,* 102 (2), 164-76.

Carroll, R. and Yellon, D. M. (1999), 'Myocardial adaptation to ischaemia--the preconditioning phenomenon', *Int J Cardiol,* 68 Suppl 1, S93-101.

Cartier, E. A., Conti, L. R., Vandenberg, C. A., and Shyng, S. L. (2001), 'Defective trafficking and function of KATP channels caused by a sulfonylurea receptor 1 mutation associated with persistent hyperinsulinemic hypoglycemia of infancy', *Proc Natl Acad Sci U S A,* 98 (5), 2882-7.

Chien, M., Morozova, I., Shi, S., Sheng, H., Chen, J., Gomez, S. M., Asamani, G., Hill, K., Nuara, J., Feder, M., Rineer, J., Greenberg, J. J., Steshenko, V., Park, S. H., Zhao, B., Teplitskaya, E., Edwards, J. R., Pampou, S., Georghiou, A., Chou, I. C., Iannuccilli, W., Ulz, M. E., Kim, D. H., Geringer-Sameth, A., Goldsberry, C., Morozov, P., Fischer, S. G., Segal, G., Qu, X., Rzhetsky, A., Zhang, P., Cayanis, E., De Jong, P. J., Ju, J., Kalachikov, S., Shuman, H. A., and Russo, J. J. (2004), 'The genomic sequence of the accidental pathogen Legionella pneumophila', *Science,* 305 (5692), 1966-8.

Chutkow, W. A., Samuel, V., Hansen, P. A., Pu, J., Valdivia, C. R., Makielski, J. C., and Burant, C. F. (2001), 'Disruption of Sur2-containing K(ATP) channels enhances insulin-stimulated glucose uptake in skeletal muscle', *Proc Natl Acad Sci U S A,* 98 (20), 11760-4.

Clement, J. P. th, Kunjilwar, K., Gonzalez, G., Schwanstecher, M., Panten, U., Aguilar-Bryan, L., and Bryan, J. (1997), 'Association and stoichiometry of K(ATP) channel subunits', *Neuron,* 18 (5), 827-38.

Cole, K S and Curtis, H J (1938), 'Electrical Impedance of Nerve during Activity', *Nature,* 142, 209-10.

Cole, K. S. (1949), 'Dynamic electrical characteristics of the squid axon membrane', *Arch. Sci. physiol,* 3, 253-8.

Cole, W. C., McPherson, C. D., and Sontag, D. (1991), 'ATP-regulated K+ channels protect the myocardium against ischemia/reperfusion damage', *Circ Res,* 69 (3), 571-81.

Cook, D. L. and Hales, C. N. (1984), 'Intracellular ATP directly blocks K+ channels in pancreatic B-cells', *Nature,* 311 (5983), 271-3.

Craig, T. J., Ashcroft, F. M., and Proks, P. (2008), 'How ATP inhibits the open K(ATP) channel', *J Gen Physiol,* 132 (1), 131-44.

Cukras, C. A., Jeliazkova, I., and Nichols, C. G. (2002a), 'Structural and functional determinants of conserved lipid interaction domains of inward rectifying Kir6.2 channels', *J Gen Physiol,* 119 (6), 581-91.

--- (2002b), 'The role of NH2-terminal positive charges in the activity of inward rectifier KATP channels', *J Gen Physiol,* 120 (3), 437-46.

Davies, N. W. (1990), 'Modulation of ATP-sensitive K+ channels in skeletal muscle by intracellular protons', *Nature,* 343 (6256), 375-7.

Dean, M., Rzhetsky, A., and Allikmets, R. (2001), 'The human ATP-binding cassette (ABC) transporter superfamily', *Genome Res,* 11 (7), 1156-66.

Dekelbab, B. H. and Sperling, M. A. (2006), 'Recent advances in hyperinsulinemic hypoglycemia of infancy', *Acta Paediatr,* 95 (10), 1157-64.

Deutsch, N., Klitzner, T. S., Lamp, S. T., and Weiss, J. N. (1991), 'Activation of cardiac ATP-sensitive K+ current during hypoxia: correlation with tissue ATP levels', *Am J Physiol,* 261 (3 Pt 2), H671-6.

Doupnik, C. A., Davidson, N., and Lester, H. A. (1995), 'The inward rectifier potassium channel family', *Curr Opin Neurobiol,* 5 (3), 268-77.

Downey, J. M. and Cohen, M. V. (1995), 'Signal transduction in ischemic preconditioning', *Z Kardiol,* 84 Suppl 4, 77-86.

Doyle, D. A., Morais Cabral, J., Pfuetzner, R. A., Kuo, A., Gulbis, J. M., Cohen, S. L., Chait, B. T., and MacKinnon, R. (1998), 'The structure of the potassium

channel: molecular basis of K+ conduction and selectivity', *Science*, 280 (5360), 69-77.

Drain, P., Li, L., and Wang, J. (1998), 'KATP channel inhibition by ATP requires distinct functional domains of the cytoplasmic C terminus of the pore-forming subunit', *Proc Natl Acad Sci U S A*, 95 (23), 13953-8.

Dunne, M. J., Kane, C., Shepherd, R. M., Sanchez, J. A., James, R. F., Johnson, P. R., Aynsley-Green, A., Lu, S., Clement, J. P. th, Lindley, K. J., Seino, S., and Aguilar-Bryan, L. (1997), 'Familial persistent hyperinsulinemic hypoglycemia of infancy and mutations in the sulfonylurea receptor', *N Engl J Med*, 336 (10), 703-6.

Dupuis, J. P., Revilloud, J., Moreau, C. J., and Vivaudou, M. (2008), 'Three C-terminal residues from the sulphonylurea receptor contribute to the functional coupling between the K(ATP) channel subunits SUR2A and Kir6.2', *J Physiol*, 586 (13), 3075-85.

Edwards, G., Ibbotson, T., and Weston, A. H. (1993), 'Levcromakalim may induce a voltage-independent K-current in rat portal veins by modifying the gating properties of the delayed rectifier', *Br J Pharmacol*, 110 (3), 1037-48.

Enkvetchakul, D., Loussouarn, G., Makhina, E., and Nichols, C. G. (2001), 'ATP interaction with the open state of the K(ATP) channel', *Biophys J*, 80 (2), 719-28.

Enkvetchakul, D., Loussouarn, G., Makhina, E., Shyng, S. L., and Nichols, C. G. (2000), 'The kinetic and physical basis of K(ATP) channel gating: toward a unified molecular understanding', *Biophys J*, 78 (5), 2334-48.

Fan, Z. and Makielski, J. C. (1997), 'Anionic phospholipids activate ATP-sensitive potassium channels', *J Biol Chem*, 272 (9), 5388-95.

--- (1999), 'Phosphoinositides decrease ATP sensitivity of the cardiac ATP-sensitive K(+) channel. A molecular probe for the mechanism of ATP-sensitive inhibition', *J Gen Physiol*, 114 (2), 251-69.

Findlay, I. (1987), 'The effects of magnesium upon adenosine triphosphate-sensitive potassium channels in a rat insulin-secreting cell line', *J Physiol,* 391, 611-29.

--- (1994), 'The ATP sensitive potassium channel of cardiac muscle and action potential shortening during metabolic stress', *Cardiovasc Res,* 28 (6), 760-1.

Furukawa, T., Virag, L., Furukawa, N., Sawanobori, T., and Hiraoka, M. (1994), 'Mechanism for reactivation of the ATP-sensitive K+ channel by MgATP complexes in guinea-pig ventricular myocytes', *J Physiol,* 479 (Pt 1), 95-107.

Gabrielsson, B. G., Karlsson, A. C., Lonn, M., Olofsson, L. E., Johansson, J. M., Torgerson, J. S., Sjostrom, L., Carlsson, B., Eden, S., and Carlsson, L. M. (2004), 'Molecular characterization of a local sulfonylurea system in human adipose tissue', *Mol Cell Biochem,* 258 (1-2), 65-71.

Garlid, K. D., Paucek, P., Yarov-Yarovoy, V., Murray, H. N., Darbenzio, R. B., D'Alonzo, A. J., Lodge, N. J., Smith, M. A., and Grover, G. J. (1997), 'Cardioprotective effect of diazoxide and its interaction with mitochondrial ATP-sensitive K+ channels. Possible mechanism of cardioprotection', *Circ Res,* 81 (6), 1072-82.

Giblin, J. P., Leaney, J. L., and Tinker, A. (1999), 'The molecular assembly of ATP-sensitive potassium channels. Determinants on the pore forming subunit', *J Biol Chem,* 274 (32), 22652-9.

Gloyn, A. L., Pearson, E. R., Antcliff, J. F., Proks, P., Bruining, G. J., Slingerland, A. S., Howard, N., Srinivasan, S., Silva, J. M., Molnes, J., Edghill, E. L., Frayling, T. M., Temple, I. K., Mackay, D., Shield, J. P., Sumnik, Z., van Rhijn, A., Wales, J. K., Clark, P., Gorman, S., Aisenberg, J., Ellard, S., Njolstad, P. R., Ashcroft, F. M., and Hattersley, A. T. (2004), 'Activating mutations in the gene encoding the ATP-sensitive potassium-channel subunit Kir6.2 and permanent neonatal diabetes', *N Engl J Med,* 350 (18), 1838-49.

Gopalakrishnan, S. M., Chen, C., and Lokhandwala, M. F. (1993), 'Identification of alpha 1-adrenoceptor subtypes in rat renal proximal tubules', *Eur J Pharmacol,* 250 (3), 469-72.

Gribble, F. M. and Ashcroft, F. M. (1999), 'Differential sensitivity of beta-cell and extrapancreatic K(ATP) channels to gliclazide', *Diabetologia,* 42 (7), 845-8.

Gribble, F. M. and Reimann, F. (2002), 'Pharmacological modulation of K(ATP) channels', *Biochem Soc Trans,* 30 (2), 333-9.

Gribble, F. M., Tucker, S. J., and Ashcroft, F. M. (1997), 'The interaction of nucleotides with the tolbutamide block of cloned ATP-sensitive K+ channel currents expressed in Xenopus oocytes: a reinterpretation', *J Physiol,* 504 (Pt 1), 35-45.

Gribble, F. M., Reimann, F., Ashfield, R., and Ashcroft, F. M. (2000), 'Nucleotide modulation of pinacidil stimulation of the cloned K(ATP) channel Kir6.2/SUR2A', *Mol Pharmacol,* 57 (6), 1256-61.

Gross, G. J. and Fryer, R. M. (1999), 'Sarcolemmal versus mitochondrial ATP-sensitive K+ channels and myocardial preconditioning', *Circ Res,* 84 (9), 973-9.

Grover, G. J., D'Alonzo, A. J., Parham, C. S., and Darbenzio, R. B. (1995), 'Cardioprotection with the KATP opener cromakalim is not correlated with ischemic myocardial action potential duration', *J Cardiovasc Pharmacol,* 26 (1), 145-52.

Gupta, A., Lawrence, A. T., Krishnan, K., Kavinsky, C. J., and Trohman, R. G. (2007), 'Current concepts in the mechanisms and management of drug-induced QT prolongation and torsade de pointes', *Am Heart J,* 153 (6), 891-9.

Halliwell, J. V., Plant, T.D., and Standen, N.B. (1994), 'Voltage Clamp Techniques', in David Ogden (ed.), *Microelectrode Techniques*

The Plymouth Workshop Handbook (second edn.; Cambridge: The Company of Biologists Limited), 17-35.

Hamaguchi, T., Hirose, T., Asakawa, H., Itoh, Y., Kamado, K., Tokunaga, K., Tomita, K., Masuda, H., Watanabe, N., and Namba, M. (2004), 'Efficacy of glimepiride in type 2 diabetic patients treated with glibenclamide', *Diabetes Res Clin Pract,* 66 Suppl 1, S129-32.

Hamill, O. P., Marty, A., Neher, E., Sakmann, B., and Sigworth, F. J. (1981), 'Improved patch-clamp techniques for high-resolution current recording from cells and cell-free membrane patches', *Pflugers Arch,* 391 (2), 85-100.

Hansen, S. B., Tao, X., and MacKinnon, R. (2012), 'Structural basis of PIP2 activation of the classical inward rectifier K+ channel Kir2.2', *Nature,* 477 (7365), 495-8.

Haverkamp, W., Breithardt, G., Camm, A. J., Janse, M. J., Rosen, M. R., Antzelevitch, C., Escande, D., Franz, M., Malik, M., Moss, A., and Shah, R. (2000), 'The potential for QT prolongation and proarrhythmia by non-antiarrhythmic drugs: clinical and regulatory implications. Report on a policy conference of the European Society of Cardiology', *Eur Heart J,* 21 (15), 1216-31.

Higgins, C. F. (2001), 'ABC transporters: physiology, structure and mechanism--an overview', *Res Microbiol,* 152 (3-4), 205-10.

Hille, B (2001), *Ion Channels of Excitable Membranes* (third edn edn.: Sunderland, Sinauer Associates).

Hoag, H. (2005), 'Expression of interest', *Nature,* 437 (7055), 164-5.

Hodgkin, A. L. and Huxley, A. F. (1952), 'Movement of sodium and potassium ions during nervous activity', *Cold Spring Harb Symp Quant Biol,* 17, 43-52.

Hough, E., Beech, D. J., and Sivaprasadarao, A. (2000), 'Identification of molecular regions responsible for the membrane trafficking of Kir6.2', *Pflugers Arch,* 440 (3), 481-7.

Hussain, K. and Cosgrove, K. E. (2005), 'From congenital hyperinsulinism to diabetes mellitus: the role of pancreatic beta-cell KATP channels', *Pediatr Diabetes,* 6 (2), 103-13.

Inagaki, N. and Seino, S. (1998), 'ATP-sensitive potassium channels: structures, functions, and pathophysiology', *Jpn J Physiol,* 48 (6), 397-412.

Inagaki, N., Gonoi, T., and Seino, S. (1997), 'Subunit stoichiometry of the pancreatic beta-cell ATP-sensitive K+ channel', *FEBS Lett,* 409 (2), 232-6.

Inagaki, N., Gonoi, T., Clement, J. P., Wang, C. Z., Aguilar-Bryan, L., Bryan, J., and Seino, S. (1996), 'A family of sulfonylurea receptors determines the pharmacological properties of ATP-sensitive K+ channels', *Neuron,* 16 (5), 1011-7.

Inagaki, N., Gonoi, T., Clement, J. P. th, Namba, N., Inazawa, J., Gonzalez, G., Aguilar-Bryan, L., Seino, S., and Bryan, J. (1995), 'Reconstitution of IKATP: an inward rectifier subunit plus the sulfonylurea receptor', *Science,* 270 (5239), 1166-70.

Inoue, I., Nagase, H., Kishi, K., and Higuti, T. (1991), 'ATP-sensitive K+ channel in the mitochondrial inner membrane', *Nature,* 352 (6332), 244-7.

Isacoff, E. Y., Jan, Y. N., and Jan, L. Y. (1990), 'Evidence for the formation of heteromultimeric potassium channels in Xenopus oocytes', *Nature,* 345 (6275), 530-4.

Isomoto, S. and Kurachi, Y. (1996), '[Molecular and biophysical aspects of potassium channels]', *Nihon Rinsho,* 54 (3), 660-6.

Isomoto, S., Kondo, C., Yamada, M., Matsumoto, S., Higashiguchi, O., Horio, Y., Matsuzawa, Y., and Kurachi, Y. (1996), 'A novel sulfonylurea receptor forms with BIR (Kir6.2) a smooth muscle type ATP-sensitive K+ channel', *J Biol Chem,* 271 (40), 24321-4.

Jiang, W., Prescott, M., Devenish, R. J., Spiccia, L., and Hearn, M. T. (2009), 'Separation of hexahistidine fusion proteins with immobilized metal ion affinity chromatographic (IMAC) sorbents derived from M(N+)-tacn and its derivatives', *Biotechnol Bioeng,* 103 (4), 747-56.

John, S. A., Weiss, J. N., Xie, L. H., and Ribalet, B. (2003), 'Molecular mechanism for ATP-dependent closure of the K+ channel Kir6.2', *J Physiol,* 552 (Pt 1), 23-34.

Jones, P. A., Tucker, S. J., and Ashcroft, F. M. (2001), 'Multiple sites of interaction between the intracellular domains of an inwardly rectifying potassium channel, Kir6.2', *FEBS Lett,* 508 (1), 85-9.

Kono, Y., Horie, M., Takano, M., Otani, H., Xie, L. H., Akao, M., Tsuji, K., and Sasayama, S. (2000), 'The properties of the Kir6.1-6.2 tandem channel co-expressed with SUR2A', *Pflugers Arch*, 440 (5), 692-8.

Koster, J. C., Sha, Q., Shyng, S., and Nichols, C. G. (1999), 'ATP inhibition of KATP channels: control of nucleotide sensitivity by the N-terminal domain of the Kir6.2 subunit', *J Physiol*, 515 (Pt 1), 19-30.

Kuo, A., Gulbis, J. M., Antcliff, J. F., Rahman, T., Lowe, E. D., Zimmer, J., Cuthbertson, J., Ashcroft, F. M., Ezaki, T., and Doyle, D. A. (2003), 'Crystal structure of the potassium channel KirBac1.1 in the closed state', *Science*, 300 (5627), 1922-6.

Kuzuya, T., Hoshida, S., Yamashita, N., Fuji, H., Oe, H., Hori, M., Kamada, T., and Tada, M. (1993), 'Delayed effects of sublethal ischemia on the acquisition of tolerance to ischemia', *Circ Res*, 72 (6), 1293-9.

Kwak, Y. G., Park, S. K., Kim, U. H., Han, M. K., Eun, J. S., Cho, K. P., and Chae, S. W. (1996), 'Intracellular ADP-ribose inhibits ATP-sensitive K+ channels in rat ventricular myocytes', *Am J Physiol*, 271 (2 Pt 1), C464-8.

Lesage, F. and Lazdunski, M. (2000), 'Molecular and functional properties of two-pore-domain potassium channels', *Am J Physiol Renal Physiol*, 279 (5), F793-801.

Li, Y. W., Whittaker, P., and Kloner, R. A. (1992), 'The transient nature of the effect of ischemic preconditioning on myocardial infarct size and ventricular arrhythmia', *Am Heart J*, 123 (2), 346-53.

Lin, Y. W., MacMullen, C., Ganguly, A., Stanley, C. A., and Shyng, S. L. (2006), 'A novel KCNJ11 mutation associated with congenital hyperinsulinism reduces the intrinsic open probability of beta-cell ATP-sensitive potassium channels', *J Biol Chem*, 281 (5), 3006-12.

Logothetis, D. E., Lupyan, D., and Rosenhouse-Dantsker, A. (2007), 'Diverse Kir modulators act in close proximity to residues implicated in phosphoinositide binding', *J Physiol*, 582 (Pt 3), 953-65.

Lorenz, E. and Terzic, A. (1999), 'Physical association between recombinant cardiac ATP-sensitive K+ channel subunits Kir6.2 and SUR2A', *J Mol Cell Cardiol*, 31 (2), 425-34.

Loughran, S. T., Loughran, N. B., Ryan, B. J., D'Souza, B. N., and Walls, D. (2006), 'Modified His-tag fusion vector for enhanced protein purification by immobilized metal affinity chromatography', *Anal Biochem*, 355 (1), 148-50.

Mannhold, R. (2004), 'KATP channel openers: structure-activity relationships and therapeutic potential', *Med Res Rev*, 24 (2), 213-66.

Marber, M. S., Latchman, D. S., Walker, J. M., and Yellon, D. M. (1993), 'Cardiac stress protein elevation 24 hours after brief ischemia or heat stress is associated with resistance to myocardial infarction', *Circulation*, 88 (3), 1264-72.

Markworth, E., Schwanstecher, C., and Schwanstecher, M. (2000), 'ATP4- mediates closure of pancreatic beta-cell ATP-sensitive potassium channels by interaction with 1 of 4 identical sites', *Diabetes*, 49 (9), 1413-8.

Matsuo, M., Kioka, N., Amachi, T., and Ueda, K. (1999), 'ATP binding properties of the nucleotide-binding folds of SUR1', *J Biol Chem*, 274 (52), 37479-82.

Matsuo, M., Dabrowski, M., Ueda, K., and Ashcroft, F. M. (2002), 'Mutations in the linker domain of NBD2 of SUR inhibit transduction but not nucleotide binding', *EMBO J*, 21 (16), 4250-8.

Matsuo, M., Tanabe, K., Kioka, N., Amachi, T., and Ueda, K. (2000), 'Different binding properties and affinities for ATP and ADP among sulfonylurea receptor subtypes, SUR1, SUR2A, and SUR2B', *J Biol Chem*, 275 (37), 28757-63.

Mikhailov, M. V., Campbell, J. D., de Wet, H., Shimomura, K., Zadek, B., Collins, R. F., Sansom, M. S., Ford, R. C., and Ashcroft, F. M. (2005), '3-D structural and functional characterization of the purified KATP channel complex Kir6.2-SUR1', *Embo J*, 24 (23), 4166-75.

Miki, T., Iwanaga, T., Nagashima, K., Ihara, Y., and Seino, S. (2001a), 'Roles of ATP-sensitive K+ channels in cell survival and differentiation in the endocrine pancreas', *Diabetes*, 50 Suppl 1, S48-51.

Miki, T., Liss, B., Minami, K., Shiuchi, T., Saraya, A., Kashima, Y., Horiuchi, M., Ashcroft, F., Minokoshi, Y., Roeper, J., and Seino, S. (2001b), 'ATP-sensitive K+ channels in the hypothalamus are essential for the maintenance of glucose homeostasis', *Nat Neurosci*, 4 (5), 507-12.

Misler, S., Gillis, K., and Tabcharani, J. (1989), 'Modulation of gating of a metabolically regulated, ATP-dependent K+ channel by intracellular pH in B cells of the pancreatic islet', *J Membr Biol*, 109 (2), 135-43.

Molecular, Devices (2008), *The Axon Guide A Guide to Electrophysiology & Biophysics Laboratory Techniques*, ed. Rivka Sherman-Gold (Third edn.; Sunnyvale: MDS Analytical Technologies) 286.

Moreau, C., Prost, A. L., Derand, R., and Vivaudou, M. (2005), 'SUR, ABC proteins targeted by KATP channel openers', *J Mol Cell Cardiol*, 38 (6), 951-63.

Murry, C. E., Jennings, R. B., and Reimer, K. A. (1986), 'Preconditioning with ischemia: a delay of lethal cell injury in ischemic myocardium', *Circulation*, 74 (5), 1124-36.

NCBI 'Structure', (updated 2009) <http://www.ncbi.nlm.nih.gov/Structure/index.shtml>, accessed 15/07/2009.

Neher, E., Sakmann, B., and Steinbach, J. H. (1978), 'The extracellular patch clamp: a method for resolving currents through individual open channels in biological membranes', *Pflugers Arch*, 375 (2), 219-28.

Nichols, C. G. and Lederer, W. J. (1991), 'The mechanism of KATP channel inhibition by ATP', *J Gen Physiol*, 97 (5), 1095-8.

Nichols, C. G. and Lopatin, A. N. (1997), 'Inward rectifier potassium channels', *Annu Rev Physiol*, 59, 171-91.

Nichols, C. G., Shyng, S. L., Nestorowicz, A., Glaser, B., Clement, J. P. th, Gonzalez, G., Aguilar-Bryan, L., Permutt, M. A., and Bryan, J. (1996), 'Adenosine diphosphate as an intracellular regulator of insulin secretion', *Science*, 272 (5269), 1785-7.

Nielsen, J. J., Kristensen, M., Hellsten, Y., Bangsbo, J., and Juel, C. (2003), 'Localization and function of ATP-sensitive potassium channels in human skeletal muscle', *Am J Physiol Regul Integr Comp Physiol*, 284 (2), R558-63.

Nishida, M. and MacKinnon, R. (2002), 'Structural basis of inward rectification: cytoplasmic pore of the G protein-gated inward rectifier GIRK1 at 1.8 A resolution', *Cell*, 111 (7), 957-65.

Noma, A. (1983), 'ATP-regulated K+ channels in cardiac muscle', *Nature*, 305 (5930), 147-8.

Ogden, D. and Stanfield, P. (1994), 'Patch Clamp Techniques for Single Channel and Whole-Cell Recordings', in David Ogden (ed.), *Microelectrode Techniques The Plymouth Workshop Handbook* (second edn.; Cambridge: The Company of Biologists Limited), 53-78.

Ohno-Shosaku, T., Zunkler, B. J., and Trube, G. (1987), 'Dual effects of ATP on K+ currents of mouse pancreatic beta-cells', *Pflugers Arch*, 408 (2), 133-8.

Patel, H. H., Hsu, A. K., Peart, J. N., and Gross, G. J. (2002), 'Sarcolemmal K(ATP) channel triggers opioid-induced delayed cardioprotection in the rat', *Circ Res*, 91 (3), 186-8.

Proks, P., Gribble, F. M., Adhikari, R., Tucker, S. J., and Ashcroft, F. M. (1999), 'Involvement of the N-terminus of Kir6.2 in the inhibition of the KATP channel by ATP', *J Physiol*, 514 (Pt 1), 19-25.

Proks, P., Reimann, F., Green, N., Gribble, F., and Ashcroft, F. (2002), 'Sulfonylurea stimulation of insulin secretion', *Diabetes*, 51 Suppl 3, S368-76.

Quayle, J. M., Nelson, M. T., and Standen, N. B. (1997), 'ATP-sensitive and inwardly rectifying potassium channels in smooth muscle', *Physiol Rev*, 77 (4), 1165-232.

Rainbow, R. D., James, M., Hudman, D., Al Johi, M., Singh, H., Watson, P. J., Ashmole, I., Davies, N. W., Lodwick, D., and Norman, R. I. (2004), 'Proximal C-terminal domain of sulphonylurea receptor 2A interacts with pore-forming Kir6 subunits in KATP channels', *Biochem J,* 379 (Pt 1), 173-81.

Reimann, F., Proks, P., and Ashcroft, F. M. (2001), 'Effects of mitiglinide (S 21403) on Kir6.2/SUR1, Kir6.2/SUR2A and Kir6.2/SUR2B types of ATP-sensitive potassium channel', *Br J Pharmacol,* 132 (7), 1542-8.

Reimann, F., Ryder, T. J., Tucker, S. J., and Ashcroft, F. M. (1999), 'The role of lysine 185 in the kir6.2 subunit of the ATP-sensitive channel in channel inhibition by ATP', *J Physiol,* 520 Pt 3, 661-9.

Ribalet, B., John, S. A., and Weiss, J. N. (2000), 'Regulation of cloned ATP-sensitive K channels by phosphorylation, MgADP, and phosphatidylinositol bisphosphate (PIP(2)): a study of channel rundown and reactivation', *J Gen Physiol,* 116 (3), 391-410.

--- (2003), 'Molecular basis for Kir6.2 channel inhibition by adenine nucleotides', *Biophys J,* 84 (1), 266-76.

Rohacs, T., Lopes, C. M., Jin, T., Ramdya, P. P., Molnar, Z., and Logothetis, D. E. (2003), 'Specificity of activation by phosphoinositides determines lipid regulation of Kir channels', *Proc Natl Acad Sci U S A,* 100 (2), 745-50.

Roper, J. and Ashcroft, F. M. (1995), 'Metabolic inhibition and low internal ATP activate K-ATP channels in rat dopaminergic substantia nigra neurones', *Pflugers Arch,* 430 (1), 44-54.

Sagen, J. V., Raeder, H., Hathout, E., Shehadeh, N., Gudmundsson, K., Baevre, H., Abuelo, D., Phornphutkul, C., Molnes, J., Bell, G. I., Gloyn, A. L., Hattersley, A. T., Molven, A., Sovik, O., and Njolstad, P. R. (2004), 'Permanent neonatal diabetes due to mutations in KCNJ11 encoding Kir6.2: patient characteristics and initial response to sulfonylurea therapy', *Diabetes,* 53 (10), 2713-8.

Sattiraju, S., Reyes, S., Kane, G. C., and Terzic, A. (2008), 'K(ATP) channel pharmacogenomics: from bench to bedside', *Clin Pharmacol Ther,* 83 (2), 354-7.

Schulz, R., Cohen, M. V., Behrends, M., Downey, J. M., and Heusch, G. (2001), 'Signal transduction of ischemic preconditioning', *Cardiovasc Res,* 52 (2), 181-98.

Schulze, D., Krauter, T., Fritzenschaft, H., Soom, M., and Baukrowitz, T. (2003), 'Phosphatidylinositol 4,5-bisphosphate (PIP2) modulation of ATP and pH sensitivity in Kir channels. A tale of an active and a silent PIP2 site in the N terminus', *J Biol Chem,* 278 (12), 10500-5.

Schwanstecher, M., Sieverding, C., Dorschner, H., Gross, I., Aguilar-Bryan, L., Schwanstecher, C., and Bryan, J. (1998), 'Potassium channel openers require ATP to bind to and act through sulfonylurea receptors', *EMBO J,* 17 (19), 5529-35.

Schwappach, B., Zerangue, N., Jan, Y. N., and Jan, L. Y. (2000), 'Molecular basis for K(ATP) assembly: transmembrane interactions mediate association of a K+ channel with an ABC transporter', *Neuron,* 26 (1), 155-67.

Seino, S. (1999), 'ATP-sensitive potassium channels: a model of heteromultimeric potassium channel/receptor assemblies', *Annu Rev Physiol,* 61, 337-62.

--- (2003), 'Physiology and pathophysiology of K(ATP) channels in the pancreas and cardiovascular system: a review', *J Diabetes Complications,* 17 (2 Suppl), 2-5.

Sherman, A. J., Shrier, A., and Cooper, E. (1999), 'Series resistance compensation for whole-cell patch-clamp studies using a membrane state estimator', *Biophys J,* 77 (5), 2590-601.

Shieh, C. C., Coghlan, M., Sullivan, J. P., and Gopalakrishnan, M. (2000), 'Potassium channels: molecular defects, diseases, and therapeutic opportunities', *Pharmacol Rev,* 52 (4), 557-94.

Shyng, S. and Nichols, C. G. (1997), 'Octameric stoichiometry of the KATP channel complex', *J Gen Physiol,* 110 (6), 655-64.

Shyng, S., Ferrigni, T., and Nichols, C. G. (1997), 'Regulation of KATP channel activity by diazoxide and MgADP. Distinct functions of the two nucleotide binding folds of the sulfonylurea receptor', *J Gen Physiol,* 110 (6), 643-54.

Shyng, S. L. and Nichols, C. G. (1998), 'Membrane phospholipid control of nucleotide sensitivity of KATP channels', *Science,* 282 (5391), 1138-41.

Shyng, S. L., Cukras, C. A., Harwood, J., and Nichols, C. G. (2000), 'Structural determinants of PIP(2) regulation of inward rectifier K(ATP) channels', *J Gen Physiol,* 116 (5), 599-608.

Speechly-Dick, M. E., Grover, G. J., and Yellon, D. M. (1995), 'Does ischemic preconditioning in the human involve protein kinase C and the ATP-dependent K+ channel? Studies of contractile function after simulated ischemia in an atrial in vitro model', *Circ Res,* 77 (5), 1030-5.

Spruce, A. E., Standen, N. B., and Stanfield, P. R. (1985), 'Voltage-dependent ATP-sensitive potassium channels of skeletal muscle membrane', *Nature,* 316 (6030), 736-8.

Standen, N. B., Quayle, J. M., Davies, N. W., Brayden, J. E., Huang, Y., and Nelson, M. T. (1989), 'Hyperpolarizing vasodilators activate ATP-sensitive K+ channels in arterial smooth muscle', *Science,* 245 (4914), 177-80.

Stanford, I. M. and Lacey, M. G. (1996), 'Electrophysiological investigation of adenosine trisphosphate-sensitive potassium channels in the rat substantia nigra pars reticulata', *Neuroscience,* 74 (2), 499-509.

Sturgess, N. C., Ashford, M. L., Cook, D. L., and Hales, C. N. (1985), 'The sulphonylurea receptor may be an ATP-sensitive potassium channel', *Lancet,* 2 (8453), 474-5.

Sunaga, Y., Gonoi, T., Shibasaki, T., Ichikawa, K., Kusama, H., Yano, H., and Seino, S. (2001), 'The effects of mitiglinide (KAD-1229), a new anti-diabetic drug, on ATP-sensitive K+ channels and insulin secretion: comparison with the sulfonylureas and nateglinide', *Eur J Pharmacol,* 431 (1), 119-25.

Tanabe, K., Tucker, S. J., Ashcroft, F. M., Proks, P., Kioka, N., Amachi, T., and Ueda, K. (2000), 'Direct photoaffinity labeling of Kir6.2 by [gamma-(32)P]ATP-[gamma]4-azidoanilide', *Biochem Biophys Res Commun,* 272 (2), 316-9.

Tanabe, K., Tucker, S. J., Matsuo, M., Proks, P., Ashcroft, F. M., Seino, S., Amachi, T., and Ueda, K. (1999), 'Direct photoaffinity labeling of the Kir6.2 subunit of the ATP-sensitive K+ channel by 8-azido-ATP', *J Biol Chem,* 274 (7), 3931-3.

Terzic, A., Jahangir, A., and Kurachi, Y. (1995), 'Cardiac ATP-sensitive K+ channels: regulation by intracellular nucleotides and K+ channel-opening drugs', *Am J Physiol,* 269 (3 Pt 1), C525-45.

Thornton, J., Striplin, S., Liu, G. S., Swafford, A., Stanley, A. W., Van Winkle, D. M., and Downey, J. M. (1990), 'Inhibition of protein synthesis does not block myocardial protection afforded by preconditioning', *Am J Physiol,* 259 (6 Pt 2), H1822-5.

Tinker, A., Jan, Y. N., and Jan, L. Y. (1996), 'Regions responsible for the assembly of inwardly rectifying potassium channels', *Cell,* 87 (5), 857-68.

Toro, L., Wallner, M., Meera, P., and Tanaka, Y. (1998), 'Maxi-K(Ca), a Unique Member of the Voltage-Gated K Channel Superfamily', *News Physiol Sci,* 13, 112-17.

Toyoda, Y., Friehs, I., Parker, R. A., Levitsky, S., and McCully, J. D. (2000), 'Differential role of sarcolemmal and mitochondrial K(ATP) channels in adenosine-enhanced ischemic preconditioning', *Am J Physiol Heart Circ Physiol,* 279 (6), H2694-703.

Trapp, S., Proks, P., Tucker, S. J., and Ashcroft, F. M. (1998), 'Molecular analysis of ATP-sensitive K channel gating and implications for channel inhibition by ATP', *J Gen Physiol,* 112 (3), 333-49.

Trapp, S., Haider, S., Jones, P., Sansom, M. S., and Ashcroft, F. M. (2003), 'Identification of residues contributing to the ATP binding site of Kir6.2', *Embo J,* 22 (12), 2903-12.

Trube, G. and Hescheler, J. (1984), 'Inward-rectifying channels in isolated patches of the heart cell membrane: ATP-dependence and comparison with cell-attached patches', *Pflugers Arch*, 401 (2), 178-84.

Tsuboi, T., Lippiat, J. D., Ashcroft, F. M., and Rutter, G. A. (2004), 'ATP-dependent interaction of the cytosolic domains of the inwardly rectifying K+ channel Kir6.2 revealed by fluorescence resonance energy transfer', *Proc Natl Acad Sci U S A*, 101 (1), 76-81.

Tsuchiya, K., Wang, W., Giebisch, G., and Welling, P. A. (1992), 'ATP is a coupling modulator of parallel Na,K-ATPase-K-channel activity in the renal proximal tubule', *Proc Natl Acad Sci U S A*, 89 (14), 6418-22.

Tucker, S. J. and Ashcroft, F. M. (1999), 'Mapping of the physical interaction between the intracellular domains of an inwardly rectifying potassium channel, Kir6.2', *J Biol Chem*, 274 (47), 33393-7.

Tucker, S. J., Gribble, F. M., Zhao, C., Trapp, S., and Ashcroft, F. M. (1997), 'Truncation of Kir6.2 produces ATP-sensitive K+ channels in the absence of the sulphonylurea receptor', *Nature*, 387 (6629), 179-83.

Tucker, S. J., Gribble, F. M., Proks, P., Trapp, S., Ryder, T. J., Haug, T., Reimann, F., and Ashcroft, F. M. (1998), 'Molecular determinants of KATP channel inhibition by ATP', *EMBO J*, 17 (12), 3290-6.

Ueda, K., Inagaki, N., and Seino, S. (1997), 'MgADP antagonism to Mg2+-independent ATP binding of the sulfonylurea receptor SUR1', *J Biol Chem*, 272 (37), 22983-6.

Ueda, K., Komine, J., Matsuo, M., Seino, S., and Amachi, T. (1999), 'Cooperative binding of ATP and MgADP in the sulfonylurea receptor is modulated by glibenclamide', *Proc Natl Acad Sci U S A*, 96 (4), 1268-72.

Uhde, I., Toman, A., Gross, I., Schwanstecher, C., and Schwanstecher, M. (1999), 'Identification of the potassium channel opener site on sulfonylurea receptors', *J Biol Chem*, 274 (40), 28079-82.

Vaxillaire, M., Populaire, C., Busiah, K., Cave, H., Gloyn, A. L., Hattersley, A. T., Czernichow, P., Froguel, P., and Polak, M. (2004), 'Kir6.2 mutations are a common cause of permanent neonatal diabetes in a large cohort of French patients', *Diabetes*, 53 (10), 2719-22.

Walker, J. E., Saraste, M., Runswick, M. J., and Gay, N. J. (1982), 'Distantly related sequences in the alpha- and beta-subunits of ATP synthase, myosin, kinases and other ATP-requiring enzymes and a common nucleotide binding fold', *Embo J*, 1 (8), 945-51.

Wibrand, F., Honore, E., and Lazdunski, M. (1992), 'Opening of glibenclamide-sensitive K+ channels in follicular cells promotes Xenopus oocyte maturation', *Proc Natl Acad Sci U S A*, 89 (11), 5133-7.

Xie, L. H., John, S. A., Ribalet, B., and Weiss, J. N. (2007), 'Activation of inwardly rectifying potassium (Kir) channels by phosphatidylinositol-4,5-bisphosphate (PIP2): interaction with other regulatory ligands', *Prog Biophys Mol Biol*, 94 (3), 320-35.

Yamada, K. and Inagaki, N. (2002), 'ATP-sensitive K(+) channels in the brain: sensors of hypoxic conditions', *News Physiol Sci*, 17, 127-30.

Yamada, M., Isomoto, S., Matsumoto, S., Kondo, C., Shindo, T., Horio, Y., and Kurachi, Y. (1997), 'Sulphonylurea receptor 2B and Kir6.1 form a sulphonylurea-sensitive but ATP-insensitive K+ channel', *J Physiol*, 499 (Pt 3), 715-20.

Yao, Z. and Gross, G. J. (1994a), 'Activation of ATP-sensitive potassium channels lowers threshold for ischemic preconditioning in dogs', *Am J Physiol*, 267 (5 Pt 2), H1888-94.

--- (1994b), 'Effects of the KATP channel opener bimakalim on coronary blood flow, monophasic action potential duration, and infarct size in dogs', *Circulation*, 89 (4), 1769-75.

Yokoshiki, H., Sunagawa, M., Seki, T., and Sperelakis, N. (1998), 'ATP-sensitive K+ channels in pancreatic, cardiac, and vascular smooth muscle cells', *Am J Physiol*, 274 (1 Pt 1), C25-37.

Zerangue, N., Schwappach, B., Jan, Y. N., and Jan, L. Y. (1999), 'A new ER trafficking signal regulates the subunit stoichiometry of plasma membrane K(ATP) channels', *Neuron*, 22 (3), 537-48.

Zhuo, M. L., Huang, Y., Liu, D. P., and Liang, C. C. (2005), 'KATP channel: relation with cell metabolism and role in the cardiovascular system', *Int J Biochem Cell Biol*, 37 (4), 751-64.

Quote from Avicenna

تا بدانجا رسيد دانش من

که بدانم همي که نادانم

All I know (what I realized) is that I know nothing

Avicenna

(Abu ʻAli al-Hussein, ibn Sina, Persian physician, scientist and philosopher,

c. 980 – 1037, note: this was mentioned by him before his passing)